1-1-1999

Characterization of structural transformations with vibrational spectroscopy.

Thomas D. Hahn
University of Massachusetts Amherst

CHARACTERIZATION OF STRUCTURAL TRANSFORMATIONS WITH VIBRATIONAL SPECTROSCOPY

A Dissertation Presented

by

THOMAS D. HAHN

Submitted to the Graduate School of the
University of Massachusetts Amherst in partial fulfillment
of the requirements for the degree of

DOCTOR OF PHILOSOPHY

February 1999

Department of Polymer Science and Engineering

CHARACTERIZATION OF STRUCTURAL TRANSFORMATIONS WITH VIBRATIONAL SPECTROSCOPY

A Dissertation Presented

by

THOMAS D. HAHN

Approved as to style and content by:

Shaw Ling Hsu, Chair

Bruce Novak, Member

Howard D. Stidham, Member

Robert Weis, Member

Richard J. Farris, Department Head
Polymer Science and Engineering

ACKNOWLEDGMENTS

I would like to express my gratitude to Professor Shaw Ling Hsu for his continued support and advice during my research. I am indebted to him for the opportunity I received. I would also like to thank the other members of my committee, Bruce Novak, Howard D. Stidham, and Robert Weis, for their time and their advice.

I wish to thank Dr. Allen Seidle of 3M Corporation for supplying several polypropylene samples which made a significant portion of this dissertation possible.

I am also appreciative to the other present and former members of my research group. I would like to thank Dorie Yontz, Xiaodong Wu, Gregory Martin, Sophie Riou, Zhaohui Su, Hun-Jan Tao, Mario Perez, Sunghoe Yoon, Chao-Cheng Chen, Bert Chien, Diana Chien, and Yong Wang. In addition, I wish to thank visiting members of the group for their collaboration, Professor Da Cheng Wu, Professor Xiaozhen Yang, Professor Saeed Al'alawe, and Hsin Fu Lin.

Many people both inside and outside of the Polymer Science and Engineering Department have played an important role in my life in the Amherst area. I especially wish to thank Naveen Agarwal, Jennifer David, and Nancy Kosloski.

I wish to thank my parents and siblings for their love and support of this endeavor.

Finally, I wish to thank my wife, Nancy, and my daughter, Grace. Nancy's constant support throughout has made my studies at the University of Massachusetts possible.

ABSTRACT

CHARACTERIZATION OF STRUCTURAL TRANSFORMATIONS

WITH VIBRATIONAL SPECTROSCOPY

FEBRUARY 1999

THOMAS D. HAHN, B.S., PENNSYLVANIA STATE UNIVERSITY

M.S., UNIVERSITY OF TENNESSEE, KNOXVILLE

Ph.D., UNIVERSITY OF MASSACHUSETTS AMHERST

Directed by: Professor Shaw Ling Hsu

The work presented in this thesis applies primarily the techniques of Raman and infrared spectroscopy to characterize the structural transformations in polymers. An overview of the problems studied is given in Chapter 1. Particular emphasis is given to mainly syndiotactic polypropylene structural transformations influenced by configurational defects (Chapter 2), and thermal history and mechanical deformation (Chapter 3). In Chapter 4, the influence of a confining surface in the structural transformation of poly(dimethyl siloxane) Langmuir films at the air-water interface is characterized.

Using a combination of Raman spectroscopy, and normal coordinate analysis of both ordered and disordered chains, it was possible to relate the Raman spectrum to the amorphous phase and ordered phase structures. With this relationship, it was possible to directly relate the Raman spectrum to the population of meso (isotactic) defects in mainly syndiotactic polypropylene. In addition, time, temperature, and mechanical stretching-dependent transformations were characterized.

With external reflectance infrared spectroscopy, it was possible to characterize chain conformation and the local environment of the polymer backbone. Dependence of band intensity and frequency was related to the average segmental orientation and the proximity of the water surface.

TABLE OF CONTENTS

LIST OF TABLES

LIST OF FIGURES

CHAPTER 1

INTRODUCTION

Polymer microstructure is markedly transformed during the process of crystal nucleation and growth, and by spreading a monolayer from an isotropic solution to a confining surface, such as the air-water interface. In the first case, the crystallization process transforms an amorphous chain to a chain with a conformation of the crystalline polymer. In the second case, the random conformation polymer in solution will align on the water surface as it spreads to form a monolayer. The structure will depend on the strength of the polymer-water interaction, separation of the nonpolar and polar groups, and available surface area. In both cases, vibrational spectroscopy can be used to characterize the microstructure associated with the transformation. In this work, factors controlling the microstructure transformation are studied. In one system, phase transformations of syndiotactic polypropylene are studied in terms of the chemical configurational defects, temperature, time, and stretching. In another system, poly(dimethyl siloxane) spread on water, the controlling factor is the confining surface and available surface area. These problems are defined below.

1.1 Syndiotactic Polypropylene Microstructural Transformations

In the last ten years interest in characterizing the physical and mechanical properties of syndiotactic polypropylene has grown. This interest is a result of the recent ability to synthesize highly syndiospecific polypropylene with metallocene catalysts.[1] With metallocene catalysts, it also became possible to control the configuration distribution of asymmetric centers in a polymer chain.[2] With increased syndiotacticity, crystal conformations and structures of form I (helical)[3] and form II (planar zigzag)[4] syndiotactic polypropylene have been confirmed and refined,[5-14] and a third crystalline state has been

observed, form III, which appears to have the conformation $(ggttggtttttt)_n$.[15-17] Likewise, ^{13}C NMR has been used to determine the configuration[18] and to study prevalent crystalline and amorphous conformations.[13,19,20]

1.1.1 Configurational Defects Transforming Polymer Microstructure

For polymers with asymmetric centers, configuration and conformation are known to be related.[21,22] In polypropylene, the isotactic polymer and syndiotactic polymer have entirely different crystal structures, as well as different mechanical and physical properties.[3,23-25] Figure 1.1 illustrates some of these differences for the most common crystalline conformations.

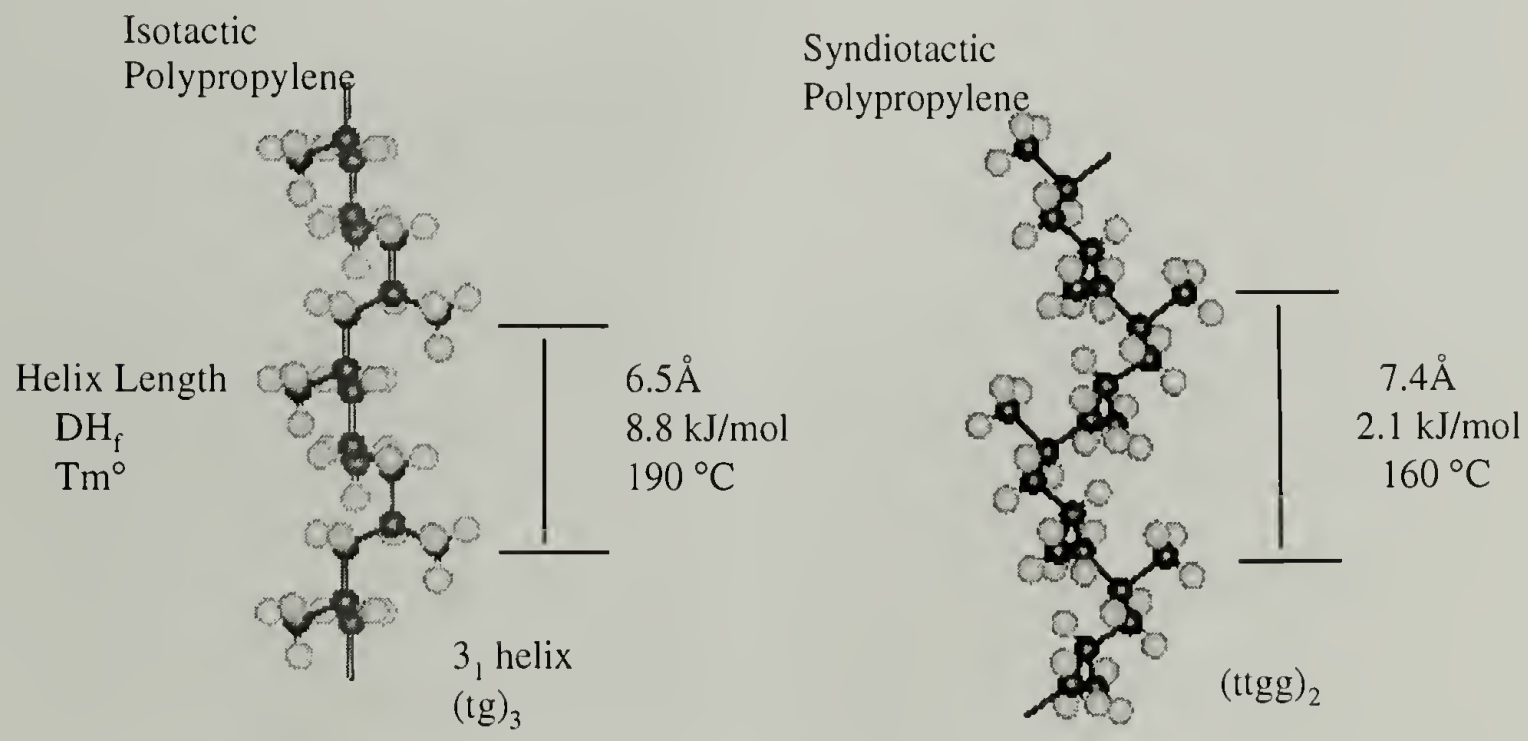

Figure 1.1 Most common crystalline conformations of isotactic and syndiotactic polypropylene.

Placing configurational defects along the backbone, like other chemical defects, is known to impact on the crystallization behavior.[26] Such defects are generally excluded

from the crystalline regions, and therefore remain in the amorphous phase. As a result, the crystallite size is limited by the sequence length between defects, and nucleation and growth rates are reduced as the noncrystallizing defects concentrate in the amorphous regions. What has not been studied is the contribution of the configurational defects to both the amorphous conformation distribution and the degree of ordering possible, whether in the crystalline phase, amorphous phase, or an ordered state in small aggregates not observable by scattering techniques.

Since at least 1960, scientists have been interested in characterizing the configurational regularity of syndiotactic polypropylene as a way to determine the stereospecificity of the catalyst.[3] Early studies have attempted to use the infrared spectrum of polypropylene to characterize the tacticity.[3,27] However, vibrational bands used for determining tacticity are dependent on the conformational ordering. Polypropylene tacticity analysis with ^{13}C NMR is possible.[28] However, interest in alternative methods for evaluating the tacticity, such as infrared and Raman spectroscopy, has persisted because these alternative methods may require less material handling, and therefore may be more rapid and less expensive to use. Masetti, et al.[29] pointed out that the Raman spectrum for syndiotactic polypropylene contains bands that may be suitable for characterizing the tacticity. Some of these bands are present only in the solid state, and other bands appear to remain in the melt. They suggested that the persistent bands, namely in the 300 to 400 cm^{-1} region, are a consequence of some of the polymer remaining in an extended helical state. However, they also note that no statement about the length of these helices is possible. As will be described below, combining the Raman spectrum with Monte Carlo calculation of an ensemble of chains to simulate the Raman spectrum makes characterization of configurational defects and their impact on syndiotactic polypropylene microstructure possible. In addition, conformational mapping makes possible a determination of the helix length required to observe the persistent bands.

1.1.2 Time-Dependent Microstructure Transformations

1.1.2.1 Time-Dependent Phase Transformations

Time-dependent ordering, such as crystallization and aggregation behavior in polymers, is strongly dependent on the crystallization temperature, as well as the environment, such as solvent, presence of impurities, nucleating agents, and chemical defects.[26] The microstructure of the crystalline phases can be established by methods such as X-ray scattering and transmission electron microscopy. However, these techniques are not suitable if the aggregation that occurs is too small to exhibit coherent scattering. Furthermore, these techniques do not give information on how the ordering process transforms the conformation distribution in the amorphous phase.

1.1.2.2 Physical Aging

Time-dependent behavior of semicrystalline polymers, as well as glassy and filled polymers, can be described in terms of physical aging. Physical aging has generated much interest in the literature, because it results in changes in physical and mechanical properties of many polymeric systems over time.[30,31] In spite of the apparent importance of a microstructural description of the aging mechanism, little direct information concerning physical aging is available. Typically, physical aging microstructure is studied in terms of free volume change by techniques which are sensitive to local chain segment or probe mobility, such as positron annihilation lifetime spectroscopy (PALS),[32-35] electron spin resonance (ESR) of a spin probe radical or spin labeled chain,[36] fluorescence spectroscopy,[37-39] and photochromic probe or labeling.[37,40] However, these techniques provide no information about the conformation change that would coincide with the changes in free volume.

1.2 Characterizing Microstructure Transformations in Syndiotactic Polypropylene

Recently, a technique has been developed that allows the application of Raman spectroscopy to characterize quantitatively both conformationally ordered and disordered states for polymer chains.[41] The technique couples Raman spectroscopy with normal coordinate analysis for ordered chains, and with Carlo simulation of an ensemble of disordered chains, to represent the features of both ordered and amorphous phase. In this work, the technique was applied to characterize the microstructural transformations that would be expected for processes of conformational ordering and physical aging in syndiotactic polypropylene with different configurational defects.

1.2.1 Raman Spectroscopy of Syndiotactic Polypropylene

Several authors[29,42-49] have assigned the spectroscopic features of the vibrational spectrum of syndiotactic and isotactic polypropylene. This work takes advantage of some of these assignments to understand how the Raman spectrum changes, going from the melt to the solid state. In the melt, two regions are interesting (Figures 1.2a and 1.2b). In the 800 to 900 cm^{-1} region, a large, broad band appears in the Raman spectra of both the syndiotactic and isotactic polymer. The frequency values are shown in Figure 1.2a. In this region, the bands are very similar, but in Figure 1.2b, it is apparent that major low frequency bands are well-separated. Masetti, et al. state that the band around 300 cm^{-1} in the syndiotactic polypropylene spectrum is a consequence of some of the racemic sequences remaining in the extended helical structure.[29] A more detailed analysis of the relationship of the peak positions and the chain conformations is possible. The means for such analysis is described below. Greater depth of analysis for the solid state spectrum is also possible. We are interested in characterizing how the microstructure changes with time, configurational defect distribution, and deformation.

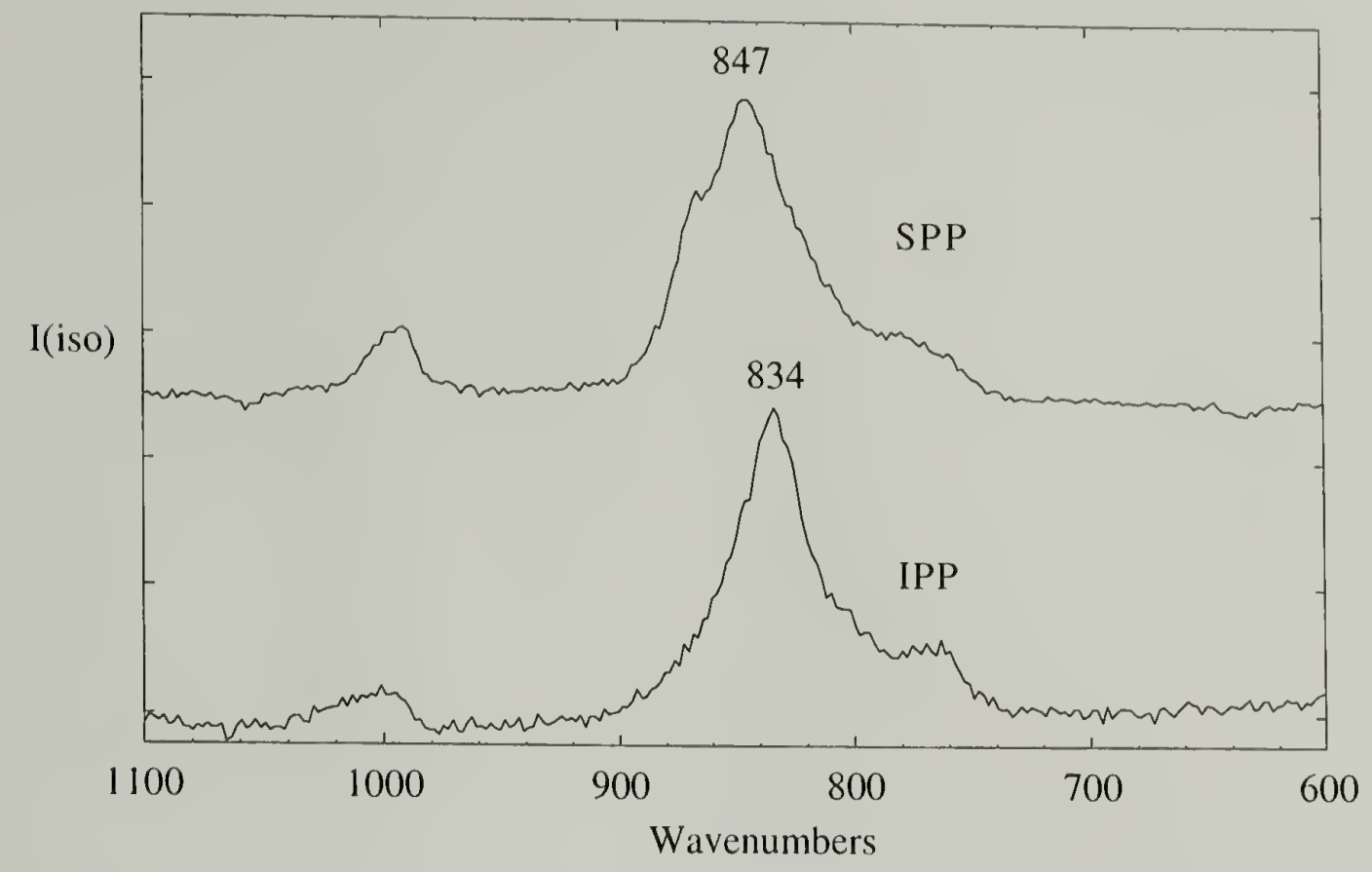

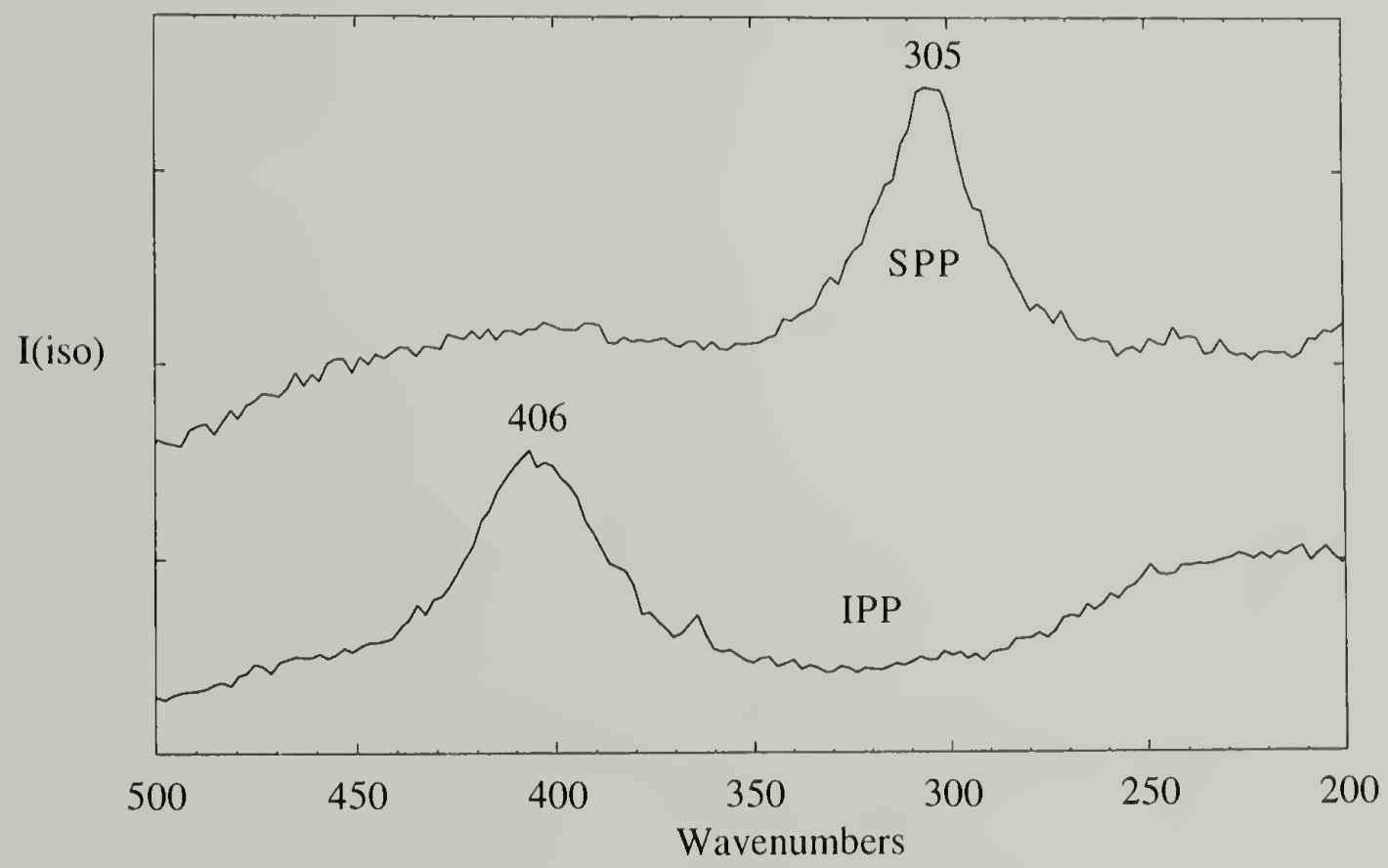

Figure 1.2 Isotropic raman melt spectrum for polypropylene.

1.2.2 Normal Coordinate Analysis and Monte Carlo Calculations of Syndiotactic Polypropylene

Snyder developed a method,[41] disordered normal coordinate analysis (DCNCA), which has been shown to represent reliably the isotropic Raman spectrum of a variety of polymers with a distribution of conformations. This method was first applied to n-alkanes.[41,50,51] More recent work applied the method to analysis of side chain behavior during polymer crystallization[52] and analysis of conformation of polyethers.[53,54] It has also been used to simulate the low frequency Raman spectrum (below ~ 600 cm^{-1}) of isotactic polypropylene, using a skeletal force field.[55] In order to understand the role of conformation and configuration on the Raman spectrum, it is necessary to be able to represent the Raman spectra of both isotactic and syndiotactic polypropylene. Furthermore, characterization of phase transformations in syndiotactic polypropylene is possible with characterization of bands in the 800 to 900 cm^{-1} region. Therefore, in this work, we applied the method of DCNCA to isotactic and syndiotactic polypropylene using a complete vibrational force field in order to simulate the isotropic Raman spectra for both ordered and disordered states. A detailed description of the procedure is given in Chapter 2. Once validated, this simulation method was used to develop a quantitative relationship between the Raman spectra and the population of configurational defects, also described in Chapter 2.

In Chapter 3, analysis of the degree of conformational ordering, based on the computational methods described in Chapter 2, made it possible to derive some information about the blockiness of the configuration distribution and the impact of configurational defects and thermal treatment on the rate and degree of ordering, and the types of phase transformations that occur.

1.3 Poly(dimethyl siloxane) Monolayer Transformation

Microstructural transformations may also result from changes in local environment and geometric confinement, such as was found in this work for poly(dimethyl siloxane) spread at the air-water interface.[56] Like other polymers and small molecules that spontaneously spread at the air-water interface,[57] poly(dimethyl siloxane) spreading results in a reduction of the surface tension. In doing so, it has been suggested that the polymer rearranges at the interface and interacts with the water substrate to a degree that depends on the surface concentration.[58-61] However, recent studies have placed some doubt on the nature of the polymer transformation.[62-66] Because of this conflict, the microstructural transformation was characterized (Chapter 4) in order to understand how the conformation, orientation, and local environment change.

1.3.1 External Reflectance Infrared Spectroscopy of Poly(dimethyl siloxane)

For polymer and surfactant thin films, such as those confined to the air-liquid interface, external reflectance infrared spectroscopy can be applied to characterize microstructural changes such as conformation and orientation.[67-69] For poly(dimethyl siloxane),[56] this technique was here to demonstrate the polymer-water interaction and to characterize the conformation change associated with a monolayer phase transition. The study takes advantage of two characteristic features of the infrared spectrum. One feature around 1000 to 1100 cm^{-1} is sensitive to the proximity of the polymer backbone to the water surface. A second feature around 1264 cm^{-1} is sensitive to the average segmental orientation. This second band is unusual because it has two vibrational bands that are assigned to the same frequency; therefore, conventional techniques could not be used to calculate an orientation function. Instead, features of the average segmental orientation were evaluated by calculating the absorbances of specific structures that may occur at the air-water interface.

1.3.2 Epifluorescence Microscopy of Poly(dimethyl siloxane)

To support the spectroscopic evidence for a structural transformation, epifluorescence microscopy was used to observe the coexistence of two different phases. This was done by adding a small amount of fluorescent probe to the polymer, spreading it at the air-water interface, and observing the fluorescence contrast. This technique has been used in the past to characterize the phase transformations and the phase structures of other monolayer films spread at the air-water interface.[70-72] It was useful in this study because it gave clear evidence that distinguishable domains of two phases were present.

1.4 References

(1) Ewen, J. A.; Jones, R. L.; Razavi, A.; Ferrara, J. D. *J. Am. Chem. Soc.* **1988**, 110, 6255.

(2) Isasi, J. R.; Mandelkern, L.; Alamo, R. G. *Polymer Preprints* **1996**, 37, 239.

(3) Natta, G.; Corradini, P. *Nuovo Chim. Suppl.* **1960**, 15, 40.

(4) Natta, G.; Peraldo, M.; Allegra, G. *Die Makromolekulare Chemie* **1964**, 75, 215.

(5) Auriemma, F.; De Rosa, C.; Corradini, P. *Macromolecules* **1993**, 26, 5719.

(6) Auriemma, F.; Born, R.; Spiess, H. W.; De Rosa, C.; Corradini, P. *Macromolecules* **1995**, 28, 6902.

(7) Auriemma, F.; Lewis, R. H.; Spiess, H. W.; De Rosa, C. *Macromol. Chem. Phys.* **1995**, 196, 4011.

(8) De Rosa, C.; Auriemma, F.; Corradini, P. *Macromolecules* **1996**, 29, 7452.

(9) Lovinger, A. J.; Lotz, B.; Davis, D. D. *Polymer* **1990**, 31, 2253.

(10) Lovinger, A. J.; Lotz, B.; Davis, D. D.; Paden, F. J. *Macromolecules* **1993**, 26, 3494.

(11) Lovinger, A. J.; Lotz, B.; Davis, D. D.; Schumacher, M. *Macromolecules* **1994**, 27, 6603.

(12) Stocker, W.; Schumacher, M.; Graff, S.; Lang, J.; Wittmann, J. C.; Lovinger, A. J.; Lotz, B. *Macromolecules* **1994**, 27, 6948.

(13) Sozzani, P.; Galimberti, M.; Balbontin, G. *Makromol. Chem. Rapid Commun.* **1992**, 13, 305.

(14) Chatani, Y.; Maruyama, H.; Noguchi, K.; Asanuma, T.; Shiomura, T. *J. Polym. Sci. Polym. Phys. Lett.* **1990**, 28, 393.

(15) Chatani, Y.; Maruyama, H.; Asanuma, T.; Shiomura, T. *J. Polym. Sci. Polym. Phys. Ed.* **1991**, 29, 1649.

(16) Asakura, T.; Aoki, A.; Takeshi, D.; Demura, M.; Asanuma, T. *Polym. J.* **1996**, 28, 24.

(17) Sozzani, P.; Simonutti, R.; Comoti, A. *Magnetic Resonance in Chemistry* **1994**, 32, s45.

(18) Tonneli, A. E.; Schilling, F. C. *Acc. Chem. Res.* **1981**, 14, 233.

(19) Sozzani, P.; Simonutti, R.; Galimberti, M. *Macromolecules* **1993**, 26, 5782.

(20) Nakaoki, T.; Hayashi, H.; Kitamaru, R. *Polymer* **1996**, 37, 4833.

(21) Flory, P. J. *Statistical Mechanics of Chain Molecules*; Interscience Publishers: New York, 1969, p 432.

(22) Mattice, W. L.; Suter, U. W. *Conformational Theory of Large Molecules. The Rotational Isomeric State Model in Macromolecular Systems*; John Wiley and Sons, Inc.: New York, 1994, p 449.

(23) Uehara, H.; Yamazaki, Y.; Kanamoto, T. *Polymer* **1996**, 37, 57.

(24) Turner-Jones, A.; Aizlewood, J. M.; Beckett, D. R. *Makromol. Chem.* **1964**, 75, 134.

(25) Corradini, P.; Natta, G.; Ganis, P.; Temussi, P. A. *Journal of Polymer Science, Part C* **1967**, 16, 2477.

(26) Gornick, F.; Mandelkern, L. *Journal of Applied Physics* **1962**, 33, 907.

(27) Boor, J. J.; Youngman, E. A. *J. Polym. Sci: Part A-1* **1966**, 4, 1861.

(28) Zambelli, A.; Locatelli, P.; Bajo, G.; Bovey, F. A. *Macromolecules* **1975**, 8, 687.

(29) Masetti, G.; Cabassi, F.; Zerbi, G. *Polymer* **1980**, 21, 143.

(30) Hutchinson, J. W. *Prog. Polym. Sci.* **1995**, 20, 703.

(31) Struik, L. C. E. *Physical Aging in Amorphous Polymers and Other Materials*; Elsevier Scientific Publishing Company: New York, 1978, p 229.

(32) Jean, Y. C.; Deng, Q. *Journal of Polymer Science: Part B: Polymer Physics Edition* **1992**, 30, 1359.

(33) Wang, Y. Y.; Nakanishi, H.; Jean, Y. C. *Journal of Polymer Science: Part B: Polymer Physics* **1990**, 28, 1431.

(34) Kobayashi, Y.; Zheng, W.; Meyer, E. F.; McGervey, J. D. *Macromolecules* **1989**, 22, 2302.

(35) Kluin, J.-E.; Yu, Z.; Vleeshouwers, S.; McGervey, J. D.; Jamieson, A. M.; Simha, R.; Sommer, K. *Macromolecules* **1993**, 26,

(36) Tsay, F. D.; Hong, S. D.; Maocanin, J.; Gupta, A. *Journal of Polymer Science: Polymer Physics Edition* **1982**, 20, 763.

(37) Royal, R. S.; Torkelson, J. M. *Macromolecules* **1992**, 25, 1705.

(38) Royal, J. S.; Victor, J. G.; Torkelson, J. M. *Macromolecules* **1992**, 25, 729.

(39) Royal, R. S.; Torkelson, J. M. *Macromolecules* **1993**, 26, 5331.

(40) Lamarre, L.; Sung, C. S. P. *Macromolecules* **1983**, 16, 1729.

(41) Snyder, R. G.; Kim, Y. *J. Phys. Chem* **1991**, 95, 602.

(42) Cyvin, S. J.; Brunvoll, J. *Journal of Molecular Spectroscopy* **1969**, 29, 159.

(43) Peraldo, M.; Cambini, M. *Spectrochimica Acta* **1965**, 21, 1509.

(44) Schachtschneider, J. H.; Snyder, R. G. *Spectrochimica Acta* **1965**, 21, 1527.

(45) Snyder, R. G.; Schachtschneider, J. H. *Spectrochim. Acta* **1964**, 20, 853.

(46) Chalmers, J. M. *Polymer* **1977**, 18, 681.

(47) Chalmers, J. M.; Edwards, H. G. M.; Lees, J. S.; Long, D. A.; Mackenzie, M. W.; Willis, H. A. *Journal of Raman Spectroscopy* **1991**, 22, 613.

(48) Zerbi, G.; Gussoni, M.; Ciampelli, F. *Spectrochimica Acta* **1967**, 23A, 301.

(49) Zerbi, G.; Piseri, L. *The Journal of Chemical Physics* **1968**, 49, 3840.

(50) Snyder, R. G. *J. Chem. Soc. Faraday Trans* **1992**, 88, 1823.

(51) Cates, D. A.; Strauss, H. L.; Snyder, R. G. *J. Phys. Chem.* **1994**, 98, 4482.

(52) Tao, H. J.; MacKnight, W. J.; Gagnon, K. D.; Lenz, R. W.; Hsu, S. L. *Macromolecules* **1995**, 28, 2016.

(53) Yang, X.; Su, Z.; Wu, D.; Hsu, S. L.; Stidham, H. D. *Macromolecules* **1997**, 30, 3796.

(54) Yoon, S.; Ichikawa, K.; Macknight, W. J.; Hsu, S. L. *Macromolecules* **1995**, 28, 4278.

(55) Hallmark, V. M.; Bohan, S. P.; Strauss, H. L.; Snyder, R. G. *Macromolecules* **1991**, 24, 4025.

(56) Hahn, T. D.; Stidham, H. D.; Hsu, S. L. *Macromolecules* **1997**, 30, 87.

(57) Adamson, A. W. *Physical Chemistry of Surfaces*; John Wiley & Sons, Inc.: New York, 1990, p 75 ff.

(58) Fox, H. W.; Taylor, P. W.; Zisman, W. A. *Industrial and Engineering Chemistry* **1947**, 1401.

(59) Garrett, W. D.; Zisman, W. A. *J. Phys. Chem.* **1970**, 70, 1796.

(60) Granick, S.; Clarson, S. J.; Formoy, T. R.; Semlyen, J. A. *Polymer* **1985**, 26, 925.

(61) Noll, W.; Steinbach, H.; Sucker, C. *Journal of Polymer Science: Part C* **1971**, 34, 123.

(62) Lee, L. T.; Mann, E. K.; Langevin, D.; Farnoux, B. *Langmuir* **1991**, 7, 3076.

(63) Lee, L. T.; Langevin, D.; Mann, E. K.; Farnoux, B. *Physica B* **1994**, 198, 83.

(64) Mann, E. K.; Langevin, D. *Langmuir* **1991**, 7, 1112.

(65) Mann, E. K.; Henon, S.; Langevin, D.; Meunier, J. *J. Phys. II, France* **1992**, 2, 1683.

(66) Mann, E. K.; Langevin, D.; Henon, S.; Meunier, J.; Lee, L. T. *Ber. Bunsenges. Phys. Chem.* **1994**, 98, 519.

(67) Ren, Y.; Shoichet, M. S.; McCarthy, T. J.; Stidham, H. D.; Hsu, S. L. *Macromolecules* **1995**, 28, 358.

(68) Baret, J. F. In *Progress in Surface and Membrane Science*; D. A. Cadenhead and J. F. Danielli, Ed.; Academic Press: New York, 1981; Vol. 14; pp 291.

(69) Chen, H.; Hsu, S. L.; Tirrell, D. A.; Stidham, H. D. *Langmuir* **1997**, 13, 4775.

(70) Weis, R. M. *Chemistry and Physics of Lipids* **1991**, 57, 227.

(71) Mohwald, H. *Annual Review of Physical Chemistry* **1990**, 41, 441.

(72) McConnell, H. M. *Annual Review of Physical Chemistry* **1991**, 42, 171.

CHAPTER 2

CONFIGURATIONAL DEFECTS TRANSFORMING SYNDIOTACTIC POLYPROPYLENE MICROSTRUCTURE

2.1 Introduction

Since the 1960s, scientists have been interested in characterizing the effects of polypropylene configuration on its structure and properties.[1-3] The earliest methods used to characterize the configuration exploited the infrared spectrum of the mainly syndiotactic polymer to measure a "syndiotacticity index".[1-3] The infrared bands used to calculate the syndiotacticity index were called ordering bands because they were sensitive to degree of ordering.[3]. If the thermal histories of all samples were matched, it was assumed that the degree of ordering, and therefore the measured syndiotacticity index, corresponded to the configuration. However, crystallinity depends on both the defect population and the defect distribution, as was recently illustrated for isotactic polypropylene.[4,5] For syndiotactic polypropylene, this effect can also be expected to influence both the degree of ordering and the syndiotacticity index. Since these early studies, it has become possible to characterize the configuration and configuration distribution with ^{13}C NMR.[6] However, the technique requires substantial sample preparation and long use times in the spectrometer to obtain sufficient signal-to-noise for analysis. Conformational analysis with ^{13}C NMR has also been done with the syndiotactic polypropylene amorphous phase.[7] However, the amorphous conformational features could not be completely separated from the crystalline features, except at high temperatures. A faster spectroscopic method would be beneficial to scientists interested in characterizing the configuration. In addition, characterizing changes in the amorphous phase conformation distribution would be beneficial in order to understand the phase transformations that occur. As Masetti, et al. pointed out, the skeletal bending modes in the low frequency Raman spectra of polypropylenes may give sufficient

differentiation between racemic (syndiotactic) and meso (isotactic) sequences to characterize the configuration.[8] They pointed out that the band around 400 cm^{-1} in isotactic polypropylene was observed both in the melt and in the solid, and likewise the band around 300 cm^{-1} in syndiotactic polypropylene was present both in the melt and in the solid. Furthermore, they indicated that these bands may be persistent due to presence of trapped in helical structure in the molten state. In order to test the possibility that the Raman spectrum can be used to characterize the configuration, and in order to understand the underlying microstructure associated with it, the Raman spectra of a range of syndiotactic polypropylenes were characterized. In what follows, the method for characterizing the microstructure is developed.

2.1.1 Crystal Structures of Syndiotactic Polypropylene

The possible crystal structures of syndiotactic polypropylene are given in Table 2.1. The first studies of the crystalline structure were done by Natta et al.[9,10] They found form I to be the most common conformation,[9] and they observed form II by quenching the polymer from the melt into ice water and stretching the sample.[10] With metallocene catalyst development,[11] synthesis of highly syndiotactic polypropylene with fewer defects and better control of the defect distribution became possible. The result of fewer defects is improved physical properties which has sparked recent interest in studying the structure of the polymer. The conformations of form I and form II were recently confirmed and refined.[12-21] In addition, a third crystalline state , form III, has been suggested which appears to have the conformation $(g_2t_2g_2t_6)_n$.[22-24] Among the refinements of the helical structure was the determination of observable antichiral packing. Furthermore, high temperature crystallization and annealing appears to yield antichiral packing in both the a and b cell directions, doubling the b unit cell dimensions.[18,25] The antichiral packing in the

b- direction was directly observed with atomic force microscopy.[19] By further study of the form II crystal structure, Chatani et al. observed two parallel chains per unit cell.[21]

Table 2.1 Published Crystal Structures for Syndiotactic Polypropylenes.

Conformation	Cell type	a(nm)	b(nm)	c(nm)	References
Helical $(ttgg)_2$ form I	$C222_1$	1.45	0.56	0.74	Natta et al.[9]
Helical $(ttgg)_2$ form I	antichiral in a direction	1.45	0.56	0.74	Lotz et al.[25]
Helical $(ttgg)_2$ form I	antichiral in a and b directions	1.45	1.12	0.74	Lovinger et al.[17]
Zigzag $(tt)_2$ form II	2 parallel chains per cell	0.522	1.117	0.506	Chatani, et al.[21]
$g_2t_2g_2t_6$ form III	triclinic P1	0.572	0.764	1.160	Chatani, et al.[22]

The preferred structure and conformation depends on the processing conditions. For example, the most common method to obtain the zigzag structure is to quench from melt into ice-water, and cold draw the sample. However, it was recently found that the planar zigzag structure forms spontaneously over an extended length of time by quenching from melt into ice water, and storing at or below 0 °C.[26,27] Form III has been observed, if a drawn sample of form II is exposed to benzene, toluene, or xylene vapor,[22] or a drawn sample is soaked in toluene for two days.[23] Both forms II and III are stable at room temperature, and revert to form I spontaneously with heating.

2.1.2 Amorphous Structures of Syndiotactic Polypropylene

Polypropylene conformation is determined by the configuration. As described above, syndiotactic polypropylene in the ordered state is found in one of three conformations. All of the ordered conformations contain the sequence $(ggtt)_n$, or $(tttt)_n$, or both. Likewise, the conformational sequences (gg) and (tt) represent local minimum energy positions in an energy contour.[28-30] In contrast, isotactic polypropylene ordered structures form a 3_1 helix with the sequence $(gt)_n$. Likewise, it is expected that the energy contour for isotactic sequence contains an energy minimum for the conformation sequence (gt).

Several studies have been done to characterize the conformational energy of syndiotactic polypropylene.[28-30] In all the studies described below, the energy contour for the bond centered on the methylene carbon were done. The contours for these studies are essentially the same, giving the low energy minima around the gg pair and the tt pair, with high energy local minima such as those described by Yang, et al. around (135°, 60°) and (180°, 90°) and their complements.[30] The energy difference between the high energy minima and the gg and tt minima are in the vicinity of 2 kcal/ mol or more,[29,30] and the barrier heights have been projected to be anywhere from about 2.5 kcal/mol[30] to around 5 kcal/mol.[29] Of these studies, only Suter and Flory[29] distinguish the energy of the gg pair from the tt pair (calculate gg as 300 cal/mol higher). Such energy differences will impact the amorphous conformation distribution observed. Details of amorphous conformation distribution determination are given in a later section.

2.2 Instrumentation and Methods

It has been shown that the skeletal bending modes in the low frequency Raman spectrum of polymers is particularly sensitive to the chain conformation.[31-37] For

example, Snyder, et al. showed that, for liquid alkanes, the conformation had a significant impact on both the vibrational frequency and the intensity of low frequency bands.[31,32] As will be shown below, syndiotactic and isotactic polypropylene have markedly different conformation distributions. This difference is expected to be manifest in the low frequency Raman spectrum, shown in Figure 1.2b. Likewise, a similar effect is observed for the crystalline conformers of the two isomers.[8] Furthermore, configurational defects, which perturb the amorphous conformation distribution are expected to have a significant impact on the frequency and intensity of the vibrational bands. Therefore, the procedure developed by Snyder, et al. is used here to develop a relationship between the configuration, conformation, and the Raman spectrum for mainly syndiotactic polypropylene. The details of the method are described below.

2.2.1 Raman Spectroscopy Theory

A vibrational mode is Raman active if the transition associated with the mode results in a change in polarizability of the molecule. If so, the exciting laser induces a dipole moment change associated with the polarizability change. The change in polarizability can be represented by an ellipsoid with the principal axes at some angle to the laboratory axes. The resultant, Raman-shifted emission will have a polarization which is related to the incident polarization and the orientation and shape of the ellipsoid associated with the change in polarizability (Figure 2.1).[38] The incident electric vector projects onto the principal axes of the differential polarizability of the mode. The projected intensity is absorbed and re-emitted with new frequency and new polarization related to the principal axes of the mode, and can be observed as a projection on the laboratory axes. If an analyzer is used to select the polarization that is collected, it is possible to obtain information about the symmetry of the mode. For example, if a mode is spherically symmetric, or isotropic, it is always possible to define the principal axes parallel to the laboratory axes, so that only scattered intensity with the same polarization as the incident

light will be observed. However, if the mode is not spherically symmetric, a portion of the scattered intensity will be polarized perpendicular to the incident intensity. For the scattering geometry shown in Figure 2.1, the degree of anisotropy is generally described by the depolarization ratio ρ:[39]

$$\rho = \frac{I_{\perp}}{I_{\parallel}} = \frac{\alpha'^{2}_{zy}}{\alpha'^{2}_{zz}} \qquad (1)$$

where α'_{ij} represents each element of the differential polarizability tensor, and is given by

$$I_{\parallel} \sim \alpha'^{2}_{zz} = \frac{45\alpha^2 + 4\beta^2}{45}, \qquad (2)$$

and

$$I_{\perp} \sim \alpha'^{2}_{zy} = \frac{\beta^2}{15}, \qquad (3)$$

where α and β represent the isotropic and anisotropic parts of the differential polarizability, respectively:

$$\alpha = \frac{1}{3}(\alpha'_1 + \alpha'_2 + \alpha'_3) = \frac{1}{3}(\alpha'_{xx} + \alpha'_{yy} + \alpha'_{zz}),$$

and (4)

$$\beta^2 = \frac{1}{2}\left[(\alpha'_1 - \alpha'_2)^2 + (\alpha'_1 - \alpha'_3)^2 + (\alpha'_3 - \alpha'_2)^2\right]$$

with (1,2,3) representing the principal axes of the polarizability derivative.[38] If a mode is completely isotropic, $\beta = 0$, and therefore ρ=0. If a vibrational mode is completely anisotropic, α=0, and the depolarization ratio becomes ρ=3/4. This relationship is illustrated by the Raman spectrum of carbon tetrachloride (CCl_4), shown in Figure 2.2. The peak near 460 cm^{-1} is totally symmetric, and therefore has a depolarization ratio of zero. On the other hand, the bands near 316 and 219 cm^{-1} are completely anisotropic and have depolarization ratios of 3/4. As will be seen in section 2.3, the intensity

parametrization method developed by Snyder uses the isotropic part of part of the Raman spectrum $I(iso) \sim \alpha^2$. From equations 2 and 3 it is possible to eliminate the anisotropic component of the spectrum to obtain the purely isotropic part:

$$I(iso) = I_{\parallel} - \frac{4}{3} I_{\perp} \sim \alpha^2 = [\frac{1}{3}(\alpha_1' + \alpha_2' + \alpha_3')]^2 \qquad (5)$$

This is illustrated in Figure 2.2 where the anisotropic part of the Raman spectrum of CCl_4 is subtracted. Since $\rho=0$ for the 460 cm^{-1} band, it remains in the isotropic Raman spectrum. However, for the bands at 316 and 219 cm^{-1}, $\rho=\frac{3}{4}$, and therefore they show no significant intensity in the isotropic Raman spectrum.

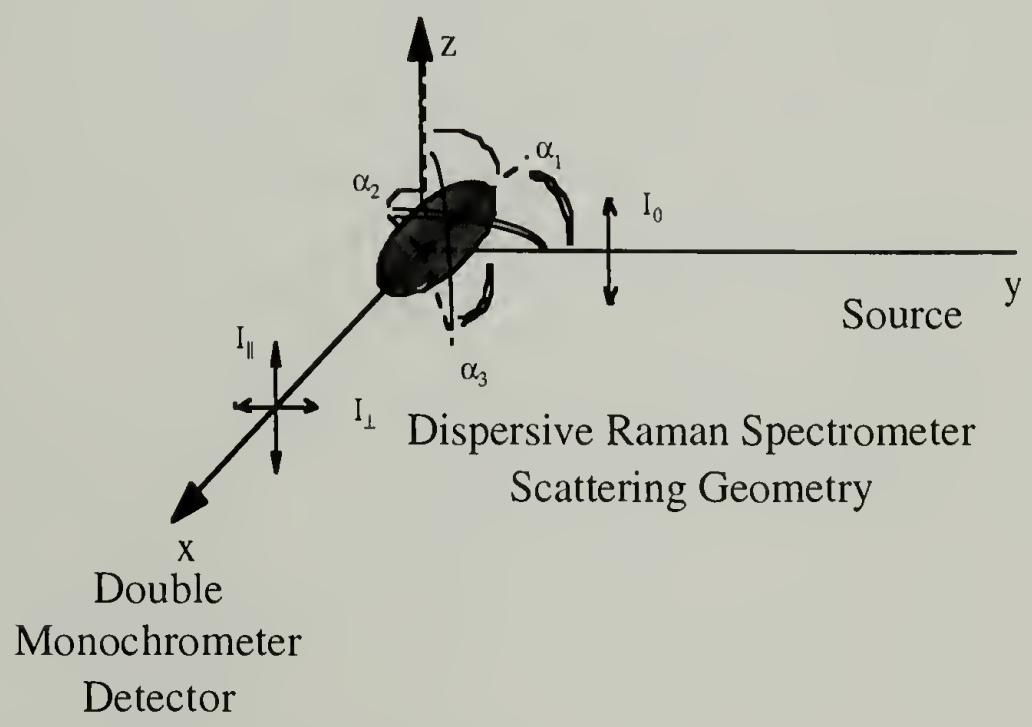

Figure 2.1 Scattering geometry schematic.

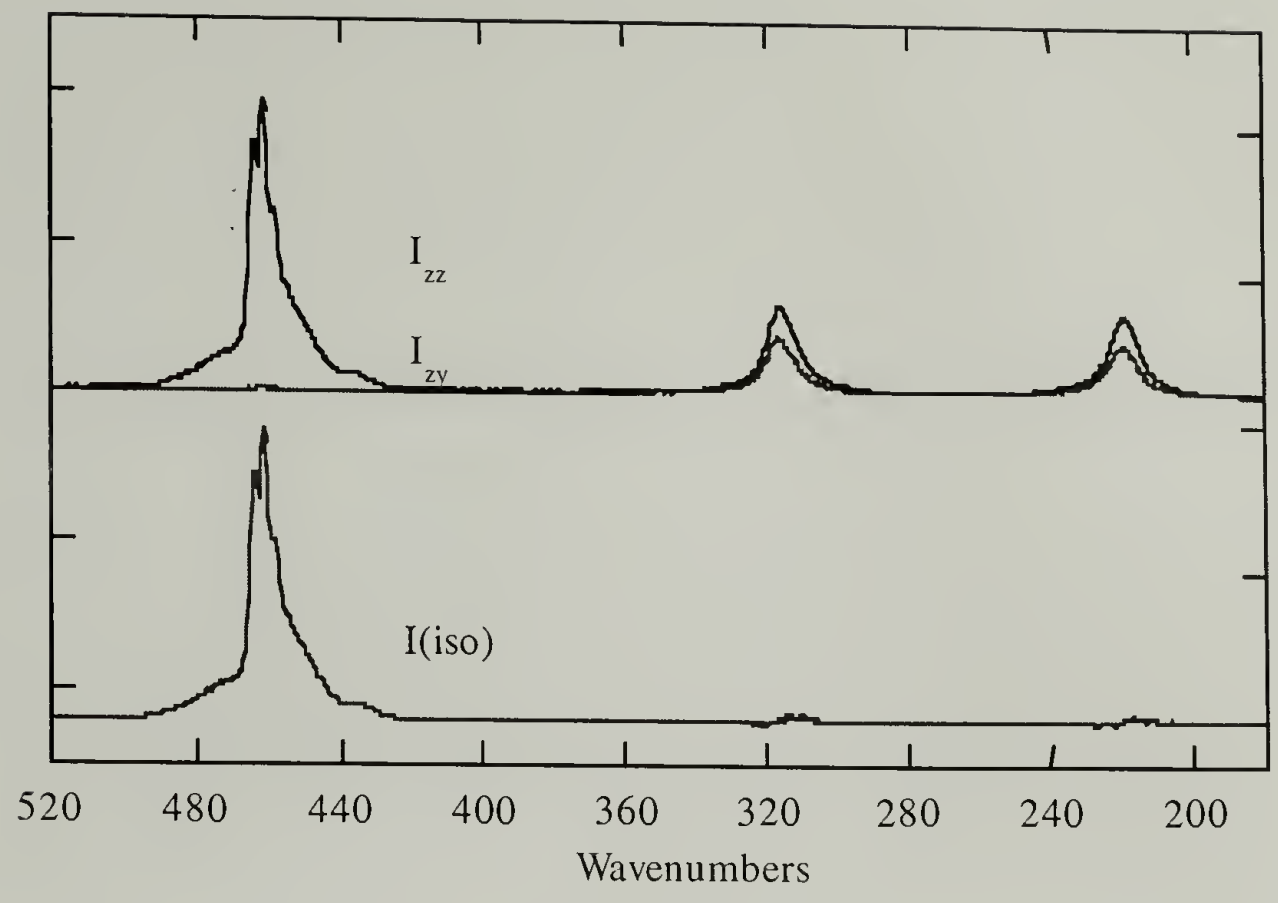

Figure 2.2 Polarized and isotropic Raman spectra of CCl_4.

2.2.2 Instrumentation

As mentioned above, quantitative description of the Raman spectrum has been possible when the isotropic component of the spectrum is measured. This is possible by subtracting out the portion of the scattered intensity that is not spherically symmetric, as illustrated by equation 4, leaving the isotropic scattering intensity. To obtain these features for the melt, the Raman spectra were obtained using a dispersive Raman spectrometer in our laboratory that has the capability to select the scattered intensity polarization with a polarizing analyzer. All Raman melt spectra were excited with 100 mW of the 514.5 nm line produced by a Spectra-Physics 165-08 Ar^+ ion laser. The scattered light was collected at 90° using custom optics to focus the scattered light through a polarization analyzer, followed by a polarization scrambler, onto a horizontal entrance slit of an Instruments SA

U-1000 double monochrometer operated at 4 cm^{-1} resolution, equipped with an RCA C31034 photomultiplier tube controlled by a Spectra Link interfaced to an IBM PC. The melt temperature was maintained by passing nitrogen gas over heating coils and through a Harney-Miller type cell containing sample stored in a capillary tube.

Raman spectra of solid isotactic and syndiotactic polypropylene samples, and samples with high populations of meso defects, were obtained using a Fourier transform Raman spectrometer produced by Bruker (model FRA 106). This is advantageous for the aging experiments because large numbers of spectra can be rapidly measured over time, with a higher level of signal-to-noise compared to the dispersive Raman spectrometer.

2.3 Simulating the Raman Spectrum

As a means to characterize microstructure, the isotropic Raman spectra for both the ordered and disordered states are calculated. To calculate the spectra, four different parts are needed. First, a model molecule of sufficient length is needed to adequately represent the polymer. Second, a suitable vibrational force field is needed to execute the normal coordinate analysis and obtain the characteristic frequencies. Third, intensity parameters need to established. Fourth, Monte Carlo simulation of an ensemble of disordered chains is necessary to generate a conformation distribution that is representative of the disordered state.

The model structures used are of the type:

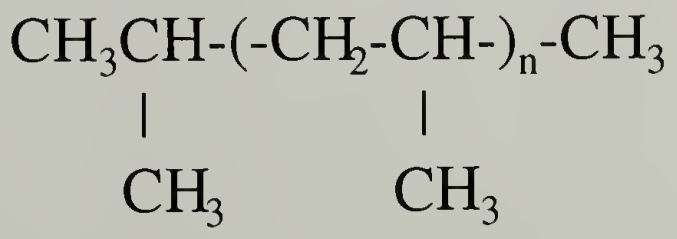

The primary model used was for n=8, named 2,4,6,8,10,12,14,16,18-nonamethylnonadecane, NMN. A skeletal model of NMN was

first used by Hallmark, et al.[34] for isotactic polypropylene using a skeletal force field, which has no explicit hydrogens. The suitability and weakness of the model structure need to be addressed. Of particular concern is the finite length of the model structure for simulation of ordered chains. Therefore, chain length dependence of the calculated spectra needs to be addressed where possible. The force fields for isotactic and syndiotactic polypropylenes used here were published in the 1960's by Snyder[40] and Schachtschneider,[41] and have since been confirmed as suitable force fields.[42]

2.3.1 Normal Coordinate Analysis

Normal coordinate analysis is based on the realization that an isolated molecule has 3N-6 (3N-5 for a linear molecule) vibrational modes, where N represents the number of atoms. These vibrational modes arrive from the coupling of all the oscillators (C-C and C-H stretching, C-C-C, C-C-H and H-C-H bending, and C-C backbone and side methyl torsions) due to their connectivity. If the harmonic oscillator approximation is used, and the force constants for the stretching, bending, torsion, etc., and their interactions are adequately determined, it is possible to calculate the normal modes for any molecule. This is done by solving the 3N simultaneous equations of motion.[43]

$$\frac{d}{dt}\left(\frac{\partial T}{\partial \dot{x}_i}\right)+\frac{\partial V}{\partial x_i}=0 \qquad (6)$$

where T is the kinetic energy, V is the potential energy, t represents time, x_i represents the position of the i^{th} mass, and $\dot{x}_i$ represents the time derivative of x_i. Diagonalization of the matrix representation of these equations gives the normal vibrational modes. The transformation matrix that diagonalizes the equations of motion is then the set of eigenvectors which describes the displacements of all the atoms in the molecule.[38]

Recently, it has been shown that these eigenvectors can be used to calculate isotropic Raman scattering intensities below ~1000 cm^{-1} by individual contributions of the

skeletal components of the modes.[31,32,44] The isotropic scattering activity for mode k can be represented as:

$$S_k(iso) \sim (\sum_i d_i L_{ik})^2 \qquad (7)$$

where L_{ik} represents the internal coordinate displacement amplitude of component **i** for eigenvector $\mathbf{L_k}$, and d_i represents the mean polarizability derivative for internal coordinate **i**. The summation in $\sum_i d_i L_{ik}$ in equation 7 is a representation of the polarizability derivative, described in terms of the internal coordinates. Therefore, it can be decomposed into the principal axis components, which makes it the same functional form as equation 5, which is used to measure the isotropic Raman intensity experimentally. The skeletal components of interest below 1000 cm^{-1} were established for n-alkanes to be C-C stretch, and C-C-C angle bending internal coordinates.[33] These terms were subsequently applied to isotactic polypropylene.[34] The components of the same type, such as C-C stretches, were assumed to give approximately the same contribution to the polarizability derivative for a given unit displacement.[44] While this assumption limits the accuracy of the intensity calculations,[31] it has the benefit of being generalizable between bonds along the chain for different conformations, with a relatively small effect on the calculations. A more specific relationship for either isotactic or syndiotactic polypropylene is:

$$S_k(iso) \sim (D_R \sum_i L_{ik}^R + D_S \sum_j L_{jk}^S + D_\omega \sum_m L_{mk}^\omega + D_\zeta \sum_n L_{nk}^\zeta)^2 \qquad (8)$$

where the elements of the eigenvector matrix, L_{ik}^R and L_{mk}^ω represent the backbone C-C stretch and C-C-C angle bending components, and L_{jk}^S and L_{nk}^ζ represent the C-C stretch and C-C-C angle bending components containing the methyl side groups for the normal

mode k. The coefficients D represent the relative contribution of the four types of internal coordinates for a unit amplitude of the respective internal coordinate displacements to the total intensity. Hallmark, et. al.[34] did not differentiate between backbone and side group intensity contributions in their isotactic polypropylene calculations, giving $D_R = D_S = 1.0$, and $D_\omega = D_\zeta = D$ (~0.3). Generally, the highly polarized, or highly isotropic, modes tend to dominate the Raman intensity.[44] As a result the isotropic calculations can be used to approximate solid spectra in which the anisotropic components are not subtracted, as long as care is taken to differentiate the anisotropic from the isotropic components. For amorphous phase features, this correction is not necessary. Since the amorphous features are a composite of many conformational spectra, the approximation that the isotropic components dominate the features becomes more reliable. In this work, both meso (isotactic), and racemic (syndiotactic) structures, as well as mixtures of the two are modeled. In an effort to parametrize both the isotactic and the syndiotactic polymers, the side groups were parametrized to best fit the experimental data. For the isotactic structures, the parameters of Hallmark et al. best fit the observations, while the syndiotactic intensity values are also the same, with the exception of the side group C-C-C angle bending intensity parameter where values of D between 0 and 0.1 best fit the observed intensities of the isotropic bands.

2.3.2 Monte Carlo Simulation of an Ensemble of Chains

Amorphous conformation distribution for polypropylene, like other polymers, is generally calculated using the rotational isomeric state model to calculate the characteristic ratio $C_\infty = \frac{\langle R^2 \rangle_o}{Nl^2}$, and its temperature dependence. The calculated temperature dependence is compared to the radius of gyration and characteristic ratio determined by methods such as light scattering and neutron scattering. For vinyl polymers, such as

polypropylene, two typical types of rotational isomeric state models are the three-state and five-state models. The three-state model (Figure 2.3) assumes that the bonds can occupy three distinct conformations (trans, gauche, and gauche' - t, g, g').[45] These torsions are assumed to be near 180, and ±60°. The relative energies of these torsions depend on the conformations of the adjacent bonds. Deviations from the butane-like model come from accounting for second-order interactions. The original three-state model parameters of Flory et al.[45] agree with the gg sequence being higher energy than the tt pair. The estimated value of E_{gg}-E_{tt}, based on Table 2.2, gives a value around 450 cal/mol, which is greater than the energy difference based on the conformational energy mapping of Suter and Flory.[29] Calculating the gg conformation pair as higher energy than the tt suggests that the presence of the tt sequence becomes more enhanced relative to the gg sequence as the temperature decreases. This change in conformantion distribution can be characterized by the Raman spectrum of the amorphous phase.[31]

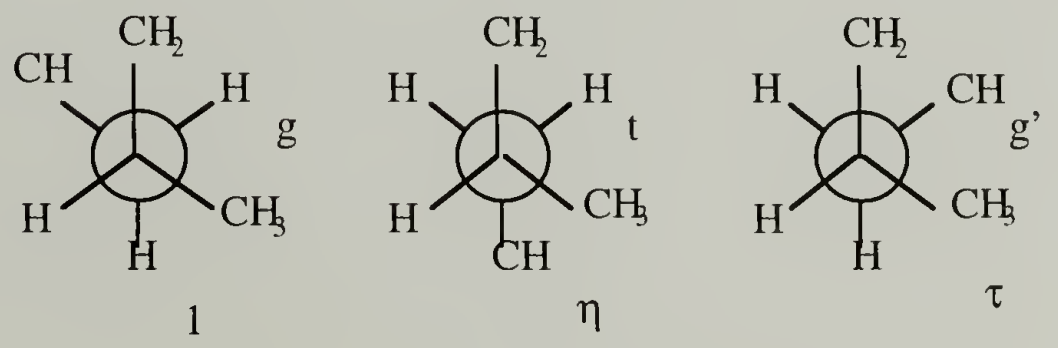

Figure 2.3 Three-state model for polypropylene.

The two stereoisomers have entirely different amorphous conformation distributions, also shown in Table 2.2, derived from the three-state model of Flory et al.[45] The conformation distributions were derived based on the variation of the characteristic ratio, observed by light scattering, with change in the chemical configuration.[45]. While the light scattering technique is sensitive to changes on the length of scale of the molecular

volume, which is influenced by the conformation distribution, it does not directly observe the local conformations (on the size order of angstroms) that are presumed to exhibit the characteristic ratio.

Table 2.2 Temperature and Configuration Dependent Amorphous Phase Conformation Distributions Based on the Flory Three-State RIS Model.[45]

p*	RT SPP 2 bonds	Melt SPP 2 bonds	RT IPP 2 bonds	Melt IPP 2 bonds
tt	0.658	0.562	0.033	0.068
tg+g't	0.014	0.065	0.033	0.084
tg'+gt	0.018	0.058	0.919	0.782
gg			0.005	0.020
gg'			0.004	0.022
g'g			0.000	0.003
gg'+g'g	0.015	0.055		
g'g'	0.295	0.261	0.005	0.020

*Differences in probabilities of low population conformers can be mostly accounted for by temperature differences of melt (~500 K) and solid (~300 K). For high population conformers, differences can be attributed to change in probability of low population conformers with changes in temperature.

The five state model[29] assumes five possible backbone torsions, t, t*, g*, g, g' which have torsion angles around 165, 130, 110, 75, and -65°. The five state model is claimed to be the more accurate model for representing the relative energies and population of the conformations, because it comes from a conformational analysis of the energies for the sequence **-($CH_2CH(CH_3)$)$_2CH_2$-**.[29] However, for the isotactic and atactic polymer, C_∞ has been accurately calculated using the three state model with suitable parametrization.[46] The three state model has been applied to ethylene-propylene copolymers because it is appropriate for the ethylene sequences.[47] The three state model

was also applied to the spectral calculations described below, because the vibrational force field parameters used were specifically optimized for the three backbone torsions that are associated with the three state model.

To apply these conformational state models to building chains with chiral centers, each center must be specified in its d-form or l-form (Figure 2.4), based on the conventions of Mattice and Suter.[47] For an isotactic polymer, all the side groups are on the same side of the chain. Each side group pair can then be described as part of a meso dyad. In the d-form, the appropriate statistical weight matrices are

$$U_d' = \begin{pmatrix} \eta & 1 & \tau \\ \eta & 1 & \tau\omega \\ \eta & \omega & \tau \end{pmatrix}, \text{ and } U_{dd}'' = \begin{pmatrix} \eta\omega'' & \tau\omega' & 1 \\ \eta & \tau\omega' & \omega \\ \eta\omega' & \tau\omega\omega'' & \omega' \end{pmatrix} \qquad (5)$$

where η and τ represent first order steric interactions (atoms separated by three bonds) dependent only on one bond rotation, and ω, ω', and ω'' represent second-order steric interactions (atoms separated by four bonds). η represents the Boltzmann factor for trans state, $\exp(-E_\eta/kT)$ with the methyl side group 60° to the backbone, and τ represents the Boltzmann factor for the gauche state with both the methyl side group and the backbone carbon at 60° to the backbone three bonds away. The second order interactions can be described as the pentane effect, which is the interaction of two atoms separated by four bonds. ω represents the second order interaction of two backbone carbons, ω' represents the interaction of a backbone carbon with a side methyl, and ω'' represents the interaction between two side methyls.

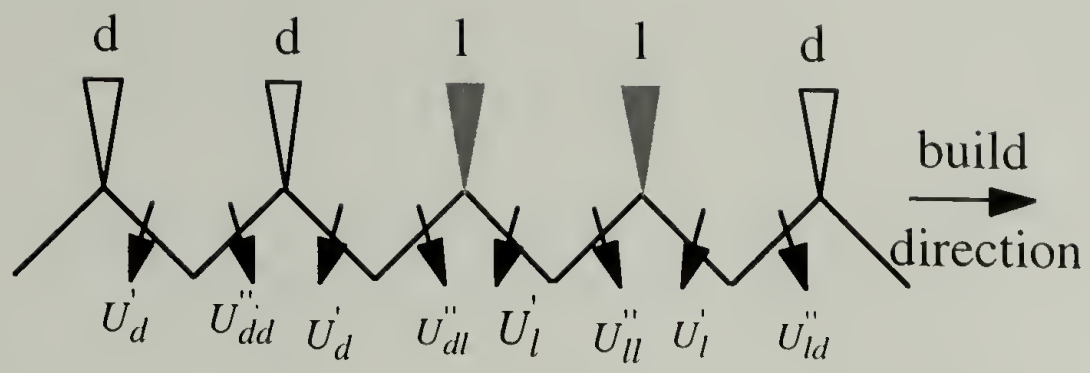

Figure 2.4. Illustration of both the d-form and l-form for a polypropylene stereochemical sequence, and the statistical weight matrices used to represent each bond conformation.

The l-form of the statistical weight matrices for the meso pair is:

$$U'_l = QU'_dQ, \text{ and } U''_{ll} = QU''_{dd}Q \tag{6}$$

where Q is the matrix transformation:

$$Q = \begin{pmatrix} 1 & 0 & 0 \\ 0 & 0 & 1 \\ 0 & 1 & 0 \end{pmatrix} \tag{7}$$

which has the property $QQ = I_3$, and I_3 is the unit diagonal matrix. For a racemic sequence, as shown in Figure 2.4, the following statistical weight matrix is also needed:

$$U''_{dl} = \begin{pmatrix} \eta & \omega' & \tau\omega'' \\ \eta\omega' & 1 & \tau\omega \\ \eta\omega' & \omega & 0 \end{pmatrix} \tag{8}$$

and $U''_{ld} = QU''_{dl}Q$.

The chain conformation partition function for a meso (isotactic) chain is represented by

$$Z_m = J^*\left(U_d^{'}U_{dd}^{''}\right)^{(n-2)/2} J = J^*\left(U_l^{'}U_{ll}^{''}\right)^{(n-2)/2} J \qquad (9)$$

where $J^* = [1 \quad 0 \quad 0]$, and $J = \begin{bmatrix} 1 \\ 1 \\ 1 \end{bmatrix}$. For the racemic chain, the partition function statistical weight matrix sequence is $U_d^{'}U_{dl}^{''}U_l^{'}U_{ld}^{''}$.[48]

In order to simulate the random chains, it is necessary to derive conditional probability matrices for each backbone conformer. Each element of the conditional probability matrix is obtained by the operation:

$$q_{lm} = \frac{J^*\left(\prod_{i=2}^{j-1} U_i\right)\tilde{U}_j \prod_{k=j+1}^{n-1} U_k J}{Z} \qquad (10)$$

where $\tilde{U}_j$ is obtained by replacing all the elements of the statistical weight matrix U_j in the partition function Z with zero, except for element u_{lm}, which remains unchanged. The various conformers along the chain are then randomly selected by weighting each random choice by the conditional probability calculated. Once the random chains are constructed, the Raman spectrum of each chain is calculated, and all are summed to obtain the total amorphous spectrum.

2.4 Spectroscopic Characterization of Polypropylene Configuration and Conformation Distribution

2.4.1 Materials

Analysis of the spectroscopic properties relating to configuration and conformation for syndiotactic polypropylene used a series of six samples. A 92 % racemic syndiotactic polypropylene was generously donated from Fina Oil Corporation. Isotactic polypropylene

was purchased from Scientific Polymer Products, Inc., Ontario, NY. Four different samples were synthesized by Dr. Alan Seidle of 3M Corporation. They are given the following designations:

One approximately 75% racemic dyad sample - R75

(measured at 76% by ^{13}C NMR supplied with samples)

Two samples with approximately 60 % racemic dyad content - R60a, and R60b

(both measured at 62% by ^{13}C NMR supplied with samples)

One sample with approximately 50% racemic dyad content - R50

(measured at 52% by ^{13}C NMR supplied with samples)

2.4.2 Results and Discussion

The room temperature FT Raman spectra of form I and form II syndiotactic polypropylene, and solid isotactic polypropylene are shown in Figure 2.5. Overall, the features of these samples are similar. Closer inspection in specific regions shows the major spectroscopic differences associated with conformation and configuration. In Figures 2.6a and 2.6b, the spectroscopic regions of interest are shown for the six samples described above. Features characteristic of the conformational ordering, and amorphous conformation distribution are discernible. The Raman spectrum for form I syndiotactic polypropylene conformation is characterized by the bands around 826 and 870 cm^{-1}.[8,42] The broad peak centered around 845 cm^{-1} is assigned as nonhelical, or amorphous.[42] Their specific assignments are given in Table 2.3 below. As would be expected with decreasing racemic content, the ordered bands decrease in intensity relative to the amorphous peak. Furthermore, as the racemic content decreases, the peak position of the amorphous band shifts slightly to lower frequency, reflecting the changing conformation distribution as a result of the change in the configuration distribution. In the 75% racemic sample, the lower frequency helical band seems to be shifted to slightly higher frequency, around 828 cm^{-1}.

The 60% racemic dyad samples show shoulders where the ordered bands are present in the more ordered 92%, and 75% racemic samples. For the purely isotactic polymer, the major bands are around 842 and 809 cm^{-1}. In this case, the amorphous features seen in the melt spectrum in Figure 1.2a, are obscured by the 842 cm^{-1} band. As will be seen in Chapter 3, these features are sensitive to both chain configuration and conformational ordering. Conformational ordering in this region is highly sensitive to the thermal history of the samples. Rapid changes occur in quenched samples, and continue to change over many hours, and even days. Because the large changes that are the result of thermal history are confounded with the small changes that are the result of configurational differences, this region is not well suited for a quantitative analysis of the racemic content.

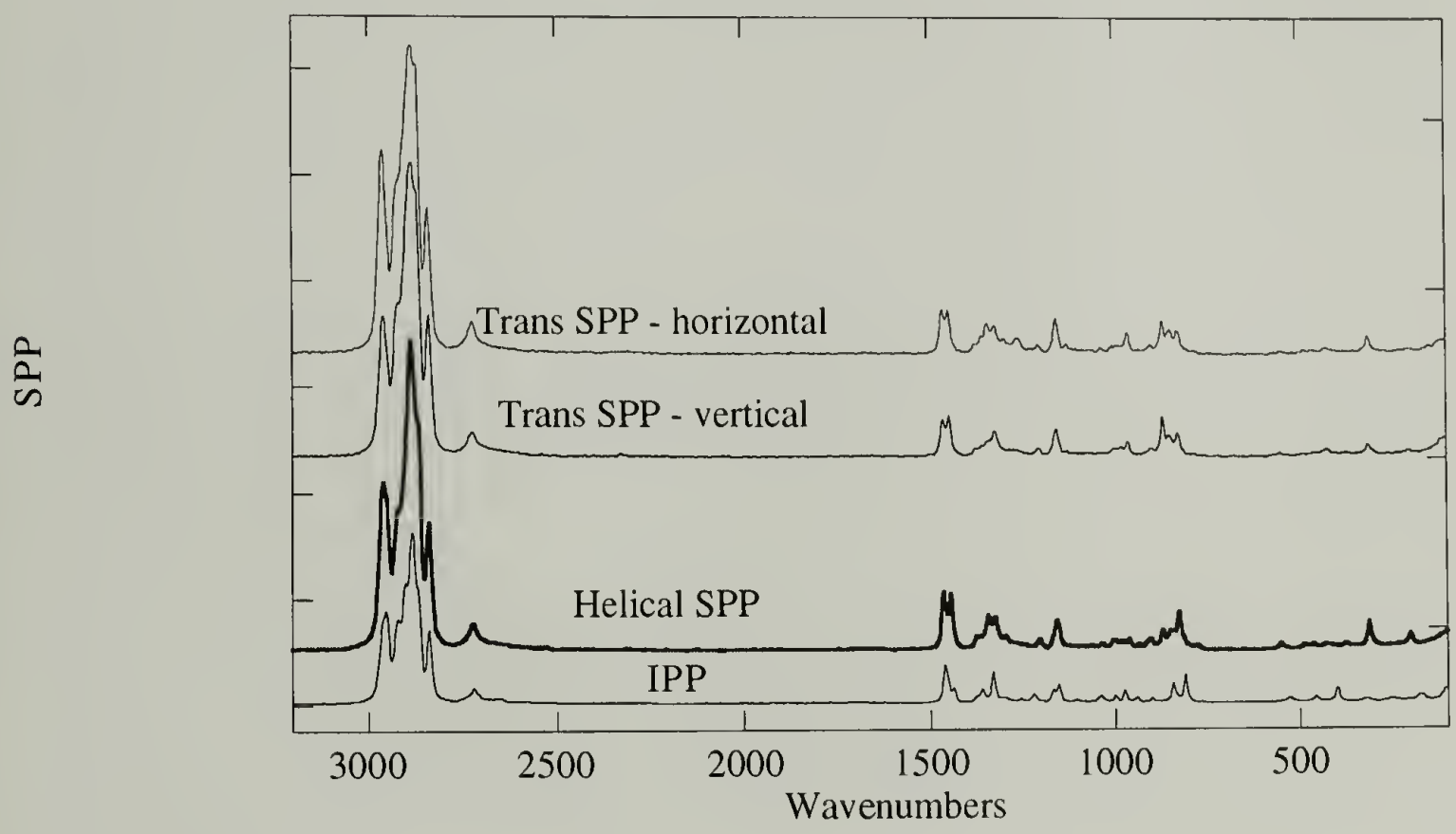

Figure 2.5 Raman spectra of solid syntiotactic and isotactic polypropylene.

Table 2.3 Calculated Assignments of Form I Syndiotactic Polypropylene.

Snyder calcn. helical	mode	P.E.D. (Snyder)	Raman Chalmers	Raman Masetti	Raman This work
2962	A	$r_a^-(91)$; $r_b^-(8)$	2962		2961
2962	A	$r_b^-(91)$; $r_a^-(8)$	2962		2961
2906	A	s(98)			
2882	A	$r^+(99)$	2873		2870
2856	A	$d_1^+(50)$; $d_2^+(50)$	2840		2841
2855	A	$d_1^+(50)$; $d_2^+(50)$	2840		2841
1463	A	$\alpha_b(77)$; $\alpha_a(7)$; $\beta_b(8)$	1466	1465	
1462	A	$\alpha_a(71)$; $\alpha_b(9)$; $\beta_a(7)$	1466	1465	
1454	A	$\delta(74)$; $\Gamma(17)$	1445	1445	1445
1452	A	$\delta(70)$; $\Gamma(15)$; α_a (8)	1445	1445	1445
1372	A	U(99)	1370?	1375	1375
1353	A	$\zeta_b(45)$; T(30); S(10)	1345	1345	1344
1339	A	$\zeta_a(48)$; T(25); R(14)	1327	1325	1325
1259	A	T(50); $\zeta_a(11)$; $\beta_a(11)$; S(10)		1242	
1191	A	T(30); $\zeta_a(14)$; S(13); $\zeta_b(7)$; $\beta_b(7)$	1204	1205	1205
1168	A	S(36); $\beta_b(18)$; $\zeta_b(14)$; $\phi(12)$	1157	1158	1157
1041	A	T(36); R(31); $\zeta_b(22)$; S(15)	1034	1035	1036
996	A	$\beta_a(38)$; T(19); $\zeta_a(18)$; $\beta_b(11)$; R(11)	1002	998	997
918	A	S(48); $\beta_b(43)$	913	912	912
839	A	S(38); $\beta_a(24)$; R(17); $\omega(14)$	828	825	826
542	A	$\omega(32)$; $\phi_a(26)$; R(8); S(8)	552	550	550
347	A	$\phi_b(33)$; $\phi^+(27)$; $\zeta^+(18)$		374	
315	A	$\phi_b(22)$; $\phi^+(10)$; S(29); $\omega(10)$		312	313
199	A	$\tau(84)$; $\phi_b(8)$		200	200
176	A	$\omega(44)$; $\phi_b(27)$; $\tau(14)$			
66	A	$\phi_a(44)$; $\tau(29)$		62	

Continued Next Page

Table 2.3 (Continued)

Snyder calcn. helical	mode	P.E.D. (Snyder)	Raman Chalmers	Raman Masetti	Raman This work
2962	B1	r_a^-(54); r_b^-(45)			
2962	B1	r_b^-(54); r_a^-(45)			
2929	B1	d^-(96)	2922		2924
2904	B1	s(95)			
2882	B1	r^+(99)			
2855	B1	d^+(99)			
1465	B1	α_b(50); α_b(26); δ(8)		1465	1464
1462	B1	α_a(50); α_b(36)		1463-1450	
1453	B1	δ(65); α_a(14)		1432	
1380	B1	U(65); W(18); S(8)		1376	1375
1357	B1	U(36); W(24); S(13); R(13)			
1352	B1	ζ_b(56); S(15); T(14)			
1275	B1	W(40); ζ_a(37); β_b(8)		1287	
1223	B1	T(45); S(11); β_a(10)	1244	1242	
1167	B1	S(28); R(12); P(11); ϕ_a(11); ζ_a(10)		1153	
1113	B1	S(37); ζ_b(24); β_b(17); R(7)		1088	
980	B1	R(25); β_a(20); β_b(16); T(11); S(9); ζ_a(8)		1005	
971	B1	β_b(34); S(25); R(19); β_a(10)	978	978	976
903	B1	β_a(36); R(23); P(22); ζ_a(10)	903	901	904
786	B1	P(41); S(38); R(13); ω(8); ζ_b(7)	776	776	776
537	B1	ϕ_b(45); ω(20); β_b(10)		535	
403	B1	ϕ^+(40); ζ^+(27); ϕ_a(13)		429;398	
264	B1	ϕ_a(55); τ(12); τ(10); S(8)		292;260	
196	B1	τ(74); ϕ_b(13)		200	200
170	B1	ω(40); ϕ_b(29); τ(15)			
62	B1	τ(85)		102?	

Continued Next Page

Table 2.3 (Continued)

Snyder calcn.		P.E.D.	Raman	Raman	Raman
helical	mode	(Snyder)	Chalmers	Masetti	This work
2962	B2	$r_b^-(59)$; $r_a^-(39)$			
2962	B2	$r_a^-(59)$; $r_b^-(40)$			
2929	B2	$d^-(95)$	2922		2924
2904	B2	s(95)			
2882	B2	$r^+(99)$			
2855	B2	$d^+(99)$			
1464	B2	$\alpha_b(78)$; $\beta_b(8)$		1463-1450	
1461	B2	$\alpha_a(86)$; $\beta_a(8)$		1463-1450	
1454	B2	$\delta(73)$; $\Gamma(20)$			
1374	B2	$\zeta_b(34)$; S(20); W(26); T(12)		1376	1375
1372	B2	U(100)	1374	1376	1375
1331	B2	$\zeta_a(57)$; W(11); R(12)		1360	
1301	B2	W(40); T(29)		1312	
1194	B2	$\zeta_b(39)$; S(14); T(11); P(10)		1205	1205
1159	B2	S(22); $\beta_b(17)$; $\beta_a(10)$; W(10); R(10)		1153	
1115	B2	R(40); T(13); S(10); $\beta_b(10)$; $\zeta_b(10)$		1106	
1044	B2	S(30); T(22); $\beta_a(16)$; $\zeta_a(12)$; R(8)	1034	1039	1043
931	B2	$\beta_b(45)$; S(38)	933	935	937
878	B2	$\beta_a(43)$; S(30); P(21); $\zeta_a(15)$	872	871	870
825	B2	P(36); S(23); R(18); $\zeta_b(7)$		812	783
476	B2	$\phi_a(45)$; $\omega(20)$; R(11); S(10)	486	484	
433	B2	$\phi^+(37)$; $\zeta^+(25)$; $\phi_b(14)$; P(12)		462	
280	B2	$\phi_b(67)$; S(8)		292;260	
202	B2	$\tau(84)$			
171	B2	$\omega(33)$; $\phi_a(28)$; $\tau(19)$; $\tau(14)$			
58	B2	$\tau(78)$; $\phi_a(10)$; $\omega(8)$		102?	

Continued Next Page

Table 2.3 (Continued)

Snyder calcn.		P.E.D.	Raman	Raman	Raman
helical	mode	(Snyder)	Chalmers	Masetti	This work
2962	B3	$r_b^-(60); r_a^-(38)$			
2962	B3	$r_a^-(60); r_b^-(39)$			
2930	B3	$d_2^+(52); d_1^+(41)$	2922		2924
2928	B3	$d_1^+(55); d_2^+(44)$	2922		2924
2903	B3	s(93);			
2882	B3	$r^+(99)$			
1464	B3	$\alpha_b(87); \beta_b(9)$		1463-1450	
1462	B3	$\alpha_a(89); \beta_a(8)$		1463-1450	
1378	B3	U(70); W(15); S(10)	1374	1376	1375
1373	B3	W(35); S(34); $\zeta_b(30)$	1374	1376	1375
1352	B3	W(34); $\zeta_a(29)$; U(22); R(13)		1345	1344
1300	B3	W(44); $\zeta_b(27)$; $\zeta_a(7)$	1293	1296	1299
1265	B3	$\zeta_a(39)$; W(33); $\zeta_b(10)$		1263	
1174	B3	S(25); $\beta_b(15)$; P(14); $\zeta_b(12)$		1168	
1096	B3	S(38); W(14); $\beta_a(14)$; P(14); $\beta_b(9)$		1094	1091
1068	B3	R(57); S(17); W(11); P(8)	1061	1060	1059
974	B3	$\beta_b(53)$; S(29)	978	978	976
902	B3	$\beta_a(53)$; P(21); $\zeta_a(16)$; S(9)	903	901	904
867	B3	P(52); S(20); $\zeta_b(10)$		871	870
829	B3	P(43); R(35); S(11)			
436	B3	$\phi^+(46); \zeta^+(32)$; P(17)	463		
410	B3	$\phi_b(86); \phi_a(9); \beta_b(9)$		429;398	
358	B3	$\phi_a(73); \phi_b(7)$; P(8)			
200	B3	$\tau(98)$		200	200
74	B3	$\tau(88)$; P(7)			
60	B3	$\tau(86)$; P(7)		102?	
	unnasigned		2725		2725
	amorphous		966		963
	amorphous		844		845

In contrast, Figure 2.6b shows spectroscopic features that are highly sensitive to configurational defects.[8] The 92% racemic sample spectrum shows an ordered helical band centered around 313 cm^{-1}, and the isotactic polymer shows an ordered helical band around 400 cm^{-1}. Other bands in this region of form I syndiotactic and ordered isotactic polypropylene are given in Table 2.3 and 2.4, respectively. As the racemic content decreases, the relative intensity of bands in the 300 cm^{-1} region decrease while bands in the 400 cm^{-1} region increase. This suggests that the region can be used as a quantitative indicator of the configuration, as proposed by Masetti, et al.[8] In the analysis that follows, this possibility is quantitatively demonstrated. As will be seen, the spectroscopic distinction is due to the preferred ordered conformations of the samples, and the accessible amorphous conformation distributions for the amorphous regions.

Table 2.4 Vibrational Assignments for Isotactic Polypropylene.

A-mode			Assignments
Snyder(calc.)	observation	P.E.D.	Zerbi, et al.
2962	2956	r^-(100)	2960
2962		r^-(100)	2960
2928		d^-(99)	2928
2906		s(98)	
2882		r^+(98)	2882
2855	2843	d^+(99)	2839
1465		α(78)	
1462		α(87)	1460
1453	1454	δ(69); α(11)	1453
1380	1378	W(27); S(26); ζ(25); U(20)	1378
1369	1365	U(89)	1359
1348	1365	ζ(65); S(12)	
1284	1305	W(37); T(36)	1304
1242	1257	ζ(37); T(19); β(15)	1256
1170	1167	S(30); β(22)	1168
1066	1044	R(51); S(31)	1045
1004	997	β(46); ζ(19)	998
969	973	β(51); S(28)	973
853	841	P(43); R(23)	841
829	841	P(29); S(32); β(20)	809
456	456	ω(81)	456
392	398	ω(62); ζ(15)	398
267		ω(58); τ(15)	251
195		τ(88)	200
140		ω(50); τ(30)	155

Continued Next Page

Table 2.4: (Continued)

E-mode			Assignments
Snyder(calc.)	observation	P.E.D.	Zerbi, et al.
2962	2956	r^-(100)	2950
2962	2951	r^-(100)	2950
2930	2925	d^-(94)	2920
2904	2907	s(94)	
2882	2880	r^+(98)	2878
2856	2868	d^+(99)	2868
1463	1459	α(88)	
1462	1459	α(78)	1462
1454		δ(69)	1437
1377	1377	U(38); W(21); ζ(21); S(16)	1377
1367	1359	U(69); ζ(19)	1359
1352	1329	ζ(52); T(15)	1328
1292	1297	W(35); ζ(25); T(13)	1295
1201	1219	T(26); ζ(20); R(19)	1220
1155	1153	S(23); R(15); ζ(13); β(13)	1155
1121	1103	R(32); β(24); ζ(16)	1104
1024		S(30); R(18); ζ(15); T(14)	1034
940	941	β(45); R(40)	941
901	900	β(49); P(17); ζ(17)	899
817	809	R(32); P(30); S(23)	809
513	528	ω(63); R(10); P(9)	528
429	408	ω(58); ζ(29); P(17)	460
311	321	ω(74)	321
198		τ(94)	210
147		ω(77); τ(16)	169
63		τ(86)	

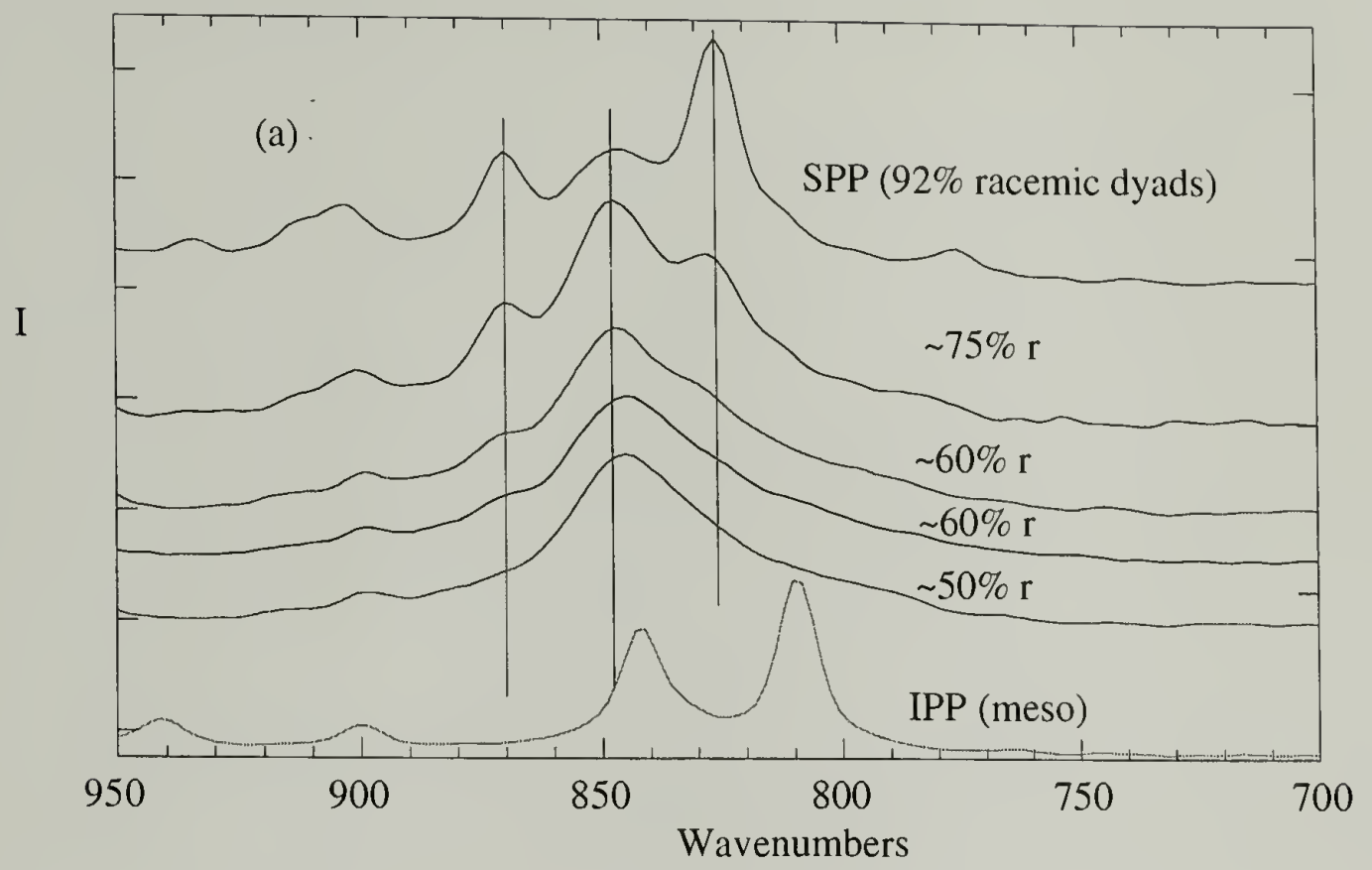

Figure 2.6 FT Raman spectra for a range of polypropylene configurations.

Distinguishing the features on the basis of ordered conformation, conformation distribution, and configuration is possible with the aide of simulation of the vibrational spectrum. This is done primarily with DCNCA, described above. The simulated spectra rely on normal coordinate analysis to calculate the vibrational frequencies, based on the force constants for small molecules with the same bonding architecture, and a bond polarizability model of only a limited number of parameters to represent the intensity. Furthermore, the calculations rely on a finite chain to represent the infinite chain geometry. As a result, some differences are to be expected. However, the main calculation features are characteristic of the experimental spectra, especially in comparison of the configurational differences described later. The population of vibrational states for the model helical structure, NMN, is plotted against the infrared and Raman spectra of the helical solid polymer in Figure 2.7. The experimentally observed frequency gaps are also observed in the population of states calculation. However, the calculated population of states is not a direct indicator of the expected intensity, either for the Raman or infrared spectrum. For the infrared spectrum, the transition moments for each mode need to be considered, and for the Raman spectrum, the change in bond polarizability associated with the vibrational modes also need to be considered. In the results that follow, comparisons of intensities of Raman spectra with simulated spectra are discussed.

Figure 2.8a compares the Fourier transform Raman spectrum of solid syndiotactic polypropylene to the ordered helical model structure of the form $(ggtt)_4$. Based on the assignments of Masetti, et al.,[8] and Chalmers, et al.,[42] and the calculations of Schachtschneider, et al.[41] only the strong band measured at 826 and a weak shoulder measured at 912 cm^{-1} should give any significant intensity in the isotropic Raman calculation. The strong 826 cm^{-1} band is calculated at 832 cm^{-1} for the NMN model structure. The absence of the calculation for the weak intensity band at 912 cm^{-1} may be due to the finite chain length of the model structure, or perhaps to its low experimental intensity. The 845 cm^{-1} band is an amorphous band which does not show up in the helical

calculation. In Figure 2.8b, the 313 cm^{-1} band is calculated at 308 cm^{-1}. This band is also an isotropic band. The weak band around 375 cm^{-1} may be calculated at 363 cm^{-1}.

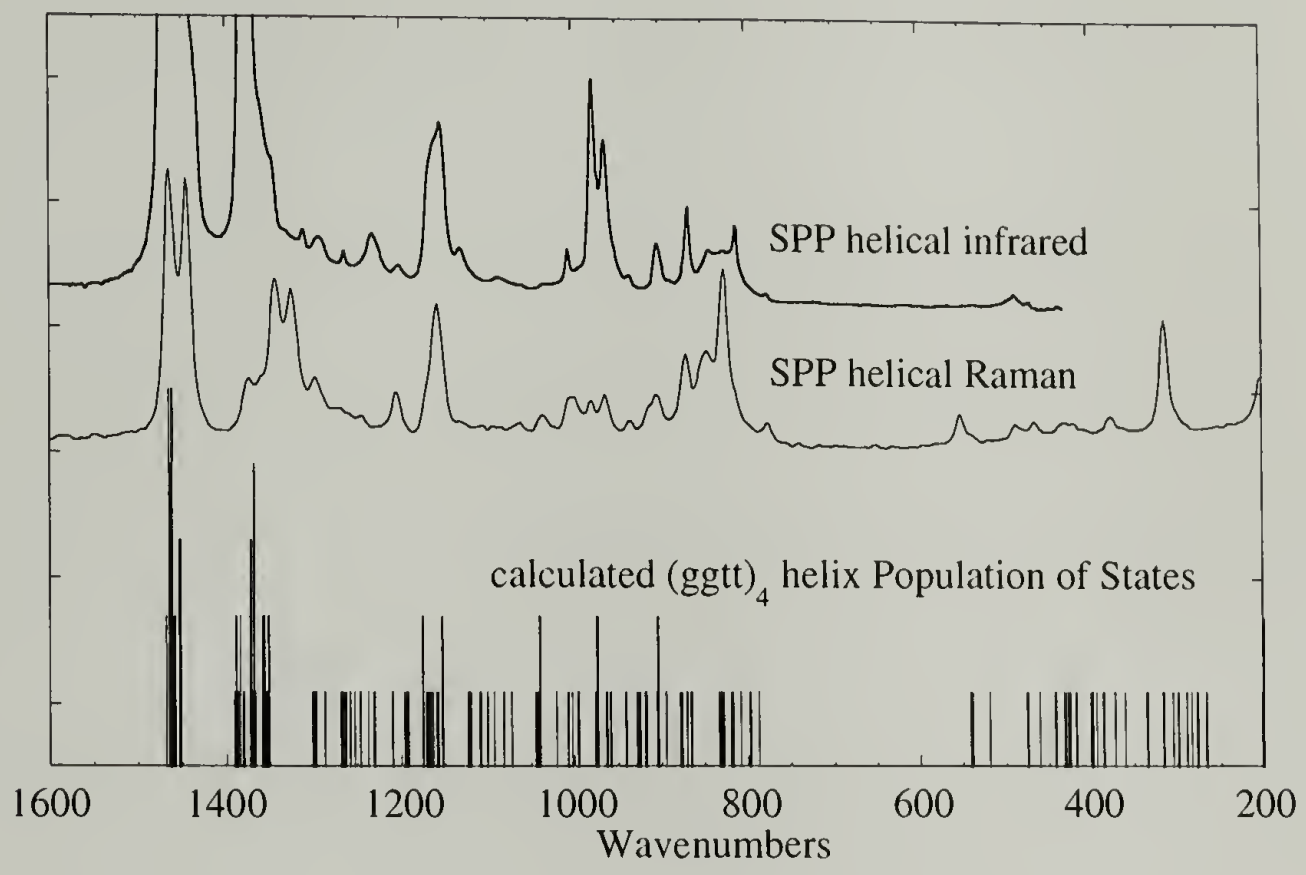

Figure 2.7 Comparison of population of states calculation with the infrared and Raman spectrum for helical syndiotactic polypropylene.

However, other weak calculated bands at higher frequencies should not be observed. It is speculated here that they show up as a consequence of the finite chain length. The conformer used, $(ggtt)_4$, is the longest number of helical turns (2) that can be simulated with the program. Nevertheless, in spite of the bands other than isotropic being calculated, the major peak for extended helical is represented.

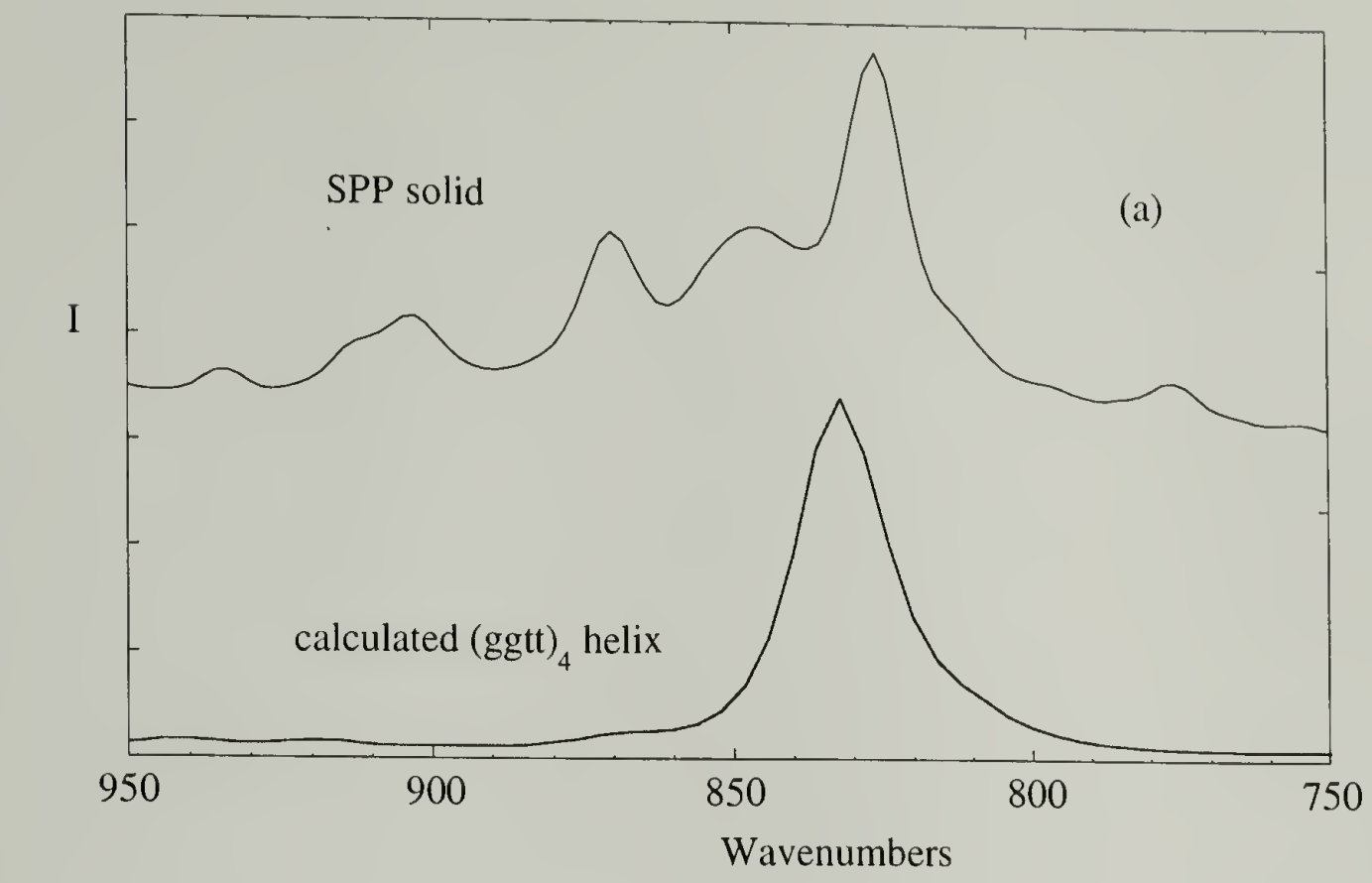

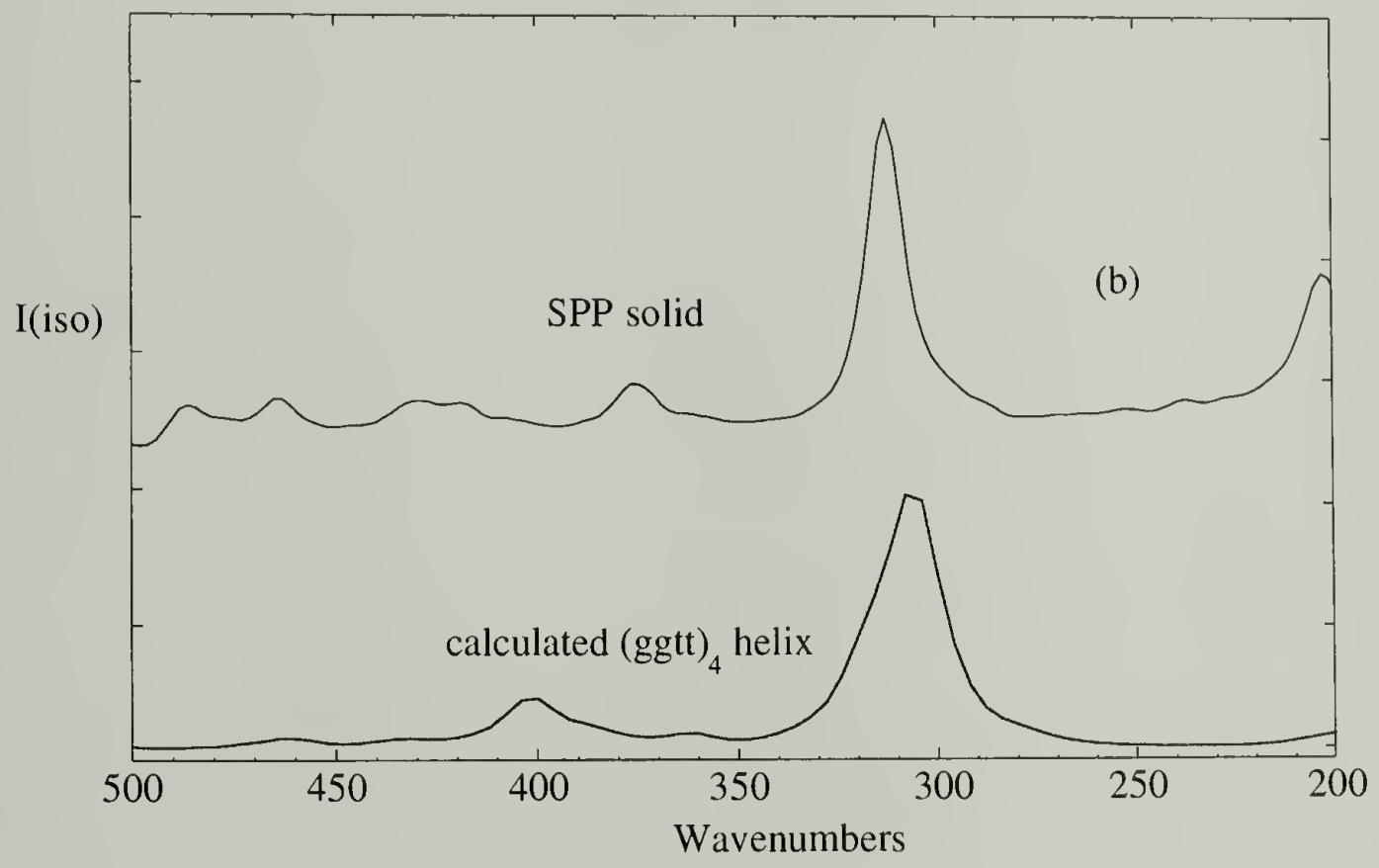

Figure 2.8 Measured and calculated Raman spectrum for solid syndiotactic polypropylene in the $(ggtt)_n$ conformation.

The 3_1 helix calculation and the Raman spectra for isotactic polypropylene are given in Figures 2.9a and 2.9b, and the assignments are given in Table 2.4. Experimentally, the two bands of interest are the 809 and 842 cm^{-1} bands (Figure 2.9a). Both of these bands should be calculated in the isotropic Raman spectrum. However, the 809 cm^{-1} peak may contain both an isotropic band, and a completely anisotropic band.[49] The isotropic bands are calculated at 829 and 852 cm^{-1}. The extra shoulder around 805 cm^{-1} in the calculation can be determined to be a consequence of the finite chain length. As the chain length increases, the high frequency band increases in intensity, and the separation between the two bands becomes more pronounced. Likewise, the main features below 500 cm^{-1} are given in Figures 2.9b. The excess calculated intensity around 456 and 265 cm^{-1} is due to the finite chain length. The length dependence is seen with the chains of length n=6 and n=9, which have two and three complete turns of the respectively. In this plot, it is evident that as the length of the chain increases, the intensity of the band around 400 cm^{-1} increases more than the other two major bands in the figure. It is anticipated that the intensity of these bands will fall in line with the experimental observations for sufficiently long calculated chains.

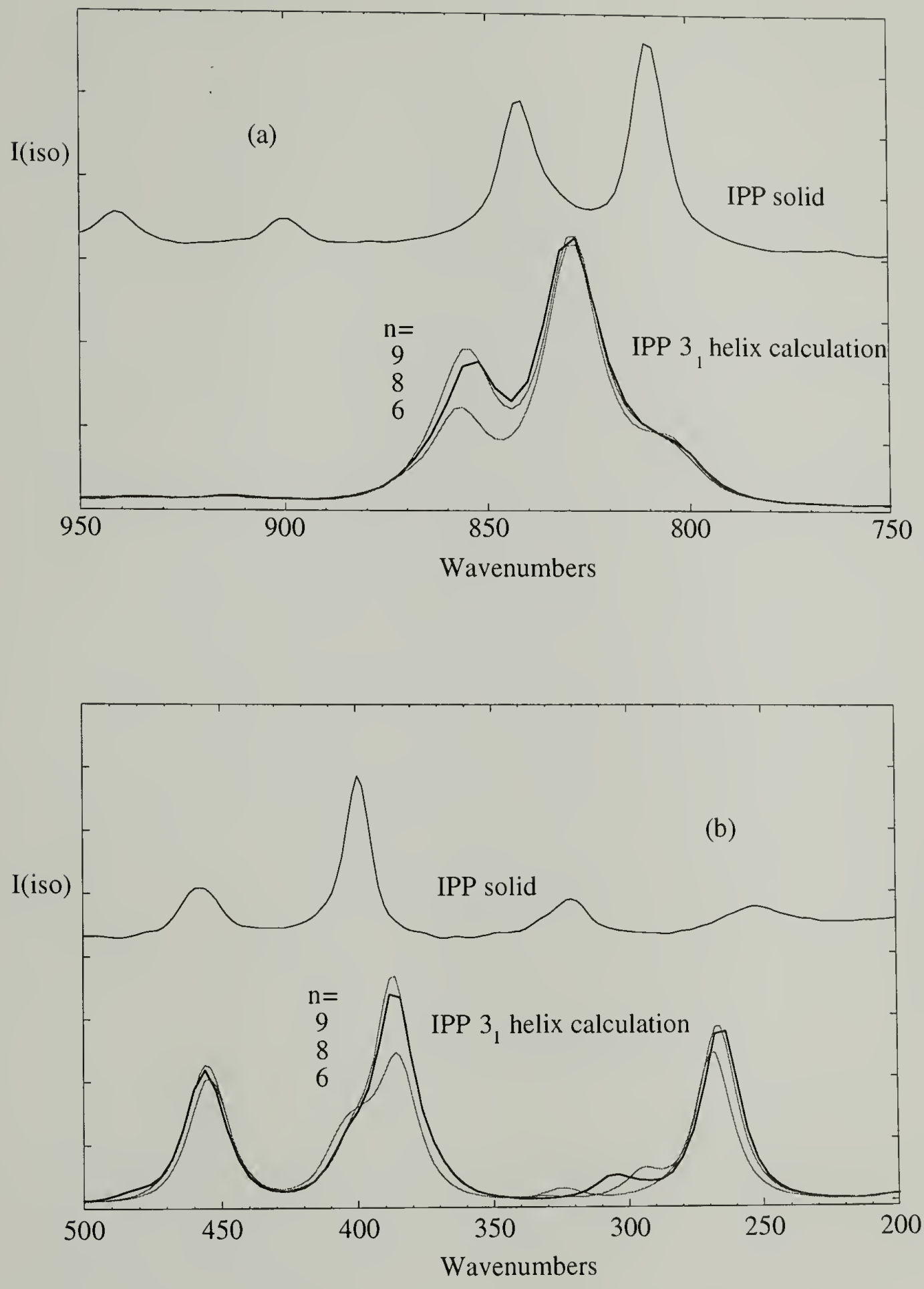

Figure 2.9 Comparison of FT Raman spectrum for isotactic polypropylene with the calculated spectrum.

The Raman spectrum of form II syndiotactic polypropylene produced by stretching the film is shown in Figures 2.10, along with the all trans simulations of different chain lengths ranging from n= 6 to n = 11. In this figure, there are three major experimental bands. They are at 868, 851 or 849 depending on the orientation of the laser relative to the stretching direction, and 827 cm^{-1}. The strongest of these peaks is around 868 cm^{-1}. In the simulated spectrum, this peak is smaller than the central peak. However, the intensity increases as the length of the trans chain increases. Plotting the relative intensity of the two simulated peaks against chain length (Figure 2.11) indicates that the higher frequency band would overcome the lower frequency band for a chain length around 13 units. This length dependence can explain the discrepancy between the observed and calculated intensity. The lowest frequency of the three bands, around 827 cm^{-1}, is a completely anisotropic mode for the zigzag model, and therefore would not calculate to have any intensity in the isotropic Raman intensity simulations. Furthermore, small amounts of ordered helical polymer that are also present contribute intensity to the 827 cm^{-1} band observed. In Figure 2.10, evidence for a small amount of helical polymer being present is the well defined, albeit small band at 313 cm^{-1}. The small peak around 425-427 cm^{-1} is more likely due to the all trans structure, or perhaps amorphous conformations. The all trans calculation has very little intensity in this region. However, the calculations by Schachtschneider, et al.[41] (Table 2.5) indicate that some Raman active bands may be present around 400, and 200 cm^{-1}.

Table 2.5 Vibrational Assignments for Trans- Syndiotactic Polypropylene.

calcn.	mode	IR observation	polarization	P.E.D.
C2v conformer		(Corradini)		
2962	A1	2959	(d)	$r_a^+(99)$
2906	A1	2916; 2905	(b)	$s(98)$
2882	A1	2880; 2868	(b)	$r^+(99)$
2856	A1			$d^+(99)$
1464	A1	1466	(b); (d)	$\alpha_a(66)$; $\delta(18)$; $\beta_a(7)$
1453	A1	1450	(d)	$\delta(59)$; $\alpha_a(24)$; $\Gamma(17)$
1373	A1	1381	(b)	$U^-(87)$; $T(9)$
1364	A1	1375	(c)	$\zeta_a(37)$; $T(32)$; $R(17)$; $U^-(15)$
1242	A1	1200	(b)	$T(34)$; $\zeta_a(27)$; $\beta_a(17)$
1152	A1	1154	(c)	$S^+(39)$; $R(22)$; $\omega(16)$; $\phi_a(16)$; $\zeta_a(13)$
971	A1	972	(b)	$\beta_a(47)$; $R(25)$; $T(20)$; $\zeta_a(21)$
863	A1	867	(b)	$R(45)$; $\beta_a(20)$; $S^+(17)$; $\omega(7)$
404	A1			$\phi^+(38)$; $\zeta^+(26)$; $\phi_a(25)$
66	A1			$\tau(97)$
2962	B1	2959	(a)	$r_b^-(99)$
2928	B1	2926	(e)	$d^-(99)$
1464	B1	~1450	(a)	$\alpha_b(88)$; $\beta_b(9)$
1370	B1	1379	(e)	$S^-(41)$; $\zeta_b(38)$; $W(36)$
1228	B1	1233	(a)	$\zeta_b(49)$; $W(40)$; $S^-(7)$
1154	B1	1130	(a)	$\beta_b(27)$; $W(26)$; $S^-(20)$; $\phi_b(10)$
949	B1	962	(a)	$\beta_b(50)$; $S^-(40)$
847	B1	831	(a)	$P(81)$; $\zeta_b(15)$
386	B1			$\phi_b(83)$; $\beta_b(8)$; $P(8)$
198	B1			$\tau(97)$
114	B1			$\tau(90)$

Table 2.5 (Continued)

calcn.	mode	IR observation	polarization	P.E.D.
C2v conformer				
2962	A2	IR INACTIVE		r_b^-(99)
2855	A2	IR INACTIVE		d^+(99)
1463	A2	IR INACTIVE		α_b(88); β_b(9)
1452	A2	IR INACTIVE		δ(78); Γ(21)
1345	A2	IR INACTIVE		ζ_b(59); T(16); S^-(8)
1185	A2	IR INACTIVE		T(50); S^-(22); β_b(19)
1082	A2	IR INACTIVE		T(35); ζ_b(33); β_b(18); S^-(16)
920	A2	IR INACTIVE		S^-(60); β_b(41)
574	A2	IR INACTIVE		ω(54); ϕ_b(28); ζ_b(9); β_b(8)
215	A2	IR INACTIVE		ϕ_b(61); ω(25); τ(14)
192	A2	IR INACTIVE		τ(84); ω(8)
2962	B2	2959	(d)	r_a^-(98)
2930	B2	2925	(b)	d^-(93)
2903	B2	2916; 2905	(b)	s(93)
2882	B2	2880; 2868	(b)	r^+(99)
1462	B2	1466	(b)	α_a(89); β_a(9)
1372	B2	1381	(b)	U(100)
1355	B2	~1350	(d)	W(49); ζ_a(28); R(7)
1330	B2	1322	(b)	ζ_a(39); W(37); ζ^+(18); R(7)
1162	B2	1153	(c)	P(26); β_a(25); R(18); ϕ^+(7)
1088	B2	1095	(b)	S^+(53); R(26); ζ_a(14)
903	B2	899	(b)	β_a(56); ζ_a(17); P(15); S^+(13)
827	B2	828	(b)	R(47); P(27); S^+(13)
447	B2	492	(b)	ϕ^+(44); ζ^+(30); W(14); P(10)
372	B2			ϕ_a(79); P(7)

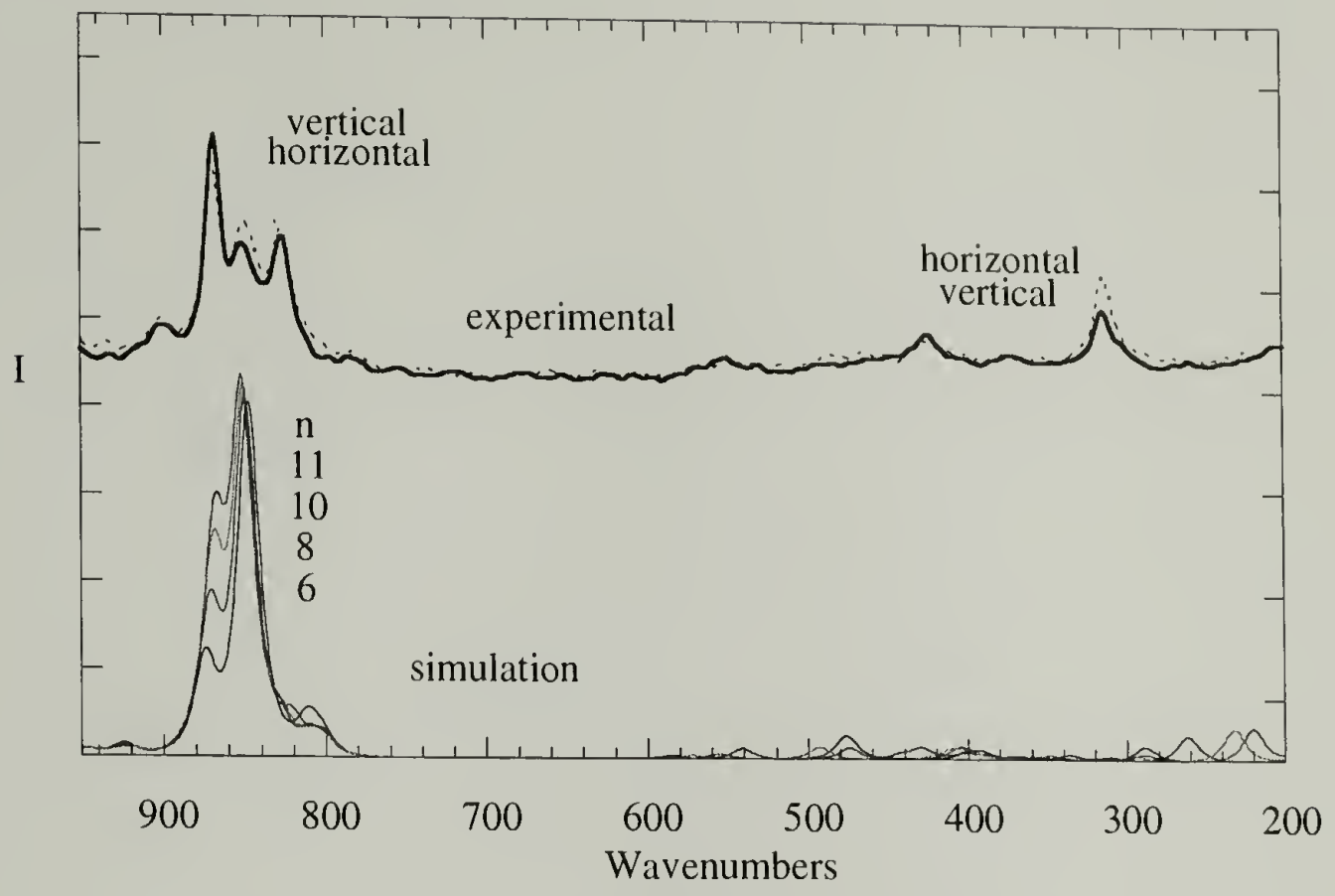

Figure 2.10 Simulated and calculated Raman spectrum for zigzag syndiotactic polypropylene.

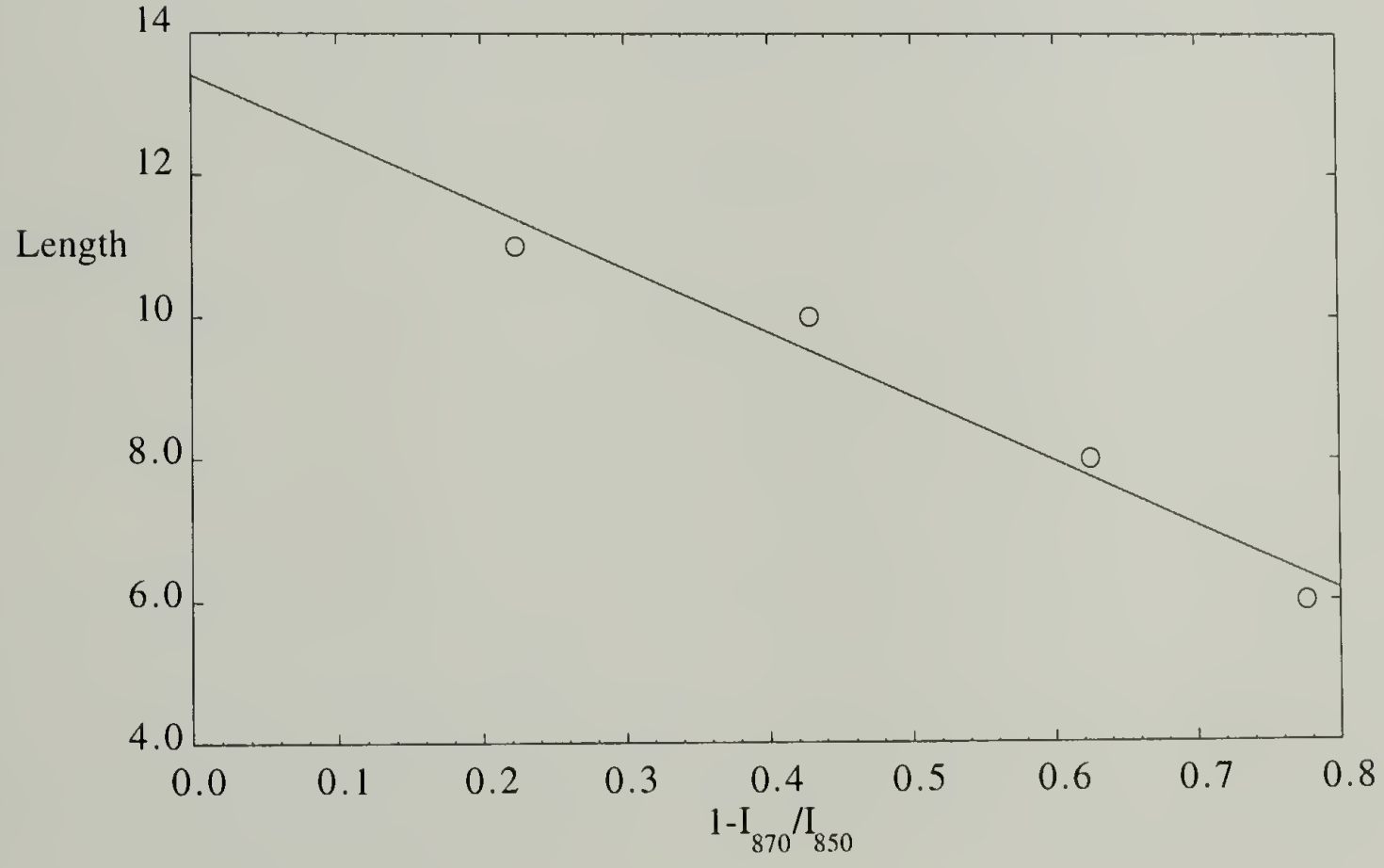

Figure 2.11 All trans chain length versus relative intensity of ~870 and ~850 cm^{-1} bands.

Mappings of the most probable conformations (i.e. combinations of ggtt and tttt) are given in Figures 2.12a through 2.13b. These mappings in Figures 2.12a and 2.12b give information about the minimum sequence length required to observe the ordered helical bands. In Figures 2.13a and 2.13b, possible alternative ordered structures are explored to consider their possible contribution to the ordered band intensities. In the high frequency region (Figures 2.12a and 2.13a) the results indicate the minimum length of chain required to observe the ordered helical band is around a sequence length of $(ggtt)_4$. Furthermore, the all trans structure gives the highest frequency isotropic bands. Likewise, the frequency shift of the band around 300 cm^{-1} (Figures 2.12b and 2.13b) indicates that at the band frequency at 313 cm^{-1} corresponds to a long helical sequence, the length of which is at least $(ggtt)_4$. However, the possibility that longer sequences are required cannot be determined with these calculations. The minimum sequence length to observe intensity around 300 cm^{-1} is either (ggtt) or $(ggtt)_2$. Based on the Flory three state RIS calculations in the melt, at least 39% of the sequences are of the form (ggtt) or (ttg'g') (Table 2.6). Therefore this band is characteristic of the most common conformation of syndiotactic polypropylene, whether in the amorphous or most stable ordered state.

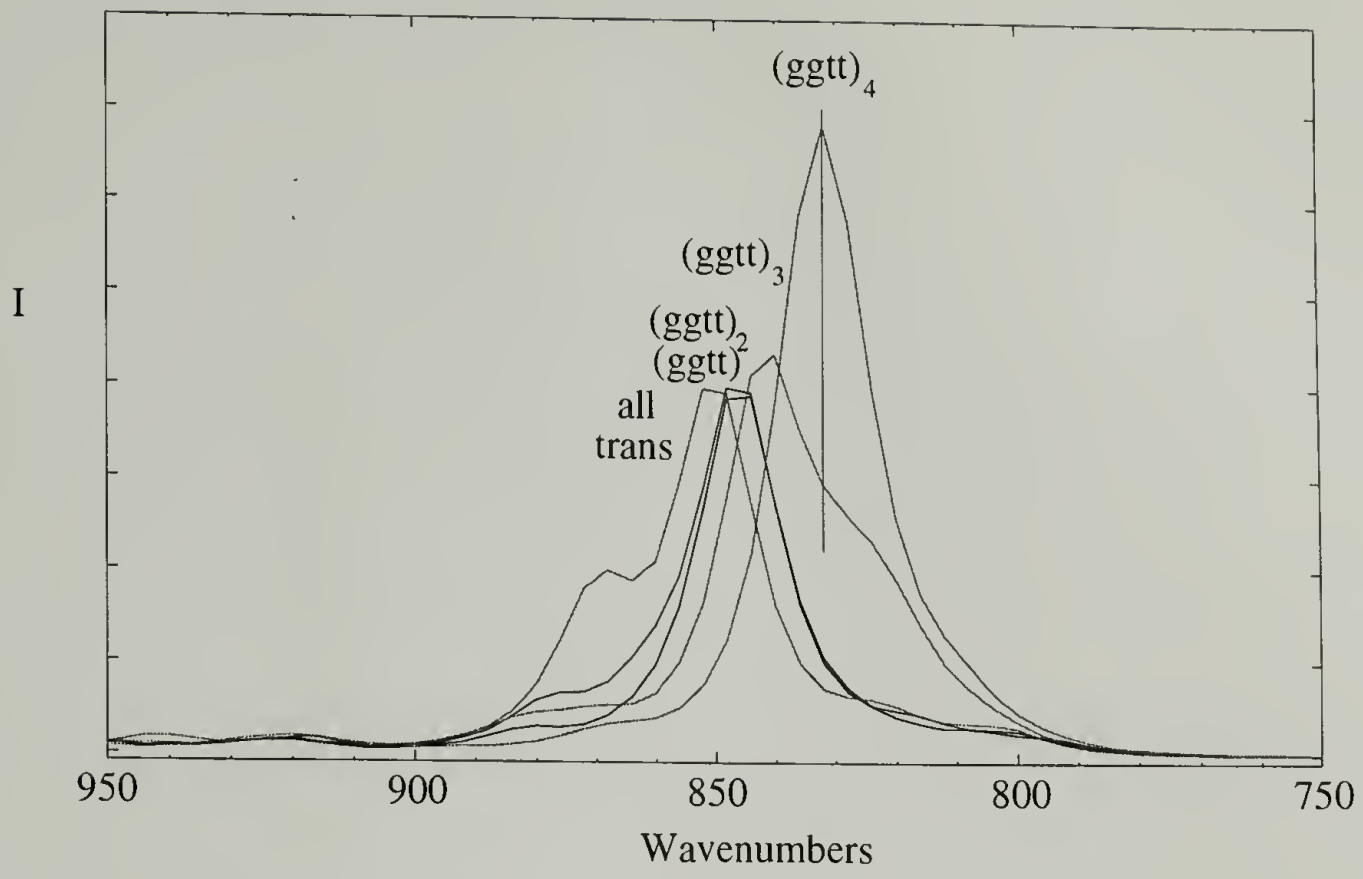

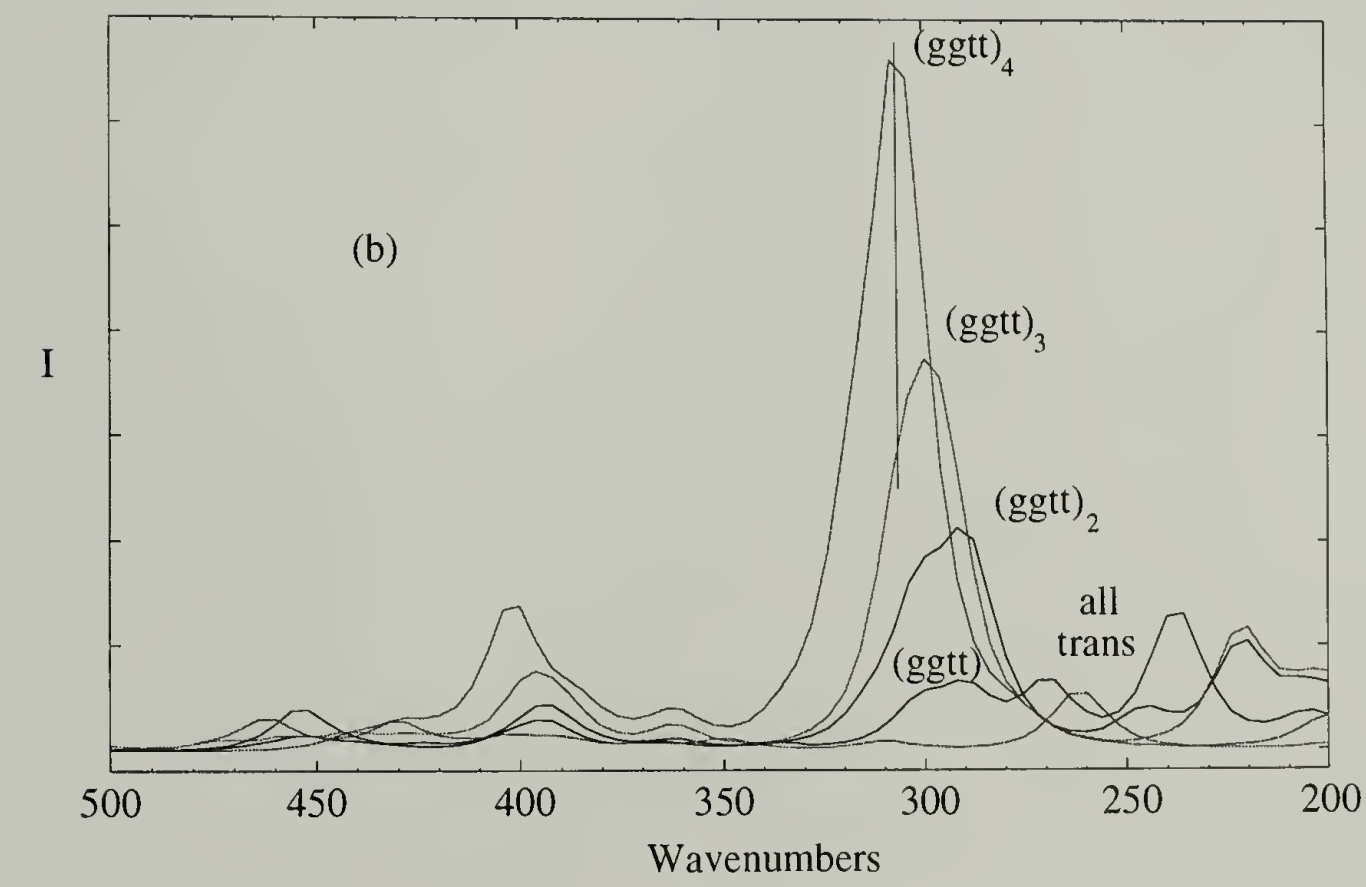

Figure 2.12 Calculations of different helical lengths for r_8.

The molten spectra for syndiotactic and isotactic polypropylene, given in Figures 1.2a and 1.2b are directly compared with Monte Carlo simulated spectra in Figures 2.14a through 2.15b. In Figure 2.14a, the shape of the experimental band around 846 cm^{-1} with a possible shoulder around 866 cm^{-1}, in comparison to the simulated spectrum suggests that the Flory three-state model may underestimate the population of tans sequences present in the molten phase. This analysis also depends on the conformational mappings in Figures 2.12a and 2.13a, described above, and the assignment of the 867 cm^{-1} in the stretched syndiotactic polypropylene to the trans structure (Figure 2.10). In Figure 2.14b, the major peak around 305 cm^{-1} is represented by the calculation around 292 cm^{-1}, and the broad bands around 400 cm^{-1}, and below 200 cm^{-1} are represented by multiple small peaks in the calculated spectrum. Comparison with the conformational mappings of the most probable chain sequences (Figures 2.12a through 2.13b) indicates that the persistence of the band around 305 cm^{-1} requires a significant population if (ggtt) sequences. The length of these sequences are most likely (ggtt)1 or (ggtt)2. These spectra also show the dependence of the calculated intensity on the side group angle bending polarizability parameter (D). This parameter has little effect on the simulated relative intensity for the racemic chain, for D close to zero. The molten spectra for isotactic polypropylene are simulated in Figures 2.15a and 2.15b. In this case, the intensity parameters were chosen to match the parameters used by Hallmark, et al.[34] In the high frequency region (Figure 2.15a) the measured melt, and calculated melt spectral peaks are in the same region. In Figure 2.15b, the major peak measured at 407 cm^{-1} is calculated at 387 cm^{-1}. The higher frequency shoulder above the 407 cm^{-1} band, and the broad band below 300 cm^{-1} are represented in the calculations by several small peaks.

Table 2.6 Calculated Populations of Most Common Conformers in Syndiotactic Polypropylene Based on the Flory Three-State RIS model.

conformation	Expectation	SPP Monte Carlo
tttt	0.263	0.271
ttg'g'+ggtt	0.395	0.385
ttg't+tgtt	0.049	
g'ttt+tttg	0.041	
gg'tt+ttg'g	0.027	

Syndiotactic polypropylene spectroscopic features below 500 cm^{-1} are significantly different from the features of isotactic polypropylene, in both the solid and the melt. The major difference is the presence of the peak around 400 cm^{-1} in the isotactic polymer, and the peak around 300 cm^{-1} for the syndiotactic polymer. This major difference is represented by the disordered calculations. Furthermore, the spectroscopic features seem to form a progression from the highly syndiotactic to the isotactic polymer, with intensity decreasing around 300 cm^{-1} as it increases around 400 cm^{-1} (Figure 2.5b). Since it is anticipated that the racemic samples with large numbers of defects are mostly amorphous, it was assumed that the differences come primarily from changes in the amorphous conformation distribution. Since the most stable conformation for ordered isotactic polypropylene is around 400 cm^{-1}, and the most stable conformer for syndiotactic polypropylene is around 300 cm^{-1}, this assumption was not necessary. However, it is convenient for simulating the Raman intensity to use for a quantitative model of the intensity. The calculations done to represent the different defect populations (Figure 2.16) are a pure racemic calculation; a calculation with two meso defect in the middle of the chain, a three meso defect in the middle, a five meso sequence in the middle, and a pure meso chain. Below 500 cm^{-1}, the overall spectroscopic features are comparable to the measured spectra in the same region. Specifically, as the configuration progress from mainly racemic

to mainly meso, intensity around 300 cm^{-1} decreases as intensity around 400 cm^{-1} increases A quantitative comparison of both the calculate and experimental data was determined by integrating all the peaks in between 350 and 500 cm^{-1}, integrating all the peaks between 250 and 350 cm^{-1}, and taking the ratio of the intensities (I_{400}/I_{300}). As Figure 2.17 shows, all the undeformed solid samples fall close to the line for racemic content. Typical errors are around 2 to 6%. Even the isotropic Raman spectrum of the syndiotactic melt falls close to the calculated line. The essentially atactic sample (R50) falls slightly below the curve. However, this is not surprising since the model assumes that the features dominating the spectrum has all the defects in blocks. The only sample that markedly deviates from the calculated intensity ratio curve is the 92% racemic sample that was stretched to induce the zigzag structure. This deviation is consistent with the simulated spectrum of the zigzag structure, in which intensity around 300 cm^{-1} is suppressed relative to the 400 cm^{-1} intensity region. The syndiotacticity index, described by Boor et al.[3] was also measured for the racemic samples using attenuated total reflectance infrared spectroscopy. The results are scaled to best match the configuration curve for the simulated intensities. These results confirm what was previously stated, that the syndiotacticity index is not a good indicator of the configuration. This is best shown by the SI values obtained for the 60% racemic samples where the range of values are in excess of possible limits for determining a tacticity.

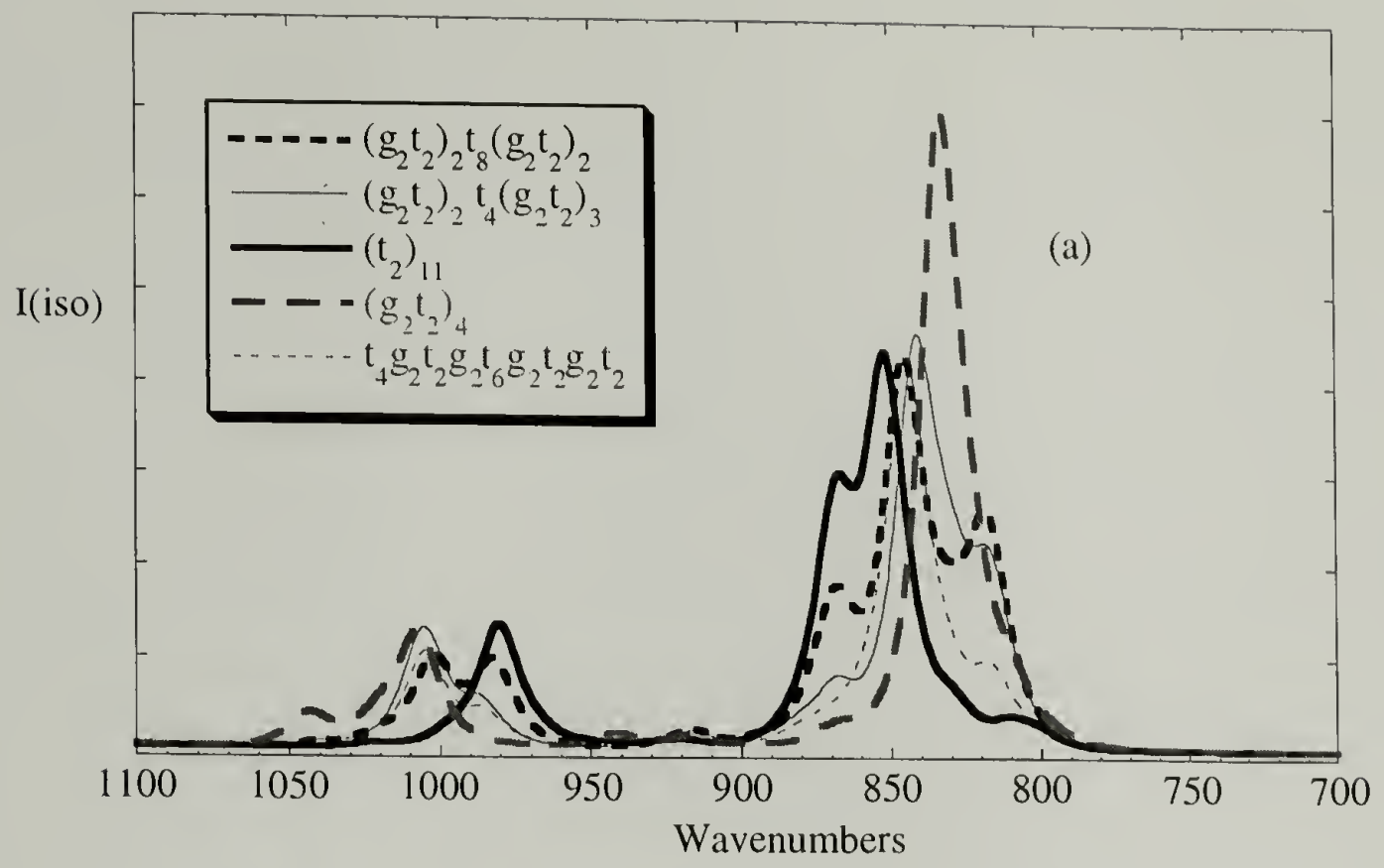

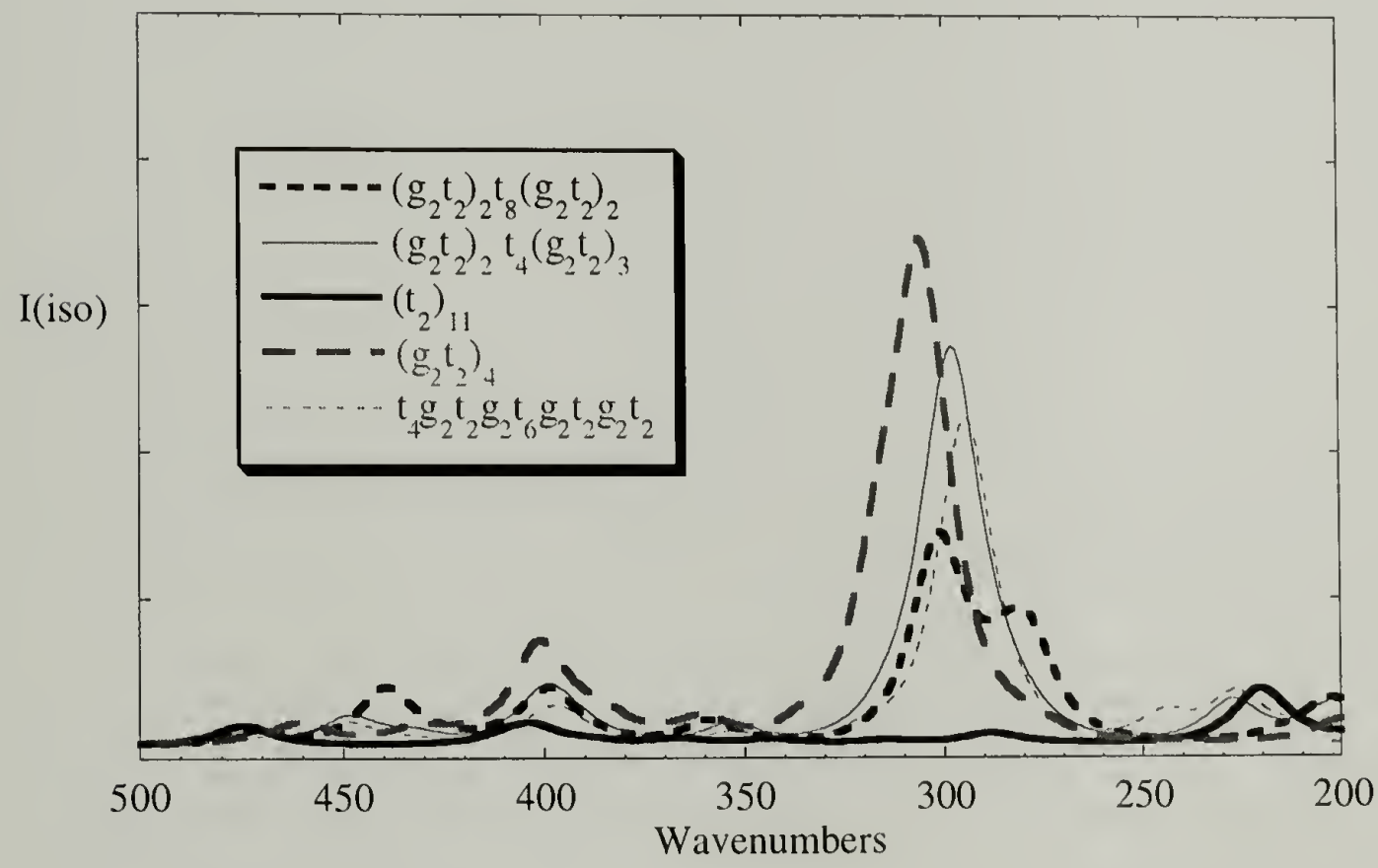

Figure 2.13 Different conformation cequences- calculated spectra.

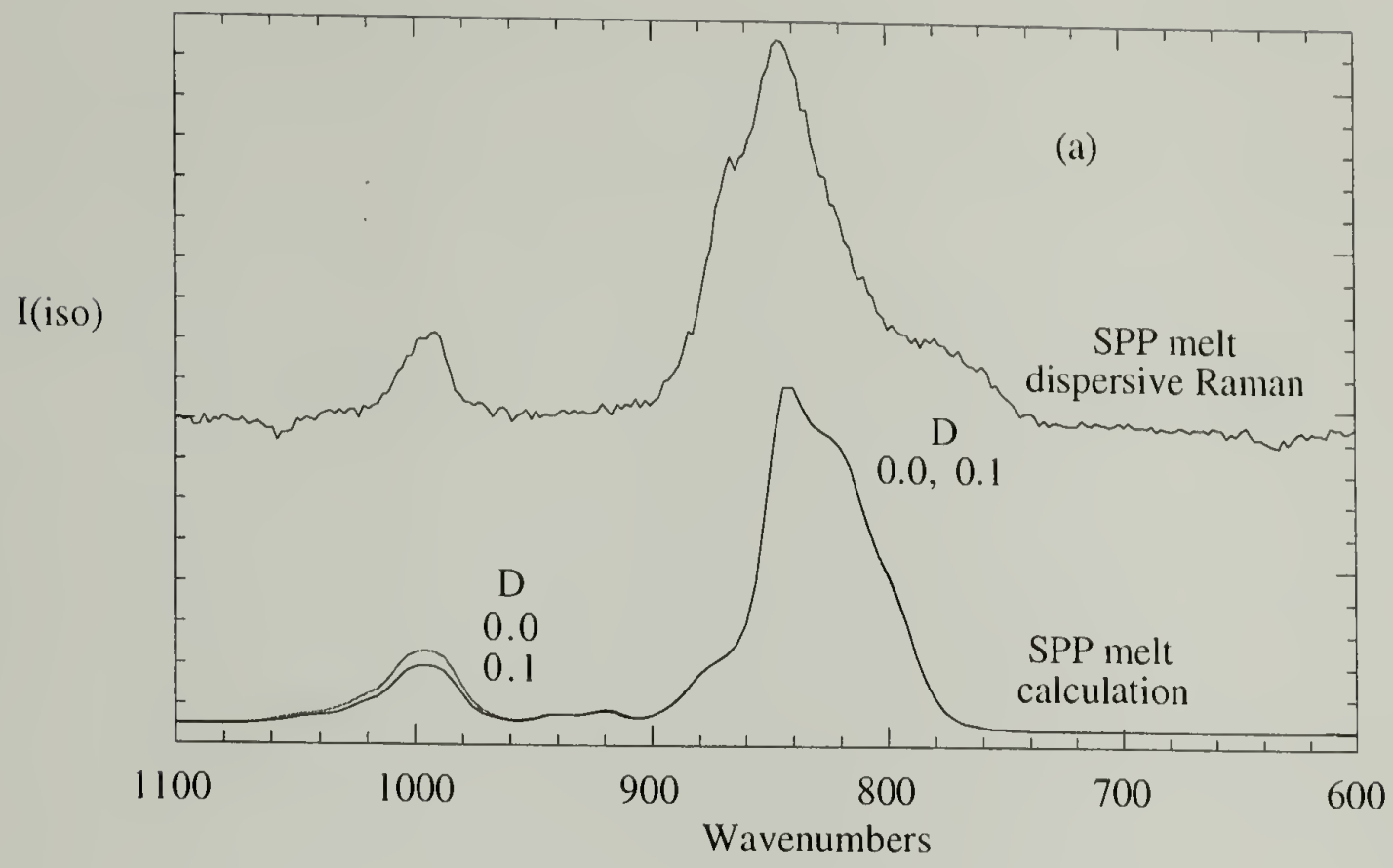

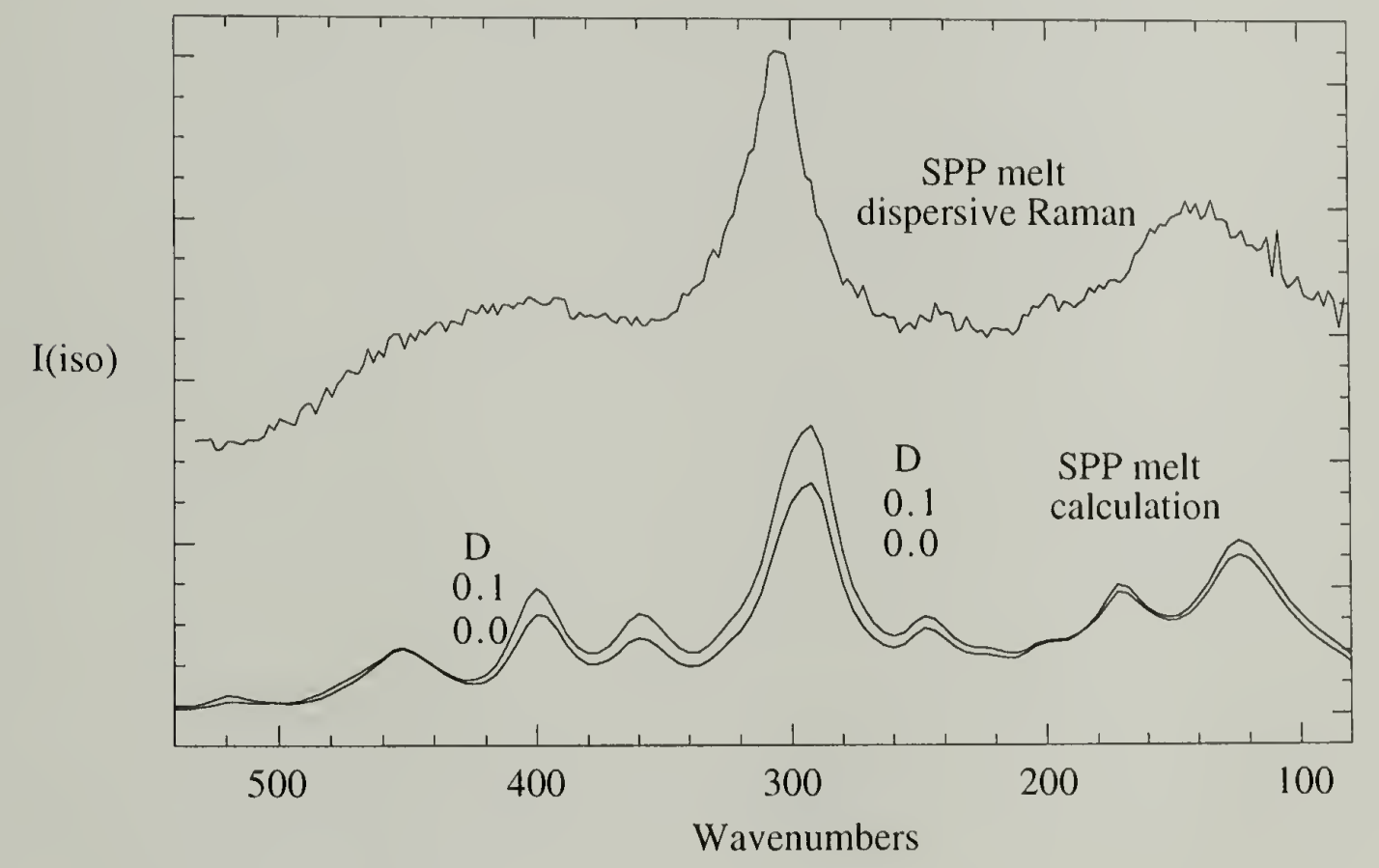

Figure 2.14 Syndiotactic polypropylene comparison of melt and calculation.

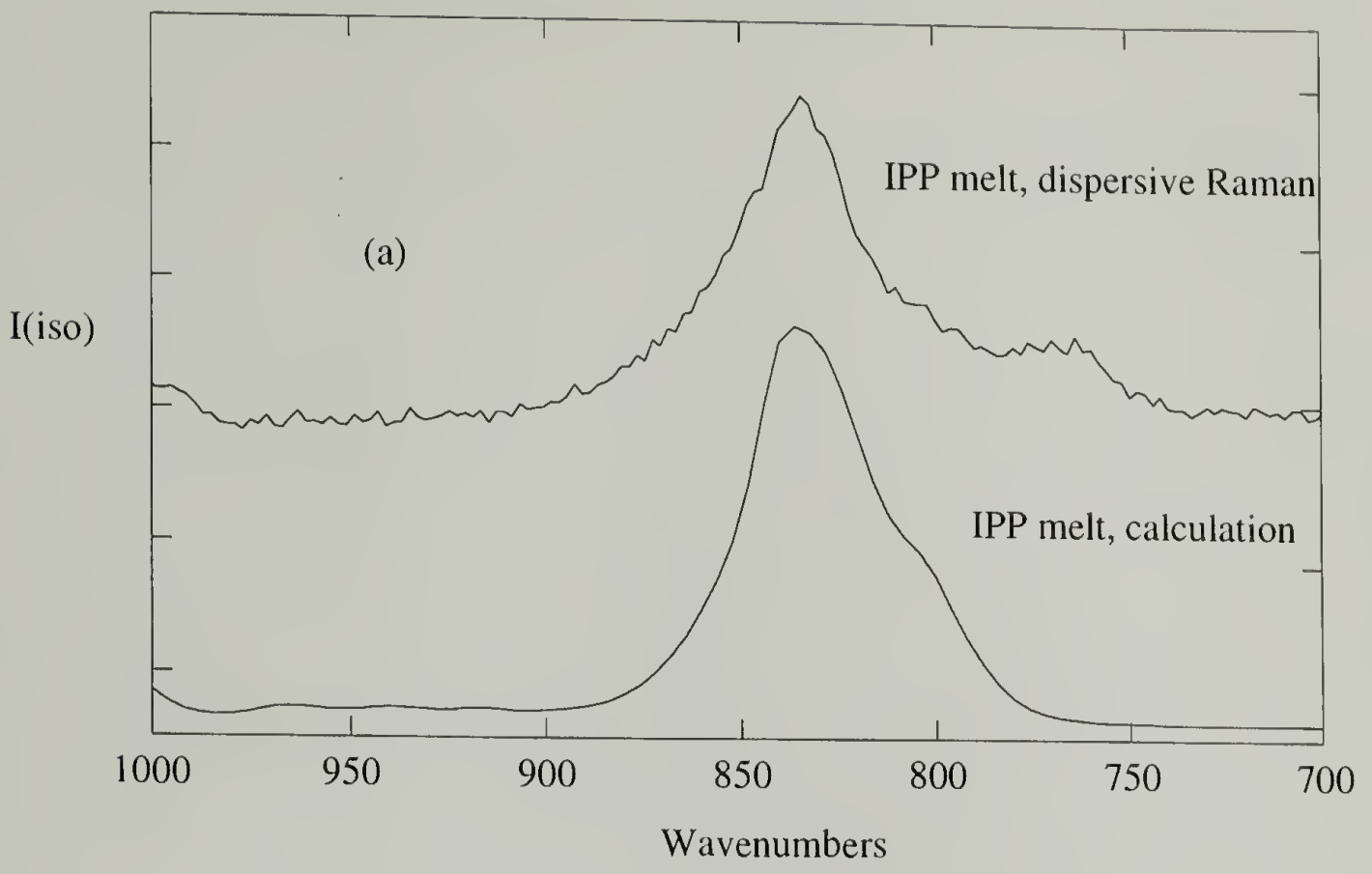

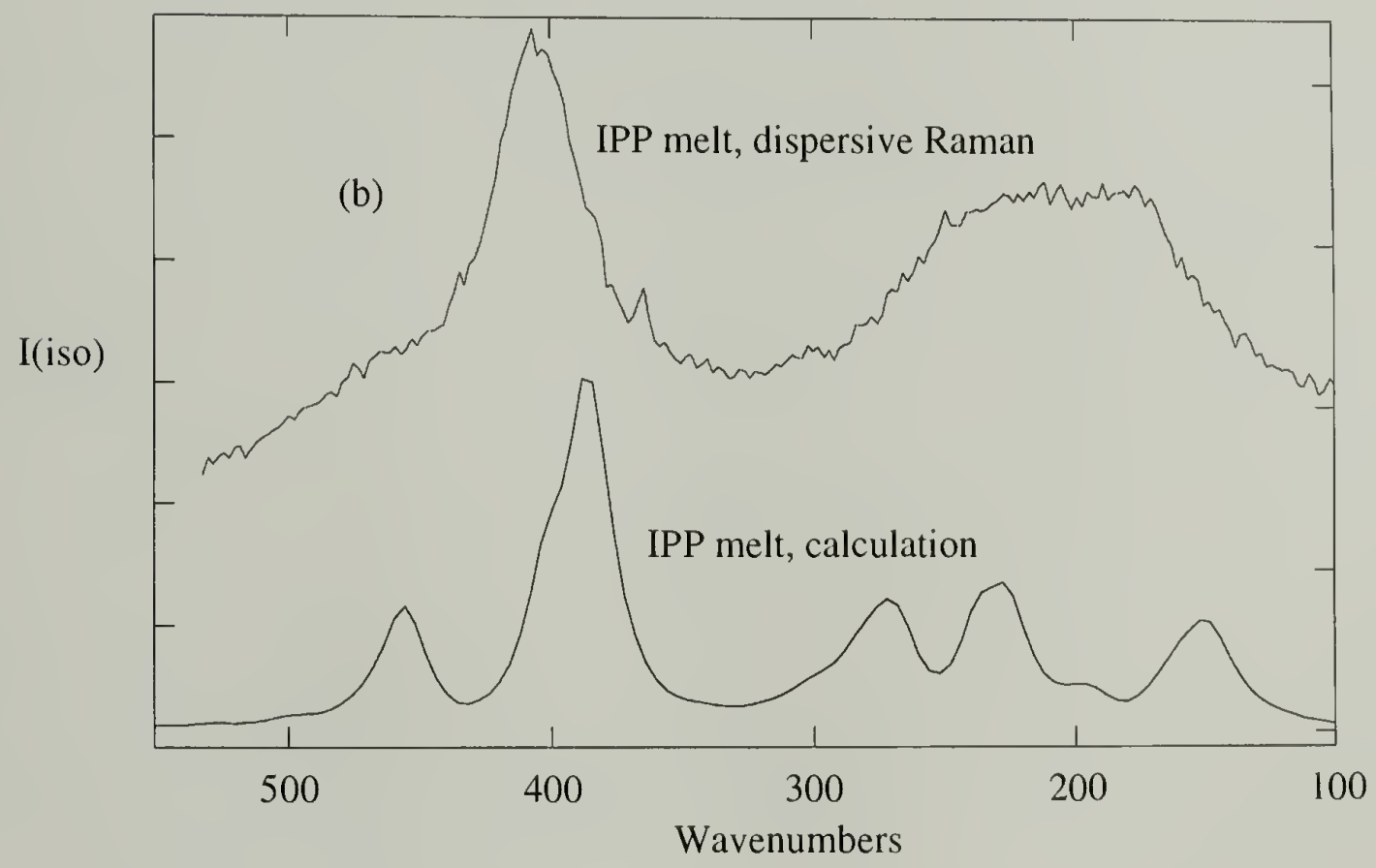

Figure 2.15 Isotactic polypropylene comparison of melt and calculation.

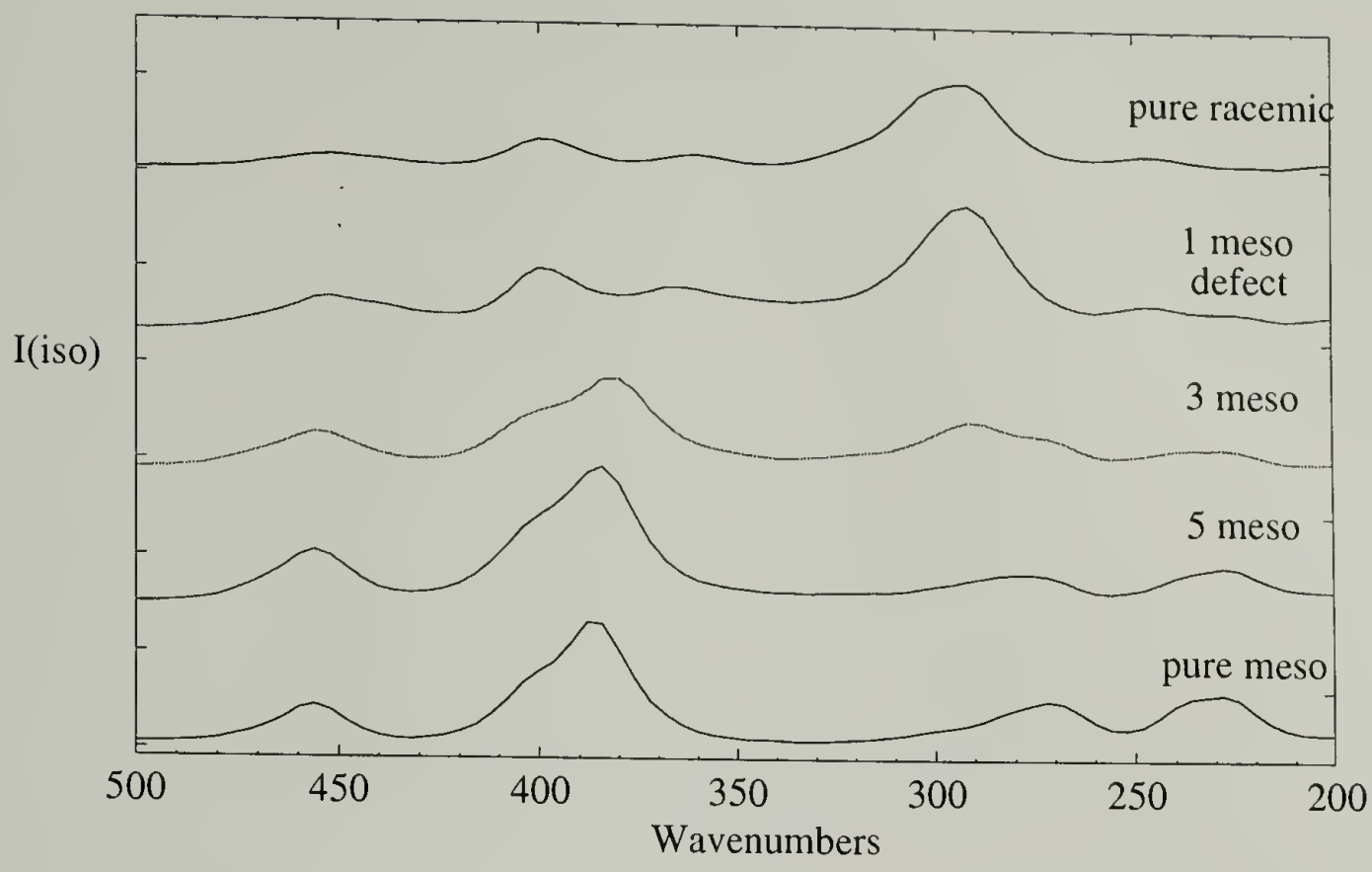

Figure 2.16 Isotropic Raman calculation spectra for a range of polypropylene configurations.

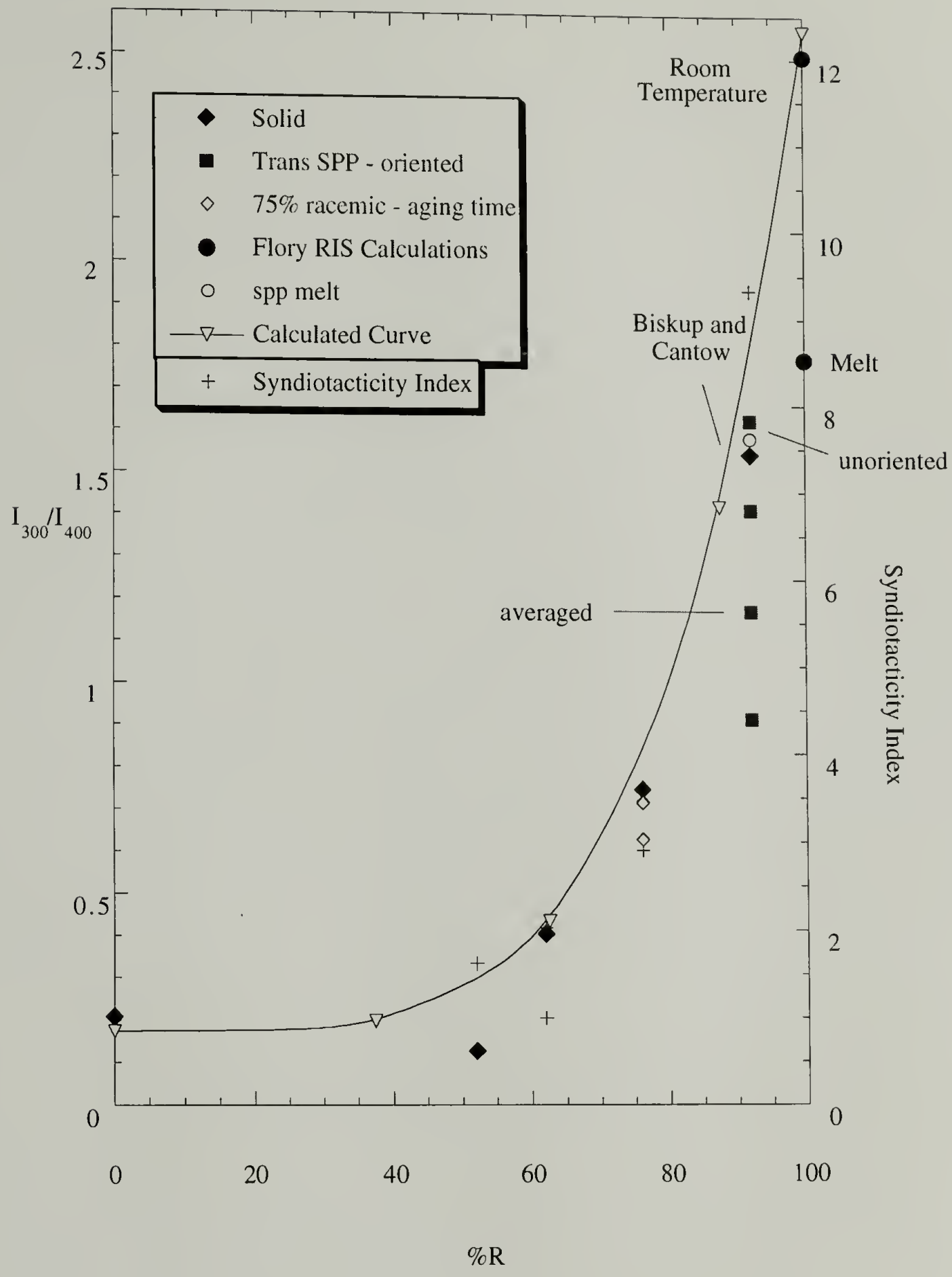

Figure 2.17 Comparison of simulated and calculated intensity ratios.

2.5 Conclusions

As the calculations indicate, it is possible to simulate the Raman spectrum of polypropylenes with different configurations. Both isotactic and syndiotactic ordered structure spectra are simulated. In these cases, the major features are represented in the 800 and 300 to 400 cm^{-1} regions. However, as has been indicated, in many cases the intensity is dependent on the chain length for short sequences. However, for representing disordered chains, this does not seem to be a significant issue. A quantitative representation of the configuration can be obtained from the Raman spectrum, at least in the range studied here (52% to 92% racemic dyads) with little or no dependence on thermal history.

Conformational mapping of both the high frequency and low frequency regions show the minimum helical length required to observe the characteristic ordered bands. The band around 826 cm^{-1} requires a minimum sequence length of $(ggtt)_4$, Likewise, the band around 300 cm^{-1} shifts to higher frequency with increasing helix length. This observation is consistent with the frequency shift observed going from the melt to the solid state. The combination of conformational mappings, analysis of the conformation distributions and ordered band simulations is a useful too for characterizing the Raman spectroscopic features. As illustrated in this chapter, it can be used l to characterize the configuration for an polypropylenes, a least in the range studied here. Further, the tool makes possible a quantitative determination of the major conformations and observed in the amorphous state. The same types of issues are important in time-dependent issues such as conformational ordering, packing, and physical aging. The usefulness of this tool for time-dependent studies is illustrated in Chapter 3.

2.6 References

(1) Peraldo, M.; Cambini, M. *Spectrochimica Acta* **1965**, 21, 1509.

(2) Zambelli, A.; Natta, G.; Pasquon, I. *Journal of Polymer Science: C* **1963**, 4, 411.

(3) Boor, J. J.; Youngman, E. A. *J. Polym. Sci: Part A-1* **1966**, 4, 1861.

(4) Alamo, R. G.; Galante, M. J.; Lucas, J. C.; Mandelkern, L. *Polymer Preprints* **1995**, 36, 285.

(5) Isasi, J. R.; Mandelkern, L.; Alamo, R. G. *Polymer Preprints* **1996**, 37, 239.

(6) Zambelli, A.; Locatelli, P.; Bajo, G.; Bovey, F. A. *Macromolecules* **1975**, 8, 687.

(7) Sozzani, P.; Simonutti, R.; Galimberti, M. *Macromolecules* **1993**, 26, 5782.

(8) Masetti, G.; Cabassi, F.; Zerbi, G. *Polymer* **1980**, 21, 143.

(9) Natta, G.; Corradini, P. *Nuovo Chim. Suppl.* **1960**, 15, 40.

(10) Natta, G.; Peraldo, M.; Allegra, G. *Die Makromolekulare Chemie* **1964**, 75, 215.

(11) Ewen, J. A.; Jones, R. L.; Razavi, A.; Ferrara, J. D. *J. Am. Chem. Soc.* **1988**, 110, 6255.

(12) Auriemma, F.; De Rosa, C.; Corradini, P. *Macromolecules* **1993**, 26, 5719.

(13) Auriemma, F.; Born, R.; Spiess, H. W.; De Rosa, C.; Corradini, P. *Macromolecules* **1995**, 28, 6902.

(14) Auriemma, F.; Lewis, R. H.; Spiess, H. W.; De Rosa, C. *Macromol. Chem. Phys.* **1995**, 196, 4011.

(15) De Rosa, C.; Auriemma, F.; Corradini, P. *Macromolecules* **1996**, 29, 7452.

(16) Lovinger, A. J.; Lotz, B.; Davis, D. D. *Polymer* **1990**, 31, 2253.

(17) Lovinger, A. J.; Lotz, B.; Davis, D. D.; Paden, F. J. *Macromolecules* **1993**, 26, 3494.

(18) Lovinger, A. J.; Lotz, B.; Davis, D. D.; Schumacher, M. *Macromolecules* **1994**, 27, 6603.

(19) Stocker, W.; Schumacher, M.; Graff, S.; Lang, J.; Wittmann, J. C.; Lovinger, A. J.; Lotz, B. *Macromolecules* **1994**, 27, 6948.

(20) Sozzani, P.; Galimberti, M.; Balbontin, G. *Makromol. Chem. Rapid Commun.* **1992**, 13, 305.

(21) Chatani, Y.; Maruyama, H.; Noguchi, K.; Asanuma, T.; Shiomura, T. *J. Polym. Sci. Polym. Phys. Lett.* **1990**, 28, 393.

(22) Chatani, Y.; Maruyama, H.; Asanuma, T.; Shiomura, T. *J. Polym. Sci. Polym. Phys. Ed.* **1991**, 29, 1649.

(23) Asakura, T.; Aoki, A.; Takeshi, D.; Demura, M.; Asanuma, T. *Polym. J.* **1996**, 28, 24.

(24) Sozzani, P.; Simonutti, R.; Comoti, A. *Magnetic Resonance in Chemistry* **1994**, 32, s45.

(25) Lotz, B.; Lovinger, A. J.; Cais, R. E. *Macromolecules* **1988**, 21, 2375.

(26) Nakaoki, T.; Ohira, Y.; Hayashi, H.; Horii, F. *Macromolecules* **1998**, 31, 2705.

(27) Wang, Y.; Hahn, T. D.; Hsu, S. L.; Stidham, H. D.; Seidle, A. **1998**, Manuscript in Preparation.

(28) Allegra, G.; Ganis, P.; Corradini, P. *Makromol. Chem.* **1963**, 61, 225.

(29) Suter, U. W.; Flory, P. J. *Macromolecules* **1975**, 8, 765.

(30) Yang, X.; He, L.; An , B.; Ma, D. *Polymer* **1993**, 34, 4542.

(31) Snyder, R. G.; Kim, Y. *J. Phys. Chem* **1991**, 95, 602.

(32) Snyder, R. G. *J. Chem. Soc. Faraday Trans* **1992**, 88, 1823.

(33) Cates, D. A.; Strauss, H. L.; Snyder, R. G. *J. Phys. Chem.* **1994**, 98, 4482.

(34) Hallmark, V. M.; Bohan, S. P.; Strauss, H. L.; Snyder, R. G. *Macromolecules* **1991**, 24, 4025.

(35) Yoon, S.; Ichikawa, K.; MacKnight, W. J.; Hsu, S. L. *Macromolecules* **1995**, 28, 5063.

(36) Yoon, S.; Ichikawa, K.; Macknight, W. J.; Hsu, S. L. *Macromolecules* **1995**, 28, 4278.

(37) Yang, X.; Su, Z.; Wu, D.; Hsu, S. L.; Stidham, H. D. *Macromolecules* **1997**, 30, 3796.

(38) Wilson Jr., E. B.; Decius, J. C.; Cross, P. C. *Molecular vibrations*; McGraw-Hill Book Company: New York, 1955.

(39) Porto, S. P. S. *Journal of the Optical Society of America* **1966**, 56, 1585.

(40) Snyder, R. G.; Schachtschneider, J. H. *Spectrochim. Acta* **1964**, 20, 853.

(41) Schachtschneider, J. H.; Snyder, R. G. *Spectrochimica Acta* **1965**, 21, 1527.

(42) Chalmers, J. M. *Polymer* **1977**, 18, 681.

(43) Woodward, L. A. *Introduction to the theory of molecular vibrations and vibrational spectroscopy*; Oxford University Press: Oxford, 1972, p 370.

(44) Tang, J.; Albrecht, A. C. In *Raman Spectroscopy: Theory and Practice*; H. A. Szymanski, Ed.; Plenum Press: New York, 1970; Vol. 2; pp 33.

(45) Flory, P. J.; Mark, J. E.; Abe, A. *Journal of the American Chemical Society* **1966**, 88, 639.

(46) Biskup, U.; Cantow, H.-J. *Macromolecules* **1972**, 5, 546.

(47) Mattice, W. L.; Suter, U. W. *Conformational Theory of Large Molecules. The Rotational Isomeric State Model in Macromolecular Systems*; John Wiley and Sons, Inc.: New York, 1994, p 449.

(48) Flory, P. J. *Statistical Mechanics of Chain Molecules*; Interscience Publishers: New York, 1969, p 432.

(49) Zerbi, G.; Piseri, L. *The Journal of Chemical Physics* **1968**, 49, 3840.

CHAPTER 3

TIME-DEPENDENT AND MECHANICALLY INDUCED PHASE TRANSFORMATIONS IN SYNDIOTACTIC POLYPROPYLENE

3.1 Introduction

In Chapter 2, a spectroscopic tool for characterizing syndiotactic polypropylene microstructure was developed. In this chapter, it is used to characterize time-dependent changes in polymer microstructure, namely ordering and changes in amorphous conformation distribution. In addition, it is used to characterize both ordered and amorphous phase structure for mechanically deformed samples with different thermal treatments and configurational defects.

Ordering can be considered in terms of crystallization or aggregation behavior. If the ordering domains are sufficiently large, they can be observed by conventional methods such as light scattering and x-ray scattering. However, domains smaller than optical dimensions do not scatter light to be observed by optical methods. Furthermore, three-dimensional packing order may be lacking, or the ordered domains may be too small have sufficient coherent scattering for methods such as x-ray scattering. In cases of low temperature ordering where small domains and many defects in the packing order are expected, vibrational spectroscopy will be useful to determine the conformational ordering.

Semicrystalline polymer also undergoes time-dependent transformations. These changes can be viewed in terms of physical aging, or as part of the crystal nucleation and growth process.[1] In either case, the method used to characterize such features needs to be sensitive to the conformation distribution in the amorphous phase. Absence of long range order in the amorphous regions limits the techniques suitable to characterizing the microstructure. Typically, physical aging is studied in terms of changes in the mechanical and physical properties, such as stiffness and density. Microstructural probes characterize free volume change by techniques which are sensitive to local chain segment or probe

mobility, such as positron annihilation lifetime spectroscopy (PALS),[2-5] electron spin resonance (ESR) of a spin probe radical or spin labeled chain,[6] fluorescence spectroscopy,[7-9] and photochromic probe or labeling.[7,10] These techniques probe the apparent free volume, or local density fluctuations, but give no information about the actual conformation distribution and how it changes with time. With the microstructural characterization tool developed in Chapter 2, it is possible to characterize the preferred conformers and how the conformation distribution changes with temperature, and possibly time.

Several studies have characterized pathways between the various crystalline structures of syndiotactic polypropylene.[11-16] However, these studies only consider a limited number of pathways to achieving the phase transformation. Specifically, the all trans, or zigzag state is achieved by either cold drawing a sample quenched from melt into ice water, or quenching and storing at or below 0°C for several days to spontaneously form the zigzag state.[16,17] None of these studies address the impact of configuration time-dependent, or mechanically induced phase transformations. With the aid of the characterization tool developed in Chapter 2 for syndiotactic polypropylene, these phase transformations are characterized to understand the influence on the transformation conditions on the ordered phase conformations and the amorphous phase conformation distribution.

3.2 Experimental

In order to consider the relative stability of the ordered phases, and the energy barriers of the of the time-dependent phase transformations that occur for mainly syndiotactic polypropylene, the polypropylene samples were prepared in a manner that initially traps high energy non-equilibrium states to follow the microstructural evolution. Different thermal histories were followed, as illustrated in Figure 3.1, for 92% racemic

dyad (syndiotactic) polypropylene samples. The samples were heated to the melt in a vacuum oven. Then, the samples were either quenched to liquid nitrogen temperatures and warmed to the target aging temperature of 20 or 40 °C, or cooled from melt directly to 20°C. In order to follow structural changes as a function of time, the quenched samples were allowed to warm to the target temperature and then the equilibration process was examined as a function of time. Two samples were quantitatively characterized, the 92% racemic dyad sample supplied by Fina Oil and Chemical Company, and the 75% racemic dyad sample supplied by 3M. These samples were described in Chapter 2.

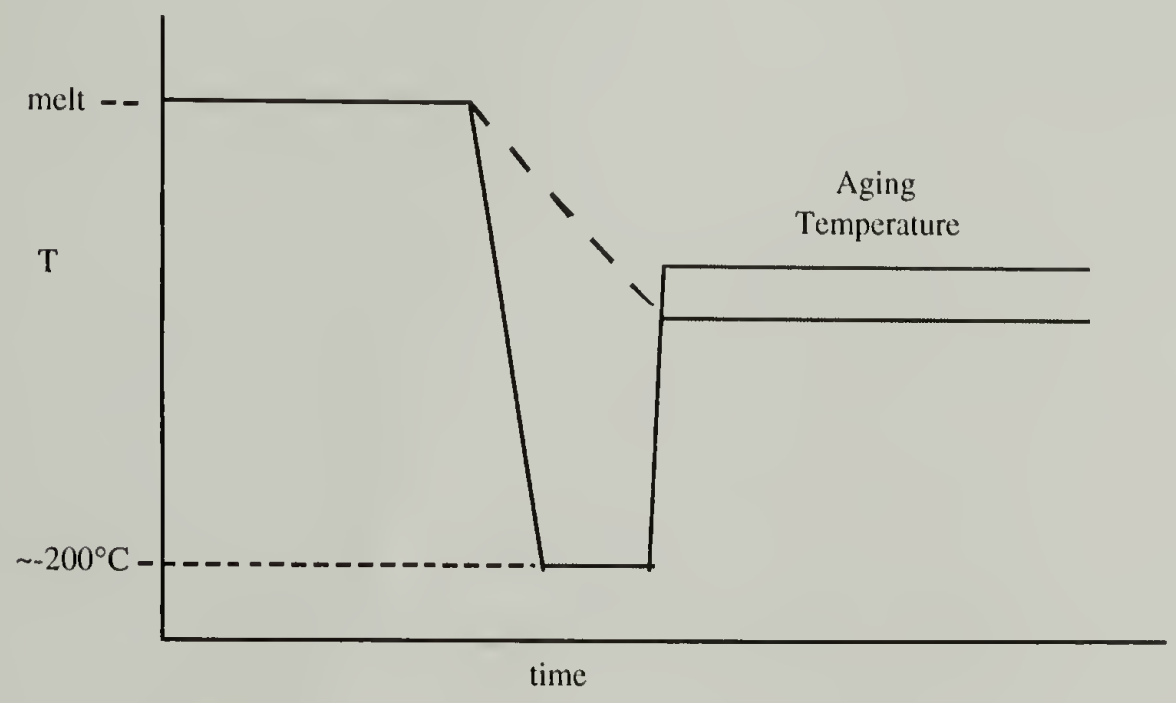

Figure 3.1 Thermal history of physical aging for mostly syndiotactic polypropylenes with different racemic content.

With these two samples, knowledge of the spectroscopic features associated with specific conformations and the conformation distribution were used to characterize the time, temperature, and configuration-dependent phase transformations associated with the ordering process. The data illustrated here was primarily for room temperature structural transformations. However, analysis takes advantage of related work[17] that characterized

the low temperature phase transformation from the amorphous state to the all trans structure.

In order to understand the impact of different thermal treatments and aging time on the phase transformation of the mechanical deformation, films were prepared in three different ways. One sample was prepared in a press set at 170 °C, and allowed to slowly cool to room temperature. After approximately 12 hours, it was mechanically deformed, and the Raman spectrum was run. A second sample was heated to melt, quenched in ice water, and mechanically stretched in the ice water. A third sample was prepared by heating it to the melt in the vacuum oven, and then removing it from the oven and allowing it to cool. During the cooling process, it was stretched. The Raman spectrum of each sample was measured, and compared with both a sample aged below 0°C, and a sample aged at room temperature.

For the 75% racemic sample, for which permanent deformation was not possible, the sample was prepared in the press at 170°C, and allowed to cool to room temperature. Subsequently, the Raman spectrum was taken before stretching, while in the deformed state, and after the deforming stress was removed.

3.3 Spectroscopic Characterization of Polypropylene Conformational Ordering, Defect Blockiness, and Amorphous Conformation Distribution

The analysis that follows uses the simulation method developed in Chapter 2 to model the time-dependent, configuration-dependent, and thermal history-dependent behavior of the samples described below. It is possible to characterize the changes in degree of ordering and conformation distribution based on the conformational mappings, and the temperature-dependent simulations of the conformation distribution for the Raman spectra.

The 92% racemic polypropylene sample shows significant time-dependent structural changes both at short times, less than 30 minutes, and longer times up to 40

hours. In a sample quenched from the melt into liquid nitrogen, structural changes were observed in the first 30 minutes as the temperature inereased, and for very short times afterward. In Figure 3.2a, the 826 cm^{-1} band, an extended helieal band, grows at the expense of the non-helieal band around 846 em^{-1}. This result clearly shows the rapid growth of ordered helieal strueture in the first 23 minutes. In addition, the amorphous band peak position starts around 849 em^{-1}, and shifts to 846 cm^{-1} at approximately six to seven minutes. Based on the amorphous ehain simulations, and the eonformational mappings in Chapter 2 (Figure 2.12a and 2.13a), the shift of the amorphous band peak to lower frequency indicates that the eonformation distribution is shifted toward more and longer helical sequences. It is not clear if the shift is due to the temperature of the ordering proeess, or it is due to the transformation of amorphous segments with long trans sequenees to helical sequenees in the ordering proeess. In Figure 3.2b, the major band rapidly shifts from approximately 305 em^{-1} to 313 em^{-1}, and beeomes more intense. In the melt speetrum shown in Figure 1.2b of Chapter 1, the major band peak position appears to be near 304 em^{-1}, whieh is consistent with the quenched sample described above. The frequeney ehange is eharaeterized based on the eonformational mappings in Chapter 2. The mappings indieate that shifting the ~306 cm^{-1} band to 313 cm^{-1} is due to growth of the length and eoneentration of the ordered helical structure from short helieal sequence lengths in the vicinity of $(ggtt)_1$ to $(ggtt)_3$ to extended helieal in the vicinity of $(ggtt)_4$ or longer (Figure 2.12b).

Wang, et al.[17] aged a sample at -5 °C, spontaneously produeing the zigzag eonformation. In their work the peak position of the amorphous phase band remained around 849 cm^{-1} over the entire time of the aging proeess. This frequeney was observed with the initial speetral observations shown in Figure 3.2a.

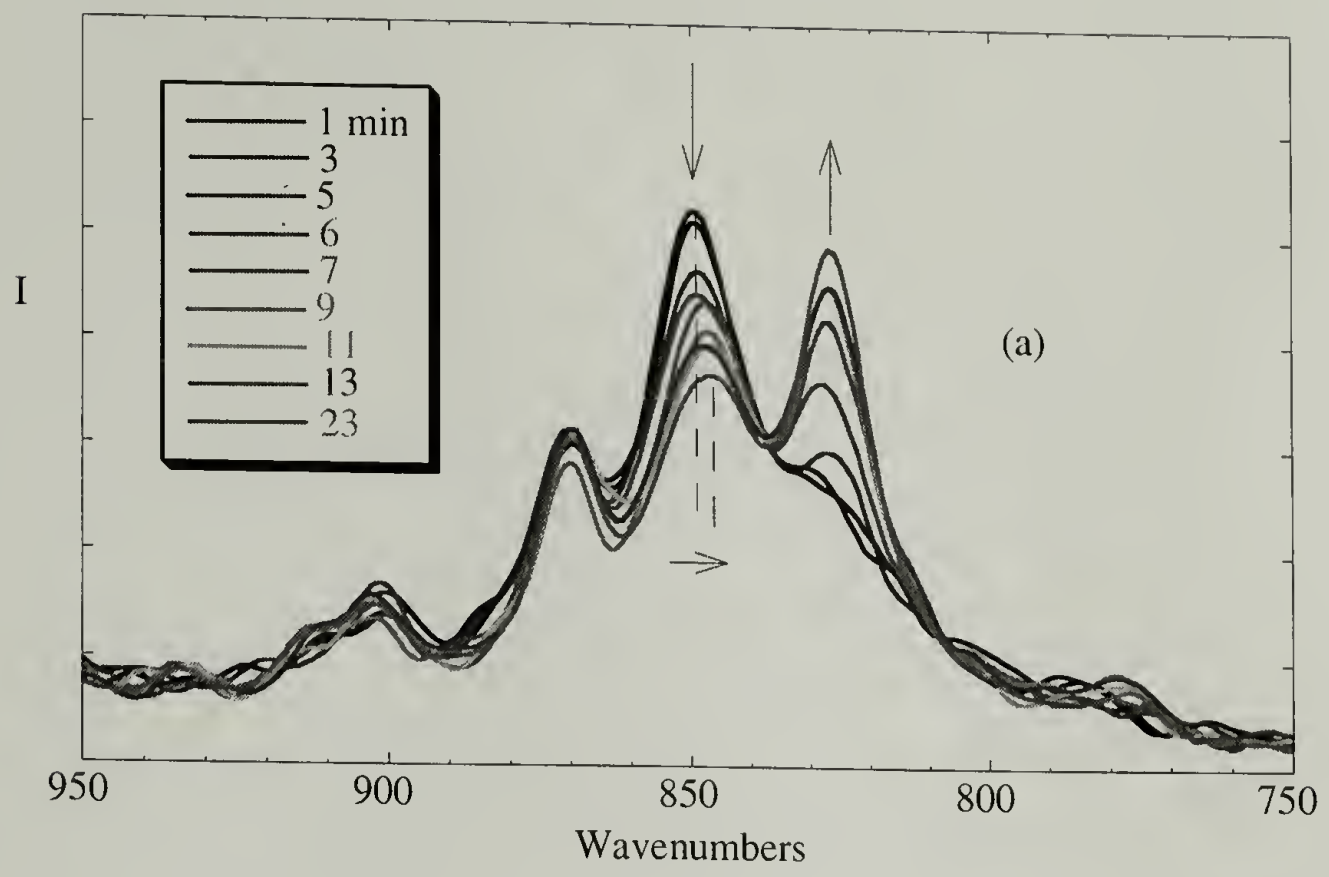

Figure 3.2 Short time changes in quenched syndiotactic polypropylene.

Unlike the short time measurements, room temperature and elevated temperature equilibration times on the order of 30 minutes to a one day for the 92% racemic sample show relatively small changes. Nevertheless, the 826 cm^{-1} band continues to increase at the expense of the 846 cm^{-1} band(Figure 3.3), indicating that the amorphous phase continues for an extended time to transform to the ordered helical phase. However, no significant changes are observed for the 313 cm^{-1} band after the first 30 minutes.

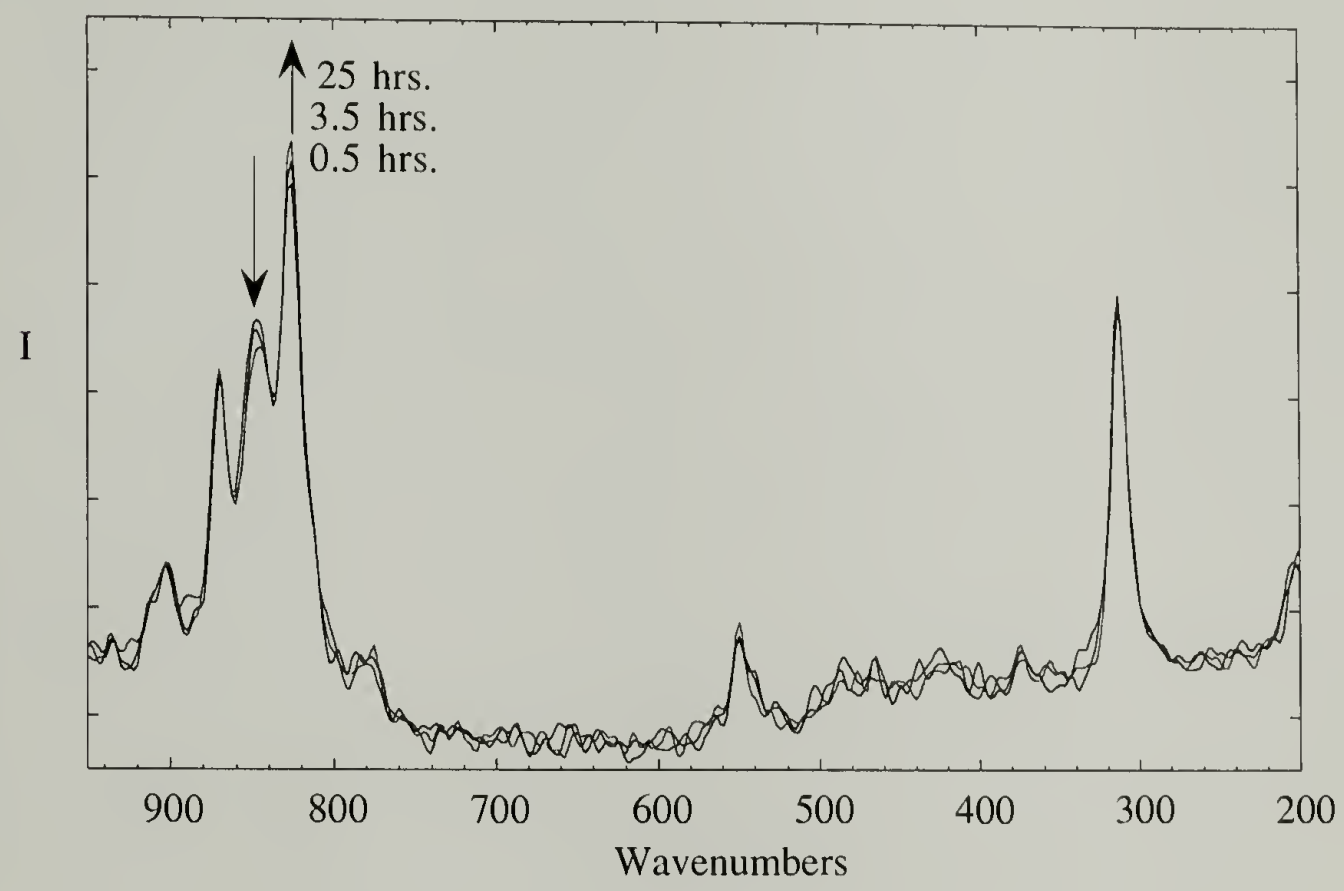

Figure 3.3 Aging of syndiotactic polypropylene.

The 75% racemic sample exhibits markedly different time dependent behavior than the 92% racemic sample. It shows no spectroscopically measurable structural development at very short times. Instead, it shows development of helical structure over extended time (around 34 hours) as shown in Figure 3.4a. Intensity of the band at 828 cm^{-1} slowly

increases at the expense of the amorphous band. The features give no information about any changes in the amorphous phase conformation distribution. Unlike the 92% racemic dyad sample, the 75% racemic dyad sample also shows significant changes in the peak position of the band around 300 cm^{-1} over long times (Figure 3.4b). This band, primarily a skeletal bending mode, shifts from about 305 cm^{-1} to 312 cm^{-1}. Again, this frequency shift indicates the growth of extended helical structure, as described above.

Spectroscopically, it is possible to determine the fraction of the material that is present in the helical state. Also, from the simulated spectra, it is possible to characterize a minimum length of helix that is necessary to spectroscopically observe conformational ordering. If the signal-to-noise ratio is high, as it is for the 92% racemic polymer, it is possible to accurately determine the relationship between the amorphous peak intensity and the helical band intensity by directly measuring the relative intensity changes between adjacent measurements and using the ratio of the changes as the intensity coefficient. If however, the signal-to-noise ratio is small, the determination requires a least squares fit of the data over the time scale of the measurements. The latter method was required for the 75% racemic sample. The results of this analytical determination are given in Figure 3.5 for the 75% racemic sample. The slope of the line represents the intensity coefficient **b**. The coefficient is used to calculate the helical fraction of material x_h:

$$x_h = \frac{I_h}{I_h + bI_{am}} \qquad (3.1)$$

where I_h represents the Raman intensity of the helical band, and I_{am} represents the intensity of the amorphous band.

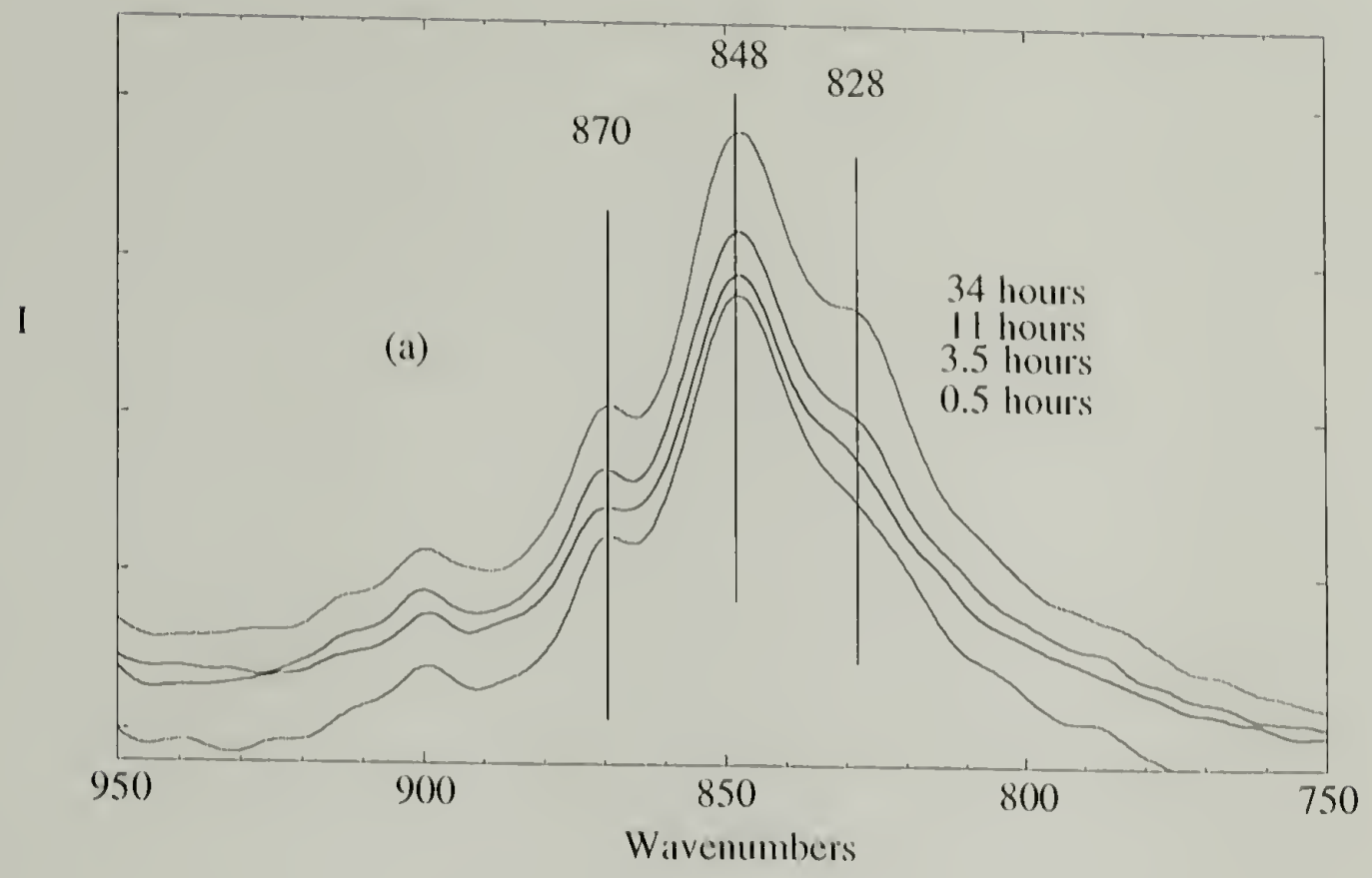

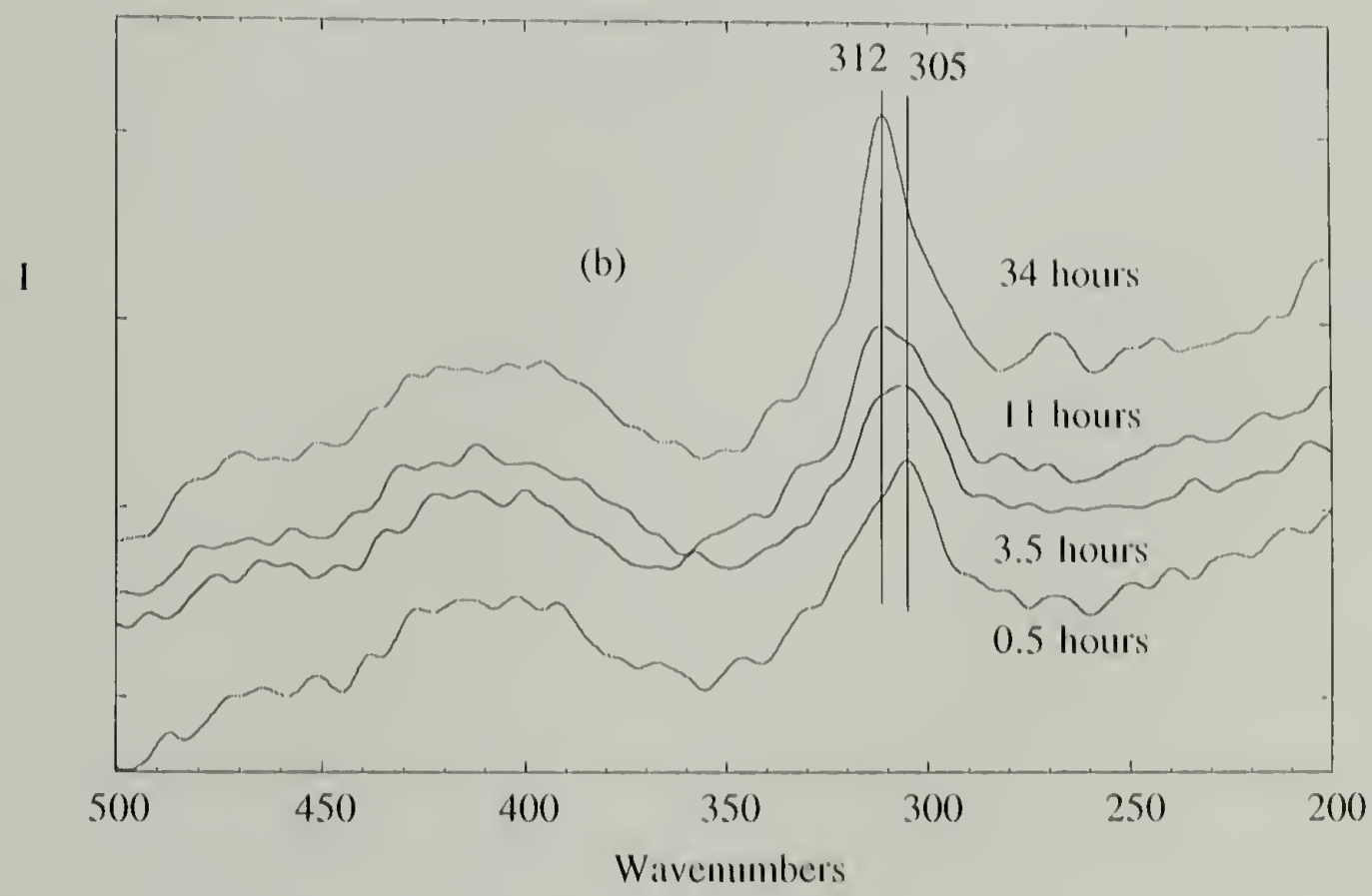

Figure 3.4 Aging spectra for 75 % racemic sample.

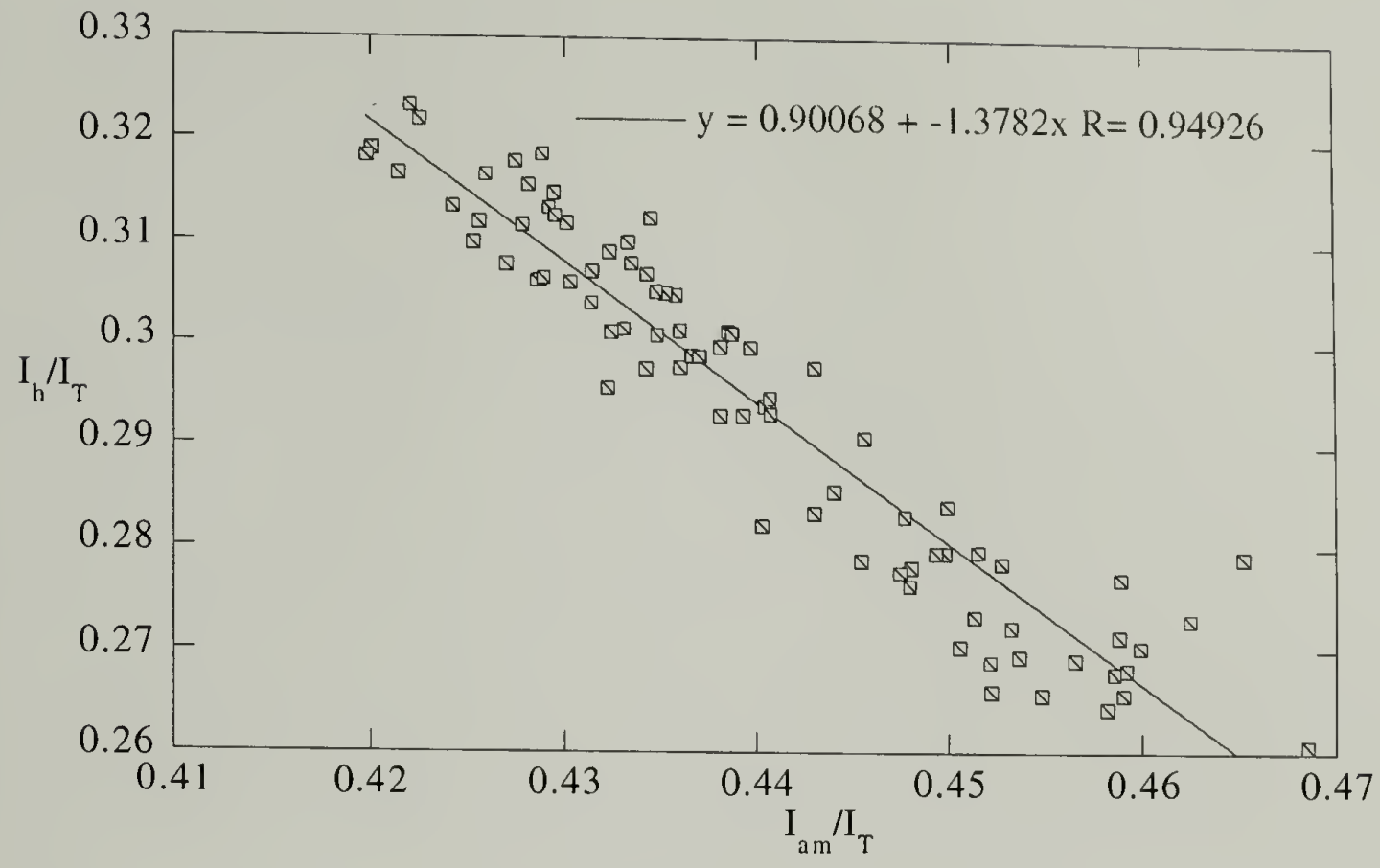

Figure 3.5 Relationship between helical and nonhelical band intensities for 75% racemic polypropylene with aging.

Based on these calculations, the fraction of extended helical polymer is plotted against time for all the samples studied (Figure 3.6). The 92% racemic polymer has more helical content than the 75% racemic sample (50 to 55% and up to 35% respectively). Based on Figure 2.12a and 2.13a, the minimum helix length required to observe the extended helical structure is $(ggtt)_4$ or longer. This requires a racemic sequence length of r_7 to r_8 (octads or nonads). For a random distribution of defects, the probability of observing racemic octads and nonads are given by:

$$P_{r_7} = P_r^7, \text{ and } P_{r_8} = P_r^8 \qquad (3.2)$$

For the 92% racemic sample, this gives an octad to nonad range of 50 to 56%, which is in line with the observed helical content. However, the 75% racemic dyad sample, based on equations 3.2 would have an octad to nonad content of only 11 to 15%, which is much

lower than the observed extended helical content of up to 35% found in Figure 3.6. This result suggests blockiness in the configurational defects.

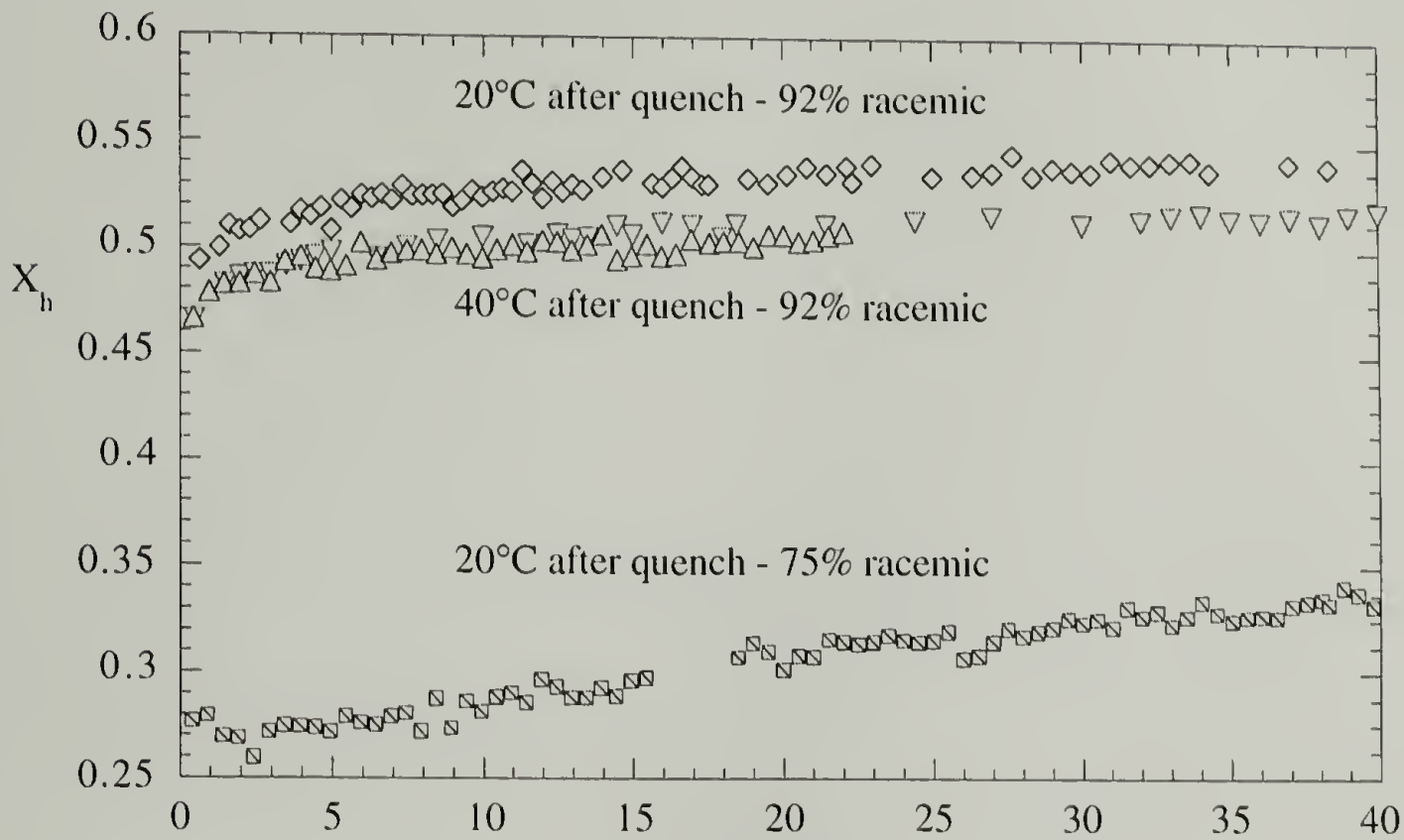

Figure 3.6 Fraction of polymer in the extended helical state.

The conventional method to obtain syndiotactic polypropylene in the all trans, or zigzag, state is to cold draw the material after quenching from the melt into ice water. The Raman spectrum of syndiotactic polypropylene drawn under these conditions is given in Figure 3.7. In contrast to the helical spectrum, the strongest band in the trans structure between 800 and 900 cm^{-1} is at 868 cm^{-1}, regardless of sample orientaiton. In addition, all trans Raman active band appear to be around 851 cm^{-1} or higher, and at 827 cm^{-1}. The peak at 313 cm^{-1} is not caused by the trans structure, but rather due to a small amount of helical polymer that is present. This assignment is based on the virtual absence of intensity in the simulated Raman spectrum around 300 cm^{-1} shown in Figure 2.10, as well as the

near coincidence of the peak position with the observed value for ordered helical syndiotactic polypropylene (Figure 2.8b). On the other hand, the very weak band around 425 cm^{-1} may be due to the trans structure. The simulated spectra of the different chain lengths give many different small peaks in this region, depending on the simulated chain length. The different intensities of the 868 and 827 cm^{-1} bands with sample orientation is a reflection of both chain alignment and the chain polarizability derivatives of the modes parallel and perpendicular to the draw direction. The same major features are shown for a sample that was stretched while cooling from the melt (Figure 2.10) or which has been aged for approximately 12 hours at room temperature (Figure 3.8). Therefore, quenching the sample prior to stretching is not necessary to observe the all trans structure. In Figure 3.9, the effects of stretching conditions are compared by overlaying the vertically oriented spectra. The room temperature aged sample, and the sample stretched while cooling from the melt virtually overlay in the 800 to 900 cm^{-1} region. In contrast, the cold drawn sample has higher amorphous band intensity, and this band is at a slightly higher frequency. In addition, the 828 cm^{-1} band for the cold drawn sample is lower intensity than the room temperature drawn samples. These observations indicate that the cold drawn sample has a higher amorphous phase concentration with the conformation distribution having more extended trans sequences, and less helical polymer present. The realization that the helical content is reduced for the ice-water stretched sample is also supported by the intensity difference in the 312 cm^{-1} band, with the ice water drawn sample having the lowest intensity.

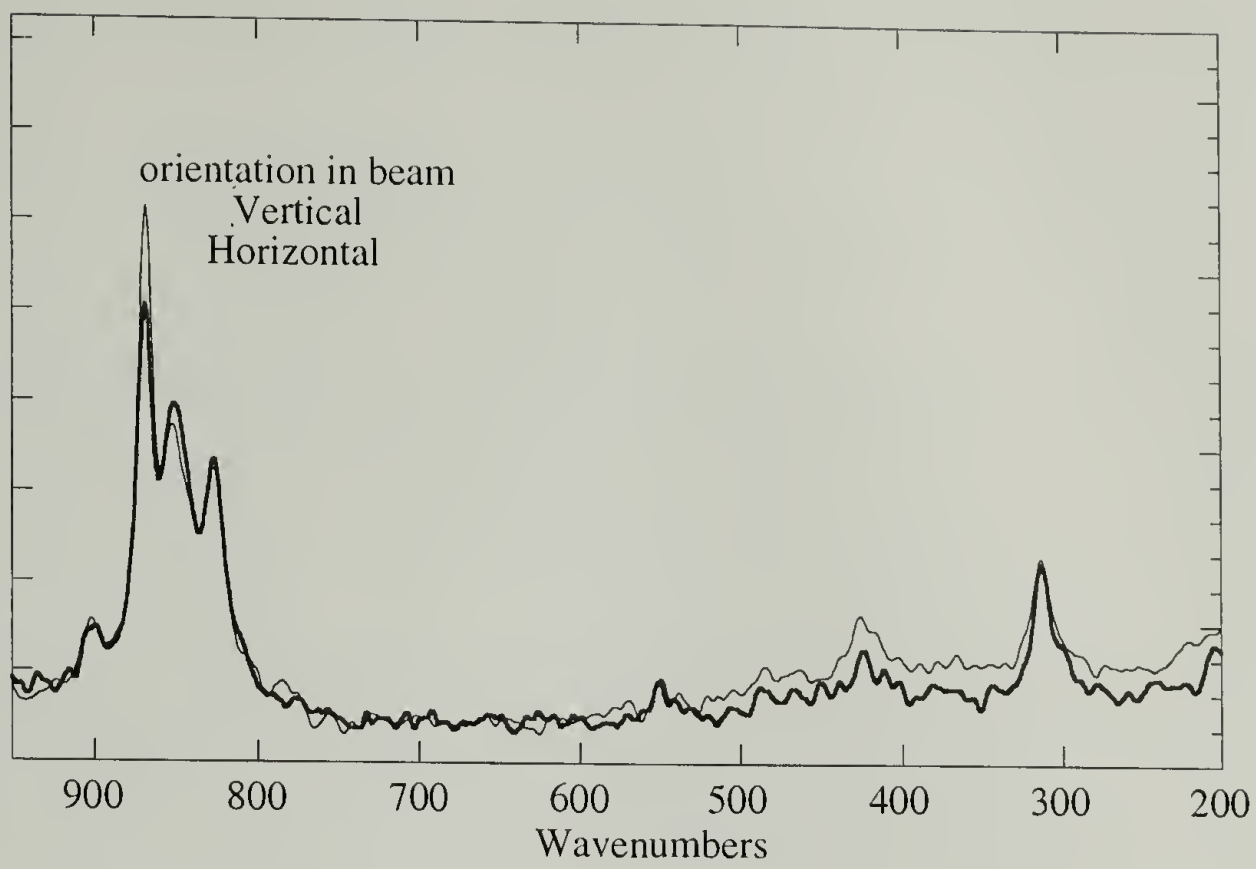

Figure 3.7 Syndiotactic polypropylene quenched from melt into ice water, and cold stretched.

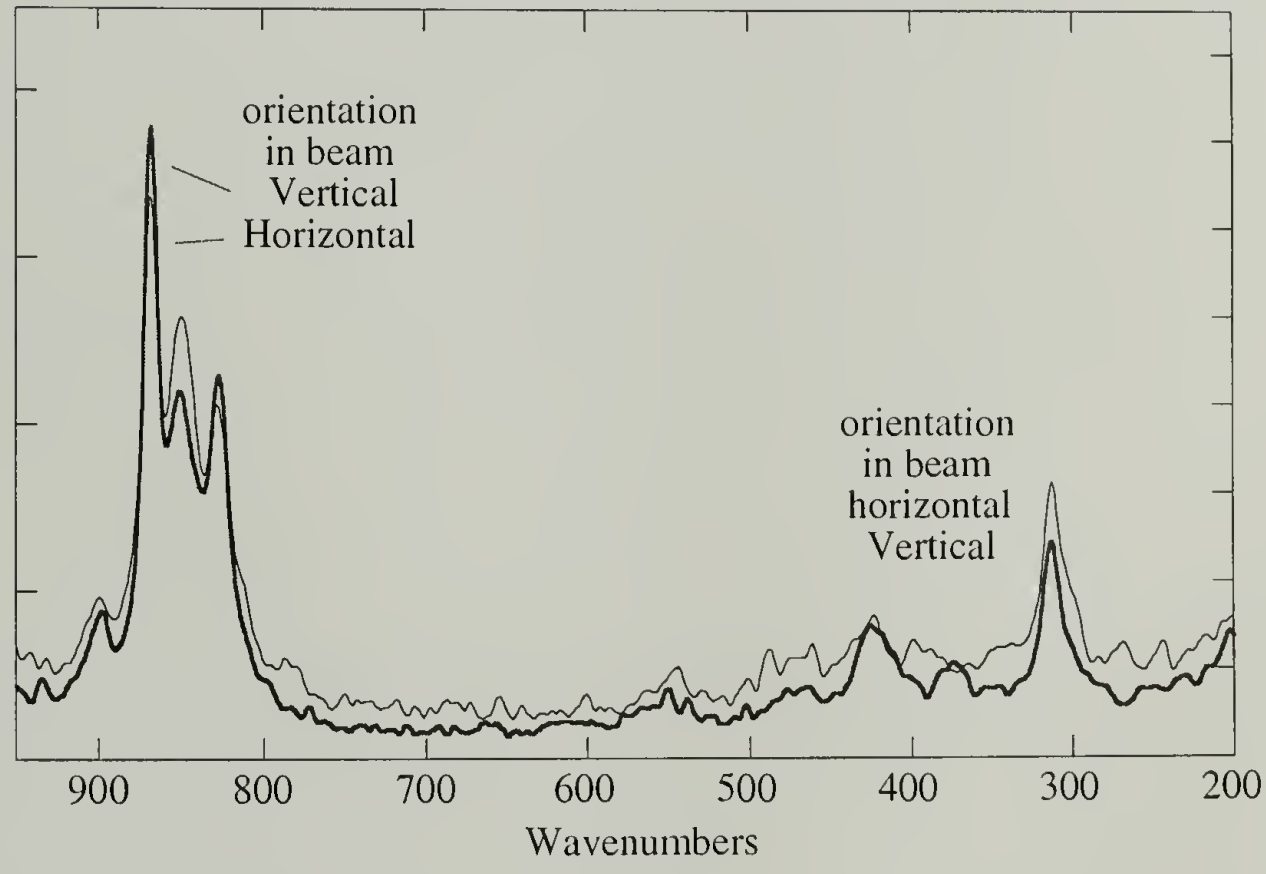

Figure 3.8 Syndiotactic polypropylene quenched from melt to room temperature, and stretched after 12 hours RT aging.

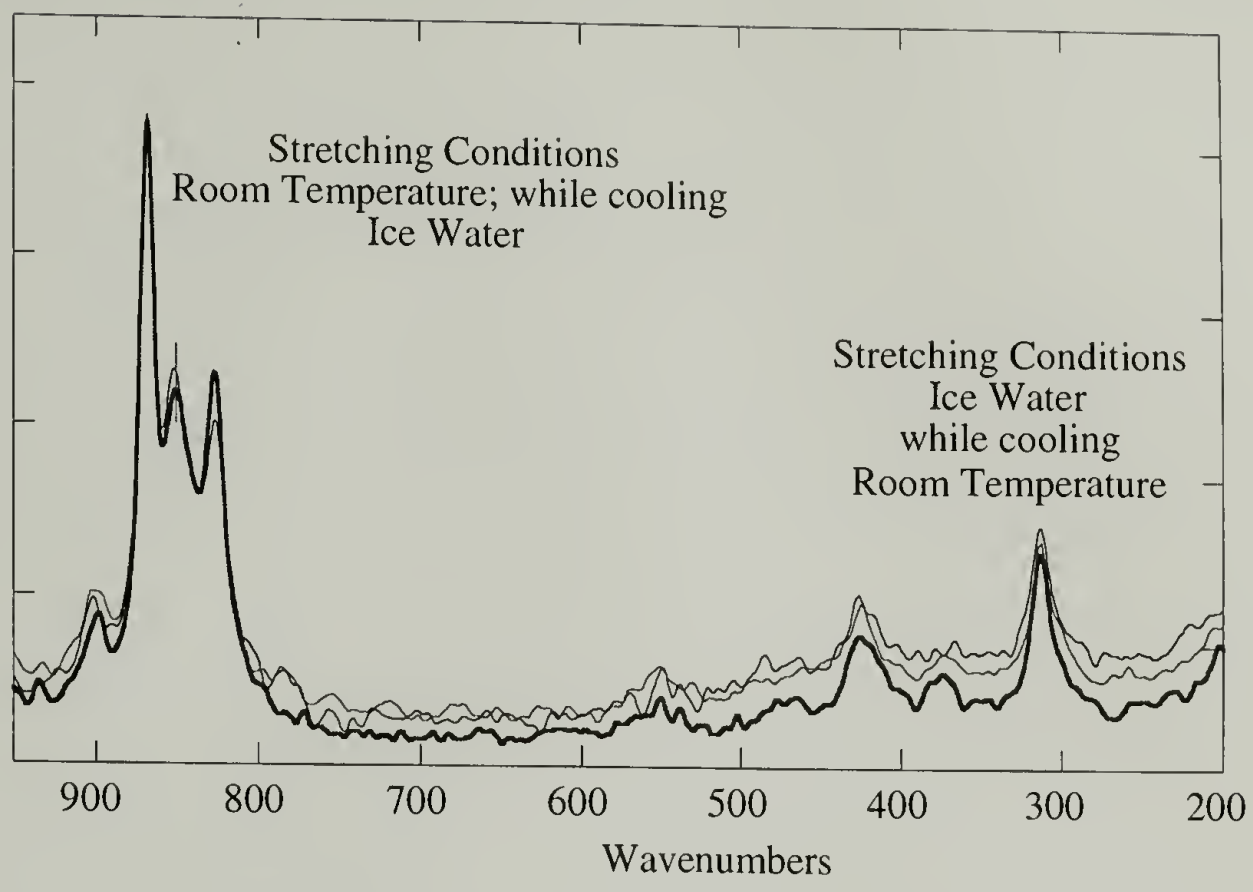

Figure 3.9 Formation of the trans conformation under different stretching conditions.

The 75% racemic polymer shows quite different response to mechanical deformation than the 92% racemic sample shows. The 75% racemic sample does not remain completely deformed after the stress is released. Therefore, studying the impact of the stretching process on the phase transformation means that the Raman spectrum of a stretch sample needs to be observed as the stress is being applied. A sample of this polymer was stretched about 1.5 days after pressing a film in the melt. The Raman spectrum was measured before deformation, while stretched, and after the stress was released. This comparison is shown in Figure 3.10. As the figure shows, deforming the sample resulted in the formation of the trans structure, much the same as shown for the 92% racemic sample. However, the concentration of the ordered trans state is quite small compared to the amorphous state in these samples. Also, upon release of the stress, the

stretched sample partially retracted toward its original dimensions, and the ordered trans structure population decreased slightly.

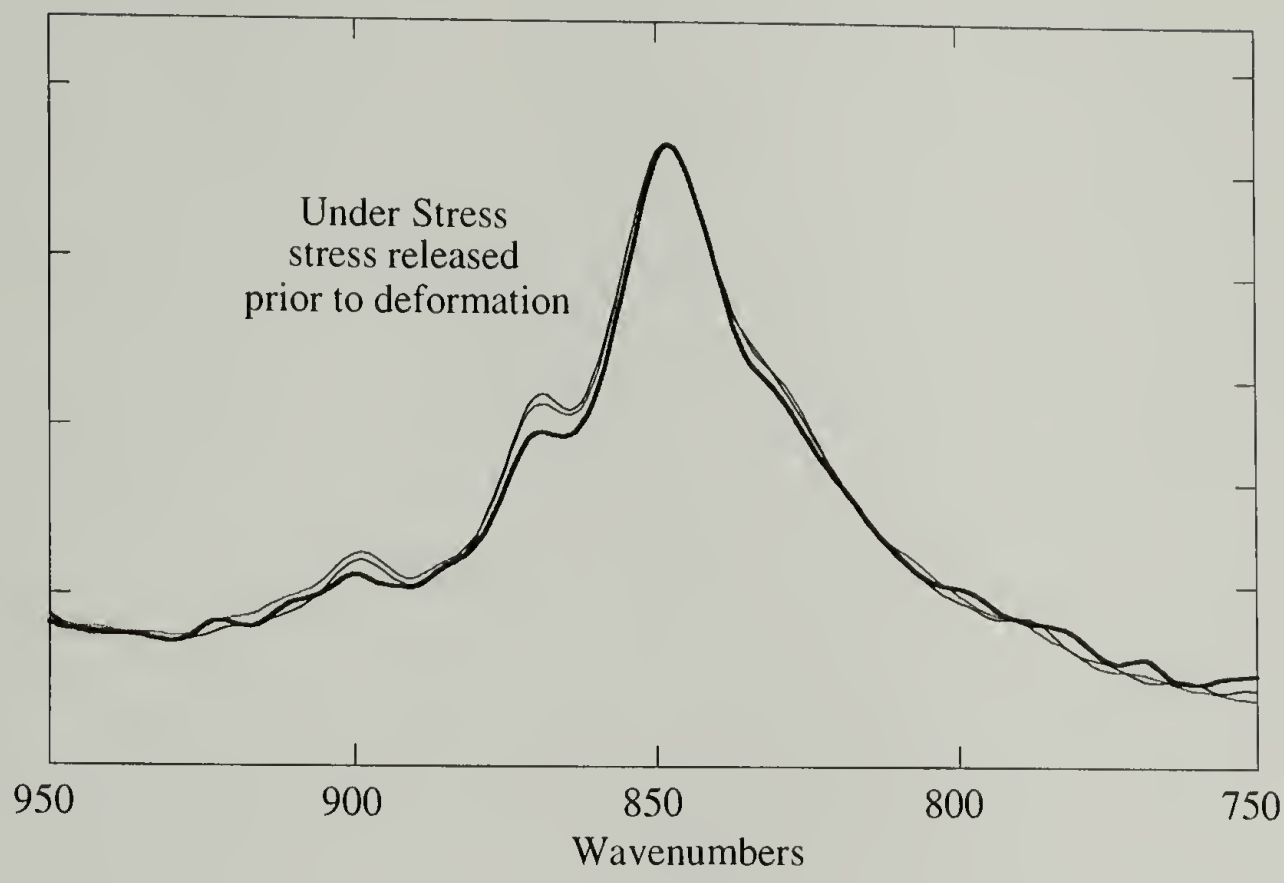

Figure 3.10 Impact of deformation on the structure development in 75% racemic polypropylene.

3.4 Conclusions

Changing the thermal history, configurational defects, aging temperature, and conditions for mechanical stretching all impact the extent and type of phase transformation that occurs. The amorphous phase conformation distribution that is observed at short times and for the duration of the analytical process depends both on the nature of the phase transformation and on the temperature at which the transformation occurs. Both the trans sample that was aged at -5°C, and the cold drawn sample have higher trans population in the amorphous phase, when compared to the samples aged or stretched at elevated temperatures.

The processing temperature also impacts the ordering structure, whether aged or stretched at the temperature of interest. Aging at moderate temperatures, around room temperature, gives the ordered helical structure. However, the helical structure can be transformed into the trans structure by mechanical deformation. This transformed sample will have higher helical population than a sample quenched from melt into ice water, and then stretched. Presence of large concentrations of configurational defects also severely impacts the nature of the observed transformation. The degree of ordering in the room temperature sample occurs to a much smaller extent for the 75% racemic sample than for the 92% racemic dyad sample. In addition, mechanically stretching the 75% racemic dyad sample induces the development of a small quantity of trans state polymer. However, this trans structure is not completely stable. Some of it reverts to amorphous phase when the stress is released.

These aging results indicate that the helical structure is kinetically the preferred crystal structure at moderate temperature, and the trans structure is the kinetically preferred state below 0°C, as illustrated by its spontaneous formation.[16,17] Under stress, syndiotactic polypropylene transforms to the planar zigzag conformation, regardless of the initial state, resulting in a high population of trans structure (Figure 2.10).

At low temperatures (<~0°C) the high energy amorphous state will tend to transform to the all trans state. This is because the energy barrier from amorphous to helical is significantly greater than the barrier from amorphous to trans.

At moderate temperatures, the energy barrier from amorphous to helical is readily overcome, and the helical state is rapidly formed as the more stable state. On the other hand, the energy barrier between the trans crystalline state to the helical energy state requires overcoming the trans crystalline lattice energy, and therefore is too high to readily occur at moderate temperatures. A more complete analysis of the lattice and conformational energies would be beneficial to test this description of the structural transformations.

The combination of low temperature and room temperature aging results with the stretched trans SPP Raman spectrum indicate that the amorphous phase conformation distribution changes with ordering temperature and mechanical stress. Below 0°C, spectroscopic evidence indicates that the amorphous phase has a greater tt population than above 0°C. This is supported both by the aging study of Wang, et al.[17] and the short time frequency shift in the 92% racemic sample (Figure 3.1a). Stretched SPP has a peak around 849 to 851 cm^{-1}, depending on the stretch direction (Figure 2.10). Two factors influence this peak position. First, the amorphous phase under stress appears to be represented by a greater tt population than the undeformed sample. Second, a small peak that comes from the zigzag structure appears to underlie the amorphous peak.

These conclusions are based on the spectroscopic evidence illustrating both frequency shifts and changes in peak intensities. The energy barriers of the phase transformations described above can be understood by more extensive temperature studies of the dynamics of the structural transformations, as well as dynamic simulation and energy minimization studies of the possible amorphous and ordered phases.

3.5 References

(1) Gornick, F.; Mandelkern, L. *Journal of Applied Physics* **1962**, 33, 907.

(2) Jean, Y. C.; Deng, Q. *Journal of Polymer Science: Part B: Polymer Physics Edition* **1992**, 30, 1359.

(3) Wang, Y. Y.; Nakanishi, H.; Jean, Y. C. *Journal of Polymer Science: Part B: Polymer Physics* **1990**, 28, 1431.

(4) Kobayashi, Y.; Zheng, W.; Meyer, E. F.; McGervey, J. D. *Macromolecules* **1989**, 22, 2302.

(5) Kluin, J.-E.; Yu, Z.; Vleeshouwers, S.; McGervey, J. D.; Jamieson, A. M.; Simha, R.; Sommer, K. *Macromolecules* **1993**, 26,

(6) Tsay, F. D.; Hong, S. D.; Maocanin, J.; Gupta, A. *Journal of Polymer Science: Polymer Physics Edition* **1982**, 20, 763.

(7) Royal, R. S.; Torkelson, J. M. *Macromolecules* **1992**, 25, 1705.

(8) Royal, J. S.; Victor, J. G.; Torkelson, J. M. *Macromolecules* **1992**, 25, 729.

(9) Royal, R. S.; Torkelson, J. M. *Macromolecules* **1993**, 26, 5331.

(10) Lamarre, L.; Sung, C. S. P. *Macromolecules* **1983**, 16, 1729.

(11) Natta, G.; Peraldo, M.; Allegra, G. *Die Makromolekulare Chemie* **1964**, 75, 215.

(12) Sozzani, P.; Galimberti, M.; Balbontin, G. *Makromol. Chem. Rapid Commun.* **1992**, 13, 305.

(13) Sozzani, P.; Simonutti, R.; Comoti, A. *Magnetic Resonance in Chemistry* **1994**, 32, s45.

(14) Chatani, Y.; Maruyama, H.; Noguchi, K.; Asanuma, T.; Shiomura, T. *J. Polym. Sci. Polym. Phys. Lett.* **1990**, 28, 393.

(15) Chatani, Y.; Maruyama, H.; Asanuma, T.; Shiomura, T. *J. Polym. Sci. Polym. Phys. Ed.* **1991**, 29, 1649.

(16) Nakaoki, T.; Ohira, Y.; Hayashi, H.; Horii, F. *Macromolecules* **1998**, 31, 2705.

(17) Wang, Y.; Hahn, T. D.; Hsu, S. L.; Stidham, H. D.; Seidle, A. **1998**, Manuscript in Preparation.

CHAPTER 4

OBSERVING A MONOLAYER TRANSITION IN POLY(DIMETHYL SILOXANE) LANGMUIR FILMS

4.1 Introduction

In chapters 2 and 3, vibrational spectroscopy was used to characterize phase transformations influenced by thermal history, mechanical deformation, and configurational defect distribution. In this chapter, the structural transformations considered pertain to spreading a polymer from solution to form a monolayer film. The consequence of the spreading is conformation change and chain orientation relative to the surface. These microstructural changes are dictated by the polymer geometry, the nature of the interface, and the polymer-substrate interaction. In the case of poly(dimethyl siloxane), which is the system described here, it is shown that the structure of the spread film also depends on the available surface area.[1]

Since at least 1947,[2] scientists have been studying the surface pressure versus surface area or surface concentration of poly(dimethyl siloxane).[3-10] Upon compression the isotherm begins at zero surface pressure at surface concentrations significantly below 0.75 mg/m^2. Around $\Gamma_1 \approx 0.75$ mg/m^2, the surface pressure π jumps substantially to about 9 mN/m, where it exhibits a plateau until about $\Gamma_2 \approx 1.6$ mg/m^2, where a small π jump occurs followed by a smaller rise. Oligomers with strongly adsorbing end groups may also show other transitions.[11] Structural features associated with the various transitions have often been debated. Particular controversy has arisen over the structural features associated with the π plateau around 9 mN/m between Γ_1 and Γ_2.[5,7,8]

Fox and coworkers constructed possible structures at the various transition points by using molecular models with tetrahedral geometry.[2] At low surface pressures, these

workers suggested a caterpillar-like structure with all the oxygens in the water, and all the methyl groups pointing away from the water surface. The structure becomes considerably twisted with an initial jump in surface pressure. Compression in the surface pressure plateau around 9 mN/m corresponds to a molecular transformation from the twisted caterpillar-like structure to a helix with the helix axis parallel to the water surface. Noll et al.[10] proposed similar structures in the π plateau region, and the caterpillar structure was suggested as the structure that adsorbs to galena in ore flotation. Thermodynamic studies of Granick and coworkers have suggested that linear and large cyclic poly(dimethyl siloxane) chains undergo similar transitions in the region of the π plateau.[4] Granick et al. also stated that a negative temperature coefficient of π suggests that decreasing the surface area of poly(dimethyl siloxane) films in the plateau region corresponds to a slight surface entropy increase. Characterization of the isotherm with damping of capillary waves supports an exchange between two structures in the vicinity of the π plateau.[3] Lenk and coworkers[11] have also pointed out that, due to the bond angle differences along the backbone with Si-O-Si ~145°, and O-Si-O ~ tetrahedral, an extended chain structure cannot persist for very many units without leaving the water surface, or twisting of the backbone. Mann and Langevin attempted to characterize the isotherm with Brewster angle ellipsometry.[7] Lee, Mann, Langevin, and Farnoux extended the work of Mann and Langevin with small angle neutron scattering,[5] and Mann, Henon, Langevin, and Meunier extended their work further with Brewster angle microscopy.[8] Collectively these three papers were unable to explain the π plateau between Γ_1 and Γ_2, and also questioned the coexistence of two structures in this region.

This chapter presents a study of the microstructural features of poly(dimethyl siloxane) CH_3-[$Si(CH_3)_2$-0]$_n$-$Si(CH_3)_3$, spread at the air-water interface in the vicinity of the π plateau at 9 mN/m. Epifluorescence microscopy has been used in the past to illustrate

the coexistence of two phases in the vicinity of a surface pressure plateau.[12-14] In addition, poly(dimethyl siloxane) spread at the air-water interface is characterized by external reflectance infrared spectroscopy.

4.2 Experimental

Poly(dimethyl siloxane) of M_W = 37,000 and M_W/M_n = 1.6 was purchased from United Chemical Technologies, Inc., and was used as supplied. The fluorescent probe 1-palmitoyl-2-[12-[(7-nitro-2-1,3-benzoxadiazol-4-yl)amino] decanoyl] phosphatidyl choline NBD-PC was purchased from Avanti Polar Lipids and was used as supplied in 1 mg/ml chloroform solution. All solutions of poly(dimethyl siloxane) were prepared using spectroscopic grade dichloromethane as solvent.

Isotherm experiments were conducted on a commercial NIMA type 611 Langmuir-Blodgett trough on deionized water. Water surface purity was established by compressing the barriers and aspirating the surface until no surface pressure change accompanied further compression or expansion. All samples were spread on water from solutions of concentrations near 20 mg/ 100 ml, and were allowed to stand at least 15 minutes to assure complete evaporation of solvent. Surface pressure measurements were made with a filter paper Wilhelmy plate suspended from an electrobalance.

Micrographs of poly(dimethyl siloxane) spread on water from 3.26 mg/ml in dichloromethane solution containing 0.0196 mg/ ml NBD-PC were obtained using a Zeiss Axioplan epifluorescence microscope equipped with a 1.6X camera eyepiece and a 32X objective focused on the air-water interface in a Langmuir trough specifically constructed to fit the microscope stage. Light from a Xenon lamp source is passed through a band pass filter that selects 450 - 490 nm radiation, followed by a dichroic mirror which reflects wavelengths shorter than 510 nm and passes wavelengths longer than 510 nm. The reflected light passes through the objective and is focused on the water surface. Fluorescence centered near 534 nm is excited by the focused light near 460 nm, returns

through the objective and is passed by the dichroic mirror. A long pass filter with a cutoff at 520 nm is set above the dichroic mirror to block scattered light. The fluorescent image is then focused on a Genisys microchannel plate photomultiplier manufactured by Dage MTI, from which a thermal print is made.

External reflectance infrared spectra were obtained with a Perkin-Elmer System 2000 FTIR equipped with a Specac Langmuir Trough reflectance attachment purchased from Specac Ltd., operated with s polarization at 30° angle of incidence. Resolution was set at 4 cm^{-1} and 2048 scans were co-added to obtain the background, 100% and sample spectra of infrared radiation reflected at the air-water interface in the trough. The surface of de-ionized water was compressed as far as possible and aspirated several times at the beginning of each run to achieve maximum surface cleanliness. Poly(dimethyl siloxane) samples were typically spread from solution concentrations approximately 20 mg/100 ml in spectroscopic grade dichloromethane and allowed to set at least 15 minutes before the sample spectra were collected.

4.3 Results and Discussion

Figure 4.1 shows a typical isotherm for poly(dimethyl siloxane) film cast on a water surface. At surface concentrations less than $\Gamma_1 \approx 0.75$ mg/m^2 π is essentially zero. Near this concentration, π rises sharply to about 9 mN/m, and remains at this value between Γ_1 and $\Gamma_2 \approx 1.6$ mg/m^2. At Γ_2, the surface pressure again rises slightly and then increases very slowly thereafter.

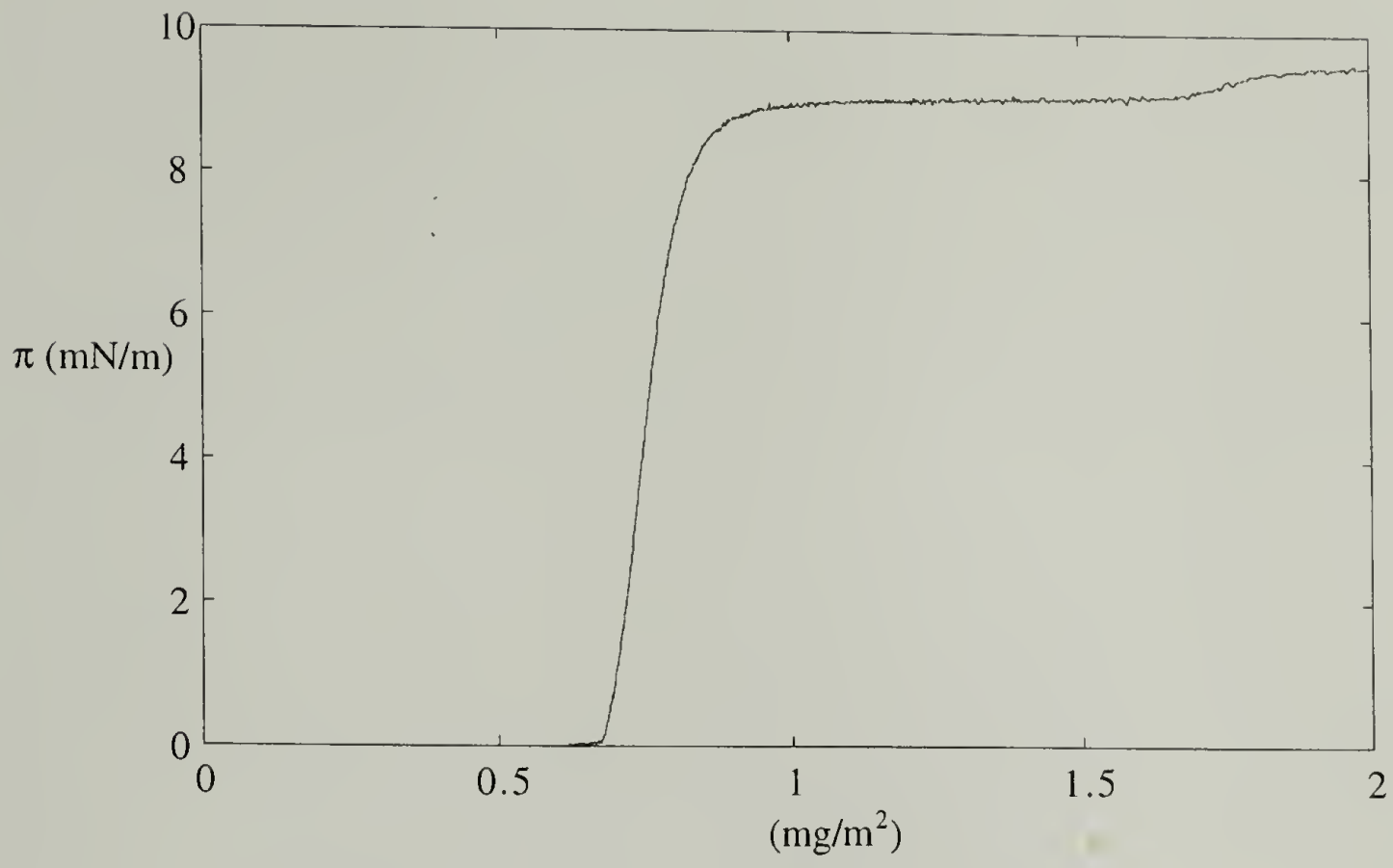

Figure 4.1. Poly(dimethyl siloxane) isotherm on water.

4.3.1 Epifluorescence Microscopy

Figure 4.2 shows bright and dark domains in a typical fluorescence micrograph for poly(dimethyl siloxane) spread on water in the plateau region at a surface concentration between Γ_1 and Γ_2. Upon further compression, the bright domains increase at the expense of the dark domains, providing evidence for the coexistence of two distinct surface structures. The relative areas of the bright and dark domains may be measured, and the fraction X of the area that is dark may be calculated. The fraction may also be calculated from the average surface concentration Γ by assuming a linear response

$$X = \frac{\Gamma - \Gamma_2}{\Gamma_1 - \Gamma_2} \qquad (1)$$

Figure 4.3 shows a plot of X calculated from the light and dark areas of a micrograph against X calculated from the linear assumption. The linear behavior of this plot strongly suggests a progression between two distinctive structures in the plateau region between Γ_1 and Γ_2. Since Γ_2 is 2.13 times as great as Γ_1, the film thickness at Γ_2 is probably about twice that at Γ_1, provided the film bulk density is not too different at the two concentrations.

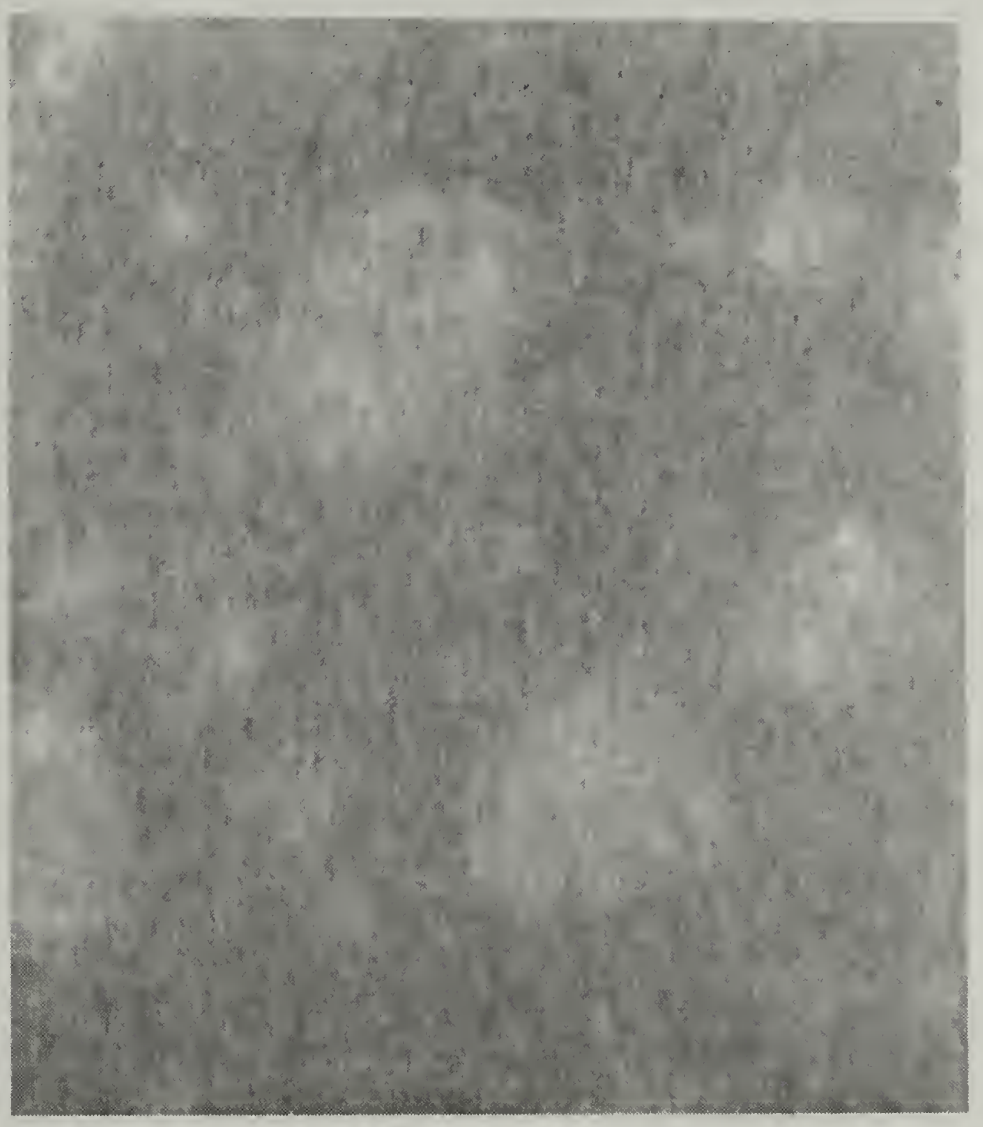

Figure 4.2. Epifluorescence microscopy micrograph for poly(dimethyl siloxane) film spread on water at 1.1 mg/m^2, with 0.6% by weight probe on polymer.

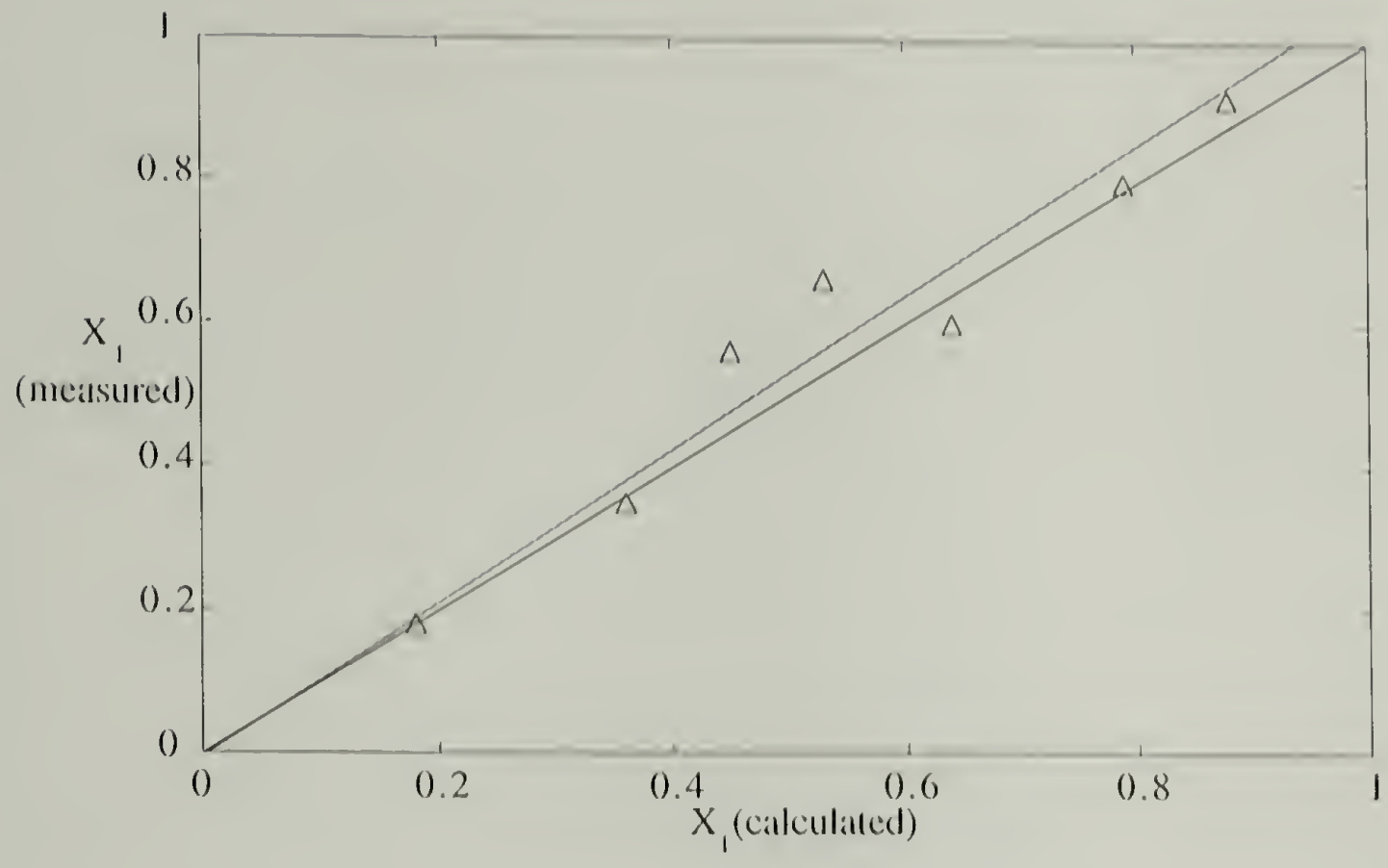

Figure 4.3. Lever rule calculated and microscopy measured component fraction of Γ_1 structure between concentrations Γ_1 and Γ_2.

4.3.2 External Reflectance Infrared Spectroscopy

External reflectance infrared spectroscopy provides further evidence for the coexistence of two structures in the plateau region between Γ_1 and Γ_2, and suggests that the structure at Γ_2 is more ordered. Representative external reflectance infrared spectra are displayed in absorbance mode in Figure 4.4, together with a 100% line for reference. The broad band in the 1000-1100 cm^{-1} region has been assigned to the asymmetric Si-O-Si stretching mode by several authors,[15,16] and the sharp band centered at 1264 cm^{-1} to the symmetric methyl deformation, consistent with the early suggestion of Wilmshurst.[17]

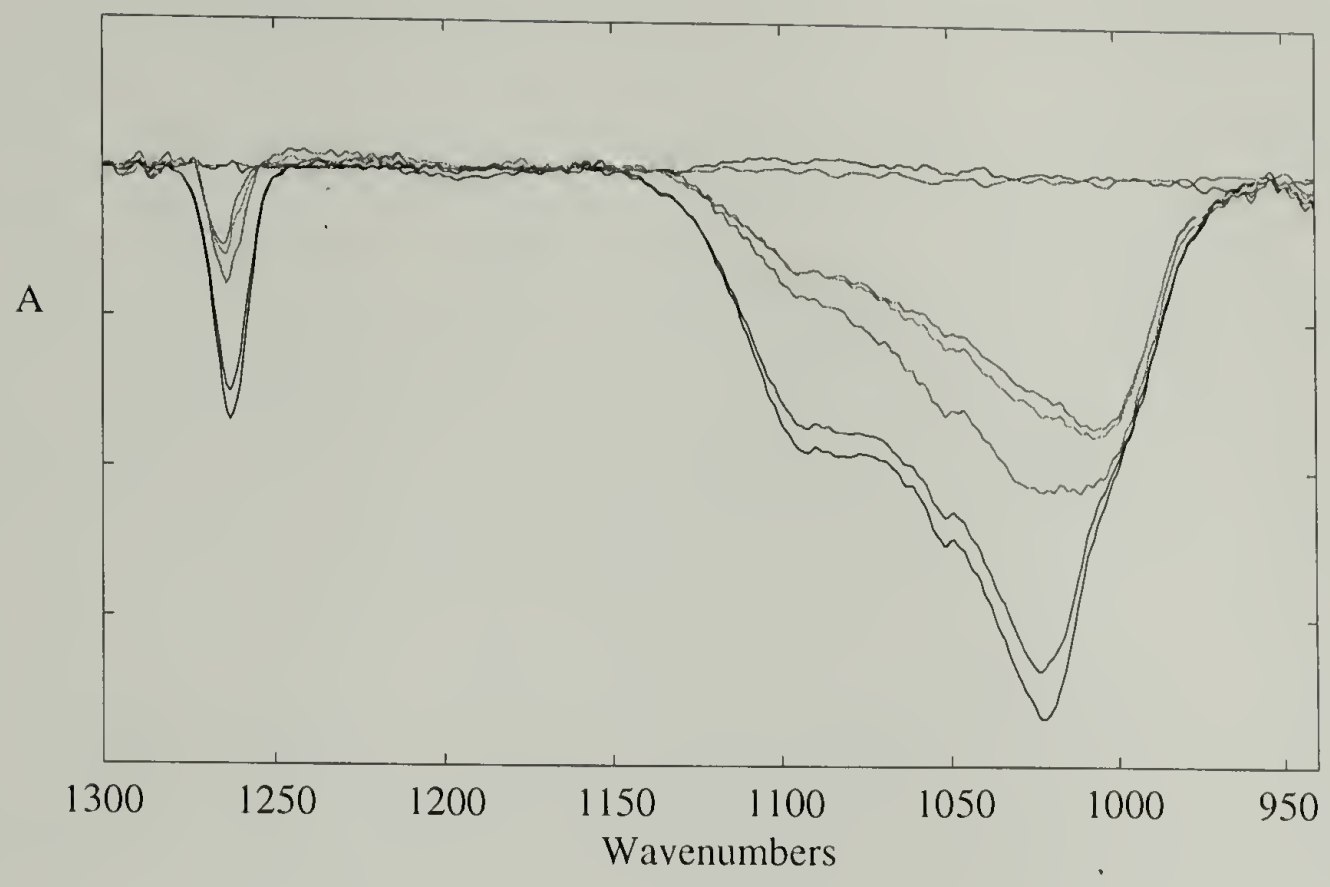

Figure 4.4. External reflectance infrared spectra for poly(dimethyl siloxane) film spread on water at several concentrations between Γ_1 and Γ_2.

4.3.2.1 Local Environment

A broad band containing several components is found in the 1000-1100 cm^{-1} region. The features of the band change significantly as the surface concentration is varied between Γ_1 and Γ_2. At Γ_1 the most intense band is at 1005 cm^{-1}. At Γ_2, the most intense peak occurs at 1020 cm^{-1}. Weaker components are found around 1055 and 1090 cm^{-1}. All components persist to some extent at all concentrations studied. In Figure 4.5, the 1000 - 1100 cm^{-1} region is plotted with all spectra normalized by division by the corresponding surface concentration. These spectra suggest that the 1020 cm^{-1} band originates in one structure and the 1005 cm^{-1} band in another. Konopka and Stojczyk[18] found that the frequency of the asymmetric Si-O-Si stretching vibration varies in solvents of varying dielectric constants and dipole moments, and showed that in many cases the frequency shifts to lower values with increasing dielectric constant in accordance with the theoretical

model due to Kirkwood, Bauer, and Magat.[19] Some cases proved better described by the later model of Allerhand and von Schleyer.[20] The dielectric constant of water is one of the highest known, and the observations of Konopka and Stojczyk suggest that Si-O-Si linkages in aqueous surroundings should usually be expected to display shifts in the asymmetric stretching frequency of the order of 15 cm^{-1} relative to the frequency of the group in surroundings of much lower dielectric constant. These expectations are consistent with the observations shown in Figures 4.4 and 4.5, the low frequency of 1005 cm^{-1} suggesting contact of the Si-O-Si groups with water in reflectance spectra obtained at low surface concentrations.

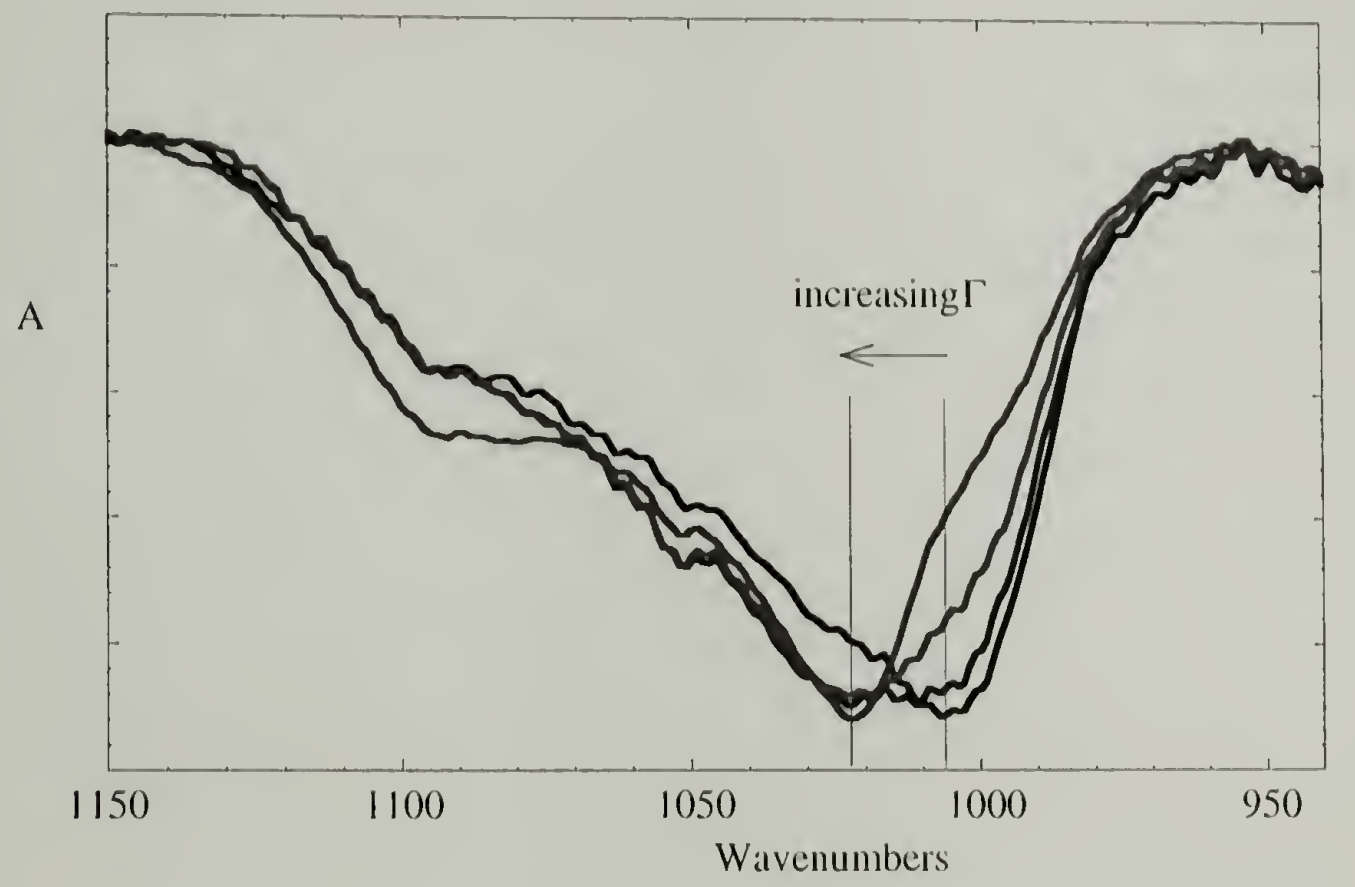

Figure 4.5. Scaled external reflectance infrared spectra of the ν_{as} band for poly(dimethyl siloxane) film spread on water at several concentrations between Γ_1 and Γ_2.

The external reflectance infrared spectrum obtained for each surface concentration can be represented as a linear combination of absorbances of the constituents measured at

each frequency. If $A_\nu(\Gamma)$ is the composite absorbance value at surface concentration Γ at a frequency ν, while $A_\nu(\Gamma_1)$ is the absorbance at ν for Γ_1 and similarly $A_\nu(\Gamma_2)$ is that for Γ_2, the composite spectrum may be constructed by superposing the contributors at each frequency as

$$A_\nu(\Gamma) = X\, A_\nu(\Gamma_1) + (1\text{-}X)\, A_\nu(\Gamma_2) \qquad (2)$$

The composite spectrum $A_\nu(\Gamma)$ synthesized in this way can then be plotted against the observed spectrum $A_\nu(\Gamma)_{exp}$ initially for the value of X with which the trough was charged. Although $A_\nu(\Gamma_1)$ and $A_\nu(\Gamma_2)$ are only available experimentally, and each of these two spectra contain evidence of traces of the dominant constituent in the other, fairly good empirical fits can be made by least squares procedures that minimize the squares of the residuals at each frequency. The residual r_ν at ν is

$$r_\nu(X) = A_\nu(\Gamma)_{exp} - [X\, A_\nu(\Gamma_1) + (1\text{-}X)\, A_\nu(\Gamma_2)] \qquad (3)$$

and X is varied to produce a minimum in the sum of the squared residuals, the sum running over all the points sampled in the frequency interval. A comparison of one such fitted spectrum with a measured spectrum is shown in Figure 4.6. Similar fits were obtained for other surface concentrations between Γ_1 and Γ_2. A comparison between values of X obtained from equation (1) and the value of X used to fit the corresponding spectrum is shown in Figure 4.7. These results support the fluorescence microscopy observation of two coexistent surface phases in the plateau region between Γ_1 and Γ_2.

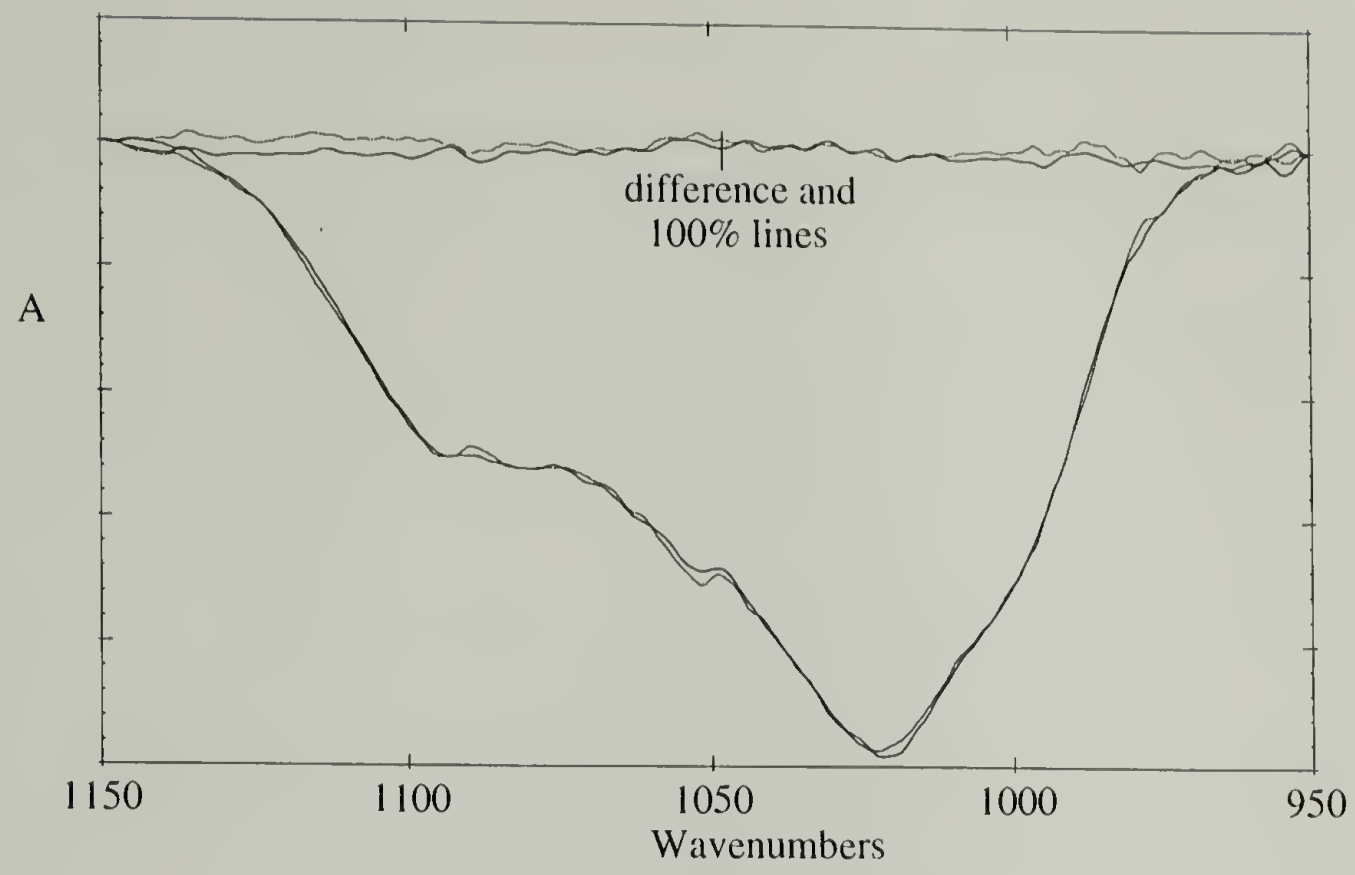

Figure 4.6. Measured and constructed spectra at $X_1 = 0.58$, for the band described in Figure 4.5.

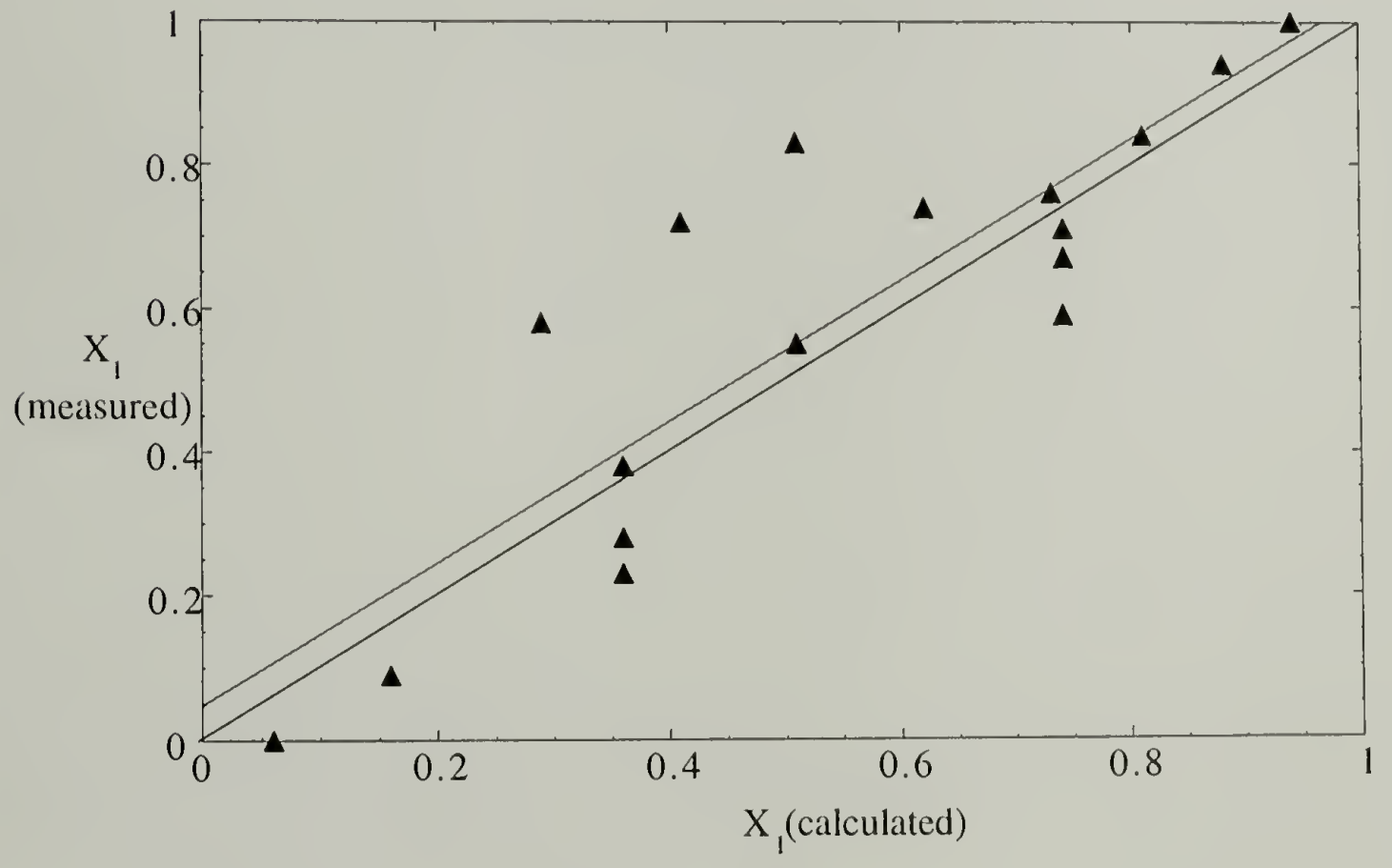

Figure 4.7. Lever rule calculated and infrared measured component fraction of Γ_1 structure between concentrations Γ_1 and Γ_2.

4.3.2.2 Average Segmental Orientation and Conformation

Figure 4.4 shows that the 1264 cm^{-1} band does not shift in frequency as surface concentration is changed, and that there is no observable splitting into several components. Figure 4.8 shows that when the integrated peak absorbance of this band is divided by surface concentration and then plotted against surface concentration, the absorbance/concentration ratio is not constant. The plot jumps between extreme values at the limiting surface concentrations Γ_1 and Γ_2. Reference to Figure 4.9 shows that the symmetric methyl deformation must have two components whose transition moments lie in the C-Si-C plane, one parallel to the angle bisector, and the other perpendicular to it. If the structure of the poly(dimethyl siloxane) molecules in the surface film at Γ_1 is one in which the hydrophobic methyl groups are as far from the air-water interface as possible while the hydrophilic O-Si-O groups are attracted to the water surface, the plane containing the C-Si-C group will tend to be perpendicular to the water surface. Spectra obtained with s polarization will then be predominantly sensitive to the components represented by the intersection between the planes of C-Si-C and water. If there is a helical structure that occurs in the phase at Γ_2, many of the planes containing C-Si-C groups have some angle significantly different from perpendicular to the water surface. Thus, the transition moments in the C-Si-C plane will tend to have greater projections onto the water surface than those at Γ_1. Figure 4.8 thus indicates that segmental orientation is different at the two extremes of surface concentration and that the intrinsic intensity of the 1264 cm^{-1} band can be used to provide a measure of the origin of the difference. The following is an account of our attempt to make these qualitative considerations more quantitative.

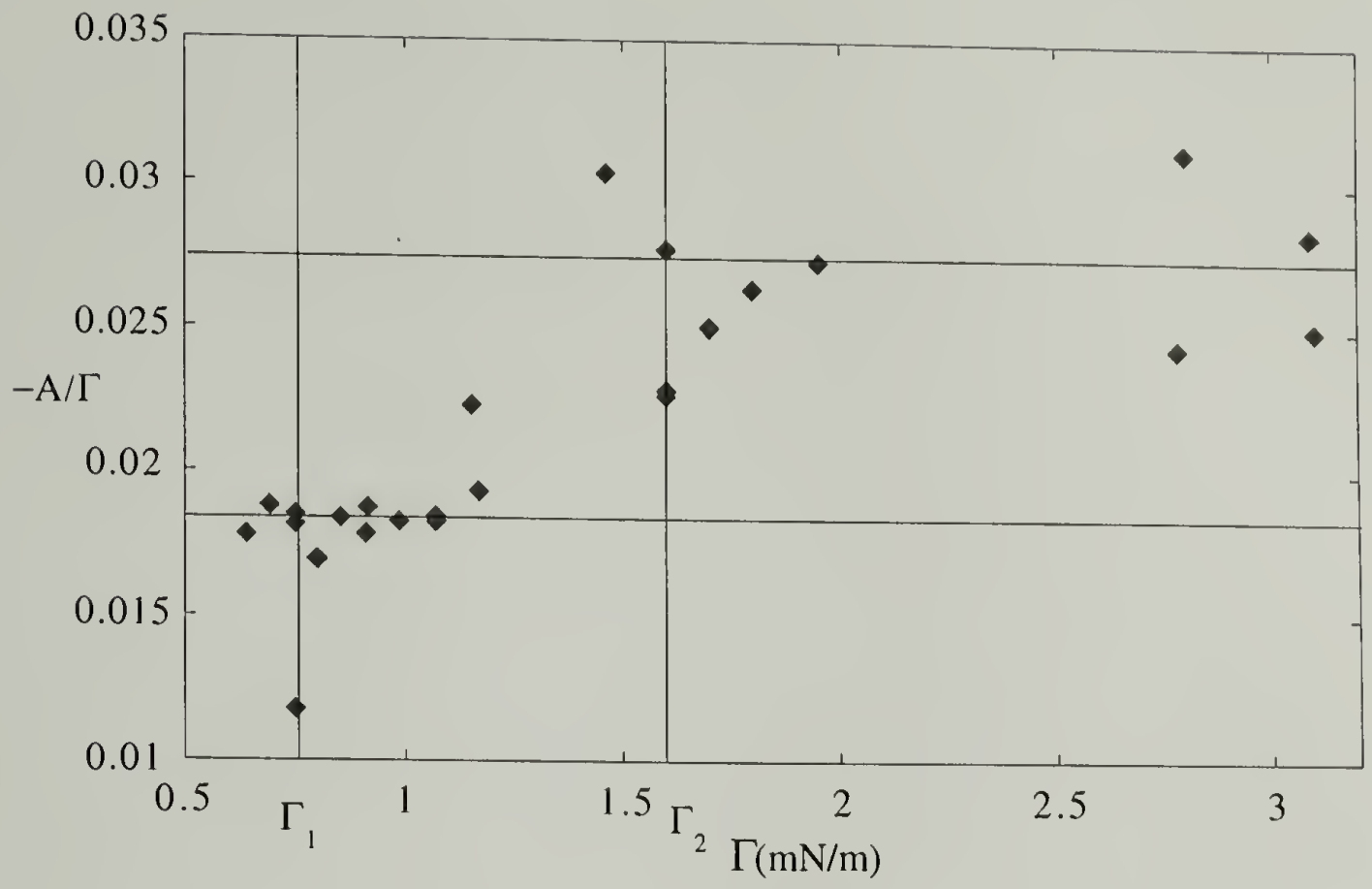

Figure 4.8. Absorbance divided by surface concentration versus surface concentration for the orientation sensitive band at 1264 cm^{-1}, as described in the text.

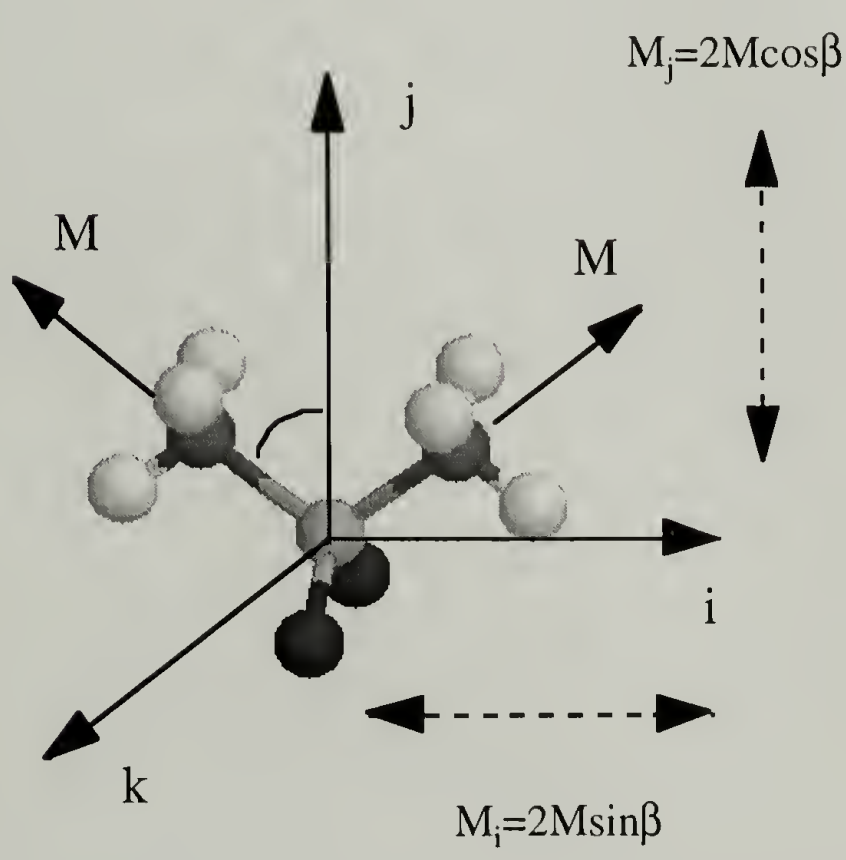

Figure 4.9. Transition moments for the band at 1264 cm^{-1}, as described in the text.

The calculation starts by projecting one transition moment $M_i = 2\ M \sin(\beta)$ for the out-of-phase symmetric deformation onto the laboratory x axis. For simplicity, the in-phase and out-of-phase deformations are represented using the same moment M, related to the transition moment for an isolated methyl group. The laboratory x axis is defined by the electric vector of the incident light. Since only s polarization was used, the x axis lies in the plane of the air-water interface. The projected transition moment $M_{X,i}$ is

$$M_{x,i} = M_i \sin(\gamma)\cos(\phi) \tag{4}$$

The average absorbance for transition moment M_i can be represented as

$$A_{x,i} = \int_0^{2\pi} \int_0^{\pi} a(\gamma,\phi) M_{x,i}^2 \sin(\gamma) d\gamma d\phi \tag{5}$$

where $a(\gamma,\phi)$ is a distribution function.[21] Since the in-phase and out-of-phase deformations are accidentally degenerate, there are two transition moments for each monomer segment at the same frequency. The calculation of the in-phase symmetric deformation absorbance is as above, with the replacement of $A_{x,i}$ with $A_{x,j}$, $M_{x,i}$ with $M_{x,j}$ and M_i with $M_j = 2\ M \cos(\beta)$. Since there is no component perpendicular to the C-Si-C plane for these vibrations, $M_k = 0$ and the total is the sum of the averaged contributions

$$A_x = A_{x,i} + A_{x,j} \tag{6}$$

For totally random orientation, $a(\gamma,\phi)$ is a constant. Since only ratios are involved in the interpretation, for simplicity $a(\gamma,\phi)=a$ is normalized to unity by writing

$$\int_0^{2\pi} \int_0^{\pi} a \sin(\gamma) d\gamma d\phi = 1 \tag{7}$$

The result for random orientation is then

$$A_x = \frac{2}{3} M^2 \tag{8}$$

If one of the three axes i, j, or k is constrained to be perpendicular to the air-water interface, the absorbance calculation involves only the plane angle ϕ. For the i^{th} component,

$$A_{X,i} = \int_0^{2\pi} a(\phi) M_{X,i}^2 d\phi \qquad (9)$$

The surface is assumed to be isotropic, and $a(\phi)=a$ is a constant. As above, $a(\phi)$ is normalized to unity, the condition for which is

$$\int_0^{2\pi} a \, d\phi = 1 \qquad (10)$$

In this case, $M_{X,i} = 0$ if the i axis is normal to the surface, but $M_{X,i} = M_i \cos \phi$ if the i axis is in the xy plane. There are three cases. If the k axis is normal to the plane, both the i and j axes lie in the plane and contribute to the total absorbance. The result is exactly $A_X = 2M^2$. However, if the j axis is perpendicular to the plane, only the i axis contributes, and the result is $A_X = 2\ M^2 \cos^2 \beta$ while if the i axis is perpendicular to the plane, only the j axis contributes and the result is $A_X = 2\ M^2 \sin^2 \beta$. When $\beta \approx 55°$ is used for a tetrahedral geometry, the result is $0.66\ M^2$ or $1.34\ M^2$. These results would be applicable to models involving the all-trans silicon-oxygen chain perpendicular to the air-water interface ($2\ M^2$), or lying flat on the surface with the j axis in the xy plane ($0.66\ M^2$) or with the i axis in the xy plane ($1.34\ M^2$), depending on how the chain was rotated about the long axis. These results are summarized in Table 4.1.

Table 4.1 Measured Absorbances, and Calculated Absorbances for Different Structures.

Structure	**Absorbance A/Γ**
$A(\Gamma_1)$	0.017
$A(\Gamma_2)$	0.026
$A(\Gamma_2)/A(\Gamma_1)$	1.5
Isotropic	2/3 M^2
Extend chains, all trans and linear:	
Perpendicular to water surface	2 M^2
parallel to water surface	0.66-1.34 M^2
Twisted Caterpillar*	1 M^2
Helical structure:	
Helix Axis perpendicular to water surface	1.22M^2
Helix axis parallel to water surface	1.34 - 1.45 M^2

* This value would be the average of the absorbance values with the chain parallel to water surface. The same absorbance value would also be measured for the 2-D random walk, assuming that the chain axis for each monomer is strictly confined to be in the xy plane.

In the twisted caterpillar model, the chain axis, which is the k axis at each monomer unit, lies in the xy plane, and the j and i axes can have any orientation relative to the surface normal. If M_i and M_j are oriented randomly with respect to the normal to the surface, each contributes equally and the average absorbance A_X is just M^2.

The crystal structure of poly(dimethyl siloxane) has been reported by Damaschun to exhibit C_2 symmetry, with six repeating monomer units per cell.[22] This structure is taken as representative of short helical segments that may form in the more compressed film at surface concentration Γ_2. To obtain the atomic coordinates, the suggested structure of Damaschun was constructed using the program Cerius^{2TM}.[23] This was used to visualize the projections required for transition moment averaging. For this purpose, it is convenient to define a set of orthogonal axes u, v, w, two of which lie in the same plane as the b and c axes of the unit cell. Then the a axis forms an angle with the third axis that is defined by

the crystal structure, in which a and b are perpendicular to c, but a is not perpendicular to b. If two of the axes u, v, w are taken in the xy plane, the third is normal to it, and it is possible to model helical structures which are aligned either parallel or perpendicular to the water surface. Figure 4.10 shows how each transition moment is projected onto the u, v, w axes by the projection cosines, which are then projected onto the x axis. The contribution of one of the monomer repeating units designated by the index σ is

$$M_{x,i}^{\sigma} = M_u^{\sigma} \cos\phi + M_v^{\sigma} \sin\phi$$

$$= M_i \cos\theta_i^{\sigma u} \cos\phi + M_i \cos\theta_i^{\sigma v} \sin\phi \qquad (11)$$

which makes a contribution to the absorbance A_x as

$$A_{x,i}^{\sigma} = \frac{1}{2} M_i^2 \{\cos^2\theta_i^{\sigma u} + \cos^2\theta_i^{\sigma v}\}$$

$$= \frac{1}{2} M_i^2 \{1 - \cos^2\theta_i^{\sigma w}\} \qquad (12)$$

Adding the in-phase and out-of-phase contributions produces the contribution from one monomer unit

$$A_x^{\sigma} = \frac{1}{2} M_i^2 \{1 - \cos^2\theta_i^{\sigma w}\} + \frac{1}{2} M_j^2 \{1 - \cos^2\theta_j^{\sigma w}\} \qquad (13)$$

The total absorbance is the average of the six individual contributions

$$A_x = \frac{1}{6} \sum_{\sigma} A_x^{\sigma} \qquad (14)$$

allowing the absorbance to be calculated for any specific orientation of the helix. If the helix axis is perpendicular to the water surface, $A_x = 1.22\ M^2$, but if the helix axis is parallel to the water surface, the slightly larger result depends on the orientation of the helix, lying between $1.34\ M^2$ and $1.45\ M^2$, as shown in Table 4.1.

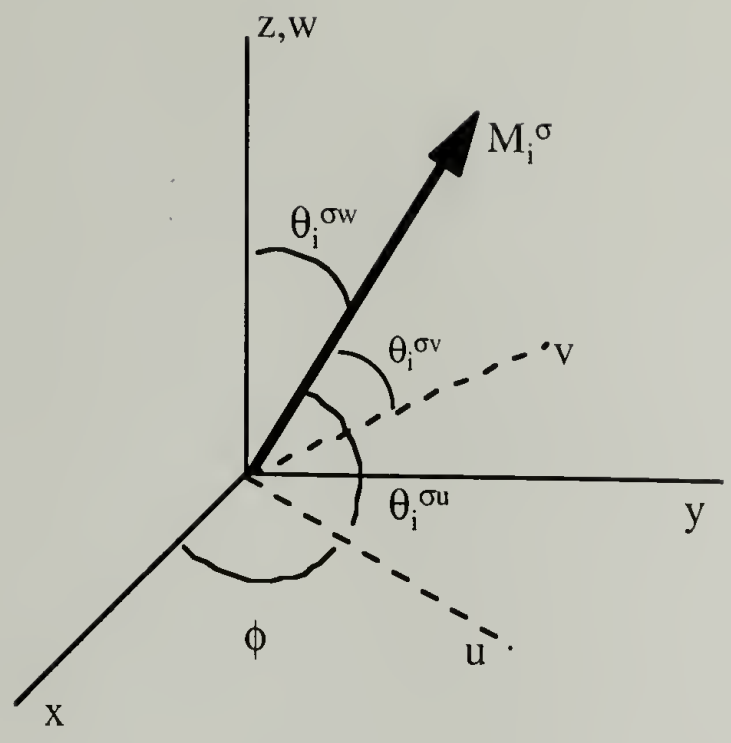

Figure 4.10. Projection of a transition moment M_i^σ from repeat unit σ onto the x- axis using projection cosines and intermediate axes (u,v,w).

The experimental values of peak absorbances A/Γ are 0.017 at Γ_1, and 0.026 at Γ_2, giving a ratio of about 1.5. The ratio of twisted caterpillar to isotropic is 1:2/3 = 1.5, suggesting that perhaps the isotropic case applies at Γ_1 and the twisted caterpillar at Γ_2. This would indicate that the structure at Γ_1 is more three-dimensional than at Γ_2, in conflict with the expectation that the film thickness at Γ_2 be about twice that at Γ_1. Alternatively, a caterpillar structure is conceivable at Γ_1 and the more ordered helical structure with the helix axis parallel to the water surface at Γ_2, since the ratio would then lie between 1.34 and 1.45, within experimental error of the observed ratio. An all trans chain structure at Γ_2 appears to be ruled out since such a structure exposes the oxygen atoms to interaction with water, and the frequency of the asymmetric Si-O-Si stretching vibration is increased by 15

cm^{-1} at Γ_2 from that at Γ_1, indicating that the oxygen atoms are largely protected from interaction with water in the structure at Γ_2. This observation argues strongly for a helical structure at Γ_2, in which the oxygen atoms are somewhat interior to the helix, and are protected from interaction with water. Additionally, most of the oxygen atoms are above the water when the helix is oriented with the helical axis parallel to the water surface. None of the other structures considered here is capable of providing similar protection. Certainly, the structure at Γ_2 must be more ordered than at Γ_1, since the experimentally determined ratio of scaled absorbances A/Γ is 1.5, and Table 4.1 shows that the introduction of structure forces the ratio to exceed unity, whether the structure at Γ_1 is taken as isotropic or twisted caterpillar. Furthermore, the 15 cm^{-1} frequency shift suggests that the structure at Γ_2 denies the oxygen atom access to water. The only structure at Γ_2 consistent with these requirements is helical with the helix axis parallel to the water surface.

4.4 Conclusions

In order to characterize the changing structures of poly(dimethyl siloxane) adsorbed to the air-water interface, both external reflectance infrared spectroscopy and epifluorescence microscopy have been used. In the vicinity of the surface pressure plateau between approximately 0.75 and 1.6 mg/m^2, the fluorescence microscopy results show bright domains and dark domains, the relative areas of which are consistent with a surface phase transition. The external reflectance infrared results indicate that the stable phase at the higher concentration is one in which the oxygen atoms of the polymer backbone are largely excluded from contact with the water surface, whereas the oxygen atoms are in intimate contact with the water surface at the lower concentration. The ratio of the scaled reflected absorbance values for the symmetric methyl deformation at 1264 cm^{-1} to the

surface concentration is not constant over the concentration range. The ratio of the scaled absorbance at the high concentration end to the scaled absorbance at the low concentration end is 1.5±0.4, consistent with the reflected absorbance ratios predicted for several possible ordered poly(dimethyl siloxane) structures. The stable structures consistent with the observed spectra at the concentration limits are the twisted caterpillar, or two-dimensional random coil, stable at the lower limit, and possibly a helical structure which has the helix axis parallel to the air-water interface at the upper limiting surface concentration.

4.5 References

(1) Hahn, T. D.; Stidham, H. D.; Hsu, S. L. *Macromolecules* **1997**, 30, 87.

(2) Fox, H. W.; Taylor, P. W.; Zisman, W. A. *Industrial and Engineering Chemistry* **1947**, 1401.

(3) Garrett, W. D.; Zisman, W. A. *J. Phys. Chem.* **1970**, 70, 1796.

(4) Granick, S.; Clarson, S. J.; Formoy, T. R.; Semlyen, J. A. *Polymer* **1985**, 26, 925.

(5) Lee, L. T.; Mann, E. K.; Langevin, D.; Farnoux, B. *Langmuir* **1991**, 7, 3076.

(6) Lee, L. T.; Langevin, D.; Mann, E. K.; Farnoux, B. *Physica B* **1994**, 198, 83.

(7) Mann, E. K.; Langevin, D. *Langmuir* **1991**, 7, 1112.

(8) Mann, E. K.; Henon, S.; Langevin, D.; Meunier, J. *J. Phys. II, France* **1992**, 2, 1683.

(9) Mann, E. K.; Langevin, D.; Henon, S.; Meunier, J.; Lee, L. T. *Ber. Bunsenges. Phys. Chem.* **1994**, 98, 519.

(10) Noll, W.; Steinbach, H.; Sucker, C. *Journal of Polymer Science: Part C* **1971**, 34, 123.

(11) Lenk, T. J.; Lee, D. H. T.; Koberstein, J. T. *Langmuir* **1994**, 10, 1857.

(12) McConnell, H. M. *Annual Review of Physical Chemistry* **1991**, 42, 171.

(13) Mohwald, H. *Annual Review of Physical Chemistry* **1990**, 41, 441.

(14) Weis, R. M. *Chemistry and Physics of Lipids* **1991**, 57, 227.

(15) Smith, A. L. *Spectrochimica Acta* **1960**, 16, 87.

(16) Wright, N.; Hunter, M. J. *The Journal of the American Chemical Society* **1947**, 69, 803.

(17) Wilmshurst, J. K. *Journal of Chemical Physics* **1957**, 26, 426.

(18) Konopka, R.; Stojczyk, B. *Acta Physica Polonica* **1971**, A40, 537.

(19) Bauer, R.; Magat, M. *J. Phys. Radium* **1938**, 9, 319.

(20) Allerhand, A.; Schleyer, P. v. R. *J. Amer. Chem. Soc.* **1963**, 85, 371.

(21) Zbinden, R. *Infrared Spectroscopy of High Polymers*; Academic Press, Inc.: New York, 1964.

(22) Damaschun, V. G. *Kolloid-Zeitschrift, Zeitschrift fur Polymere* **1962**, 180, 65.

(23) This program was developed by Molecular Simulations Incorporated.

CHAPTER 5

GENERAL CONCLUSIONS AND FUTURE WORK

5.1 General Conclusions

The characterization of microstructural transformations in this dissertation used infrared and Raman spectroscopy. Characterizing the microstructure came in part from Monte Carlo calculations of chain conformation coupled with normal coordinate analysis of isotropic Raman scattering intensity. By changing the chemical configuration defect population of syndiotactic polypropylene, we were able to quantitatively relate the Raman spectrum to configuration and conformation. Further, by quenching from the melt state to enhance the amorphous state population at moderate temperatures (near room temperature), we were able to characterize the conformation change over time. This work, coupled with related studies, made it possible to characterize the ordered phase conformation, and amorphous phase conformation distribution for several different polypropylene structures under different thermal treatments and deformation conditions. Finally, we addressed the issue of microstructure transformation for a polymer in a restricted geometry. This system was poly(dimethyl siloxane) spread at the air-water interface. Clarification of the structure and how it transforms was done with external reflectance infrared spectroscopy. It was possible to characterize how the polymer-water interaction changed, and it was possible to relate the average segmental orientation to the chain conformation.

Monte Carlo calculations coupled with normal coordinate analysis and Raman spectra, described in Chapter 2, indicate that spectroscopic distinction of different polypropylene racemic dyad populations is possible. Spectroscopic differences result because the amorphous phase conformation distribution is perturbed by the presence of configurational defects. In the vicinity of 300 to 400 cm^{-1}, the prominent spectroscopic features are representative of both amorphous conformation distribution, and ordered helical structure for syndiotactic and isotactic polypropylene. The isotactic, or meso

sequence ordered conformation, and amorphous conformation distribution, spectral features are primarily in the vicinity of 400 cm^{-1}. Likewise, the most stable ordered conformation, and amorphous conformation distribution spectroscopic features for syndiotactic, or racemic, sequences are mainly in the vicinity of 300 cm^{-1}. As a result, both highly ordered samples, and samples with little ordering exhibit Raman scattering features in these two regions that are a reflection of the configuration. Even a sample which has been aged below the glass transition temperature to enhance the all trans state was appropriately assigned to the known configuration by the features of the Raman spectrum in this region. The notable exception to the universality of this characterization method is the syndiotactic polypropylene which was mechanically deformed to induce the formation of a highly all-trans structure. Using the Raman spectrum of this sample underestimates the racemic dyad population. This effect agrees with expectations, based the model chain conformational mapping calculations, which show that spectroscopic features in the vicinity of 300 cm^{-1} are suppressed when the polymer is in the all trans state.

In Chapter 3, degree of conformational ordering in a 92% and a 75% racemic dyad population polypropylene was quantitatively characterized using Raman vibrational bands in the 800 to 900 cm^{-1} region. In addition, the metastable trans state, which was recently discovered to spontaneously form at or below the glass transition temperature for syndiotactic polypropylene,[1,2] was eliminated as a possible structure that is forming for the 75% racemic sample at room temperature. Coupling this analysis with analysis of stretched syndiotactic polypropylene in the trans state, and conformational mapping of the vibrational spectrum in the 800 to 900 cm^{-1} region has served to both improve the assignment of the bands in this region, and to characterize the dependence of amorphous phase conformation distribution on temperature and mechanical deformation. The analysis indicated that a minimum helical length $(ggtt)_4$ is required in order to observe the band characteristic of the helix (around 826 cm^{-1}), which means that a minimum racemic sequence length (r_7 or r_8) is required. Therefore, it was possible to relate the expected helical content, based on the

racemic content and defect distribution to the actual helical content present. The analysis showed that the 92 % racemic dyad sample exhibited ordered helical content around 50-55%. Based on the calculations, the extended helical features observed have at least seven to eight racemic sequences in a row, corresponding to racemic octads (r_7) or nonads (r_8). For the 92% racemic dyad population, random distribution of defects would correspond with octad to nonad populations of 50 to 56%. This is consistent with the helical fractions that were observed.

In contrast to the 92% racemic polypropylene, the room temperature ordering rate for the 75% racemic polypropylene is much slower, and the degree of ordering is significantly greater than expected, albeit less than the syndiotactic sample. Up to 35% of the polymer is determined to be in this extended helical state. If a random distribution of racemic and meso sequences is assumed for the 75% racemic sample, the octad to nonad population would be expected to be in the range 10 to 13%. After eliminating the all trans ordered structure as a significant component, it was determined that the 75% racemic dyad sample ordered features correspond to extended helical features with blockiness of racemic sequences.

Deformation experiments showed that there are several conditions which induce formation of the all trans syndiotactic polypropylene, other than cold drawing and aging of a quenched sample below 0°C. All trans structure can be formed by stretching a warm sample, or stretching a sample that had been at room temperature for at least 12 hours after melting. The amount of helical polymer in the stretched sample is reduced if the sample is cold drawn. The spectroscopic evidence also suggests that both low temperature (<~0 °C) aging, and cold drawing enhance the trans population in the amorphous phase relative to comparable treatment conditions at room temperature.

In Chapter 4, the phase transformation of poly(dimethyl siloxane) confined to the air-water interface was studied with external reflectance infrared spectroscopy, and epifluorescence microscopy. The data supports earlier studies that claim the surface

pressure plateau region corresponds to a transition between a "twisted caterpillar" and a local helical structure with the helix axis parallel to the water surface.[3,4] In this analysis, a number of different conformations were considered, including a three-dimensional random coil, and a variety of extended chain and helical structures with different orientations. For an insoluble chain, the three-dimensional random coil, as well as all the helical structures, and the extended chain structures oriented away from the water surface do not allow for sufficient interaction with the water surface at the low concentration to allow for the observed frequency shift of the skeletal asymmetric stretch vibration with increasing concentration. Furthermore, based on the models studied, the increase in scaled intensity for the symmetric methyl deformation with increased surface concentration requires that conformational ordering increases. Among all the combinations available from these choices, only the "twisted caterpillar" to local helical with the helix axis parallel to the water surface was consistent with the experimental observations. Evidence for this transformation being a phase transition came from epifluorescence microscopy observations. They showed the presence of two different types of domains in the region of the surface pressure plateau. As the concentration increased, the relative bright and dark domain populations changed in a manner that is consistent with the lever rule calculation for a phase transition.

Overall, this dissertation characterized transformations in the polymer microstructure by applying appropriate model structures and vibrational spectroscopy in order to test potential transformations. From these models it was possible to develop a quantitative relationship between the Raman spectrum and the population of meso defects in the mainly syndiotactic polymer. For syndiotactic polypropylene, the rate and extent of the conformational transformation was influenced by configurational defects. In the restricted geometry of the air-water interface, poly(dimethyl siloxane) goes through a phase transformation to accommodate the available surface area, while still stabilizing the air-

water interface. These observations are consistent with the knowledge that the backbone is highly polar, and the methyl groups are nonpolar, making the chain surface active.

5.2 Future Work

In addition to the structural characterization derived from the Raman vibrational bands in the 800-900 and 300-400 cm^{-1} regions, further insight into the structures may be possible by studying the high frequency regions of the Raman spectrum, such as the 2900 to 3100 cm^{-1} region, in which changes may be assigned to packing differences.[5] It may also be desirable to relate the characterized spectroscopic features to changes in mechanical and physical properties such as those observed with crystallization kinetics and physical aging. Furthermore, a complete interpretation of the normal modes for the all trans syndiotactic polypropylene structure is possible with the addition of the all trans structure Raman spectrum. In addition, an analysis of the different phase transformations illustrated with this work and other studies in this and other laboratories,[1,2,6-10] will be valuable to understand the temperature dependence of the phase transformations observed.

Application of Raman spectroscopy to characterize microstructure transformations for other polymers is possible. However, doing so requires both the ability to spectroscopically distinguish the physical states, and suitable vibrational force field and rotational isomeric states description for the polymers. For isotactic polypropylene, features associated with the amorphous phase are largely obscured by the ordered phase spectroscopic features, because the disordered phase is dominated by the same conformation (gt) that is present in the ordered helical structure. Therefore, the description of amorphous phase changes in the solid samples with the same regions studied for isotactic polypropylene is not realistic. However, it may be possible to study other systems which have suitably described vibrational force fields, for ordering and physical aging mechanisms.

Confinement of polymers to interfaces changes their equilibrium microstructures. The flexibility and chemical structure of both the backbone and the side groups therefore affect the conformation and orientation of polymers spread and adsorbed at interfaces. External reflectance infrared spectroscopy is a useful technique to characterize such features.[11-14] The method has potential application for more complex systems, such as the phase behavior of mixed monolayers. Furthermore, the technique can be applied to more complex siloxanes, such as poly(diethyl siloxane), poly(methyl phenyl siloxane), and copolymers containing dimethylsiloxane sequences as part of the backbone, in which the bulkiness, flexibility, and hydrophilicity of the side groups or copolymer are expected to impact the polymer spreading behavior.

5.3 References

(1) Nakaoki, T.; Ohira, Y.; Hayashi, H.; Horii, F. *Macromolecules* **1998**, 31, 2705.

(2) Wang, Y.; Hahn, T. D.; Hsu, S. L.; Stidham, H. D.; Seidle, A. **1998**, Manuscript in Preparation.

(3) Fox, H. W.; Taylor, P. W.; Zisman, W. A. *Industrial and Engineering Chemistry* **1947**, 1401.

(4) Noll, W.; Steinbach, H.; Sucker, C. *Journal of Polymer Science: Part C* **1971**, 34, 123.

(5) Chalmers, J. M. *Polymer* **1977**, 18, 681.

(6) Chatani, Y.; Maruyama, H.; Noguchi, K.; Asanuma, T.; Shiomura, T. *J. Polym. Sci. Polym. Phys. Lett.* **1990**, 28, 393.

(7) Chatani, Y.; Maruyama, H.; Asanuma, T.; Shiomura, T. *J. Polym. Sci. Polym. Phys. Ed.* **1991**, 29, 1649.

(8) Sozzani, P.; Galimberti, M.; Balbontin, G. *Makromol. Chem. Rapid Commun.* **1992**, 13, 305.

(9) Sozzani, P.; Simonutti, R.; Comoti, A. *Magnetic Resonance in Chemistry* **1994**, 32, s45.

(10) Asakura, T.; Aoki, A.; Takeshi, D.; Demura, M.; Asanuma, T. *Polym. J.* **1996**, 28, 24.

(11) Ren, Y.; Shoichet, M. S.; McCarthy, T. J.; Stidham, H. D.; Hsu, S. L. *Macromolecules* **1995**, 28, 358.

(12) Ren, Y.; Meuse, C. W.; Hsu, S. L. *J. Phys. Chem.* **1994**, 98, 8424.

(13) Riou, S. A.; Hsu, S. L.; Stidham, H. D. *J. Polym. Sci., Polym. Phys. Ed.* **1997**, 35, 2843.

(14) Chen, H.; Hsu, S. L.; Tirrell, D. A.; Stidham, H. D. *Langmuir* **1997**, 13, 4775.

APPENDIX A

VALIDATION OF THE INPUT GEOMETRY AND FORCE FIELD FOR DCNCA

A.1 Frequency Tables

In this appendix, issues relating to the reliability of the geometry input and force constant definitions used for the disordered normal coordinate analysis are discussed. These issues are addressed by comparing the measured values of frequencies calculated by myself with both DCNCA and another normal coordinate analysis program with published values for the frequencies with the same geometry. DCNCA force constant and input geometry, as well as the DCNCA program are given in Appendix B.

Demonstration that the method of geometry input is correct for DCNCA is first shown for simple alkane structures, namely propane and the two butane conformers by comparing the calculated frequencies with the values published by Snyder.[1] Then, validation of the input force field and geometry for polypropylene analogs is completed. This step ran into several complications which are discussed here, and satisfactorily resolved to the extent needed for the reliable use of the program DCNCA.

Frequency comparisons for propane, trans-butane, and gauche-butane are given in Tables A.1, A.2, and A.3. In Table A.1, the calculated frequencies for propane are mostly within 1 cm^{-1} of Snyder's calculations, with only one deviating by 3 cm^{-1}. The trans-butane calculation given in Table A.2 does not exceed the published values by more than 2 cm^{-1}, and most calculations are within 1 cm^{-1} of the published values. Calculation of gauche-butane, is given in Table A.3. In this case, all the calculated frequencies by DCNCA are within 1 cm^{-1} of the published values.

In an effort to evaluate the polypropylene force field input, an attempt was made to explicitely generate the frequencies and potential energy distributions using the program "mv.f" for the isotactic polypropylene 3_1 helix.. However, this effort to date has been unsuccessful, for reasons that have yet to be determined. The A-mode calculation

frequencies do not deviate much from Snyder's published frequencies (Table A.4), but the E-mode frequencies show numerous deviations (Table A.5).

In an effort to differentiate geometry error from force constant error, a small molecule analog was tested using both DCNCA and the "mv.f" program. The results are given in Table A.6. These results indicate some systematic deviations from the expected observations. However, after systematic elimination of geometric input errors in the "mv.f" calculations, it was determined that any remaining errors must be due to either incorrect definition of force constants, or error in the published frequencies. Therefore a careful review of the force constants was done. After eliminating any errors due to incorrect force constant definitions that are unambiguous, attention was turned to the force constants that are difficult to interpret. All of these force constants have a relatively small effect on the calculated frequencies. It was found that the same systematic errors occured, even if the ambiguous force constants were removed from consideration. This find gave us confidence that both the force constants and the geometry input were correct, and therefore it was possible to reliably generate spectral calculations that accurately represent the applied force field and the planned geometry.

Table A.1 Calculated Frequencies for Propane, Compared to Snyder's Original Calculations.[1]

sym	snyder	DCNCA	diff.
A1	2967	2967	0
A2	2965	2966	1
B2	2965	2965	0
B1	2963	2964	1
B2	2918	2918	0
A1	2877	2878	1
B1	2877	2877	0
A1	2855	2856	1
A1	1470	1469	-1
B1	1463	1463	0
B2	1460	1461	1
A2	1457	1457	0
A1	1452	1453	1
B1	1382	1381	-1
A1	1370	1369	-1
B1	1334	1332	-2
A2	1281	1281	0
B2	1183	1183	0
A1	1145	1146	1
B1	1048	1049	1
B1	923	926	3
A2	898	898	0
A1	863	863	0
B2	743	743	0
A1	379	379	0
B2	220	221	1
A2	200	200	0

Table A.2 Calculated Frequencies for Trans-Butane, Compared to Snyder's Original Calculations.[1]

Ag	2965	2965	0
Au	2965	2965	0
Bg	2965	2965	0
Bu	2965	2965	0
Bg	2923	2923	0
Au	2914	2914	0
Ag	2877	2877	0
Bu	2877	2877	0
Ag	2859	2859	0
Bu	2852	2852	0
Bu	1473	1473	0
Ag	1467	1467	0
Au	1459	1459	0
Bg	1459	1459	0
Bu	1457	1458	1
Ag	1452	1453	1
Bu	1378	1377	-1
Ag	1375	1373	-2
Ag	1360	1360	0
Bg	1301	1301	0
Bu	1286	1284	-2
Au	1260	1260	0
Bg	1179	1179	0
Ag	1148	1150	2
Ag	1055	1055	0
Bu	1011	1011	0
Bu	974	976	2
Au	948	948	0
Ag	830	831	1
Bg	800	800	0
Au	728	728	0
Ag	432	432	0
Bu	270	269	-1
Bg	225	225	0
Au	194	194	0
Au	102	102	0

Table A.3 Calculated Frequencies for Gauche-Butane, Compared to Snyder's Original Calculations.[1]

A	2965	2965	0
A	2965	2965	0
B	2965	2965	0
B	2965	2965	0
A	2921	2921	0
B	2916	2916	0
A	2877	2877	0
B	2877	2877	0
A	2857	2857	0
B	2854	2854	0
A	1468	1469	1
B	1466	1467	1
A	1459	1459	0
B	1459	1459	0
A	1458	1457	-1
B	1455	1455	0
A	1376	1376	0
B	1376	1376	0
B	1345	1345	0
A	1344	1344	-1
A	1266	1266	0
B	1250	1249	-1
A	1177	1177	0
B	1130	1130	0
A	1078	1078	0
A	984	984	0
B	963	963	0
B	947	947	0
A	832	832	0
A	798	799	1
B	751	751	0
B	449	449	0
A	308	308	0
A	197	197	0
B	196	195	-1
A	100	100	0

Table A.4 Calculated Frequencies for the A-Mode Frequencies of Isotactic Polypropylene 3_1 Helix, Compared to the Calculations of Snyder, et al.[2]

Hahn	Snyder(calc.)	difference	P.E.D. (Snyder)
2961	2962	1	r^-(100)
2961	2962	1	r^-(100)
2928	2928	0	d^-(99)
2905	2906	1	s(98)
2882	2882	0	r^+(98)
2855	2855	0	d^+(99)
1467	1465	-2	α(78)
1462	1462	0	α(87)
1452	1453	1	δ(69); α(11)
1382	1380	-2	W(27); S(26); ζ(25); U(20)
1368	1369	1	U(89)
1353	1348	-5	ζ(65); S(12)
1280	1284	4	W(37); T(36)
1241	1242	1	ζ(37); T(19); β(15)
1166	1170	4	S(30); β(22)
1065	1066	1	R(51); S(31)
1009	1004	-5	β(46); ζ(19)
968	969	1	β(51); S(28)
851	853	2	P(43); R(23)
826	829	3	P(29); S(32); β(20)
456	456	0	ω(81)
391	392	1	ω(62); ζ(15)
267	267	0	ω(58); τ(15)
193	195	2	τ(88)
140	140	0	ω(50); τ(30)

Table A.5 Calculated Frequencies for the E-mode Frequencies of Isotactic Polypropylene 3_1 Helix, Compared to the Calculations of Snyder, et al.[2]

Hahn	Sndyer	difference	P.E.D. (Snyder)
2961	2962	1	r^-(100)
2961	2962	1	r^-(100)
2930	2930	0	d^-(94)
2904	2904	0	s(94)
2882	2882	0	r^+(98)
2856	2856	0	d^+(99)
1504	1463	-41	α(88)
1463	1462	-1	α(78)
1455	1454	-1	δ(69)
1451	1377	-74	U(38); W(21); ζ(21); S(16)
1373	1367	-6	U(69); ζ(19)
1363	1352	-11	ζ(52); T(15)
1278	1292	14	W(35); ζ(25); T(13)
1192	1201	9	T(26); ζ(20); R(19)
1142	1155	13	S(23); R(15); ζ(13); β(13)
1108	1121	13	R(32); β(24); ζ(16)
1038	1024	-14	S(30); R(18); ζ(15); T(14)
949	940	-9	β(45); R(40)
905	901	-4	β(49); P(17); ζ(17)
792	817	25	R(32); P(30); S(23)
513	513	0	ω(63); R(10); P(9)
430	429	-1	ω(58); ζ(29); P(17)
296	311	15	ω(74)
196	198	2	τ(94)
147	147	0	ω(77); τ(16)
62	63	1	τ(86)

Table A.6 Calculated Frequencies for the 2,4-dimethylpentane in the C_2 Conformation, Compared to the Calculations of Bohan et al.[3]

Bohan et al.	MV calcn. 1	diff.	MV calcn. 2	diff.	DCNCA	diff.
1276	1276	0	1276	0	1274	2
1227	1231	-4	1225	2	1233	-6
1177	1179	-2	1179	-2	1178	-1
1176	1174	2	1174	2	1170	6
1164	1165	-1	1166	-2	1162	2
1154	1152	2	1152	2	1152	2
1087	1088	-1	1088	-1	1091	-4
1040	1038	2	1037	3	1046	-6
973	974	-1	974	-1	975	-2
962	963	-1	963	-1	966	-4
949	948	1	948	1	951	-2
923	924	-1	923	0	926	-3
922	923	-1	922	0	925	-3
913	914	-1	914	-1	913	0
876	873	3	876	0	876	0
816	815	1	815	1	815	1
815	812	3	812	3	811	4
471	475	-4	475	-4	476	-5
437	437	0	436	1	431	6
400	406	-6	407	-7	404	-4
394	394	0	394	0	393	1
372	360	12	360	12	360	12
294	295	-1	295	-1	295	-1
205	202	3	202	3	202	3
202	200	2	200	2	200	2
199	197	2	197	2	197	2
199	197	2	197	2	197	2
162	157	5	157	5	157	5
71	72	-1	72	-1	72	-1
51	50	1	50	1	50	1

A.2 References

(1) Snyder, R. G. *J. Chem. Phys.* **1967**, 47, 1316.

(2) Snyder, R. G.; Schachtschneider, J. H. *Spectrochim. Acta* **1964**, 20, 853.

(3) Bohan, S. P.; Strauss, H. L.; Snyder, R. G. *Journal of Physical Chemistry* **1990**, 94, 2801.

APPENDIX B

DOCUMENTATION OF DCNCA VERSION USED FOR POLYPROPYLENE SIMULATIONS USED IN CHAPTERS 2 AND 3

B.1 Description of Programs and Input

The primary program used for the calculations described in Chapters 2 and 3 is called DC8, which stands for "Disordered Normal Coordinate Analysis, version 8" revised by X. Yang. An early version of this program, called DCNCA has been available in our labs for several years. The contents of this appendix are are described below.

In Section B.2, input geometry for calculating the $(ggtt)_4$ structure for 2,4,6,8,10,12,14,16,18-nonamethylnonadecane (helical SPP), and the corresponding group coordinates for calculatingthe intensities are given. In section B.3, the force field parameters for both polypropylene, and n-alkanes are given. Finally, section B.4 gives the code for program DC8. The contents of these input files are illustrted in a different text font from the rest of this thesis in order to preserve the column sensitive formatting.

B.2 Input for 2,4,6,8,10,12,14,16,18-nonamethylnonadecane

B.2.1 Geometry

```
DC8--PP config.: r8,or (dl)8d, D=(1,1,.3,0,0),SPP in 8
h=0.7, t=0.4, w=0.0726, w1=0.0441,Sat Sep 27 10:39:13 PDT 1997
     1  1  1  0  9
48765492 9354827 300.
 15
    1.540000    1.093000    0.000000   60.000000  -60.000000  120.000000
 -120.000000    1.007825   12.01115   180.000000   67.000000  -67.000000
    1.410000   15.994915   77.139999
 86 85  0 27
  1  0  0  0  0  0  0  8
  2  1  0  0  2  0  0  9
```

3	2	1	0	1	3	0	9
4	2	1	3	2	3	7	8
5	2	1	3	2	3	6	8
6	3	2	1	1	3	10	9
7	3	2	6	1	3	7	9
8	3	2	6	2	3	6	8
9	6	3	2	1	3	10	9
10	6	3	9	2	3	6	8
11	6	3	9	2	3	7	8
12	9	6	3	1	3	10	9
13	9	6	12	2	3	7	8
14	9	6	12	1	3	6	9
15	12	9	6	1	3	10	9
16	12	9	15	2	3	6	8
17	12	9	15	2	3	7	8
18	15	12	9	1	3	10	9
19	15	12	18	1	3	7	9
20	15	12	18	2	3	6	8
21	18	15	12	1	3	10	9
22	18	15	21	2	3	6	8
23	18	15	21	2	3	7	8
24	21	18	15	1	3	10	9
25	21	18	24	2	3	7	8
26	21	18	24	1	3	6	9
27	24	21	18	1	3	10	9
28	24	21	27	2	3	6	8
29	24	21	27	2	3	7	8
30	27	24	21	1	3	10	9
31	27	24	30	1	3	7	9
32	27	24	30	2	3	6	8
33	30	27	24	1	3	10	9
34	30	27	33	2	3	6	8
35	30	27	33	2	3	7	8
36	33	30	27	1	3	10	9
37	33	30	36	2	3	7	8
38	33	30	36	1	3	6	9
39	36	33	30	1	3	10	9
40	36	33	39	2	3	6	8
41	36	33	39	2	3	7	8
42	39	36	33	1	3	10	9
43	39	36	42	1	3	7	9
44	39	36	42	2	3	6	8
45	42	39	36	1	3	10	9
46	42	39	45	2	3	7	8
47	42	39	45	2	3	6	8
48	45	42	39	1	3	10	9
49	45	42	48	2	3	7	8
50	45	42	48	1	3	6	9
51	48	45	42	1	3	10	9
52	48	45	51	2	3	6	8
53	48	45	51	2	3	7	8
54	51	48	45	1	3	10	9
55	51	48	54	1	3	7	9
56	51	48	54	2	3	6	8

```
57 54 51 48  2  3 10  8
58 54 51 57  2  3  6  8
59 54 51 57  2  3  7  8
60  7  3  2  2  3  5  8
61  7  3  2  2  3  4  8
62  7  3  2  2  3 10  8
63 14  9  6  2  3  4  8
64 14  9  6  2  3 10  8
65 14  9  6  2  3  5  8
66 19 15 12  2  3  5  8
67 19 15 12  2  3  4  8
68 19 15 12  2  3 10  8
69 26 21 18  2  3  4  8
70 26 21 18  2  3 10  8
71 26 21 18  2  3  5  8
72 31 27 24  2  3  5  8
73 31 27 24  2  3  4  8
74 31 27 24  2  3 10  8
75 38 33 30  2  3  4  8
76 38 33 30  2  3 10  8
77 38 33 30  2  3  5  8
78 43 39 36  2  3  5  8
79 43 39 36  2  3  4  8
80 43 39 36  2  3 10  8
81 50 45 42  2  3  4  8
82 50 45 42  2  3 10  8
83 50 45 42  2  3  5  8
84 55 51 48  2  3  5  8
85 55 51 48  2  3  4  8
86 55 51 48  2  3 10  8
 1  2  2  1  1  2  2  1  2  1  1  2  1  2  2  1  1  2  2  1  2  1  1  2
 1  2  2  1  1  2  2  1  2  1  1  2  1  2  2  1  1  2  2  1  2  1  1  2
 1  2  2  1  1  2  2  1  1  1  1  1  1  1  1  1  1  1  1  1  1  1  1  1
 1  1  1  1  1  1  1  1  1  1  1  1  1  1
 2  1  3  2  4  2  5  2  6  3  7  3  8  3  9  6 10  6 11  6 12  9 13  9
14  9 15 12 16 12 17 12 18 15 19 15 20 15 21 18 22 18 23 18 24 21 25 21
26 21 27 24 28 24 29 24 30 27 31 27 32 27 33 30 34 30 35 30 36 33 37 33
38 33 39 36 40 36 41 36 42 39 43 39 44 39 45 42 46 42 47 42 48 45 49 45
50 45 51 48 52 48 53 48 54 51 55 51 56 51 57 54 58 54 59 54 60  7 61  7
62  7 63 14 64 14 65 14 66 19 67 19 68 19 69 26 70 26 71 26 72 31 73 31
74 31 75 38 76 38 77 38 78 43 79 43 80 43 81 50 82 50 83 50 84 55 85 55
86 55
 2  2  0  0    0.000000
 5  2  1  9    0.000000
 8  2  2 12    0.000000
11  2  3 15    0.000000
14  2  4 18    0.000000
17  2  1 21    0.000000
20  2  2 24    0.000000
23  2  3 27    0.000000
26  2  4 30    0.000000
29  2  1 33    0.000000
32  2  2 36    0.000000
35  2  3 39    0.000000
```

```
38  2  4 42     0.000000
41  2  1 45     0.000000
44  2  2 48     0.000000
47  2  3 51     0.000000
50  2  4 54     0.000000
53  2  0  0     0.000000
 6  2  0  0     0.000000
13  2  0  0     0.000000
18  2  0  0     0.000000
25  2  0  0     0.000000
30  2  0  0     0.000000
37  2  0  0     0.000000
42  2  0  0     0.000000
49  2  0  0     0.000000
54  2  0  0     0.000000
 4
 3  0
10  4  5
    0.459911    0.515681    0.024408          d
    0.470563    0.527624    0.001813
    0.881466    0.071755    0.046780
 3  0
10  4  5
    0.945626    0.031083    0.023290          dl
    0.053132    0.898018    0.048851
    0.449021    0.550979    0.000000
 3  0
10  4  5
    0.459911    0.024408    0.515681          l
    0.881466    0.046780    0.071754
    0.470563    0.001813    0.527624
  3  0
 10  4  5
    0.945626    0.023290    0.031083          ld
    0.449021    0.000000    0.550979
    0.053132    0.048851    0.898018
1600.             .1          4.
 13 62 62
 18 18    1.0       0.
  1     1.0          1.0          1.0
  1     1.0          1.0          1.0
  1     1.0          1.0          1.0
  1     1.0          1.0          1.0
  1     1.0          1.0          1.0
  1     1.0          1.0          1.0
  1     1.0          1.0          1.0
  1     1.0          1.0          1.0
  1     1.0          1.0          1.0
  1     1.0          1.0          1.0
  1     1.0          1.0          1.0
  1     1.0          1.0          1.0
  1     1.0          1.0          1.0
  1     1.0          1.0          1.0
  1     1.0          1.0          1.0
```

```
 1      1.0          1.0          1.0
 1      1.0          1.0          1.0
 1      1.0          1.0          1.0
 9  9     1.0        0.
 1      1.0          1.0          1.0
 1      1.0          1.0          1.0
 1      1.0          1.0          1.0
 1      1.0          1.0          1.0
 1      1.0          1.0          1.0
 1      1.0          1.0          1.0
 1      1.0          1.0          1.0
 1      1.0          1.0          1.0
 1      1.0          1.0          1.0
17 17     0.3        0.
 1      1.0          1.0          1.0
 1      1.0          1.0          1.0
 1      1.0          1.0          1.0
 1      1.0          1.0          1.0
 1      1.0          1.0          1.0
 1      1.0          1.0          1.0
 1      1.0          1.0          1.0
 1      1.0          1.0          1.0
 1      1.0          1.0          1.0
 1      1.0          1.0          1.0
 1      1.0          1.0          1.0
 1      1.0          1.0          1.0
 1      1.0          1.0          1.0
 1      1.0          1.0          1.0
 1      1.0          1.0          1.0
 1      1.0          1.0          1.0
 1      1.0          1.0          1.0
 1      1.0          1.0          1.0
 1      1.0          1.0          1.0
 1  1     0.0        0.
end 1
 1      1.0          1.0          1.0
 2  2     0.0        0.                                          r pair 1
 1      1.0          1.0          1.0
 1      1.0          1.0          1.0
 2  2     0.0        0.                                          r pair 2
 1      1.0          1.0          1.0
 1      1.0          1.0          1.0
 2  2     0.0        0.                                          r pair 3
 1      1.0          1.0          1.0
 1      1.0          1.0          1.0
 2  2     0.0        0.                                          r pair 4
 1      1.0          1.0          1.0
 1      1.0          1.0          1.0
 2  2     0.0        0.                                          r pair 5
 1      1.0          1.0          1.0
 1      1.0          1.0          1.0
 2  2     0.0        0.                                          r pair 6
 1      1.0          1.0          1.0
 1      1.0          1.0          1.0
 2  2     0.0        0.                                          r pair 7
 1      1.0          1.0          1.0
```

```
  1      1.0            1.0            1.0
  2   2    0.0          0.
  1      1.0            1.0            1.0                                  r pair 8
  1      1.0            1.0            1.0
  1   1    0.0          0.
  1      1.0            1.0            1.0                                     end 2
  1
  7
1 2 2 1 1 2 2 1 1 2 2 1 1 2 2 1 1 1 1 1 1 1 1 1 1 1 1.0
----------------------------------------
27 C-C; 35 C-C-C.
```

B.2.2 Group Coordinates for Intensity Parametrization

```
 1   59      1.
 2   60      1.
 3   62      1.
 4   63      1.
 5   65      1.
 6   66      1.
 7   68      1.
 8   69      1.
 9   71      1.
10   72      1.
11   74      1.
12   75      1.
13   77      1.
14   78      1.
15   80      1.
16   81      1.
17   83      1.
18   84      1.
19   61      1.
20   64      1.
21   67      1.
22   70      1.
23   73      1.
24   76      1.
25   79      1.
26   82      1.
27   85      1.
28   95      1.
29  103      1.
30  113      1.
31  121      1.
32  131      1.
33  139      1.
34  149      1.
35  157      1.
36  167      1.
37  175      1.
38  185      1.
39  193      1.
```

```
40 203      1.
41 211      1.
42 221      1.
43 229      1.
44 239      1.
45  96      1.
46  97      1.
47 114      1.
48 115      1.
49 132      1.
50 133      1.
51 150      1.
52 151      1.
53 168      1.
54 169      1.
55 186      1.
56 187      1.
57 204      1.
58 205      1.
59 222      1.
60 223      1.
61 240      1.
62 241      1.

  18 (cc); 9 s(cc); 17 (ccc); 18 s(ccc).
```

B.3 Force Field Inputs for DC8

B.3.1 Alkanes

```
VFF 11095 N-ALKANES
 1    4698680              1   1   2   0   0   0   1   1   2
 2     032039              5   1   1
 3    4537625              1   1   2   0   0   0   1   2   2
 4     019285              5   3   3
 7     174285              8  31  12
                           31  10
 8     539216              2   1   2   1   1   2
 9     533050              2   1   2   1   2   2
10     617944              2   1   2   2   1   1
11    -030793             11  10  10   2   2
12     662674              2   1   2   2   1   2
13    -019438             11  12  12   2   2
14     021121             11  12  12   1   2
16    1032144              2   2   2   2   1   1
17     302874              8  31  16
18    -022086             11  12  16   2   2
21     008150              4   2   2   1   1   2   1   1   1
22     073275 180.        12  12  12
                           10  12
                           10  10
23    -058134  60.        12  12  12
```

```
                                 10 12
                                 10 10
 24    008150                    4  2  2  1  1  2  1  1  2
 25   -097028                    9 31 12
 31   4532150                    1  2  2
 35    097139 180.              12 16 16
 36    073379 180.              12 12 16
                                 10 16
 37   -063996  60.              12 12 16
                                 10 16
 38    083168                    5 31 31
 40   -009139 120.              13 12 12
                                 10 12
 41   -003937   0.              13 12 12
                                 10 12
 42    009700 180.              14 12 12
                                 10 12
 43    012133  60.              14 12 12
                                 10 12
 44   -004707  60.              12 16 16
-04
```

B.3.2 Polypropylenes

```
VFF 1965snyder et al. HC's
  1   4699000                   1  1  2  0  0  0  1  1  2
  2   4554000                   1  1  2  0  0  0  1  2  2
  3   4588000                   1  1  2  0  0  0  2  2  2
  4   4387000                   1  2  2  1  1  1  1  2  2
  5   4337000                   1  2  2  2  2  1  2  1  1
  6    540000                   2  1  2  1  1  2
  7    550000                   2  1  2  1  2  2
  8    645000                   2  1  2  2  1  1
  9    655000                   2  1  2  2  1  2
 10    657000                   2  1  2  2  2  2
 11   1130000                   2  2  2  2  1  1
 12   1084000                   2  2  2  2  1  2
 13    008000                   4  2  2  2  2  1  2  1  1
 14    008000                   4  2  2  2  2  1  1  1  1
 15    043000                   5  1  1
 16    006000                   5  2  2
 17    101000                   5  4  4
                                   4  5
                                   5  5
 18   -012000                  11  8  8  2  2
 19   -021000                  11  9  9  2  2
 20    012000                  11  9  9  1  2
 21    417000                   8  5 11
                                   4 12
                                   5 12
 22   -031000                  11 11  9  2  2
                               11 12 10  2  2
```

```
23    328000              8  4  8
                             5  9
                             4 10
                             5 10
24    079000              9  4 10
                             5  9
                             5 10
25    127000 180.        12  8 10
                             9 10
26   -005000  60.        12  8 10
                             9 10
27   -011000 180.        12 11 12
28    010000  60.        12 11 12
29    049000 180.        12 11 10
                            12  8
                            12  9
30   -052000  60.        12 11 10
                            12  8
                            12  9
31    009000 120.        13  8 10
                             9 10
32    002000   0.        13  8 10
                             9 10
33   -014000 180.        14  9 10
34   -025000  60.        14  9 10
35   -041000             11 12 12  2  2
36   -005000 -60.        12  8 10
                             9 10
 37    010000 -60.       12 11 12
 30   -052000 -60.       12 11 10
                            12  8
                            12  9
 38    009000-120.       13  8 10
                             9 10
 39   -025000 -60.       14  9 10
-04
```

B.4 DC8 Source Code

```
PROGRAM DCNCA
C
C   This program is for Normal Coordinate Analysis of Disordered Chains
C            modified by Xiaozhen Yang, May 8, 1995
C    << VERSION 8 >>          Modified by Xiaozhen Yang, June 16, 1996
C     HOE/FEB.03/94
C     INCLUDES ABILITY TO PRODUCE SYMMETRIZED Z AND G MATRICES
C
      PARAMETER  (MXNEL=4000)
      PARAMETER  (MXNAQ=400)
      PARAMETER  (MXNAQ2=MXNAQ**2)
      PARAMETER  (MXNAQE=MXNAQ*2)
      PARAMETER  (MXNOB=4000)
      PARAMETER  (MXNOAT=120)
      PARAMETER  (MXSPAR=100)
      PARAMETER  (MXPOLP=20)
      PARAMETER  (MXTOR=50)
      PARAMETER  (MXNC=MXTOR+3)
C
      INTEGER NRBB(MXNOB),NCBB(MXNOB),NOB
      INTEGER NRU(MXNAQ2),NCU(MXNAQ2)
      INTEGER NOSPAR,NXC(MXNOAT,8),IFTAU
      INTEGER  NINGP(MXPOLP),NGPSET,NICTOT,NGPTOT
      INTEGER  NGC(MXNAQ),KIC(MXNAQ),NGPC(MXPOLP)
      INTEGER  CAX(MXNAQ),IC(MXNC),JC(MXNC),KC(MXNC),NUMC
      INTEGER  TC(MXNC), DSEED,GSEED
C
      REAL  B(MXNOB),WTINV(MXNAQ)
      REAL  SM1(MXNAQ,MXNAQ),SM2(MXNAQ,MXNAQ),SM3(MXNAQ,MXNAQ)
      REAL  FP(MXNAQ),FR(MXNAQ)
      REAL  ED(MXNAQE),ROWDAT(MXNAQ2)
      REAL  DU(MXNAQ2),GMAT(MXNAQ,MXNAQ),SM4(MXNAQ,MXNAQ)
      REAL  UMAT(MXNAQ,MXNAQ),DA(MXNAQ)
      REAL  TEMP,AQQ(50,3,3)
      REAL  SPAR(MXSPAR),KON(50),XC(3,120)
      REAL  DS(MXNEL),SA(MXNEL),RI(MXNEL)
      REAL  DIJ(MXNOAT,MXNOAT),COF(MXNAQ),DIPMAG(MXPOLP,2)
      REAL  DIPCOM(MXNAQ,3),TRC(MXNC,3,3)
C
      COMMON  /PROBN/ REC(36)
      COMMON  /ATOM/  NOAT
      COMMON  /MAINC/ IFR,IFL,NMOL,NCM,NMTOT
      COMMON  /BOND1/ CAR(120,3),NOBOND,NB1(120),NB2(120)
      COMMON  /BOND2/ KWT(120),KB1(120),KB2(120)
      COMMON  /CORD1/ NIC(370,4),NCOD(370),NONIC,NOCTOT
      COMMON  /CORD2/ NICT(101,6,4),NCODT(101,6),NOCOMP(101),NT
      COMMON  /CORD3/ NOC,NAT,NLIN
      COMMON  /LINR/  NATLIN(370)
      COMMON  /TORC/  KBTOR(50),KBON(50)
      COMMON  /ETORS/ KTNUM(50),NSTATE(50),KTTYP(50),KTANG(50,3),
     1                TENER(50,3),KTYN,KARTAU(50)
      COMMON  /ANGT/  ANGTAU(50)
```

```
      COMMON  /ENVIR/ KBN(120,4),KT(120),KTSK(120)
      COMMON  /FCON1/ NOK(105),KND(105,10),KODE(105),NOF
      COMMON  /FCON2/ VAL(105),ANGLE(105),ZFACT(105)
      COMMON  /FCON3/ KIFC(105,20),KJFC(105,20),NOEQ(105)
      COMMON  /ASS02/ NUZZ(20),NIIQ(20),NOASS2
      COMMON  /STRUC/ X(3,120),W(120),KIND(120)
      COMMON  /ZEEEL/ COEF(2001),NRW(2001),NCL(2001),NF(2001),NZ
      COMMON  /B12/   FH,FL,FDEL,NEL
C
      CHARACTER*32 FNAME1,FNAME2,FNAME3,FNAME4,FNAME5
      EQUIVALENCE  (SM2,ROWDAT)
C
C           Open files
C
      WRITE(*,*)'              **************************8**** '
      WRITE(*,*)'              *                           * '
      WRITE(*,*)'              *           DCNCA           * '
      WRITE(*,*)'              *                           * '
      WRITE(*,*)'              *        Dr. Hsu/s LAB      * '
      WRITE(*,*)'              *            -1996          * '
      WRITE(*,*)'              **x*z*******************yang* '
      WRITE(*,*)' '
      WRITE(*,*)'     Filename for input: '
      read(*,100)FNAME1
      WRITE(*,*)'     Filename for output: '
      read(*,100)FNAME2
      WRITE(*,*)'     Filename for Force Constants: '
      read(*,100)FNAME3
C
c          FNAME1='DCNCA.OPT'
c          FNAME2='JUNK.OUT'
c          FNAME3='FORCONST.ETHER'
      OPEN(1,FILE=FNAME1,STATUS='OLD')
      OPEN(2,FILE=FNAME3,STATUS='OLD')
      OPEN(16,FILE=FNAME2,STATUS='UNKNOWN')
C
C                    Main Loop
C
      NCM=0
      NMTOT=0
  100 FORMAT(A)
  110 READ(1,1104) (REC(I),I=1,36)
 1104 FORMAT(18A4)
      READ(1,1105) NMOL,IFS,IFR,IFU,IFL
 1105 FORMAT(I6,4I3)
      WRITE(16,1108) (REC(I),I=1,36),NMOL,IFS,IFR,IFU,IFL
 1108 FORMAT(///2X,'<PROGRAM DCNCA>'//,2(/2X,18A4),//2X,'NUMBER OF',
     1' CONFORMERS =',I6,3X,'IFS =',I3,3X,'IFR =',I3,3X,'IFU =',I3,3X,
     2'IFL =',I3)
C
      IF(IFR .NE. 0) THEN
      CALL CONFORM1(DSEED,GSEED,TEMP)
      ELSE
      read(1,*)DSEED,GSEED,temp
```

```
      WRITE(16,120)
  120   FORMAT(//2X,'CONFORMERS ARE DEFINED.')
      ENDIF
      CALL GETSPNCRT(SPAR,NOSPAR,MXSPAR,NXC,MXNOAT)
      CALL KARTO(SPAR,MXSPAR,NXC,MXNOAT,X,W,0,GSEED)
C---------------------- Modified here-----------------------
ccc      Modified DATIN(IFTAU) into the one below
C
      CALL DATIN(IFTAU,AQQ)
C---------------------- Modified end-----------------------
C
      IF (IFS .NE. 0) THEN
      write(*,*)' Filename for the group coordinates:'
      read(*,100)FNAME4
      write(*,*)' Filename for the spectrum:'
      read(*,100)FNAME5
c         FNAME4='GROUP.OPT'
      open(8,file=FNAME4,status='OLD')
      CALL PLOT1(MXNEL,DS,SA)
      CALL INTIN1(NGC,COF,MXNAQ,DIPMAG,KIC,SM1,NICTOT,NINGP,MXPOLP,
     1    NGPSET,NGPC,NGPTOT,DIPCOM,IC,JC,KC,NUMC,MXNC,CAX,TC)
      ENDIF
C
      IF(IFR .NE. 0) CALL CONFM2(AQQ,TEMP)
      CALL KORD
      CALL FCIN
C
      DO 200 I=1,NMOL
      CALL CONFM3(AQQ,DSEED,NXC,MXNOAT,SPAR,MXSPAR,KON,WTS)
      IF(IFR .NE. 0) THEN
        NCM=1
        CALL KARTO(SPAR,MXSPAR,NXC,MXNOAT,X,W,0,GSEED)
        CALL KORDT
        IF (IFTAU .NE. 0) CALL KARTO(SPAR,MXSPAR,NXC,MXNOAT,XC,W,1,
     1                                  GSEED)
      ENDIF
C***
      IF ( IFL.EQ.2) THEN
         CALL LISTX(X,XC)
      ENDIF
C***
C***    CALL LISTX(X,XC)
      IF ((IFTAU .EQ. 0).OR.(IFR .EQ. 0)) THEN
        CALL OVERLP(IFOVER,X)
      ELSE
        CALL OVERLP(IFOVER,XC)
      ENDIF
      IF (IFOVER .EQ. 0) GO TO 200
      CALL COUNT(KON)
      NMTOT=NMTOT+1
      CALL ZDIAG
      CALL ZINTER
C       CALL LISTZ
      IF ((IFTAU .EQ. 0).OR.(IFR .EQ. 0)) THEN
```

```
        CALL BGENER(MXNOB,NOB,NRBB,NCBB,B,MXNOAT,MXNAQ,X)
      ELSE
        CALL BGENER(MXNOB,NOB,NRBB,NCBB,B,MXNOAT,MXNAQ,XC)
      ENDIF
      CALL FORMB(MXNOB,NRBB,NCBB,B,NOB,SM1,MXNAQ,NOCTOT)
      IF(IFU .NE. 0) CALL ZGSYM(SM1,MXNAQ,NOCTOT,NRU,NCU,DU,MXNAQ2,
     1                          GMAT,SM4,UMAT,SM3,DA)
      IF (IFS .NE. 0) THEN
        IF ((IFTAU .EQ. 0).OR.(IFR .EQ. 0)) THEN
          CALL TFORM(TRC,MXNC,NUMC,IC,JC,KC,TC,X)
        ELSE
          CALL TFORM(TRC,MXNC,NUMC,IC,JC,KC,TC,XC)
        ENDIF
      ENDIF
      CALL FREQNC(MXNAQ,FP,FR,SM1,SM2,SM3,ED,MXNAQ2,ROWDAT,
     1            MXNAQE,WTINV,MXNOAT,CAX,NGPTOT)
C***    IF (IFL .EQ. 1) CALL OUTL(MXNAQ,FP,FR,SM2,XC,IFTAU,IFR)
C***    CALL LISTFR(MXNAQ,FP,FR,SM2)
      CALL LISTFR(MXNAQ,FP,FR,SM2,IFL,IFS)
      IF (IFS .NE. 0) THEN
        CALL INTIN2(NGC,COF,MXNAQ,DIPMAG,SM1,SM2,SM3,NNEWNO,RI,IFREOR,
     1    NICTOT,NGPC,MXPOLP,KIC,NGPSET,MXNTOR,KON,NGPTOT,TRC,CAX,
     2    DIPCOM,MXNC,FR)
ccc          CALL LISTRI(MXNAQ,FP,FR,SM2,RI)
        CALL ADD2(MXNEL,DS,SA,MXNAQ,FP,FR,SM2,RI,WTS)
      ENDIF
  200 CONTINUE
C
      IF (IFS .NE. 0) THEN
      IF (NMTOT .NE. 0) CALL PLOT3(MXNEL,DS,SA,TEMP)
      CALL STAT(MXNEL,DS,SA)
      IF (NMTOT .NE. 0) CALL RESULT1(MXNEL,DS,SA,IFL,temp,FNAME5)
      ENDIF
C
C     ------------------------------------------ S T O P
      STOP
      END
      SUBROUTINE CONFORM1(DSEED,GSEED,TEMP)
      REAL TEMP
      INTEGER DSEED,GSEED
C
C
      READ(1,10) DSEED,GSEED,TEMP
   10 FORMAT(2I8,F12.6)
      WRITE(16,20) DSEED,GSEED,TEMP
   20 FORMAT(//2X,'CONFORMERS ARE DETERMINED RANDOMLY:',//2X,'DSEED,',
     1' GSEED = ',2I9,5X,'TEMP = ',F6.1)
C
C
      RETURN
      END
      SUBROUTINE GETSPNCRT(SPAR,NOSPAR,MXSPAR,NXC,MXNOAT)
      INTEGER  NOSPAR,MXSPAR,MXNOAT,NXC(MXNOAT,8)
      REAL  SPAR(MXSPAR)
```

```
      COMMON  /ATOM/  NOAT
      COMMON  /BOND1/ CAR(120,3),NOBOND,NB1(120),NB2(120)
      COMMON  /CORD2/ NICT(101,6,4),NCODT(101,6),NOCOMP(101),NT
      COMMON  /OOP/   IOOP(25,5),NOOP,NDIR(25)
C
C
      READ(1,10) NOSPAR
   10 FORMAT(I3)
      READ(1,20) (SPAR(I),I=1,NOSPAR)
   20 FORMAT(6F12.6)
      WRITE(16,30) (SPAR(I),I=1,NOSPAR)
   30 FORMAT(//2X,'LIST OF STRUC. PAR. (SPAR(I)  :',/(5X,5F12.6))
C
      READ(1,2) NOAT,NOBOND,NOOP,NT
    2 FORMAT(4I3)
      WRITE(16,8) NOAT,NOBOND,NOOP,NT
    8 FORMAT(//2X,'NOAT =',I3,3X,'NOBOND =',I3,3X,'NOOP =',I3,3X,
     2'NT =',I3)
C
      DO 50 I=1,NOAT
      READ(1,60) (NXC(I,L),L=1,8)
   60   FORMAT(8I3)
   50 CONTINUE
C
C
      RETURN
      END
      SUBROUTINE KARTO(SPAR,MXSPAR,NXC,MXNOAT,X,W,IFVAR,GSEED)
      DIMENSION COR(120,3),XT(120,3),VBA(3),VCA(3),
     1 RJA(3),TRANS(3,3),PRC(3),DNER(3,3),CM(3),TR(3,3),
     2 RT(500),NR(1500),NCO(1500),DAT(1500),D(120),RR(3),
     3 XM(4),ED(6),DROW(6)
      REAL  SPAR(MXSPAR),X(3,120),W(120)
      INTEGER  MXSPAR,MXNOAT,NXC(MXNOAT,8),IFVAR,GSEED
      COMMON  /MAINC/ IFR, IFL,NMOL,NCM,NMTOT
      COMMON  /ATOM/  NOAT
      COMMON  /CORD2/ NICT(101,6,4),NCODT(101,6),NOCOMP(101),NT
      COMMON  /BOND1/ CAR(120,3),NOBOND,NB1(120),NB2(120)
      COMMON  /BOND2/ KWT(120),KB1(120),KB2(120)
      COMMON  /TORC/  KBTOR(50),KBON(50)
      COMMON  /OOP/   IOOP(25,5),NOOP,NDIR(25)
      COMMON  /ETORS/ KTNUM(50),NSTATE(50),KTTYP(50),KTANG(50,3),
     1                TENER(50,3),KTYN,KARTAU(50)
      COMMON  /ANGT/  ANGTAU(50)
C
C
      CON=.174532925E-01
      IF (NCM .EQ. 0) THEN
      WRITE(16,40)
   40   FORMAT(//2X,'CART INPUT FOLLOWS'/)
      ENDIF
      JOKE=0
      CALL TRANSLT(SPAR,MXSPAR,NXC,MXNOAT,1,NO,NA,NB,NC,R,TE,PH,WT)
      N1=NO
```

```
      W(NO)=WT
      COR(NO,1)=0.0
      COR(NO,2)=0.0
      COR(NO,3)=0.0
      CALL TRANSLT(SPAR,MXSPAR,NXC,MXNOAT,2,NO,NA,NB,NC,R,TE,PH,WT)
      COR(NO,1)=R
      COR(NO,2)=0.0
      COR(NO,3)=0.0
      W(NO)=WT
      CALL TRANSLT(SPAR,MXSPAR,NXC,MXNOAT,3,NO,NA,NB,NC,R,TE,PH,WT)
      IF(TE)120,118,120
  118 CS=-0.33333333
      SS= 0.94280907
      TE=109.47122
      GO TO 121
  120 CS=COS(CON*TE)
      SS=SIN(CON*TE)
  121 W(NO)=WT
      IF(NA-N1)128,122,128
  122 COR(NO,1)=COR(NA,1)+R*CS
      GO TO 129
  128 COR(NO,1)=COR(NA,1)-R*CS
  129 COR(NO,2)=R*SS
      COR(NO,3)=0.0
      IF (NOAT-3) 131,161,130
  131 WRITE(16,134)
  134 FORMAT(//2X,'ERROR!! CANNOT HAVE < 3 ATOMS!')
      CALL EXIT
  130 DO 160 I=4,NOAT
      CALL TRANSLT(SPAR,MXSPAR,NXC,MXNOAT,I,NO,NA,NB,NC,R,TE,PH,WT)
C
C IF AT LEAST 1 TORSION HAS NON-ZERO ANGLE DEVIATION THEN VARY THE
C DESIGNATED TORSIONS (NOTE THAT INPUT X MATRIX IS ACTUALLY XC FOR
C THIS CASE).
C
c---------------------------------------XXXXX
c       write(*,*)'----------------> IFVAR=',IFVAR
      IF (IFVAR .NE. 0) THEN
      IFX=0
      DO 300 K=1,NT
        IF (I .EQ. KARTAU(K)) THEN
          IFX=1
          GO TO 310
        ENDIF
  300   CONTINUE
  310   CONTINUE
      IF (IFX .NE. 0) CALL VARTAU(NXC(I,7),PH,ANGTAU(K),SPAR,MXSPAR,
     1                            GSEED,I)
      ENDIF
C
      W(NO)=WT
      IF(TE)133,132,133
  132 CS=-0.33333333
      SS= 0.94280907
```

```
      TE=109.47122
      GO TO 135
  133 CS=COS(CON*TE)
      SS=SIN(CON*TE)
  135 DSQ=0.0
      DO 138 M=1,3
      VBA(M)=COR(NB,M)-COR(NA,M)
      VCA(M)=COR(NC,M)-COR(NA,M)
  138 DSQ=DSQ+VBA(M)**2
      RAB=SQRT(DSQ)
      SCALE=0.0
      DO 142 M=1,3
      TRANS(M,1)=VBA(M) / RAB
  142 SCALE=SCALE+ TRANS(M,1)*VCA(M)
      DSQ=0.0
      DO 146 M=1,3
      RJA(M)=VCA(M)-SCALE*TRANS(M,1)
  146 DSQ=DSQ+RJA(M)**2
      RAJ=SQRT(DSQ)
      DO 148 M=1,3
  148 TRANS(M,2)=RJA(M) / RAJ
      TRANS(1,3)=TRANS(2,1)*TRANS(3,2)-TRANS(3,1)*TRANS(2,2)
      TRANS(2,3)=TRANS(3,1)*TRANS(1,2)-TRANS(1,1)*TRANS(3,2)
      TRANS(3,3)=TRANS(1,1)*TRANS(2,2)-TRANS(2,1)*TRANS(1,2)
      PRC(1)=R*CS
      PRC(2)=R*SS*COS(CON*PH)
      PRC(3)=R*SS*SIN(CON*PH)
      DO 160 M=1,3
      COR(NO,M)=COR(NA,M)
      DO 160 K=1,3
  160 COR(NO,M)=COR(NO,M)+TRANS(M,K)*PRC(K)
  161 IF(NOAT .NE. 0) GO TO 168
      WRITE(16,60)
   60 FORMAT(/1X,'ATOM NO.',9X,'X',11X,'Y',11X,'Z',9X,'MASS'/)
      DO 164 I=1,NOAT
  164 WRITE(16,62)I,(COR(I,M),M=1,3),W(I)
   62 FORMAT(4X,I3,3X,3F12.6,F13.6)
C
C  FIND CENTER OF MASS
C
  168 WT=0.0
      DO 170 I=1,NOAT
  170 WT=WT+W(I)
      IF(WT)172,172,175
  172 DO 173 I=1,NOAT
      W(I)=1.0
  173 WT=WT+1.0
  175 DO 180 M=1,3
      CM(M)=0.0
      DO 179 I=1,NOAT
  179 CM(M)=CM(M)-W(I)*COR(I,M)
  180 CM(M)=CM(M)/ WT
  184 DO 185 I=1,NOAT
      RT(I)=0.0
```

```
      DO 185 M=1,3
      XT(I,M)=COR(I,M)+CM(M)
  185 RT(I)=RT(I)+(XT(I,M))**2
      DO 190 I=1,3
      DO 190 J=1,3
      DNER(I,J)=0.0
      DO 190 K=1,NOAT
      IF(I-J)189,187,189
  187 DNER(I,J)=DNER(I,J)+W(K)*(RT(K)-XT(K,I)*XT(K,I))
      GO TO 190
  189 DNER(I,J)=DNER(I,J) -W(K)* XT(K,I)*XT(K,J)
  190 CONTINUE
      IF(NOAT .NE. 0) GO TO 195
      WRITE(16,80) WT,(CM(M),M=1,3)
   80 FORMAT(//5X,'TOTAL MASS =',F12.6/5X,'CENTER OF MASS =',3F12.6)
      WRITE(16,8190)
 8190 FORMAT(//5X,'MOMENT OF INERTIA TENSOR ='//)
  193 DO 192 I=1,3
  192 WRITE(16,82)(DNER(I,J),J=1,3)
   82 FORMAT(10X,3F12.6)
  195 NR1=0
C
C  FIND TRANSFORMATION TO PRINCIPAL AXES.
C
      N=0
      DO 255 I=1,3
      DO 255 J=I,3
      N=N+1
      DROW(N)=DNER(I,J)
      IF (ABS(DROW(N)) .LT. 0.000001) DROW(N)=0.0
  255 CONTINUE
      CALL DSPEV(1,DROW,VBA,TRANS,3,3,ED,6)
C
      DO 257 I=1,3
      DNER(I,I)=VBA(I)
      DO 257 J=1,3
        TR(I,J)=TRANS(I,J)
  257     CONTINUE
C
  200 IF(NOAT .NE. 0) GO TO 205
      WRITE(16,84)(DNER(I,I),I=1,3)
   84 FORMAT(/' PRINCIPAL MOMENTS =',3F12.6)
      WRITE(16,2201)
 2201 FORMAT(//5X,'TRANSFORMATION MATRIX ='/)
  201 DO 202 I=1,3
  202 WRITE(16,85)(TR(I,J),J=1,3)
   85 FORMAT(10X,3F12.6)
C
C  ROTATE TO PRINCIPAL AXES.
C
  205 DO 210 I=1,NOAT
      DO 210 J=1,3
      CAR(I,J)=0.0
      DO 210 K=1,3
```

```
  210 CAR(I,J)=CAR(I,J)+TR(K,J)*XT(I,K)
C
C USE NEXT 4 LINES FOR UN-TRANSLATED COORDINATES
C
      DO 220 I=1,NOAT
      DO 220 J=1,3
       CAR(I,J)=COR(I,J)
  220 CONTINUE
C
      DO 1200 I=1,3
      DO 1200 J=1,NOAT
 1200 X(I,J)=CAR(J,I)
C
c-----------------------------------------XXXXX
c       write(*,*)'--------------------> NCM=',NCM
      IF (NCM .NE. 0) RETURN
      WRITE(16,86)
   86 FORMAT(//,'PRINCIPAL CARTESIAN COORDINATES')
      WRITE(16,60)
      DO 215 I=1,NOAT
  215 WRITE(16,62)I,(CAR(I,M),M=1,3),W(I)
      RETURN
      END
      SUBROUTINE TRANSLT(SPAR,MXSPAR,NXC,MXNOAT,IN,NO,NA,NB,NC,
     1                   R,TE,PH,WT)
      INTEGER  MXSPAR,NO,NA,NB,NC,IN,NXC(MXNOAT,8),MXNOAT
      REAL  R,TE,PH,WT,SPAR(MXSPAR)
      COMMON  /MAINC/ IFR, IFL,NMOL,NCM,NMTOT
C
C
      NO=NXC(IN,1)
      NA=NXC(IN,2)
      NB=NXC(IN,3)
      NC=NXC(IN,4)
       R=SPAR(NXC(IN,5))
      TE=SPAR(NXC(IN,6))
      PH=SPAR(NXC(IN,7))
      WT=SPAR(NXC(IN,8))
      IF(NCM .EQ. 0) THEN
      WRITE(16,19)NO,NA,NB,NC,R,TE,PH,WT
   19   FORMAT(4I4,4F12.6)
      ENDIF
C
C
      RETURN
      END
      SUBROUTINE VARTAU(J,PH,TAUDEV,SPAR,MXSPAR,GSEED,NTOR)
      INTEGER  J,MXSPAR,NTOR,GSEED
      REAL  PH,TAUDEV,SPAR(MXSPAR)
      DIMENSION  RD(2)
      COMMON  /CON4/ VTOTSQ(50)
C
C
  120 CALL DNRAND(GSEED,2,RD,AUX,1)
```

```
      VT=TAUDEV*RD(1)
C
      VTOTSQ(NTOR)=VTOTSQ(NTOR)+VT**2
      PH=SPAR(J)+VT
C     WRITE(16,71) VT,SPAR(J),PH,VTOTSQ(NTOR)
C  71 FORMAT(10X,'VT, SPAR(J), PH, VTOTSQ(NTOR)=',4F10.4)
ccc      WRITE(16,94) J,GSEED,RD(1),VT,PH
   94 FORMAT(/2X,'J,GSEED,RD(1),VT,PH =',I3,I10,3F12.6)
C
C
      RETURN
      END
      SUBROUTINE DATIN(IFTAU,AQQ)
      INTEGER  IFTAU
      REAL TEMP,AQQ(50,3,3)
      COMMON  /ATOM/  NOAT
      COMMON  /BOND1/ CAR(120,3),NOBOND,NB1(120),NB2(120)
      COMMON  /CORD2/ NICT(101,6,4),NCODT(101,6),NOCOMP(101),NT
      COMMON  /STRUC/ X(3,120),W(120),KIND(120)
      COMMON  /BOND2/ KWT(120),KB1(120),KB2(120)
      COMMON  /TORC/  KBTOR(50),KBON(50)
      COMMON  /ETORS/ KTNUM(50),NSTATE(50),KTTYP(50),KTANG(50,3),
     1                TENER(50,3),KTYN,KARTAU(50)
      COMMON  /ANGT/  ANGTAU(50)
      COMMON  /OOP/   IOOP(25,5),NOOP,NDIR(25)
C
C
      READ(1,1640) (KIND(I),I=1,NOAT)
 1640 FORMAT(24I3)
      READ(1,64) (NB1(I),NB2(I),I=1,NOBOND)
   64 FORMAT(12(2I3))
      DO 1644 I=1,NOBOND
      KB1(I)=NB1(I)
      KB2(I)=NB2(I)
 1644 CONTINUE
      WRITE(16,1019) (KIND(I),I=1,NOAT)
 1019 FORMAT(/3X,'ATOM KINDS'/(2X,15I4))
      WRITE(16,1119)  (KB1(I),KB2(I),I=1,NOBOND)
 1119 FORMAT(/3X,'BOND PAIRS'/(8(I5,I3)))
C
C READ IN OUT-OF-PLANE BEND - BEND INTERACTION DEFINITIONS
C
      IF(NOOP .GT. 0) THEN
      WRITE(16,243) NOOP
  243   FORMAT(//3X,'OUT-OF-PLANE INTERACTIONS',//10X,'NOOP= ',I3,
     1      //5X,'ATOMS DEFINING OOP BEND AND POSITIVE INCREASE IN COORD
     2INATE'/)
      DO 246 KK=1,NOOP
        READ(1,244) (IOOP(KK,JJ),JJ=1,5)
  244     FORMAT(5I3)
        WRITE(16,245) (IOOP(KK,JJ),JJ=1,5)
  245     FORMAT(10X,5I3)
  246   CONTINUE
      ENDIF
```

```
C
      IF(NT .GT. 0) THEN
      DO 5 I=1,NT
        READ(1,10) KBON(I),KBTOR(I),KTNUM(I),KARTAU(I),ANGTAU(I)
    5   CONTINUE
      ENDIF
   10 FORMAT(4I3,F12.6)
      WRITE(16,60)
   60 FORMAT(//3X,'TORSIONS',/10X,'# KBON KBTOR KTNUM KARTAU ANGTAU')
      DO 68 I=1,NT
      WRITE(16,65) I,KBON(I),KBTOR(I),KTNUM(I),KARTAU(I),ANGTAU(I)
   65   FORMAT(7X,2I4,1X,I4,2X,I4,3X,I4,2X,F8.2)
   68 CONTINUE
C
      IFTAU=0
      DO 300 I=1,NT
      IF ((ANGTAU(I).NE.0.0).AND.(KTNUM(I).GT.0)) THEN
        IFTAU=1
        GO TO 310
      ENDIF
  300 CONTINUE
  310 CONTINUE
C
      READ(1,15) KTYN
   15 FORMAT(I3)
      IF(KTYN .NE. 0) THEN
      DO 20 I=1,KTYN
        READ(1,25) NSTATE(I),KTTYP(I)
   25     FORMAT(2I3)
        READ(1,30) (KTANG(I,J),J=1,NSTATE(I))
   30     FORMAT(3I3)
C---------------------- Modified here-----------------------
C    IF KTTYP=0, then read in Conditional Probabilities of RIS
C
      IF(KTTYP(I).EQ.0) THEN
        READ(1,33) ((AQQ(I,J,K),K=1,3),J=1,3)
      ELSE
        READ(1,33) (TENER(I,J),J=1,3)
      ENDIF
C---------------------- Modified end-----------------------
   33     FORMAT(3F12.6)
   20   CONTINUE
      DO 40 I=1,KTYN
        WRITE(16,45) I,NSTATE(I),(KTANG(I,J),J=1,3)
   45     FORMAT(//3X,'TORSION DEFINITION NO. ',I3,//6X,'NSTATE =',I3,
     1           5X,'SPAR FOR TORS. =',3I3)
C---------------------- Modified here-----------------------
        WRITE(16,50) KTTYP(I)
      IF(KTTYP(I).EQ.0) THEN
        WRITE(16,51) ((AQQ(I,J,K),K=1,3),J=1,3)
       ELSE
        WRITE(16,51) (TENER(I,J),J=1,3)
      ENDIF
   50     FORMAT(/6X,'KTTYP =',I3,5X,' TORS PARAMS. '/)
```

```
   51     FORMAT(20X,3F12.6)
C---------------------- Modified END-----------------------
   40   CONTINUE
      ENDIF
C
C
      RETURN
      END
      SUBROUTINE PLOT1(MXNEL,DS,SA)
      INTEGER  MXNEL
      REAL  DS(MXNEL),SA(MXNEL)
      COMMON  /B12/ FH,FL,FDEL,NEL
C
C
      READ(1,10) FH,FL,FDEL
   10 FORMAT(3F12.6)
      WRITE(16,12) FH,FL,FDEL
   12 FORMAT(/2X,'PLOTING PAR.'/5X,'HIGH FREQ. LIM. (FH) =',F7.1
     1  /5X,'LOW FREQ. LIM. (FL) =',1X,F7.1/5X,'INTERVAL (FDEL) =',5X,
     2  F7.1)
C
      NEL=(FH-FL)/FDEL+0.5
C
      IF(NEL .GT. 2000) THEN
      WRITE(16,14) NEL
   14   FORMAT(//2X,'*** ERROR *** : NEL EXCEEDS 2000. NEL=',I6)
      CALL EXIT
       ENDIF
C
      WRITE(16,20) NEL
   20 FORMAT(5X,'NO. OF INTERVALS (NEL) =',I6)
C
      DO 130 I=1,NEL
      SA(I)=0.0
      DS(I)=0.0
  130   CONTINUE
C
C
      RETURN
      END
      SUBROUTINE INTIN1(NGC,COF,MXNAQ,DIPMAG,KIC,SM1,NICTOT,NINGP,
     1  MXPOLP,NGPSET,NGPC,NGPTOT,DIPCOM,IC,JC,KC,NUMC,MXNC,CAX,TC)
      INTEGER  NGC(MXNAQ),NINGP(MXPOLP),MXPOLP
      INTEGER  MXNAQ,KIC(MXNAQ),NGPSET,NGPC(MXPOLP),NGPTOT
      INTEGER  IC(MXNC),JC(MXNC),KC(MXNC),CAX(MXNAQ),MXNC,NUMC
      INTEGER  TC(MXNC)
      REAL  SM1(MXNAQ,MXNAQ),COF(MXNAQ),DIPMAG(MXPOLP,2)
      REAL  DIPCOM(MXNAQ,3)
      COMMON  /ATOM/  NOAT
      COMMON  /CORD2/ NICT(101,6,4),NCODT(101,6),NOCOMP(101),NT
C
C  READ IN GROUP COORD. DEF. IN SETS OF SIMILAR GROUP COORD.
C    NGPSET = NO. OF SETS OF GROUP COORD.
C    NICTOT = TOTAL NO. OF INTERNAL COORD.
```

```
C     NGPTOT = TOTAL NO. OF GROUP COORD.
C
      READ(1,10) NGPSET,NGPTOT,NICTOT
   10 FORMAT(3I3)
      WRITE(16,16) NGPSET,NGPTOT,NICTOT
   16 FORMAT(/2X,'GROUP COORD. DEFINED IN SETS'
     1  /10X,'NO. OF SETS (NGPSET) =',I3
     2  /10X,'TOTAL NO. OF GRP. COORD. (NGPTOT) =',I3
     3  /10X,'TOTAL NO. OF INTERNAL COORD. (NICTOT) =',I3)
C
C
      DO 117 I=1,NICTOT
      READ(8,110) NGC(I),KIC(I),COF(I)
  110   FORMAT(2I3,F12.6)
  117   CONTINUE
C
      IFX=1
      IF (IFX .EQ. 0) THEN
        WRITE(16,109)
  109     FORMAT(//2X,'U MATRIX COEFFICIENTS',/11X,'NO.',4X,'NGC',4X,'KI
     1C',7X,'COF')
        DO 118 I=1,NICTOT
          WRITE(16,111) I,NGC(I),KIC(I),COF(I)
  111       FORMAT(10X,3(I3,4X),F8.4)
  118       CONTINUE
      ENDIF
C
      NGR=0
      NICIN=0
      NGP=1
  121   NGR=NGR+1
        READ(1,123) NGPC(NGR),NINGP(NGR),DIPMAG(NGR,1),DIPMAG(NGR,2)
  123     FORMAT(2I3,2F12.6)
        NICIN=NICIN+NINGP(NGR)
        DO 300 I=1,NGPC(NGR)
          READ(1,305) CAX(NGP),DIPCOM(NGP,1),DIPCOM(NGP,2),
     1      DIPCOM(NGP,3)
  305       FORMAT(I3,3(F12.6))
          NGP=NGP+1
  300     CONTINUE
      IF (NGR .LT. NGPSET) GO TO 121
C
      IF (NICIN .NE. NICTOT) THEN
        WRITE(16,125)
  125     FORMAT(//5X,'ERROR !!! TOT. NUMBER OF IC IN U DOES NOT MATCH N
     1ICTOT IN INPUT FILE!')
      ENDIF
C
      READ(1,361) NUMC
  361   FORMAT(I3)
      DO 355 I=1,NUMC
        READ(1,360) TC(I),IC(I),JC(I),KC(I)
  360     FORMAT(4(I3))
  355   CONTINUE
```

```
C
      NGPRV=1
      RN=COF(1)**2
      DO 130 I=2,NICTOT
        IF(NGC(I) .EQ. NGC(I-1)) THEN
          RN=RN+COF(I)**2
        ELSE
          RNORM=1.0/SQRT(RN)
          DO 133 J=I-1,NGPRV,-1
            COF(J)=RNORM*COF(J)
  133         CONTINUE
          RN=COF(I)**2
          NGPRV=I
         ENDIF
  130   CONTINUE
      RNORM=1.0/SQRT(RN)
      DO 135 I=NICTOT,NGPRV,-1
        COF(I)=RNORM*COF(I)
  135   CONTINUE
C
      DO 200 I=1,NICTOT
      II=NGC(I)
      JJ=KIC(I)
      SM1(II,JJ)=COF(I)
  200   CONTINUE
C
      KK=0
      II=0
      DO 230 I=1,NGPSET
      WRITE(16,210) I
  210   FORMAT(//5X,'GROUP COORDINATE SET NO.',I3)
      WRITE(16,213) NGPC(I)
  213   FORMAT(5X,'NUMBER OF GROUP COORDINATES IN SET = ',I3)
      WRITE(16,215) NINGP(I)
  215   FORMAT(5X,'NUMBER OF INTERNAL COORDINATES IN SET = ',I3)
ALA07020
      WRITE(16,454) I,DIPMAG(I,1),DIPMAG(I,2)
  454   FORMAT(5X,'DIPOLE MOMENT DERIVATIVES FOR SET NO.',I3,' =',
ALA07040
     1  2F12.6)
ALA07050
      DO 235 J=1,NINGP(I)
        KK=KK+1
        IF (KK .NE. 1) THEN
          IF (NGC(KK) .EQ. NGC(KK-1)) THEN
            GO TO 226
          ENDIF
        ENDIF
        II=II+1
        WRITE(16,223) II
  223     FORMAT(/10X,'GROUP COORDINATE NO.',I3)
ALA07190
        WRITE(16,240) II,II,II,II
```

```
  240     FORMAT(13X,'CAX(',I3,')',2X,'DIPCOM(',I3,',X)',2X,'DIPCOM(',
ALA07210
     1    I3,',Y)',2X,'DIPCOM(',I3,',Z)')
ALA07220
        WRITE(16,245) CAX(II),DIPCOM(II,1),DIPCOM(II,2),DIPCOM(II,3)
  245     FORMAT(16X,I3,7X,F7.3,2(9X,F7.3))
ALA07240
        WRITE(16,225)
  225     FORMAT(16X,'NGC',4X,'KIC',8X,'COF')
ALA07260
  226     WRITE(16,227) NGC(KK),KIC(KK),COF(KK)
  227     FORMAT(16X,2(I3,4X),F12.6)
ALA07280
  235     CONTINUE
ALA07290
  230   CONTINUE
ALA07300
C
ALA07310
      WRITE(16,270)
  270 FORMAT(//2X,'ATOMS USED TO DEFINE LOCAL X,Y,Z AXES',/3X,'TYPE',
ALA07330
     14X,'IC',4X,'JC',4X,'KC')
ALA07340
      DO 260 I=1,NUMC
ALA07350
      WRITE(16,265) TC(I),IC(I),JC(I),KC(I)
  265   FORMAT(1X,4(I6))
ALA07370
  260 CONTINUE
ALA07380
C
ALA07390
      IFX=1
ALA07400
      IF(IFX .EQ. 0) THEN
ALA07410
        WRITE(16,36)
   36     FORMAT(//2X,'POL. WEIGHTED U-MATRIX FOR GROUP COORD.'/)
ALA07430
        LIM=1
        NNQQ=NOAT*3-6
        DO 214 I=1,LIM
C         DO 214 I=1,NICTOT
ALA07470
          WRITE(16,47) (SM1(I,J),J=1,NNQQ)
   47       FORMAT(10X,10F5.1)
ALA07490
  214       CONTINUE
ALA07500
      ENDIF
ALA07510
C
ALA07520
```

```
      DO 220 IA=1,NICTOT-1
ALA07530
      DO 218 IB=IA+1,NICTOT
        DOT=0.0
        DO 216 J=1,NICTOT
          DOT=DOT+SM1(IA,J)*SM1(IB,J)
  216       CONTINUE
          IF(ABS(DOT) .GT. 0.000001) THEN
             WRITE(16,48) IA,IB
   48             FORMAT(//2X,'*** ERROR***'//10X,'INT. COORD.',I4,1X,
     1            'AND',I4,1X,'ARE NOT ORTHOG.')
             CALL EXIT
             ENDIF
  218     CONTINUE
ALA07650
  220   CONTINUE
ALA07660
C
ALA07670
C
ALA07680
      RETURN
ALA07690
      END
ALA07700
      SUBROUTINE CONFM2(AQQ,TEMP)
      REAL  AQQ(50,3,3),TEMP,QQ(3,3)
      COMMON  /ETORS/ KTNUM(50),NSTATE(50),KTTYP(50),KTANG(50,3),
     1                TENER(50,3),KTYN,KARTAU(50)
C
C
CCC       NOQQ=0
CCC       DO 10 I=1,KTYN
CCC         IF(KTTYP(I) .EQ. 0) THEN
CCC           CALL PEPQ(QQ,TENER(I,1),TENER(I,2),TENER(I,3),TEMP)
CCC           DO 15 J=1,3
CCC           DO 15 K=1,3
CCC             AQQ(I,J,K)=QQ(J,K)
CCC    15     CONTINUE
CCC         ENDIF
CCC    10 CONTINUE
C
C
      RETURN
      END
      SUBROUTINE PEPQ(QQ,EG,EGG,EGGP,TEMP)
ALA03040
      REAL  QQ(3,3),EG,EGGP,EGG,TEMP
      PARAMETER (RCONST=1.987)
ALA03060
      LOGICAL DUM(6)
ALA03070
      REAL  U(3,3),UU(3,3),B(3,3),PP(3,3),P(3)
ALA03080
```

```
      REAL  SWA(6),DET(2)
ALA03090
      REAL  EVAL(3),A(3,3)
ALA03100
      COMPLEX EVALC(3),AC(3,3)
ALA03110
C
ALA03210
C  FORM U
ALA03220
C
ALA03230
      U1=EXP(-EG/(RCONST*TEMP))
ALA03240
      U2=EXP(-EGGP/(RCONST*TEMP))
ALA03250
      U3=EXP(-EGG/(RCONST*TEMP))
ALA03260
C
ALA03270
      DO 140 I=1,3
ALA03280
      DO 138 J=1,3
        IF(J .EQ. 1) U(I,J)=1.0
        IF(J .NE. 1) U(I,J)=U1
  138     CONTINUE
ALA03320
  140   CONTINUE
ALA03330
      U(2,3)=U(2,3)*U2
ALA03340
      U(3,2)=U(2,3)
ALA03350
      U(2,2)=U(2,2)*U3
ALA03360
      U(3,3)=U(2,2)
ALA03370
  600 WRITE(16,14) ((U(I,J),J=1,3),I=1,3)
   14 FORMAT(/6X,'U-MATRIX ='/(10X,3F10.6))
C
ALA03400
C  DIAG. U-MATRIX
ALA03410
C
ALA03420
      DO 150 I=1,3
ALA03430
      DO 148 J=1,3
        UU(I,J)=U(I,J)
  148     CONTINUE
ALA03460
  150   CONTINUE
ALA03470
```

```
      CALL DGEEV(1,UU,3,EVALC,AC,3,DUM,3,SWA,6)
ALA03480
C
ALA03490
C  KEEP REAL PART ONLY (ASSUME IMAG. = 0)
ALA03500
C
ALA03510
      DO 152 I=1,3
ALA03520
      EVAL(I)=EVALC(I)
      DO 151 J=1,3
        A(I,J)=AC(I,J)
  151     CONTINUE
ALA03560
  152   CONTINUE
ALA03570
       WRITE(16,18)
   18 FORMAT(//2X,'A-MATRIX ='/)
ALA03590
       WRITE(16,20) ((A(I,J),J=1,3),I=1,3)
   20 FORMAT(10X,3F10.6)
ALA03610
C
ALA03620
C  CALC. B, THE INVERSE OF A
ALA03630
C
ALA03640
      DO 160 I=1,3
ALA03650
      DO 158 J=1,3
        B(I,J)=A(I,J)
  158     CONTINUE
ALA03680
  160   CONTINUE
ALA03690
      CALL DGEICD(B,3,3,0,RCOND,DET,DDUM,NDUM)
ALA03700
C     WRITE(16,24)
C  24 FORMAT(//2X,'B-MATRIX ='/)
ALA03720
C     WRITE(16,26) ((B(I,J),J=1,3),I=1,3)
C  26 FORMAT(10X,3F10.6)
ALA03740
C
ALA03750
C  FIND POSITION OF LARGEST EIGENVALUE
ALA03760
C
ALA03770
C     WRITE(16,28) (EVAL(I),I=1,3)
C  28 FORMAT(//2X,'EVAL(I) =',3F10.6)
ALA03790
```

```
      EMAX=0.0
ALA03800
      LMAX=0
ALA03810
      DO 210 I=1,3
ALA03820
      IF(EVAL(I) .GT. EMAX) THEN
          EMAX=EVAL(I)
          LMAX=I
        ENDIF
  210   CONTINUE
ALA03870
C
ALA03880
C  CALC. FIRST ORDER PROB.
ALA03890
C
ALA03900
      DO 220 I=1,3
ALA03910
      P(I)=A(I,LMAX)*B(LMAX,I)
  220   CONTINUE
ALA03930
C
ALA03940
C  CALC. SECOND-ORDER A PRIORI PROBABILITIES
ALA03950
C
ALA03960
      DO 230 I=1,3
ALA03970
      DO 228 J=1,3
        PP(I,J)=U(I,J)*A(J,LMAX)*B(LMAX,I)/EVAL(LMAX)
  228     CONTINUE
ALA04000
  230   CONTINUE
ALA04010
C
ALA04020
C  CALC. SECOND-ORDER CONDITIONAL PROBABILITIES
ALA04030
C
ALA04040
      DO 240 I=1,3
ALA04050
      DO 238 J=1,3
        QQ(I,J)=U(I,J)*A(J,LMAX)/(A(I,LMAX)*EVAL(LMAX))
  238     CONTINUE
ALA04080
  240   CONTINUE
ALA04090
C
ALA04100
      WRITE(16,30)
```

```
   30 FORMAT(/6X,'CALC. PROB.'/10X,'P',18X,'PP',24X,'QQ')
ALA04120
      DO 310 I=1,3
ALA04130
  310   WRITE(16,32) P(I),(PP(I,J),J=1,3),(QQ(I,J),J=1,3)
   32   FORMAT(8X,F7.4,5X,3F7.4,5X,3F7.4)
ALA04150
C
ALA04160
C
ALA04170
      RETURN
ALA04180
      END
ALA04190
      SUBROUTINE KORD
C
C
      CALL KORDIN
      CALL KORDSB
      CALL KORDT
C
C
      RETURN
      END
      SUBROUTINE KORDIN
      DIMENSION  NSKEL(200),NTEMPT(200),NTEMPS(200),
     1NR(4),NCO(4),DAT(4),RR(3),NTERM(200),
     2DH(200),NOLD(200),DHOK(6),MXOK(6)
      COMMON  /ATOM/  NOAT
      COMMON  /CORD2/ NICT(101,6,4),NCODT(101,6),NOCOMP(101),NT
      COMMON  /BOND1/ CAR(120,3),NOBOND,NB1(120),NB2(120)
      COMMON  /ENVIR/ KBN(120,4),KT(120),KTSK(120)
      COMMON  /BOND2/ KWT(120),KB1(120),KB2(120)
      COMMON  /STRUC/ X(3,120),W(120),KIND(120)
C
C  IDENTIFY ALL ATOMS BONDED TO ATOM I. STORE THESE IN KBN(I,N).
C
      DO 34 I=1,NOAT
      KT(I)=0
   34 KTSK(I)=0
      DO 50 I=1,NOAT
   35 DO 50 J=1,NOBOND
      J1=KB1(J)
      J2=KB2(J)
      IF(I-J1) 38,36,38
   36 NSUR=J2
      GO TO 40
   38 IF(I-J2) 50,39,50
   39 NSUR=J1
   40 KT(I)=KT(I)+1
      N=KT(I)
      KBN(I,N)=NSUR
   50 CONTINUE
```

```
C
C  IDENTIFY TERMINAL AND NON-TERMINAL (SKELETAL) ATOMS
C  LIST NON-TERMINAL ATOMS FIRST IN KBN(I,N)
C
      K=0
      DO 58 I=1,NOAT
      N=KT(I)
      IF(N-1) 56,56,58
   56 K=K+1
      NTERM(K)=I
   58 CONTINUE
      NOTERM=K
      DO 80 I=1,NOAT
      N=KT(I)
      NTT=0
      NS=0
   60 DO 68 J=1,N
      L=KBN(I,J)
      DO 64 K=1,NOTERM
      M=NTERM(K)
      IF(L-M) 64,62,64
   62 NTT=NTT+1
      NTEMPT(NTT)=L
      GO TO 68
   64 CONTINUE
      NS=NS+1
      NTEMPS(NS)=L
   68 CONTINUE
      IF(NS) 74,74,69
   69 KTSK(I)=NS
      DO 70 J=1,NS
   70 KBN(I,J)=NTEMPS(J)
   74 IF(NTT) 80,80,76
   76 DO 78 K=1,NTT
      KK=NS+K
   78 KBN(I,KK)=NTEMPT(K)
   80 CONTINUE
      DO 84 I=1,NOAT
   84   KWT(I)=W(I)
      IFX=0
      IF(IFX .EQ. 0) RETURN
      WRITE(16,1024)
 1024 FORMAT(/3X,'KBN AFTER REARRANGED  ')
      DO 55 I=1,NOAT
      NJ=KT(I)
   55 WRITE(16,1023) I,(KBN(I,J),J=1,NJ)
 1023 FORMAT(I8,I6,9I4)
C
C
      RETURN
      END
      SUBROUTINE KORDSB
      DIMENSION  R(3),EL(3),EM(3),EN(3),DD(3),CROS(3),BX(3),EA(3),EB(3),
     1  AX(3),ITMP(4)
```

```
      COMMON  /ATOM/  NOAT
      COMMON  /CORD1/ NIC(370,4),NCOD(370),NONIC,NOCTOT
      COMMON  /CORD3/ NOC,NAT,NLIN
      COMMON  /ENVIR/ KBN(120,4),KT(120),KTSK(120)
      COMMON  /LINR/  NATLIN(370)
      COMMON  /BOND2/ KWT(120),KB1(120),KB2(120)
      COMMON  /STRUC/ X(3,120),W(120),KIND(120)
      COMMON  /OOP/   IOOP(25,5),NOOP,NDIR(25)
C
C
      NONIC=0
      NLIN=0
C
C  DISPLAY NUMBER OF BONDS FOR EACH ATOM
C
C     WRITE(16,1027) (KT(I),I=1,NOAT)
C1027 FORMAT(/3X,'KT NUMBERS '/(5X,15I4))
C
C  DEFINE BOND STRETCHING COORD.
C
C  DEFINE C-H (C-D) STRETCHES
C
      CALL HSTR(NOAT,12)
      CALL HSTR(NOAT,13)
C     IF(NONIC .NE. 0) THEN
C         WRITE(16,1028)
C1028     FORMAT(/3X,'C-H AND C-D STRETCHES')
C         WRITE(16,1029) (I,NCOD(I),NIC(I,1),NIC(I,2),I=1,NONIC)
C1029     FORMAT(10X,4I4)
C       ENDIF
C
C  DEFINE N-H STRETCH
C
      NBEG=NONIC+1
      CALL HSTR(NOAT,14)
C     IF(NONIC .GE. NBEG) THEN
C         WRITE(16,1031)
C1031     FORMAT(/3X,'N-H STRETCHES')
C         WRITE(16,1029) (I,NCOD(I),NIC(I,1),NIC(I,2),I=NBEG,NONIC)
C       ENDIF
C
C  OTHER HYDGROGEN STRECTHES
C
      NBEG=NONIC+1
      CALL HSTRX(NOAT)
C     IF(NONIC .GE. NBEG) THEN
C         WRITE(16,2030)
C2030     FORMAT(/3X,'OTHER X-H STRETCHES')
C         WRITE(16,1029) (I,NCOD(I),NIC(I,1),NIC(I,2),I=NBEG,NONIC)
C       ENDIF
C
C  DEFINE OTHER TERMINAL ATOM STRETCHES
C
  119 NBEG=NONIC+1
```

```
      DO 130 I=1,NOAT
      N=KT(I)
      IF(N-1)130,120,130
  120 IF(KWT(I) .EQ. 1 .OR. KWT(I) .EQ. 2) GO TO 130
      K=KBN(I,1)
      CALL KFOR(1,K,I,0,0)
  130 CONTINUE
C     DEFINE SKELETAL STRETCHES
  132 NBST=NONIC+1
      NCN=NONIC
      DO 150 I=1,NOAT
      N=KT(I)
      IF(N-1) 150,150,134
  134 NK=KTSK(I)
      IF(NK .EQ. 0) GO TO 150
      DO 148 J=1,NK
      K=KBN(I,J)
C     CHECK FOR DUPLICATE STRETCHES
      IF(NONIC-NCN) 140,140,138
  138 NCK=NONIC
      DO 139 L=NBST,NCK
      CALL COMPARB(I,K,NIC(L,1),NIC(L,2),NX)
      IF(NX) 139,148,148
  139 CONTINUE
  140 NONIC=NONIC+1
      NCOD(NONIC)=1
      NIC(NONIC,1)=I
      NIC(NONIC,2)=K
      NIC(NONIC,3)=0
      NIC(NONIC,4)=0
  148 CONTINUE
  150 CONTINUE
      NEST=NONIC
C     DEFINE BENDS FOR XY4 GROUPS
 1510 NBEG=NONIC+1
      DO 210 I=1,NOAT
      NJ=KT(I)
      IF(NJ-4) 210,152,210
  152 NJSK=KTSK(I)
      GO TO (154,168,174,192)NJSK
C     XST3 GROUP
  154 DO 158 M=2,3
      MM=M+1
      DO 158 N=MM,4
      NONIC=NONIC-1
      NCOD(NONIC+4)=2
      NIC(NONIC+4,1)=KBN(I,M)
      NIC(NONIC+4,2)=I
      NIC(NONIC+4,3)=KBN(I,N)
  158 NIC(NONIC+4,4)=0
      NONIC=NONIC+6
      DO 162 M=2,4
      NONIC=NONIC+1
      NCOD(NONIC)=2
```

```
      NIC(NONIC,1)=KBN(I,M)
      NIC(NONIC,2)=I
      NIC(NONIC,3)=KBN(I,1)
  162 NIC(NONIC,4)=0
      GO TO 210
C     XS2T2 GROUP
  168 NONIC=NONIC+1
      NCOD(NONIC)=2
      NIC(NONIC,1)=KBN(I,3)
      NIC(NONIC,2)=I
      NIC(NONIC,3)=KBN(I,4)
      NIC(NONIC,4)=0
      DO 172 M=3,4
      DO 172 N=1,2
      NONIC=NONIC+1
      NCOD(NONIC)=2
      NIC(NONIC,1)=KBN(I,M)
      NIC(NONIC,2)=I
      NIC(NONIC,3)=KBN(I,N)
  172 NIC(NONIC,4)=0
      NONIC=NONIC+1
      NCOD(NONIC)=2
      NIC(NONIC,1)=KBN(I,1)
      NIC(NONIC,2)=I
      NIC(NONIC,3)=KBN(I,2)
      NIC(NONIC,4)=0
      GO TO 210
C     XS3T GROUP
  174 DO 176 M=1,3
      NONIC=NONIC+1
      NCOD(NONIC)=2
      NIC(NONIC,1)=KBN(I,4)
      NIC(NONIC,2)=I
      NIC(NONIC,3)=KBN(I,M)
  176 NIC(NONIC,4)=0
      DO 180 M=1,2
      MM=M+1
      DO 180 N=MM,3
      NONIC=NONIC+1
      NCOD(NONIC)=2
      NIC(NONIC,1)=KBN(I,M)
      NIC(NONIC,2)=I
      NIC(NONIC,3)=KBN(I,N)
  180 NIC(NONIC,4)=0
  190 GO TO 210
C     XS4 GROUP
  192 DO 196 M=1,4
      MM=M+1
      IF(M-4) 194,193,194
  193 MM=1
  194 NONIC=NONIC+1
      NCOD(NONIC)=2
      NIC(NONIC,1)=KBN(I,M)
      NIC(NONIC,2)=I
```

```
      NIC(NONIC,3)=KBN(I,MM)
  196 NIC(NONIC,4)=0
      DO 200 M=1,2
      MM=M+2
      NONIC=NONIC+1
      NCOD(NONIC)=2
      NIC(NONIC,1)=KBN(I,M)
      NIC(NONIC,2)=I
      NIC(NONIC,3)=KBN(I,MM)
  200 NIC(NONIC,4)=0
  210 CONTINUE
C     DEFINE BENDS FOR XY3 GROUP
  212 NBEG=NONIC+1
      IDIR=0
      DO 250 I=1,NOAT
      IF(KT(I)-3) 250,220,250
C     TEST FOR PLANARITY OF THE XY3 GROUP
  220 L=KBN(I,1)
      M=KBN(I,2)
      N=KBN(I,3)
      CALL DIST(I,L,R(1))
      CALL DIST(I,M,R(2))
      CALL DIST(I,N,R(3))
      DO 230 K=1,3
      EL(K) = (X(K,I)-X(K,L))/R(K)
      EM(K) = (X(K,I)-X(K,M))/R(K)
  230 EN(K) = (X(K,I)-X(K,N))/R(K)
      CROSDT = (EM(2)*EN(3) - EM(3)*EN(2))*EL(1) - (EM(1)*EN(3) -EM(3)*
     1EN(1))*EL(2) + (EM(1)*EN(2) - EM(2)*EN(1))*EL(3)
C     WRITE(16,1038) I
C1038 FORMAT(//2X,'ATOM ',I3,' IS CENTER OF XY3 GROUP')
C     WRITE(16,1037) CROSDT,L,M,N
C1037 FORMAT(/5X,'CROSDT=', F10.6, ' FOR PLANE DEFINED BY ATOMS',3I3)
      IF(ABS(CROSDT)-0.015) 235,235,234
C     NOT PLANAR IN EXCESS OF ONE DEGREE
  234 IPLANE=-1
      GO TO 236
C     PLANAR
  235 IPLANE=1
C     BENDS FOR BOTH PLANAR AND NON-PLANAR CASES
  236 DO 240 J=1,2
      NONIC=NONIC+1
      NIC(NONIC,1) = KBN(I,J)
      NIC(NONIC,2)=I
      NIC(NONIC,3)=KBN(I,3)
      NIC(NONIC,4)=0
  240 NCOD(NONIC)=2
C     OUT-OF-PLANE COORD. FOR SP2 ATOM GROUP
C     CHECK FOR TWO BONDS OF EQUAL LENGTH
      IF(IPLANE) 250,250,241
C
C DEFINE OOP BEND AND POSITIVE INTERACTION
C
  241 IFOP=0
```

```
      DO 4000 M=1,NOOP
      DO 4010 K=1,4
        ITMP(K)=0
 4010   CONTINUE
      ITMP(2)=I
      DO 4030 N=1,KT(I)
      DO 4030 K=1,4
        IF(IOOP(M,K) .EQ. KBN(I,N)) ITMP(K)=KBN(I,N)
 4030   CONTINUE
      IFZE=0
      DO 4020 K=1,4
        IF(ITMP(K) .EQ. 0) IFZE=1
 4020   CONTINUE
      IF(IFZE .EQ. 0) IFOP=IFOP+1
      IF(IFOP .EQ. 1) THEN
        NONIC=NONIC+1
        NCOD(NONIC)=3
        DO 4040 K=1,4
          NIC(NONIC,K)=ITMP(K)
 4040     CONTINUE
        IDIR=IDIR+1
        NDIR(IDIR)=NONIC
      ELSEIF(IFOP .GT. 1) THEN
        WRITE(16,4050)
 4050     FORMAT(//2X,'ERROR!! OOP BEND HAS >1 INTERACTION DEFINITION!')
        CALL EXIT
      ENDIF
 4000 CONTINUE
      IF(IFOP .EQ. 0) THEN
      WRITE(16,4060)
 4060   FORMAT(//2X,'ERROR!! PLANAR XY3 GROUP HAS NO INTERACTION',1X,
     1          'DEFINITION!')
      CALL EXIT
      ENDIF
C
  250 CONTINUE
C     BENDING COORD. FOR XY2 GROUP
  252 NBEG=NONIC+1
      DO 254 I=1,NONIC
  254 NATLIN(I)=0
      DAI=1.0
      DO 300 I=1,NOAT
      IF(KT(I)-2) 300,260,300
C     TEST FOR LINEARITY OF XY2 GROUP. IF LINEAR, BEND IS LESS
C     THAN ONE DEGREE.
  260 L=KBN(I,1)
      M=KBN(I,2)
      CALL ANGIK(L,I,M,ALF)
C     WRITE(16,1041)  ALF,L,I,M
C1041 FORMAT(  /'   ANGLE=',F8.2,' FOR ATOMS',3I3)
      IF(ABS(ALF)-1.0) 272,270,270
C     NON-LINEAR
  270 NONIC=NONIC+1
      NCOD(NONIC)=2
```

```
      NIC(NONIC,1)=L
      NIC(NONIC,2)=I
      NIC(NONIC,3)=M
      NIC(NONIC,4)=0
      NATLIN(NONIC)=0
      GO TO 300
C     LINEAR
C     FIND POINT A
C     FIRST FIND POINT B
  272 NCOM=0
      DO 274, K=1,3
  274 EB(K)=0.0
C     CHECK FOR LINEARITY WITH L AND I
      CALL DIST(I,L,RL)
      DO 275 K=1,3
  275 EL(K) = (X(K,I)-X(K,L))/RL
      DO 280 K=1,3
      IF(ABS(EL(K))-1.0) 276,280,276
  276 EB(K)=1.0
      GO TO 284
  280 CONTINUE
C     BI CROSS IL
  284 CROS(1) = (EL(2)*EB(3) - EL(3)*EB(2))
      CROS(2) =-(EL(1)*EB(3) - EL(3)*EB(1))
      CROS(3) = (EL(1)*EB(2) - EL(2)*EB(1))
      AISQ=0.0
      DO 288 K=1,3
  288 AISQ = AISQ+CROS(K)**2
C     DAI=SQRT(AISQ)
      DO 290 K=1,3
      EA(K) = CROS(K)/DAI
  290 AX(K) = X(K,I)-EA(K)
  291 NONIC=NONIC+1
      NLIN=NLIN+1
C     WRITE(16,1042) NONIC,(AX(K),K=1,3)
C1042 FORMAT(/'COORD. OF POINT A FOR LINEAR BEND COORD. NO.',I3/(3F12.6)
C    1 )
      NCOD(NONIC)=6
      NIC(NONIC,1)=L
      NIC(NONIC,2)=I
      NIC(NONIC,3)=M
      NIC(NONIC,4)=0
      N=NOAT+NLIN
      NATLIN(NONIC)=N
      DO 292 K=1,3
  292 X(K,N)=AX(K)
      IF(NCOM) 293,293,300
  293 NCOM=NCOM+1
      CROS(1) = EA(2)*EL(3)-EA(3)*EL(2)
      CROS(2) =-EA(1)*EL(3)+EA(3)*EL(1)
      CROS(3) = EA(1)*EL(2)-EA(2)*EL(1)
      DO 295 K=1,3
  295 AX(K)=X(K,I)-CROS(K)
      GO TO 291
```

```
  300 CONTINUE
C     IF(NBEG .GT. NONIC) RETURN
C3000 WRITE(16,1044) (I,NCOD(I),(NIC(I,J2),J2=1,3),I=NBEG,NONIC)
C1044 FORMAT(/3X,'BEND COORD. FOR XY2 GROUP'/(10X,5I4))
C
C
      RETURN
      END
      SUBROUTINE KORDT
      COMMON  /MAINC/ IFR, IFL,NMOL,NCM,NMTOT
      COMMON  /BOND2/ KWT(120),KB1(120),KB2(120)
      COMMON  /CORD2/ NICT(101,6,4),NCODT(101,6),NOCOMP(101),NT
      COMMON  /ENVIR/ KBN(120,4),KT(120),KTSK(120)
      COMMON  /TORC/  KBTOR(50),KBON(50)
C
C
      DO 180 NIY=1,NT
      IY=KBON(NIY)
      IT=0
      NA=KB1(IY)
      NB=KB2(IY)
      IF(KT(NA) .LT. KT(NB)) THEN
        NA=KB2(IY)
        NB=KB1(IY)
      ENDIF
      IM=KT(NA)
      IN=KT(NB)
C
      IF(IM .LE. 1 .OR. IN .LE. 1) THEN
        WRITE(16,12) NIY,NA,NB,KBTOR(NIY),IM,IN
   12     FORMAT(//2X,'ERROR IN DEFINING TORSION NO.',I3
     1     //10X,'NA,NB,KBTOR(NIY),IM,IN =',5I3)
        CALL EXIT
      ENDIF
C
      DO 170 M=1,IM
      LA=KBN(NA,M)
      IF(LA .EQ. NB) GO TO 170
      CALL ANGIK(LA,NA,NB,ALF)
      IF(ABS(ALF) .LT. 5.0) THEN
          WRITE(16,16) ALF,LA,NA,NB
   16       FORMAT(/2X,'THE ANGLE (',F7.2,',) FORMED BY ATOMS',3I4,
     1       ' IS WITHIN 5 DEG. OF BEING LINEAR.'/5X,'NOT USED IN',
     2       ' DEFINING A TORS. COORD.')
          GO TO 170
      ENDIF
C
      DO 160 N=1,IN
        LB=KBN(NB,N)
      IF(LB .EQ. NA) GO TO 160
      CALL ANGIK(NA,NB,LB,ALF)
      IF(ABS(ALF) .LT. 5.0) THEN
          WRITE(16,16) ALF,NA,NB,LB
          GO TO 160
```

```
        ENDIF
C
C  ALL POSSIBLE COMBINATIONS
C
      IF(KBTOR(NIY) .EQ. 1) GO TO 140
      CALL TRAGA(LA,NA,NB,LB,TAU,MX)
      ATAU=ABS(TAU)
C     WRITE(16,99) NIY,M,N,LA,NA,NB,LB,TAU
C  99 FORMAT(7I3,F12.6)
C
C  TRANS COMBINATIONS ONLY
C
      IF(KBTOR(NIY) .EQ. 2) THEN
        IF(ABS(ATAU-180.0) .LT. 30.0) GO TO 140
      ENDIF
C
C  CIS COMBINATIONS ONLY
C
      IF(KBTOR(NIY) .EQ. 3) THEN
        IF(ATAU .LT. 30.0) GO TO 140
      ENDIF
C
C  AROMATIC CCCC TORSIONS
C
      IF(KBTOR(NIY) .EQ. 4) THEN
        IF(ATAU .LT. 30.0) THEN
            IF(KWT(LA) .NE. 12 .OR. KWT(NA) .NE. 12) GO TO 160
            IF(KWT(NB) .EQ. 12 .AND. KWT(LB) .EQ. 12) GO TO 140
          ENDIF
      ENDIF
C
C ALL COMBINATIONS NOT INVOLVING H-X-X-H TORSIONS
C
      IF(KBTOR(NIY) .EQ. 5) THEN
      IF((KWT(LA) .NE. 1 .AND. KWT(LA) .NE. 2) .OR.
     1     (KWT(LB) .NE. 1 .AND. KWT(LB) .NE. 2)) GO TO 140
      ENDIF
C
      GO TO 160
C
  140 IF(IT .EQ. 0) THEN
        MCOD=4
      ELSE
        MCOD=0
      ENDIF
      IT=IT+1
C
      CALL KFORT(NIY,MCOD,LA,NA,NB,LB,IT)
  160 CONTINUE
  170 CONTINUE
      NOCOMP(NIY)=IT
  180 CONTINUE
C
C  WRITE TORSIONAL COORD.
```

```
C
      IF(NCM .GT. 0) RETURN
      NNT=0
      WRITE(16,30) NT
   30 FORMAT(///2X,'TORSIONAL COORDINATES.  NT =',I3/)
      IF(NT .EQ. 0) RETURN
      DO 260 I=1,NT
      DO 270 J=1,NOCOMP(I)
        IF(NCODT(I,J) .EQ. 4) NNT=NNT+1
        WRITE(16,32) NNT,NCODT(I,J),(NICT(I,J,K),K=1,4)
   32     FORMAT(19X,2I4,2X,4I3)
  270     CONTINUE
  260   CONTINUE
C
C
      RETURN
      END
      SUBROUTINE KFOR(I,J,K,L,M)
      COMMON  /CORD1/ NIC(370,4),NCOD(370),NONIC,NOCTOT
C
C
      NONIC=NONIC+1
      NCOD(NONIC)=I
      NIC(NONIC,1)=J
      NIC(NONIC,2)=K
      NIC(NONIC,3)=L
      NIC(NONIC,4)=M
C
C
      RETURN
      END
      SUBROUTINE KFORT(NIY,MCOD,I,J,K,L,IT)
      COMMON  /CORD2/ NICT(101,6,4),NCODT(101,6),NOCOMP(101),NT
C
C
      NCODT(NIY,IT)=MCOD
      NICT(NIY,IT,1)=I
      NICT(NIY,IT,2)=J
      NICT(NIY,IT,3)=K
      NICT(NIY,IT,4)=L
C
C
      RETURN
      END
      SUBROUTINE HSTR(NOAT,KX)
      COMMON  /ENVIR/ KBN(120,4),KT(120),KTSK(120)
COM00050
      COMMON  /BOND2/ KWT(120),KB1(120),KB2(120)
COM00090
C
C
      DO 120 I=1,NOAT
      IF(KT(I) .EQ. 1) THEN
          IF(KWT(I) .EQ. 1 .OR. KWT(I) .EQ. 2) THEN
```

```
            J=KBN(I,1)
            IF(KWT(J) .EQ. KX) CALL KFOR(1,I,J,0,0)
            ENDIF
          ENDIF
  120 CONTINUE
C
C
      RETURN
      END
      SUBROUTINE HSTRX(NOAT)
      COMMON  /CORD1/ NIC(370,4),NCOD(370),NONIC,NOCTOT
      COMMON  /ENVIR/ KBN(120,4),KT(120),KTSK(120)
      COMMON  /BOND2/ KWT(120),KB1(120),KB2(120)
C
C
      DO 120 I=1,NOAT
      IF(KT(I) .EQ. 1) THEN
          IF(KWT(I) .EQ. 1 .OR. KWT(I) .EQ. 2) THEN
            J=KBN(I,1)
            IF(NONIC .EQ. 0) THEN
                CALL KFOR(1,I,J,0,0)
              ELSE
                DO 118 N=1,NONIC
                  IF(I .EQ. NIC(N,1)) GO TO 120
  118                 CONTINUE
                CALL KFOR(1,I,J,0,0)
              ENDIF
            ENDIF
          ENDIF
  120   CONTINUE
C
C
      RETURN
      END
      SUBROUTINE DIST(I,J,DFAR)
      DIMENSION  R(3)
      COMMON  /STRUC/ X(3,120),W(120),KIND(120)
C     THIS SUBROUTINE COMPUTES THE DISTANCE BETWEEN ATOMS I AND J.
      RIJSQ=0.0
      DO 110 M=1,3
      R(M)=X(M,I)-X(M,J)
  110 RIJSQ=RIJSQ+R(M)**2
      DFAR=SQRT(RIJSQ)
      RETURN
      END
      SUBROUTINE COMPARB(LA,LB,MA,MB,NX)
C     THIS SUBROUTINE COMPARES THE VALUES OF THE PAIR LA AND LB WITH THE
C     PAIR MA AND MB IN ALL POSSIBLE PERMUTATIONS.  IF THEY ARE THE SAME
C     NX=1.   IF DIFFERENT NX=-1.
      IF(LA-MA) 110,112,110
  110 IF(LA-MB) 120,111,120
  111 IF(LB-MA) 120,124,120
  112 IF(LB-MB) 120,124,120
  120 NX=-1
```

```
      GO TO 126
  124 NX=1
  126 RETURN
      END
      SUBROUTINE ANGIK(I,J,K,ALF)
      COMMON  /STRUC/ X(3,120),W(120),KIND(120)
C     THIS SUBROUTINE COMPUTES THE ANGLE FORMED BY THE ATOMS I-J-K.
C     THE ANGLE IN DEGREES IS CALLED ALF.
      DIMENSION  EL(3),EM(3)
      CALL DIST(J,I,RI)
      CALL DIST(K,J,RK)
      DOT=0.0
      DO 120 M=1,3
      EL(M)=(X(M,I)-X(M,J))/RI
      EM(M)=(X(M,J)-X(M,K))/RK
  120 DOT=DOT+EL(M)*EM(M)
      DEL=ABS(DOT)-1.0
      IF(DEL)150,140,140
  140 IF(DOT)148,144,144
  144 DOT=1.0
      GO TO 150
  148 DOT=-1.0
  150 ALF=ASIN(DOT)
      ALF=ALF/0.0174532925-90.0
      RETURN
      END
      SUBROUTINE FCIN
      DIMENSION  KTT(10),KFOR(10)
      DIMENSION  RECIN(18)
      COMMON  /ATOM/ NOAT
      COMMON  /CORD1/ NIC(370,4),NCOD(370),NONIC,NOCTOT
      COMMON  /CORD2/ NICT(101,6,4),NCODT(101,6),NOCOMP(101),NT
      COMMON  /ENVIR/ KBN(120,4),KT(120),KTSK(120)
      COMMON  /FCON1/ NOK(105),KND(105,10),KODE(105),NOF
      COMMON  /FCON2/ VAL(105),ANGLE(105),ZFACT(105)
      COMMON  /FCON3/ KIFC(105,20),KJFC(105,20),NOEQ(105)
      COMMON  /STRUC/ X(3,120),W(120),KIND(120)
C
C
C  THE TORSIONAL COORD. WILL BE DEFINED IN THE
C  SAME FORMAT AS THE STRETCHING COORD.
C
C  NOCTOT = THE TOTAL NUMBER OF INT. COORD.
C
      NOCTOT=NONIC+NT
C
      DO 250 IT=1,NT
      I=NONIC+IT
      NCOD(I)=4
      NIC(I,1)=NICT(IT,1,2)
      NIC(I,2)=NICT(IT,1,3)
  250   CONTINUE
C
      WRITE(16,52)
```

```
   52 FORMAT(//2X,'INTERNAL COORD. WITH TORSIONS DEFINED IN A STRETCH',
     1  1X,'FORMAT'//5X,'NO.',2X,'NCOD',3X,'N1 N2 N3 N4'/)
      WRITE(16,54) (I,NCOD(I),(NIC(I,J),J=1,4),I=1,NOCTOT)
   54 FORMAT(4X,I3,5X,I1,3X,4I3)
C
C  READ IN FORCE CONSTANTS
C
      READ(2,100) (RECIN(I),I=1,18)
  100 FORMAT(18A4)
      WRITE(16,110) (RECIN(I),I=1,18)
  110 FORMAT(//2X,'VFF USED =',/18A4)
      N=0
      M=0
  304 READ(2,60) K,V,A,KE,(KFOR(I),I=1,10),ZFAK
   60 FORMAT(I3,2F10.6,11I3,F10.6)
C
      IF(N .NE. 0 .AND. K .EQ. 0) THEN
        M=M+1
        KIFC(N,M)=KFOR(1)
        KJFC(N,M)=KFOR(2)
C         WRITE(16,867) N,M,KIFC(N,M),KJFC(N,M)
C 867     FORMAT(2X,'N,M,KIFC(N,M),KJFC(N,M) =',4I3)
        GO TO 304
      ELSEIF(N .NE. 0) THEN
        NOEQ(N)=M
        IF(K .LT. 0) GO TO 324
      ENDIF
C
      N=N+1
      M=1
      NOK(N)=K
      VAL(N)=V
      ANGLE(N)=A
      KODE(N)=KE
      DO 320 I=1,10
      KND(N,I)=KFOR(I)
  320   CONTINUE
      KIFC(N,M)=KFOR(1)
      KJFC(N,M)=KFOR(2)
      ZFACT(N)=ZFAK
      GO TO 304
C
  324 NOF=N
      WRITE(16,64) NOF
   64 FORMAT(/5X,'NOF =',I4)
      DO 330 I=1,NOF
      IF(ZFACT(I) .EQ. 0.0) ZFACT(I)=1.0
  330   CONTINUE
C
C  IF IFYY=1, THE F.C. WILL BE PRINTED
C
      IFYY=1
      IF(IFYY .EQ. 0) RETURN
C
```

```
      WRITE(16,66)
   66   FORMAT(///2X,'FORCE CONSTANTS'//1X,'NO.',2X,'F.NO.',3X,
     1    'VAL.',5X,'ANGLE',2X,'KODE',1X,'K1',1X,'K2',1X,'K3',1X,
     2    'K4',1X,'K5',1X,'K6',1X,'K7',1X,'K8',1X,'K9',1X,'K10',
     3    1X,'ZFACT')
C
      DO 350 I=1,NOF
        DO 340 J=1,NOEQ(I)
          IF(J .EQ. 1) THEN
            WRITE(16,68) I,NOK(I),VAL(I),ANGLE(I),KODE(I),
     1           (KND(I,K),K=1,10),ZFACT(I)
   68           FORMAT(1X,I3,I6,F10.6,F9.1,2X,11I3,F8.4)
          ELSE
            WRITE(16,70) I,NOK(I),KIFC(I,J),KJFC(I,J)
   70           FORMAT(1X,I3,I6,24X,2I3)
          ENDIF
  340        CONTINUE
  350     CONTINUE
C
C
      RETURN
      END
      SUBROUTINE CONFM3(AQQ,DSEED,NXC,MXNOAT,SPAR,MXSPAR,KON,WTS)
c
c      Generate specific torsion angles for rotating bonds
c           Modification:
c             When IFL=9, it will read in the RIS code for each
c         torsional bond along the chain.
c                    Xiaozhen Yang July 10, 1996
c
      REAL  AQQ(50,3,3),SPAR(MXSPAR),Q(3)
      INTEGER  MXNOAT,NXC(MXNOAT,8),MXSPAR,KON(50) ,DSEED
      COMMON  /ATOM/  NOAT
      COMMON  /MAINC/ IFR, IFL,NMOL,NCM,NMTOT
      COMMON  /BOND2/ KWT(120),KB1(120),KB2(120)
      COMMON  /TORC/  KBTOR(50),KBON(50)
      COMMON  /CORD2/ NICT(101,6,4),NCODT(101,6),NOCOMP(101),NT
      COMMON  /ETORS/ KTNUM(50),NSTATE(50),KTTYP(50),KTANG(50,3),
     1                TENER(50,3),KTYN,KARTAU(50)
C
C       The modified
C
      if(IFL.eq.9) then
        read(1,*)(KON(i),i=1,NT),WTS
      do 200 i=1,NT
          IST=ABS(KTNUM(I))
          NXC(KARTAU(I),7)=KTANG(IST,KON(i))
  200 continue
        goto 666
      endif
C-----------------------------------------------
C                  O L D    P A R T
C-----------------------------------------------
      DO 10 I=1,NT
```

```
      IST=ABS(KTNUM(I))
C
      IF (KTNUM(I) .GT. 0) THEN
        IF (I .EQ. 1) THEN
          KK=1
        ELSE
          KK=KON(I-1)
        ENDIF
        IF (KTTYP(IST) .EQ. 0) THEN
          DO 50 J=1,NSTATE(IST)
            Q(J)=AQQ(IST,KK,J)
   50       CONTINUE
        ELSEIF(KTTYP(IST) .EQ. 1) THEN
          DO 165 II=1,3
            Q(II)=TENER(IST,II)
  165       CONTINUE
        ENDIF
      ENDIF
C
      IF(KTNUM(I) .EQ. 0) THEN
        KON(I)=1
      ELSE
        IF ((KTNUM(I) .LT. 0).AND.(NCM .EQ. 0)) THEN
          DO 40 K=1,NSTATE(IST)
            IF(NXC(KARTAU(I),7) .EQ. KTANG(IST,K)) KON(I)=K
   40       CONTINUE
        ELSEIF (KTNUM(I) .GT. 0) THEN
          CALL SELECT(Q,DSEED,KSEL,IST)
          KON(I)=KSEL
          NXC(KARTAU(I),7)=KTANG(IST,KSEL)
        ENDIF
      ENDIF
C
    10 CONTINUE
C
  666 continue
      WRITE(16,160) (KON(I),I=1,NT)
  160 FORMAT(2X,'KON= ',50I1)
C
C
      RETURN
      END
      SUBROUTINE SELECT(Q,DSEED,KSEL,IST)
      REAL  Q(3)
      INTEGER  KSEL,IST,DSEED
      DIMENSION  PP(4)
      COMMON  /MAINC/ IFR, IFL,NMOL,NCM,NMTOT
      COMMON  /ETORS/ KTNUM(50),NSTATE(50),KTTYP(50),KTANG(50,3),
     1                TENER(50,3),KTYN,KARTAU(50)
C
C  A RANDOM CONFORMATIONAL SEQUENCE IS GENERATED WITH THE USE OF A
C  THE ROW Q(I) OF THE CONDITIONAL PROB. MATRIX.
ALA09200
```

```
C
ALA09210
      CALL DURAND(DSEED,1,R)
ccc      write(16,*) DSEED,R
      PP(1)=0.0
C
ALA09240
      DO 111 K=1,NSTATE(IST)
ALA09250
      PP(K+1)=PP(K)+Q(K)
      IF(PP(K+1) .GE. R .AND. PP(K) .LT. R) THEN
          KSEL=K
          RETURN
        ENDIF
  111   CONTINUE
ALA09310
C
ALA09320
      IF(PP(4) .LT. 0.98 .OR. PP(4) .GT. 1.02) THEN
ALA09330
        WRITE(16,4) PP(4)
    4     FORMAT(//2X,'*** ERROR*** IN SR SELECT.'
ALA09350
     1    /5X,'SUM OF ONE ROW OF THE COND. PROB. MATRIX =',F7.4)
ALA09360
        CALL EXIT
      ENDIF
C
ALA09390
      IF(R .GT. 0.98) THEN
ALA09400
        KSEL=3
        RETURN
      ENDIF
C
ALA09440
      WRITE(16,13) NMOL
   13 FORMAT(//2X,'ERROR **** SR SELECT FAILED FOR NMOL =',I4)
ALA09460
      WRITE(16,17) R,(Q(I),I=1,3)
   17 FORMAT(10X,'R,Q(I)=',4F10.4)
ALA09480
      CALL EXIT
ALA09490
C
ALA09500
C
ALA09510
      RETURN
ALA09520
      END
ALA09530
      SUBROUTINE OVERLP(IFOVER,X)
ALA12430
```

```
      INTEGER  IFOVER
      REAL  X(3,120)
      COMMON  /MAINC/ IFR, IFL,NMOL,NCM,NMTOT
      COMMON  /BOND1/ CAR(120,3),NOBOND,NB1(120),NB2(120)
      COMMON  /BOND2/ KWT(120),KB1(120),KB2(120)
      COMMON  /ATOM/  NOAT
C
C
      IFOVER=1
      DO 140 I=1,NOAT-1
      DO 140 J=I+1,NOAT
      DO 150 K=1,NOBOND
        CALL COMPAR(I,J,KB1(K),KB2(K),NX)
        IF (NX .NE. 0) GO TO 140
  150   CONTINUE
      CALL DIST2(I,J,DD,X)
C***    IF(DD .LT. 1.5) THEN
ALA12590
      IF(DD .LT. 0.1) THEN
        IFOVER=0
        WRITE(16,160) NMTOT,I,J,DD
  160     FORMAT(//2X,'CONFORMER ',I5,' SKIPPED - ATOMS ',I3,' AND ',I3,
     1                ' OVERLAPPED.',/10X,'DISTANCE = ',F12.6)
        RETURN
       ENDIF
  140 CONTINUE
C
C
      RETURN
      END
      SUBROUTINE DIST2(I,J,DFAR,X)
      REAL  X(3,120)
      DIMENSION  R(3)
C THIS SUBROUTINE COMPUTES THE DISTANCE BETWEEN ATOMS I AND J.
C (NOTE X IS PASSED IN INSTEAD OF BEING IN A COMMON)
      RIJSQ=0.0
      DO 110 M=1,3
      R(M)=X(M,I)-X(M,J)
  110 RIJSQ=RIJSQ+R(M)**2
      DFAR=SQRT(RIJSQ)
      RETURN
      END
      SUBROUTINE COUNT(KON)
      INTEGER  KON(50)
      COMMON  /MAINC/ IFR, IFL,NMOL,NCM,NMTOT
      COMMON  /CORD2/ NICT(101,6,4),NCODT(101,6),NOCOMP(101),NT
      COMMON  /STAT1/ KOUNT(7),KOUNTB(50,3)
ALA12730
C
C  THIS SR DETERMINES THE FIRST AND SECOND ORDER STATISTICS FOR
C THE  3-FOLD CONFORMATIONAL STATES T, G, AND G*.
C
      IF(NMOL .EQ. 1) THEN
ALA12800
```

```
        DO 106 K=1,7
  106       KOUNT(K)=0
ALA12820
      ENDIF
C
ALA12840
      DO 140 K=1,NT
ALA12850
      KK=KON(K)
      KOUNT(KK)=KOUNT(KK)+1
      KOUNTB(K,KK)=KOUNTB(K,KK)+1
      IF(NT .EQ. 1 .OR. K .EQ. 1) GO TO 140
C
ALA12900
      IF(KON(K-1) .NE. 1) GO TO 120
          IF(KON(K) .NE. 1) KK=5
          IF(KON(K) .EQ. 1) KK=4
          GO TO 138
C
ALA12950
  120   IF(KON(K) .NE. 1) GO TO 122
ALA12960
          KK=5
          GO TO 138
C
ALA12990
  122   IF(KON(K) .EQ. KON(K-1)) KK=6
ALA13000
      IF(KON(K) .NE. KON(K-1)) KK=7
C
ALA13020
  138   KOUNT(KK)=KOUNT(KK)+1
ALA13030
  140   CONTINUE
ALA13040
C
ALA13050
C
ALA13060
      RETURN
ALA13070
      END
ALA13080
      SUBROUTINE ZDIAG
      DIMENSION  V1(3),V2(3),C(3),D(3),CD(3),CI(3),CJ(3),DI(3),DJ(3)
      DIMENSION  DX(3)
      COMMON  /CORD1/ NIC(370,4),NCOD(370),NONIC,NOCTOT
      COMMON  /FCON1/ NOK(105),KND(105,10),KODE(105),NOF
      COMMON  /FCON2/ VAL(105),ANGLE(105),ZFACT(105)
      COMMON  /MISC1/ NOCO(20),KKA(20),KKB(20),NUM(20),NOASS
      COMMON  /MISC2/ KOKIND(401)
      COMMON  /ASS02/ NUZZ(20),NIIQ(20),NOASS2
      COMMON  /ZEEEL/ COEF(2001),NRW(2001),NCL(2001),NF(2001),NZ
C
```

```
C
      NZ=0
C
C  ASSIGN F.C. AT THE 1-ST LEVEL.
C
      DO 190 I=1,NOCTOT
C     DO 190 I=1,2
      NOASS=0
C
C
      IF(NCOD(I) .EQ. 1 .OR. NCOD(I) .EQ. 4) THEN
          DO 150 J=1,NOF
            IF(KODE(J) .NE. 1 .AND. KODE(J) .NE. 4) GO TO 155
            IF (KODE(J) .NE. NCOD(I)) GO TO 155
            CALL COMP2(I,1,2,J,1,2,IQ2)
            IF(IQ2 .EQ. 0) GO TO 155
            CALL ADDASS(I,J,IQ2)
            GO TO 150
C
  155         IF (KODE(J) .NE. 29) GO TO 150
            CALL COMP2(I,1,2,J,1,2,IQ2)
            IF(IQ2 .EQ. 0) GO TO 150
            IF(IQ2 .EQ. 1) THEN
            I1=NIC(I,1)
            I2=NIC(I,2)
            ELSE
            I1=NIC(I,2)
            I2=NIC(I,1)
            ENDIF
            CALL COMKND(I,J,I2,9,I3)
            IF(I3 .EQ. 0) GO TO 150
            CALL COMKND(I,J,I3,10,I4)
            IF(I4 .EQ. 0) GO TO 150
C             WRITE(16,519) I,J,I1,I2,I3,I4
C 519         FORMAT(//2X,'ATOMS FOR I,J',2I3,' ARE',4I3)
            CALL TRAGA(I1,I2,I3,I4,TAU,MX)
            IF(ABS(TAU) .GT. 180.0) THEN
            IF(TAU .GE. 0.0) THEN
              TAU=360.0 -TAU
            ELSE
              TAU=360.0+TAU
            ENDIF
            ENDIF
C             WRITE(16,517) TAU
C 517         FORMAT('TAU= ',F12.6)
            DEL=ANGLE(J)-ABS(TAU)
            IF (ABS(DEL) .GT. 30.0) GO TO 150
            CALL ADDASS(I,J,IQ2)
  150         CONTINUE
C
C
        ELSEIF(NCOD(I) .EQ. 2) THEN
          DO 160 J=1,NOF
            IF(KODE(J) .NE. 2) GO TO 165
```

```
            CALL COMP1(I,2,J,2,IQ1)
            IF(IQ1 .EQ. 0) GO TO 165
            CALL COMP2(I,1,3,J,1,3,IQ2)
            IF(IQ2 .EQ. 0) GO TO 165
            CALL ADDASS(I,J,IQ2)
            GO TO 160
C
  165         IF(KODE(J) .NE. 27) GO TO 167
            CALL COMP1(I,2,J,2,IQ1)
            IF(IQ1 .EQ. 0) GO TO 167
            CALL COMP2(I,1,3,J,1,3,IQ2)
            IF(IQ2 .EQ. 0) GO TO 167
            IF (IQ2 .EQ. 1) THEN
            I1=NIC(I,1)
            I3=NIC(I,3)
            ELSE
            I1=NIC(I,3)
            I3=NIC(I,1)
            ENDIF
            I2=NIC(I,2)
            CALL COMKND(I,J,I3,6,I4)
            IF(I4 .EQ. 0) GO TO 160
            CALL TRAGA(I1,I2,I3,I4,TAU,MX)
            IF(ABS(TAU) .GT. 180.0) THEN
            IF(TAU .GE. 0.0) THEN
              TAU=360.0 -TAU
            ELSE
              TAU=360.0+TAU
            ENDIF
            ENDIF
C             WRITE(16,520) I,J,I1,I2,I3,I4
C 520         FORMAT(//2X,'ATOMS FOR I,J',2I3,' ARE',4I3)
C             WRITE(16,515) TAU
C 515         FORMAT('TAU= ',F12.6)
            DEL=ANGLE(J)-ABS(TAU)
            IF (ABS(DEL) .GT. 30.0) GO TO 160
            CALL ADDASS(I,J,IQ2)
            GO TO 160
C
  167         IF(KODE(J) .NE. 28) GO TO 160
            CALL COMP1(I,2,J,2,IQ1)
            IF(IQ1 .EQ. 0) GO TO 160
            CALL COMP2(I,1,3,J,1,3,IQ2)
            IF(IQ2 .EQ. 0) GO TO 160
            IF(IQ2 .EQ. 1) THEN
            I1=NIC(I,1)
            I3=NIC(I,3)
            ELSE
            I1=NIC(I,3)
            I3=NIC(I,1)
            ENDIF
            I2=NIC(I,2)
            NCC=I2
            CALL COMKND(I,J,I2,6,NB)
```

```
            IF(NB .EQ. 0) GO TO 160
            CALL COMKND(I,J,NB,7,NA)
            IF(NA .EQ. 0) GO TO 160
C             WRITE(16,94) NA,NB,NCC,I1,I2,I3
C  94         FORMAT(/2X,'NA,NB,NCC =',3I3,3X,'I1,I2,I3 =',3I3)
            CALL GENVEC(NB,NA,1,V1)
            CALL GENVEC(NB,NCC,1,V2)
            CALL GENVEC(NCC,NB,1,D)
            CALL GENVEC(I2,I1,1,CI)
            CALL GENVEC(I2,I3,1,CJ)
            CALL CROSP(V1,V2,1,C)
            CALL CROSP(C,D,1,CD)
            CALL ADDVEC(CI,CJ,1,C)
            CALL CROSP(C,D,1,DX)
            CALL CROSP(D,DX,1,DI)
            CALL DOTVEC(DI,CD,1,TAU)
C             WRITE(16,514) TAU
C 514         FORMAT('TAU= ',F12.6)
            DEL=ANGLE(J)-ABS(TAU)
            IF (ABS(DEL) .GT. 30.0) GO TO 160
            CALL ADDASS(I,J,IQ2)
  160         CONTINUE
C
C
        ELSEIF(NCOD(I) .EQ. 3) THEN
          DO 170 J=1,NOF
            IF(KODE(J) .NE. 3) GO TO 170
            CALL COMP1(I,1,J,1,IQ1)
            IF (IQ1 .EQ. 0) GO TO 170
            CALL COMP1(I,2,J,2,IQ1)
            IF (IQ1 .EQ. 0) GO TO 170
            CALL COMP2(I,1,3,J,1,3,IQ2)
            CALL ADDASS(I,J,IQ2)
  170         CONTINUE
C
C
        ELSE
          WRITE(16,11) I,NCOD(I)
   11       FORMAT(//2X,'ERROR IN INT. COORD. NO.',I3,2X,'NCOD =',I2)
        ENDIF
      CALL ROUTE1(I,NGO)
      IF(NGO .EQ. 0) THEN
          CALL ASSSEC(I)
          CALL ROUTE2(I)
        ENDIF
  190   CONTINUE
C
C
C
      RETURN
      END
      SUBROUTINE ROUTE1(I,NGO)
      COMMON  /MISC1/ NOCO(20),KKA(20),KKB(20),NUM(20),NOASS
C
```

```
C
C  THIS SR ROUTES THE PROGRAM AFTER THE 1-ST LEVEL F.C. SEARCH.
C    NGO IS SET TO 0, IF A SECOND ORDER SEARCH IS NEEDED.
C
      NGO=1
C
C  CASE WHERE NO F.C. HAVE BEEN ASSIGNED.
C
      IF(NOASS .EQ. 0) THEN
          WRITE(16,10) I
   10       FORMAT(//2X,'NO DIAG. F.C. FOUND FOR INT COORD. NO.',I3)
          RETURN
C
C  CASE WHERE ONE F.C. HAS BEEN ASSIGNED
C
        ELSEIF(NOASS .EQ. 1) THEN
          CALL ADDZ(I)
          RETURN
C
C  CASE WHERE MORE THAN ONE F.C. HAS BEEN ASSIGNED AT THE 1-ST LEVEL.
C
        ELSEIF(NOASS .GT. 1) THEN
          IFXX=1
          IF(IFXX .NE. 0) GO TO 160
          WRITE(16,20) NOASS,I
   20       FORMAT(//2X,I2,1X,'FORCE CONSTANTS ASSIGNED TO INT. COORD.',
     1       ' NO.',I3)
          WRITE(16,22) (NOCO(L),L=1,NOASS)
   22       FORMAT(5X,'F.C. NUMBERS ARE',10I3)
  160       NGO=0
        ENDIF
C
C
      RETURN
      END
      SUBROUTINE ASSSEC(I)
      COMMON  /CORD1/ NIC(370,4),NCOD(370),NONIC,NOCTOT
      COMMON  /FCON1/ NOK(105),KND(105,10),KODE(105),NOF
      COMMON  /MISC1/ NOCO(20),KKA(20),KKB(20),NUM(20),NOASS
      COMMON  /ASS02/ NUZZ(20),NIIQ(20),NOASS2
C
C  IN THIS SR, MULTIPLE F.C. ASSIGNMENTS ARE RESOLVED AT THE SECOND
C  ORDER LEVEL
C
      NOASS2=0
C
C  STRETCHING AND TORSIONAL
C
      IF(NCOD(I) .EQ. 1 .OR. NCOD(I) .EQ. 4) THEN
        DO 141 JD=1,NOASS
          IA=KKA(JD)
          IB=KKB(JD)
          J=NUM(JD)
          CALL COMP3(I,IA,J,3,5,IIQ1)
```

```
            CALL COMP3(I,IB,J,6,8,IIQ2)
            IF (KND(J,1).EQ.KND(J,2) .AND. ((IIQ1.EQ.-1).OR.
     1           (IIQ2.EQ.-1))) THEN
              CALL COMP3(I,IA,J,6,8,IIQ1)
              CALL COMP3(I,IB,J,3,5,IIQ2)
            ENDIF
            IF(IIQ1 .NE. -1 .AND. IIQ2 .NE. -1) THEN
              NOASS2=NOASS2+1
              NUZZ(NOASS2)=NOCO(JD)
              NIIQ(NOASS2)=IIQ1+IIQ2
              ENDIF
  141         CONTINUE
          ENDIF
C
C  BENDING
C
        IF(NCOD(I) .EQ. 2) THEN
          DO 151 JD=1,NOASS
C             IA=KKA(JD)
C             IB=KKB(JD)
            J=NUM(JD)
            CALL COMP3(I,NIC(I,2),J,4,5,IIQ1)
            IF(IIQ1 .NE. -1) THEN
              NOASS2=NOASS2+1
              NUZZ(NOASS2)=NOCO(JD)
              NIIQ(NOASS2)=IIQ1
              ENDIF
  151         CONTINUE
          ENDIF
C
C  OUT-OF-PLANE BENDING
C
        IF(NCOD(I) .EQ. 3) THEN
          DO 161 JD=1,NOASS
            IA=KKA(JD)
            IB=KKB(JD)
            J=NUM(JD)
            CALL COMP3(I,IA,J,5,7,IIQ1)
            CALL COMP3(I,IB,J,8,10,IIQ2)
            IF(IIQ1 .NE. -1 .AND. IIQ2 .NE. -1) THEN
              NOASS2=NOASS2+1
              NUZZ(NOASS2)=NOCO(JD)
              NIIQ(NOASS2)=IIQ1+IIQ2
              ENDIF
  161         CONTINUE
          ENDIF
C
C
        RETURN
        END
        SUBROUTINE ROUTE2(I)
        COMMON  /MISC1/ NOCO(20),KKA(20),KKB(20),NUM(20),NOASS
        COMMON  /ASS02/ NUZZ(20),NIIQ(20),NOASS2
C
```

```
C  THIS SR DETERMINES THE PROGRAM ROUTE AFTER THE 2-ND LEVEL
C  F.C. SEARCH.
C
C
      IF(NOASS2 .EQ. 0) THEN
        WRITE(16,12) I
   12     FORMAT(/5X,'NO DIAG. F.C. CAN BE ASSIGNED TO INT. COORD. NO.',
     1       I3,' AT THE SECOND LEVEL')
        RETURN
      ELSEIF(NOASS2 .EQ. 1) THEN
        NOCO(1)=NUZZ(1)
        CALL ADDZ(I)
        RETURN
      ELSE
          CALL RANK(N,NUZ)
          IF(N .EQ. 1) THEN
            NOCO(1)=NUZ
            CALL ADDZ(I)
            ELSE
            WRITE(16,16) I,(NUZZ(J),J=1,NOASS2)
   16         FORMAT(/5X,'MORE THAN ONE DIAG. F.C. CAN BE ASSIGNED TO',
     1           /5X,'INT. COORD. NO.',I3,' AT THE SECOND LEVEL',
     2           /7X,'THESE ARE NO.',10I3)
          ENDIF
      ENDIF
C
C
      RETURN
      END
      SUBROUTINE RANK(N,NUZ)
      COMMON  /ASS02/ NUZZ(20),NIIQ(20),NOASS2
C
C
      MAX=0
      DO 110 I=1,NOASS2
      IF(NIIQ(I) .GT. MAX) MAX=NIIQ(I)
  110   CONTINUE
C
      N=0
      DO 118 I=1,NOASS2
      IF(NIIQ(I) .EQ. MAX) THEN
          N=N+1
          NUZ=NUZZ(I)
        ENDIF
  118   CONTINUE
C
C
      RETURN
      END
      SUBROUTINE COMP1(I,NI,J,NJ,IQ1)
      COMMON  /CORD1/ NIC(370,4),NCOD(370),NONIC,NOCTOT
      COMMON  /FCON1/ NOK(105),KND(105,10),KODE(105),NOF
      COMMON  /STRUC/ X(3,120),W(120),KIND(120)
C
```

```
C
C  IN THIS SR, THE KIND NO. OF ATOM NI OF INT. COORD. I IS COMPARED
C  WITH THE KIND NO. KND(J,NJ) WHICH IS PART OF THE DEF. OF FORCE
C  CONSTANT:
C    IF NOT ALIKE, THEN IQ1=0
C    IF ALIKE, THEN     IQ1=1
C
      LI=KIND(NIC(I,NI))
      LJ=KND(J,NJ)
      IQ1=0
      IF(LI .EQ. LJ) IQ1=1
C
C
      RETURN
      END
      SUBROUTINE COMP2(I,NI1,NI2,J,NJ1,NJ2,IQ2)
      COMMON  /CORD1/ NIC(370,4),NCOD(370),NONIC,NOCTOT
      COMMON  /FCON1/ NOK(105),KND(105,10),KODE(105),NOF
      COMMON  /STRUC/ X(3,120),W(120),KIND(120)
C
C
C  IN THIS SR, THE KIND NO.'S OF THE PAIR OF ATOMS NI1 AND NI2 OF
C  INT. COORD. NO. I ARE COMPARED WITH THE KIND NO.'S KND(J,NJ1) AND
C  KND(J,NJ2), WHICH ARE PART OF THE DEF. OF F.C. NO. J:
C      IQ2=0, IF NOT ALIKE.
C         =1, IF ALIKE IN THE ORDER GIVEN.
C         -1, IF ALIKE AFTER THE ORDER OF ONE PAIR HAS BEEN REVERSED.
C
      LI1=KIND(NIC(I,NI1))
      LI2=KIND(NIC(I,NI2))
      LJ1=KND(J,NJ1)
      LJ2=KND(J,NJ2)
C
      IQ2=0
      IF(LI1 .EQ. LJ1 .AND. LI2 .EQ. LJ2) IQ2=1
      IF(LI1 .EQ. LJ2 .AND. LI2 .EQ. LJ1) IQ2=-1
C
C
      RETURN
      END
      SUBROUTINE COMP3(I,IC,J,J1,J2,IQ3)
      DIMENSION  NQUAL(10),A(20),B(20)
      COMMON  /CORD1/ NIC(370,4),NCOD(370),NONIC,NOCTOT
      COMMON  /ENVIR/ KBN(120,4),KT(120),KTSK(120)
      COMMON  /FCON1/ NOK(105),KND(105,10),KODE(105),NOF
      COMMON  /STRUC/ X(3,120),W(120),KIND(120)
C
C
C  THIS SR COMPARES TWO SETS OF KIND NUMBERS.
C    ONE SET IS ASSOCIATED WITH THE ATOMS BONDED TO ATOM IC OF INT.
C    COORD. NO. I.  ANY ATOM THAT IS USED IN THE INT. COORD. DEF.
C    IS EXCLUDED FROM THE SET OF ATOMS BONDED TO ATOM IC.
C    THE SECOND SET CONSISTS OF A SPECIFIED SEQUENCE OF KIND NUMBERS
C    (KND(J,JD),JD=J1,J2) USED IN THE DEF. OF THE J-TH F.C.
```

```
C     IQ3=-1, IF THE SETS DO NOT MATCH
C     IQ3=0,  IF ALL THE SPECIFIED KND(J,JD) EQUAL 0
C     IQ3=1,  IF THE SETS MATCH
C
C
C  FIRST CHECK FOR ARGUMENT AND FORCE-CONSTANT DEF. ERRORS
C
      NJSEQ=J2-J1+1
      N=0
C
      DO 120 JN=J1,J2
      IF(KND(J,JN) .NE. 0) N=N+1
  120   CONTINUE
      IF(N .EQ. 0) THEN
        IQ3=0
        RETURN
      ELSEIF(N .NE. NJSEQ) THEN
        WRITE(16,10) N,NJSEQ
   10     FORMAT(/2X,'*** ERROR *** N AND NJSEQ =',2I3)
        WRITE(16,12) J,J1,J2,(KND(J,JN),JN=J1,J2)
   12     FORMAT(//2X,'*** ERROR *** FOR F.C. NO.',I3,1X,'EITHER IN',
     1       1X,'KND(J,JN) RANGE JN=',I2,1X,'THRU',I2
     2       /5X,'OR IN THE F.C. DEF.  KND(J,JN) =',10I3)
        CALL EXIT
      ENDIF
C
C  CHECK TO SEE IF THE SETS HAVE THE SAME NO. OF MEMBERS
C
      NAC=4
      IF(NCOD(I) .LE. 3) NAC=NCOD(I)+1
C
      N=0
      DO 136 L=1,KT(IC)
      LI=KBN(IC,L)
      DO 130 M=1,NAC
        IF(LI .EQ. NIC(I,M)) GO TO 136
  130     CONTINUE
      N=N+1
      NQUAL(N)=LI
  136   CONTINUE
      NISEQ=N
C
      IF(NISEQ .NE. NJSEQ) THEN
        WRITE(16,16) IC,I,J,NISEQ,NJSEQ
   16     FORMAT(//2X,'*** ERROR *** NO. OF QUALIFIED ATOMS BONDED',
     1    1X,'TO ATOM',I3,' OF INT. COORD.',I3/2X,'IS NOT EQUAL TO',
     2    1X,'THE NUMBER OF KND(J,JD) TERMS SPECIFIED'/2X,'FOR F.C. NO.'
     3    ,I3//5X,'NISEQ AND NJSEQ ARE EQUAL TO',2I3)
        CALL EXIT
      ENDIF
C
C  COMPARE SEQUENCES
C
      DO 210 LI=1,NISEQ
```

```
      A(LI)=KIND(NQUAL(LI))
  210   CONTINUE
      LJ=0
      DO 214 JN=J1,J2
      LJ=LJ+1
      B(LJ)=KND(J,JN)
  214   CONTINUE
C
      CALL COMP4(A,B,NISEQ,IQ4)
      IQ3=-1
      IF(IQ4 .EQ. 0) IQ3=1
C
C
      RETURN
      END
      SUBROUTINE COMP4(A,B,NDIM,IQ4)
      DIMENSION  A(20),B(20),KMATCH(20)
C
C
C  IN THIS SR, TWO SETS OF INTEGERS (A(I) AND B(I),I=1,NDIM) ARE
C  COMPARED TO SEE IF THEY MATCH. THE ORDER IS UNIMPORTANT.
C
C    IQ4 = THE NO. OF UNMATCHED ELEMENTS OF ONE SET.
C
      DO 110 K=1,NDIM
      KMATCH(K)=1
  110   CONTINUE
C
      M=0
      DO 130 I=1,NDIM
      DO 120 K=1,NDIM
        IF(KMATCH(K) .EQ. 0) GO TO 120
        IF(A(I) .EQ. B(K)) THEN
            M=M+1
            KMATCH(K)=0
            GO TO 130
          ENDIF
  120     CONTINUE
  130   CONTINUE
C
      IQ4=NDIM-M
C
C
      RETURN
      END
      SUBROUTINE ADDASS(I,J,IQ)
      COMMON  /CORD1/ NIC(370,4),NCOD(370),NONIC,NOCTOT
      COMMON  /FCON1/ NOK(105),KND(105,10),KODE(105),NOF
      COMMON  /MISC1/ NOCO(20),KKA(20),KKB(20),NUM(20),NOASS
C
C
C  IN THIS SR, THE F.C. ASSIGNMENTS MADE AT THE 1-ORDER ARE STORED.
C
      NOASS=NOASS+1
```

```
      NOCO(NOASS)=NOK(J)
      NUM(NOASS)=J
C
C  KKA(NOASS) AND KKB(NOASS) GIVES THE ORDER OF THE "END" ATOMS IN AN
C  INT. COORD. THIS ORDER CORRESPONDS TO THAT GIVEN IN THE F.C. DEF.
C
C  STRETCHING AND TORSIONAL
C
      IF(NCOD(I) .EQ. 1 .OR. NCOD(I) .EQ. 4) THEN
        IF(IQ .EQ. 1) THEN
            KKA(NOASS)=NIC(I,1)
            KKB(NOASS)=NIC(I,2)
          ELSEIF(IQ .EQ. -1) THEN
            KKA(NOASS)=NIC(I,2)
            KKB(NOASS)=NIC(I,1)
          ENDIF
      ENDIF
C
C  BENDING
C
      IF(NCOD(I) .EQ. 2) THEN
        IF(IQ .EQ. 1) THEN
            KKA(NOASS)=NIC(I,1)
            KKB(NOASS)=NIC(I,3)
          ELSEIF(IQ .EQ. -1) THEN
            KKA(NOASS)=NIC(I,3)
            KKB(NOASS)=NIC(I,1)
          ENDIF
      ENDIF
C
C  OUT-OF-PLANE BENDING
C
      IF(NCOD(I) .EQ. 3) THEN
        IF(IQ .EQ. 1) THEN
            KKA(NOASS)=NIC(I,3)
            KKB(NOASS)=NIC(I,4)
          ELSEIF(IQ .EQ. -1) THEN
            KKA(NOASS)=NIC(I,4)
            KKB(NOASS)=NIC(I,3)
          ENDIF
      ENDIF
C
      RETURN
      END
      SUBROUTINE ADDZ(I)
      COMMON  /MISC1/ NOCO(20),KKA(20),KKB(20),NUM(20),NOASS
      COMMON  /MISC2/ KOKIND(401)
      COMMON  /ZEEEL/ COEF(2001),NRW(2001),NCL(2001),NF(2001),NZ
C
C
      NZ=NZ+1
      N=I
C
      NRW(NZ)=N
```

```
      NCL(NZ)=N
      NF(NZ)=NOCO(1)
      COEF(NZ)=1.0
      KOKIND(N)=NOCO(1)
C     WRITE(16,910) NZ,NRW(NZ),NCL(NZ),NF(NZ),KOKIND(NZ)
C 910 FORMAT(2X,'NZ,NRW,NCL,NF =',I4,3X,2I4,2X,I4,3X,'KOKIND =',I3)
C
C
      RETURN
      END
      SUBROUTINE ZINTER
      DIMENSION  IS(20),JS(20)
      DIMENSION  V1(3),V2(3),C(3),D(3),CD(3),CI(3),CJ(3),DI(3),DJ(3)
      DIMENSION  DX(3)
      COMMON  /CORD1/ NIC(370,4),NCOD(370),NONIC,NOCTOT
      COMMON  /ENVIR/ KBN(120,4),KT(120),KTSK(120)
      COMMON  /FCON1/ NOK(105),KND(105,10),KODE(105),NOF
      COMMON  /FIJSUP/ KIJSUP(4),PIJSUP(4)
      COMMON  /INTER/ COFF,KEY(51)
      COMMON  /MISC2/ KOKIND(401)
      COMMON  /STRUC/ X(3,120),W(120),KIND(120)
C
C
C  IN THIS SR INTERACTION FORCE CONSTANTS ARE ASSIGNED.
C
C  FIRST FIND VALUES FOR KEY(L), WHERE L IS A F.C. KODE NUMBER.
C     IF KEY(L)=1, THEN F.C. TYPE L (KODE) IS PRESENT IN THE F.C. SET.
C     OTHERWISE, KEY(L)=0.
C
      KLARG=0
      DO 128 L=1,NOF
      IF(KODE(L) .GT. KLARG) KLARG=KODE(L)
      KEY(KODE(L))=1
  128   CONTINUE
   15 CONTINUE
C
C  CHECK ALL POSSIBLE INT. COORD. PAIRS FOR INTERACTION.
C
      DO 440 I=1,NOCTOT-1
      DO 430 J=I+1,NOCTOT
        CALL COMATM(I,J,IS,JS,NCOM)
C         WRITE(16,82) I,J,NCOM
C  82     FORMAT(5X,'I,J,NCOM =',3I3)
        IF(NCOM .EQ. 0) GO TO 210
C         WRITE(16,83) (IS(INN),INN=1,NCOM)
C  83     FORMAT(10X,'IS(INN) =',4I3)
C         WRITE(16,84) (JS(JNN),JNN=1,NCOM)
C  84     FORMAT(10X,'JS(JNN) =',4I3)
        COFF=1.0
C
C  STRETCH-STRETCH (KON=5)
C
        IF(NCOD(I) .EQ. 1 .AND. NCOD(J) .EQ. 1) THEN
            IF(KEY(5) .EQ. 0) GO TO 430
```

```
            CALL ADDZIN(I,J,5)
            GO TO 430
          ENDIF
C
C  STRETCH-BEND (KON=8 AND 9)
C
        NOR=0
        IF(NCOD(I) .EQ. 1 .AND. NCOD(J) .EQ. 2) NOR=1
        IF(NCOD(I) .EQ. 2 .AND. NCOD(J) .EQ. 1) NOR=-1
        IF(NOR .EQ. 0) GO TO 210
C
C    KON=8,  TWO ATOMS IN COMMON
C
        IF(NCOM .EQ. 2) THEN
            IF(KEY(8) .EQ. 0) GO TO 430
            CALL ADDZIN(I,J,8)
            GO TO 430
          ENDIF
C
C    KON=9,  ONLY THE CENTRAL ATOM OF THE BEND IS IN COMMON.
C
        IF(KEY(9) .EQ. 0) GO TO 430
        IF(NOR .EQ. 1 .AND. JS(1) .EQ. 2) CALL ADDZIN(I,J,9)
        IF(NOR .EQ. -1 .AND. IS(1) .EQ. 2) CALL ADDZIN(I,J,9)
        GO TO 430
C
C  BEND-BEND INTERACTIONS (KON= 11 THRU 14 AND 26)
C
  210 IF(NCOD(I) .NE. 2 .OR. NCOD(J) .NE. 2) GO TO 300
C
C  KON= 11 AND 12
C
        IF(NCOM .EQ. 2) THEN
C
C  KON= 11
C
            IF(NIC(I,2) .EQ. NIC(J,2)) THEN
              IF(KEY(11) .EQ. 1) THEN
                  KIJSUP(1)=KIND(NIC(I,IS(1)))
                  KIJSUP(2)=KIND(NIC(I,IS(2)))
                  CALL ADDZIN(I,J,11)
                  GO TO 430
                ENDIF
C
C  KON= 12
C
            ELSE
              IF(KEY(12) .EQ. 1) THEN
C
C  DIFINE DIHEDRAL ANGLE: MA-MB-MC-MD
C
                MA=0
                MD=0
                DO 218 K=1,2
```

```
                    IF(IS(K) .EQ. 1) MA=NIC(I,3)
                    IF(IS(K) .EQ. 3) MA=NIC(I,1)
                    IF(JS(K) .EQ. 1) MD=NIC(J,3)
                    IF(JS(K) .EQ. 3) MD=NIC(J,1)
  218                   CONTINUE
C           WRITE(16,93) MA,NIC(I,2),NIC(J,2),MD
C  93       FORMAT(/2X,'MA,MB,MC,MD =',4I3)
                  CALL TRAGA(MA,NIC(I,2),NIC(J,2),MD,TAU,MX)
                  IF(ABS(TAU) .GT. 180.0) THEN
                    IF(TAU .GE. 0.0) THEN
                       TAU=360.0 -TAU
                     ELSE
                       TAU=360.0+TAU
                     ENDIF
                    ENDIF
                  PIJSUP(1)=TAU
                  CALL ADDZIN(I,J,12)
                  GO TO 430
                ENDIF
              GO TO 430
              ENDIF
          ELSEIF(NCOM .EQ. 1) THEN
              IF(NIC(I,2) .NE. NIC(J,2)) THEN
C
C  KON=13
C
                IF (KEY(13) .EQ. 0) GO TO 430
                IF(IS(1) .NE. 2 .AND. JS(1) .EQ. 2) THEN
                  IF(IS(1) .EQ. 3) THEN
                    NA=NIC(I,1)
                  ELSE
                    NA=NIC(I,3)
                  ENDIF
                  NB=NIC(I,2)
                  NCC=NIC(I,IS(1))
                  I1=NIC(J,1)
                  I2=NIC(J,2)
                  I3=NIC(J,3)
                ELSEIF(IS(1) .EQ. 2 .AND. JS(1) .NE. 2) THEN
                  IF(JS(1) .EQ. 3) THEN
                     NA=NIC(J,1)
                   ELSE
                     NA=NIC(J,3)
                   ENDIF
                  NB=NIC(J,2)
                  NCC=NIC(J,JS(1))
                  I1=NIC(I,1)
                  I2=NIC(I,2)
                  I3=NIC(I,3)
                  ELSE
                  GO TO 430
                  ENDIF
C     WRITE(16,94) NA,NB,NCC,I1,I2,I3
C  94 FORMAT(/2X,'NA,NB,NCC =',3I3,3X,'I1,I2,I3 =',3I3)
```

```
C
                CALL GENVEC(NB,NA,1,V1)
                CALL GENVEC(NB,NCC,1,V2)
                CALL GENVEC(NCC,NB,1,D)
                CALL GENVEC(I2,I1,1,CI)
                CALL GENVEC(I2,I3,1,CJ)
                CALL CROSP(V1,V2,1,C)
                CALL CROSP(C,D,1,CD)
C
                CALL ADDVEC(CI,CJ,1,C)
                CALL CROSP(C,D,1,DX)
C
                CALL CROSP(D,DX,1,DI)
                CALL DOTVEC(DI,CD,1,TAU)
C
                PIJSUP(1)=TAU
C     WRITE(16,94) TAU,I,J
C  94 FORMAT(2X,'TAU= ',F8.2,' FOR INTERACTION ',2I4)
                CALL ADDZIN(I,J,13)
                GO TO 430
              ELSE
C
C KON=26
C
                IF(KEY(26) .EQ. 0) GO TO 430
                CALL ADDZIN(I,J,26)
                GO TO 430
              ENDIF
C
C  KON=14
C
        IF(NCOM .EQ. 0) THEN
            IF(KEY(14) .EQ. 0) GO TO 430
            DO 224 K=1,KTSK(NIC(J,2))
              IF(NIC(I,2) .EQ. KBN(NIC(J,2),K)) GO TO 230
  224           CONTINUE
            GO TO 430
  230         CALL GENVEC(NIC(I,2),NIC(I,1),1,CI)
            CALL GENVEC(NIC(I,2),NIC(I,3),1,DI)
            CALL GENVEC(NIC(J,2),NIC(J,1),1,CJ)
            CALL GENVEC(NIC(J,2),NIC(J,3),1,DJ)
            CALL GENVEC(NIC(I,2),NIC(J,2),1,CD)
C
            CALL ADDVEC(CI,DI,1,C)
            CALL ADDVEC(CJ,DJ,1,D)
C
            CALL CROSP(C,CD,1,CI)
            CALL CROSP(D,CD,1,CJ)
C
            CALL DOTVEC(CI,CJ,1,TAU)
            PIJSUP(1)=TAU
            CALL ADDZIN(I,J,14)
            GO TO 430
```

```
          ENDIF
C
C BEND - OUT-OF-PLANE BEND INTERACTIONS
C
C KON=30
C
  300     NOR=0
        IF(NCOD(I) .EQ. 2 .AND. NCOD(J) .EQ. 3) NOR=1
        IF(NCOD(I) .EQ. 3 .AND. NCOD(J) .EQ. 2) NOR=-1
        IF(NOR .EQ. 0) GO TO 350
        IF(KEY(30) .EQ. 0) GO TO 430
        IF(NCOM .EQ. 2) THEN
          IF(NOR .EQ. 1) THEN
            I2=NIC(I,2)
            I4=NIC(J,1)
            IF(NIC(I,3) .EQ. NIC(J,2)) THEN
            I1=NIC(I,1)
            I3=NIC(I,3)
            ELSE
            I1=NIC(I,3)
            I3=NIC(I,1)
            ENDIF
          ELSEIF(NOR .EQ. -1) THEN
            I2=NIC(J,2)
            I4=NIC(I,1)
            IF(NIC(J,3) .EQ. NIC(I,2)) THEN
            I1=NIC(J,1)
            I3=NIC(J,3)
            ELSE
            I1=NIC(J,3)
            I3=NIC(J,1)
            ENDIF
          ENDIF
            CALL TRAGA(I1,I2,I3,I4,TAU,MX)
            IF(ABS(TAU) .GT. 180.0) THEN
            IF(TAU .GE. 0.0) THEN
              TAU=360.0 -TAU
            ELSE
              TAU=360.0+TAU
            ENDIF
            ENDIF
C             WRITE(16,520) I,J,I1,I2,I3,I4
C 520         FORMAT(//2X,'ATOMS FOR I,J',2I3,' ARE',4I3)
C             WRITE(16,515) TAU
C 515         FORMAT('TAU= ',F12.6)
            PIJSUP(1)=TAU
            CALL ADDZIN(I,J,30)
            GO TO 430
        ENDIF
C
C KON=31
C
  350     IF((NCOD(I) .EQ. 3 .AND. NCOD(J) .EQ. 4) .OR.
     1       (NCOD(J) .EQ. 4 .AND. NCOD(J) .EQ. 3)) THEN
```

```
          IF(KEY(31) .EQ. 0) GO TO 430
          IF(NCOM .EQ. 2) THEN
            CALL ADDZIN(I,J,31)
          ENDIF
        ENDIF
  430     CONTINUE
  440   CONTINUE
C
C
      RETURN
      END
      SUBROUTINE COMKND(I,J,I3,INK,I4)
      INTEGER  I,J,I3,INK,I4
      DIMENSION ING(3)
      COMMON  /FCON1/ NOK(105),KND(105,10),KODE(105),NOF
      COMMON  /ENVIR/ KBN(120,4),KT(120),KTSK(120)
      COMMON  /STRUC/ X(3,120),W(120),KIND(120)
      COMMON  /CORD1/ NIC(370,4),NCOD(370),NONIC,NOCTOT
C
C THIS SUBROUTINE RETURNS IN I4 THE ATOM WHOSE TYPE MATCHES
C THAT LISTED IN FORCE CONSTANT J, POSITION INK.
C THIS ATOM IS CONNECTED TO ATOM I3 IN INTERNAL COORDINATE
C I, BUT IS NOT PART OF THE COORDINATE DEFINITION.  THIS
C SUBROUTINE IS USED FOR KODE=27, 28 AND 29.
C
C
      L=0
      I4=0
      DO 205 K=1,KT(I3)
      IF(KIND(KBN(I3,K)) .EQ. KND(J,INK)) THEN
        DO 208 INN=1,NCOD(I)+1
          IF (KBN(I3,K) .EQ. NIC(I,INN)) GO TO 205
  208     CONTINUE
        L=L+1
        ING(L)=KBN(I3,K)
      ENDIF
  205 CONTINUE
      IF(L .EQ. 1) THEN
      I4=ING(1)
      ELSEIF(L .GT. 1) THEN
      WRITE(16,510) (ING(K),K=1,L)
  510   FORMAT(//2X,'ERROR! MULTIPLE MATCHES FOR ATOM ',
     1              'TYPE ',/'ATOM NOS. =',4I3)
      CALL EXIT
      ENDIF
C
C
      RETURN
      END
      SUBROUTINE ADDZIN(I,J,KON)
      DIMENSION  NUZ2(10)
      COMMON  /FCON1/ NOK(105),KND(105,10),KODE(105),NOF
      COMMON  /FCON2/ VAL(105),ANGLE(105),ZFACT(105)
      COMMON  /FCON3/ KIFC(105,20),KJFC(105,20),NOEQ(105)
```

```
      COMMON  /FIJSUP/ KIJSUP(4),PIJSUP(4)
      COMMON  /INTER/ COFF,KEY(51)
      COMMON  /MISC2/ KOKIND(401)
      COMMON  /ZEEEL/ COEF(2001),NRW(2001),NCL(2001),NF(2001),NZ
      COMMON  /CORD1/ NIC(370,4),NCOD(370),NONIC,NOCTOT
      COMMON  /OOP/   IOOP(25,5),NOOP,NDIR(25)
C
C
      NDUPZ=0
      DO 140 L=1,NOF
      IF(KODE(L) .NE. KON) GO TO 140
      DO 136 JJ=1,NOEQ(L)
        CALL COMPAR(KIFC(L,JJ),KJFC(L,JJ),KOKIND(I),KOKIND(J),NX)
c         WRITE(16,81) L,JJ,KIFC(L,JJ),KJFC(L,JJ),KOKIND(I),KOKIND(J),NX
c  81     FORMAT(/2X,2I3,5X,2I3,2X,2I3,5X,I3)
        IF(NX .EQ. 0) GO TO 136
C
C        CONSIDER SPECIAL CONDITIONS, IF ANY.
C
  118     IF(KON .EQ. 11) THEN
          IJ=KIJSUP(1)
          IK=KIJSUP(2)
          CALL COMPAR(IK,IJ,KND(L,3),KND(L,4),NX)
          IF(NX .EQ. 0) GO TO 136
        ELSEIF(KON .GE. 12 .AND. KON .LE. 14 .OR. KON .EQ. 30) THEN
          TAU=PIJSUP(1)
          DEL=ANGLE(L)-ABS(TAU)
          IF(ABS(DEL) .GT. 30.0) GO TO 136
        ENDIF
        NZ=NZ+1
        NRW(NZ)=I
        NCL(NZ)=J
        NF(NZ)=NOK(L)
        COEF(NZ)=COFF*ZFACT(L)
        NDUPZ=NDUPZ+1
        NUZ2(NDUPZ)=NF(NZ)
        IF(KON .EQ. 30) THEN
          IFNEG=0
          DO 10 KK=1,NOOP
            IF(NDIR(KK) .EQ. I) THEN
            CALL DIROOP(NIC(I,1),NIC(I,2),NIC(I,3),IOOP(KK,5),
     1                  NIC(J,1),NIC(J,2),NIC(J,3),IFNEG)
            GO TO 20
            ELSEIF(NDIR(KK) .EQ. J) THEN
            CALL DIROOP(NIC(J,1),NIC(J,2),NIC(J,3),IOOP(KK,5),
     1                  NIC(I,1),NIC(I,2),NIC(I,3),IFNEG)
            GO TO 20
            ENDIF
   10       CONTINUE
   20       CONTINUE
          IF(IFNEG .EQ. 1) NF(NZ)=-NF(NZ)
        ENDIF
  136     CONTINUE
  140   CONTINUE
```

```
C
      IF(NDUPZ .EQ. 1) THEN
C         WRITE(16,8) NZ,NRW(NZ),NCL(NZ),NF(NZ),COEF(NZ)
C    8    FORMAT(5X,'INTER FC =',I3,2X,3I4,2X,F7.4)
      ELSEIF(NDUPZ .GT. 1) THEN
        WRITE(16,17) I,J,(NUZ2(K),K=1,NDUPZ)
   17   FORMAT(//2X,'*** ERROR *** MORE THAN 1 INTERACTION CONSTANT',
     1       1X,'ASSIGNED'/10X,'INT. COORD. NO.',I3,' AND',I3
     2       /10X,'F.C. ASSIGNED =',10I3)
      ENDIF
C
C
      RETURN
      END
      SUBROUTINE DIROOP(I,J,K,IP,I2,J2,K2,IFNEG)
      INTEGER I,J,K,IP,I2,J2,K2,IFNEG,MX
      REAL  TAU1,TAU2
      COMMON  /STRUC/ X(3,120),W(120),KIND(120)
C
      CALL TRAGA(I,J,K,IP,TAU1,MX)
      IF(ABS(TAU1) .GT. 180.0) THEN
      IF(TAU1 .GE. 0.0) THEN
        TAU1=360.0 -TAU1
      ELSE
        TAU1=360.0+TAU1
      ENDIF
      ENDIF
      IF(I2 .EQ. J) THEN
      CALL TRAGA(I,J,K,K2,TAU2,MX)
      ELSE
      CALL TRAGA(I,J,K,I2,TAU2,MX)
      ENDIF
      IF(ABS(TAU2) .GT. 180.0) THEN
      IF(TAU2 .GE. 0.0) THEN
        TAU2=360.0 -TAU2
      ELSE
        TAU2=360.0+TAU2
      ENDIF
      ENDIF
C
      IF(TAU1 .EQ. 0.0 .OR. TAU2 .EQ. 0.0) THEN
      WRITE(16,10) TAU1,TAU2
   10   FORMAT(//2X,'ERROR!! DEFINITION OF OOP BEND INTERACTION IS',
     1          'INCORRRECT!'//,'TAU1,TAU2= ',2F12.6)
      CALL EXIT
      ENDIF
C
      IFNEG=0
      IF(TAU1 .GT. 0.0 .AND. TAU2 .LT. 0.0) IFNEG=1
      IF(TAU1 .LT. 0.0 .AND. TAU2 .GT. 0.0) IFNEG=1
C
C
      RETURN
      END
```

```
      SUBROUTINE COMATM(I,J,IS,JS,N)
      DIMENSION  IS(20),JS(20)
      COMMON  /CORD1/ NIC(370,4),NCOD(370),NONIC,NOCTOT
C
C
      IN=NCOD(I)+1
      IF(NCOD(I) .EQ. 4) IN=2
      JN=NCOD(J)+1
      IF(NCOD(J) .EQ. 4) JN=2
C
      N=0
      DO 120 I1=1,IN
      DO 110 J1=1,JN
        IF(NIC(I,I1) .EQ. NIC(J,J1)) THEN
            N=N+1
            IS(N)=I1
            JS(N)=J1
          ENDIF
  110     CONTINUE
  120   CONTINUE
C
C
      RETURN
      END
      SUBROUTINE COMPAR(I,J,M,N,NX)
C
C
      NX=0
      IF(I .EQ. M .AND. J .EQ. N) THEN
        NX=1
        RETURN
      ENDIF
      IF(I .EQ. N .AND. J .EQ. M) NX=-1
C
C
      RETURN
      END
      SUBROUTINE GENVEC(I,J,IFUNIT,V)
      DIMENSION  V(3)
      COMMON  /STRUC/ X(3,120),W(120),KIND(120)
C
C
C  IF IFUNIT=1, V IS CONVERTED TO A UNIT VECTOR
C
      S=0.0
      DO 108 M=1,3
      V(M)=X(M,J)-X(M,I)
      S=S+V(M)**2
  108   CONTINUE
C
      IF(IFUNIT .EQ. 1) THEN
          S=SQRT(S)
          DO 116 M=1,3
            V(M)=V(M)/S
```

```
  116          CONTINUE
       ENDIF
C
C
       RETURN
       END
       SUBROUTINE ADDVEC(V1,V2,IFUNIT,C)
       DIMENSION  V1(3),V2(3),C(3)
C
C
       S=0.0
       DO 109 M=1,3
       C(M)=V1(M)+V2(M)
       S=S+C(M)**2
  109    CONTINUE
C
       IF(IFUNIT .EQ. 1) THEN
         S=SQRT(S)
         DO 113 M=1,3
           C(M)=C(M)/S
  113        CONTINUE
       ENDIF
C
C
       RETURN
       END
       SUBROUTINE DOTVEC(V1,V2,IFORM,DAT)
       DIMENSION  V1(3),V2(3)
C
C  IF IFORM=0, THEN DOT IS RETURNED.
C  IF IFORM=1, THEN TAU IS RETURNED.
C
       DOT=0.0
       DO 124 M=1,3
       DOT=DOT+V1(M)*V2(M)
  124    CONTINUE
C
       IF(IFORM .EQ. 0) THEN
         DAT=DOT
       ELSE
         DEL=ABS(DOT)-1.0
         IF(DEL .EQ. 0.0) THEN
             DOT=1.0
             IF(DOT .LE. 0.0) DOT=-1.0
           ENDIF
C
C CORRECT FOR ROUND-OFF
C
         IF (ABS(DOT) .GT. 1.0) DOT=1.0
         DAT=-((ASIN(DOT)/0.0174532925)-90.0)
       ENDIF
C
C
       RETURN
```

```
      END
      SUBROUTINE CROSP(V1,V2,IFUNIT,C)
      DIMENSION  V1(3),V2(3),C(3)
C
C
C  IF IFUNIT=1, THEN C IS CONVERTED TO A UNIT VECTOR
C
      C(1)= V1(2)*V2(3)-V1(3)*V2(2)
      C(2)=-V1(1)*V2(3)+V1(3)*V2(1)
      C(3)= V1(1)*V2(2)-V1(2)*V2(1)
C
      IF(IFUNIT .EQ. 1) THEN
        S=0.0
        DO 120 M=1,3
          S=S+C(M)**2
  120       CONTINUE
        S=SQRT(S)
        DO 124 M=1,3
          C(M)=C(M)/S
  124       CONTINUE
      ENDIF
C
C
      RETURN
      END
      SUBROUTINE TRAGA(LA,NA,NB,LB,TAU,MT)
C     THIS SUBROUTINE COMPUTES THE DIHEDRAL ANGLE DEFINED BY THE SEQUENC
C     E OF ATOMS LA,NA,NB,LB. IF TRANS MT IS SET =1, IF GAUCHE =2.
      DIMENSION  RIJ(3),RKJ(3),RLK(3),UVJ(3),UVK(3),CPJK(3)
      COMMON  /STRUC/ X(3,120),W(120),KIND(120)
      I=LA
      J=NA
      K=NB
      L=LB
      DIJSQ=0.0
      DKJSQ=0.0
      DLKSQ=0.0
      DO 210 M=1,3
      RIJ(M)=X(M,I)-X(M,J)
      RKJ(M)=X(M,K)-X(M,J)
      RLK(M)=X(M,L)-X(M,K)
      DIJSQ=DIJSQ+RIJ(M)**2
      DKJSQ=DKJSQ+RKJ(M)**2
  210 DLKSQ=DLKSQ+RLK(M)**2
      DIJR=SQRT(DIJSQ)
      DKJR=SQRT(DKJSQ)
      DLKR=SQRT(DLKSQ)
      UVJ(1)=(RIJ(2)*RKJ(3)-RIJ(3)*RKJ(2))
      UVJ(2)=-(RIJ(1)*RKJ(3)-RIJ(3)*RKJ(1))
      UVJ(3)=(RIJ(1)*RKJ(2)-RIJ(2)*RKJ(1))
      UVK(1)=-(RKJ(2)*RLK(3)-RKJ(3)*RLK(2))
      UVK(2)=(RKJ(1)*RLK(3)-RKJ(3)*RLK(1))
      UVK(3)=-(RKJ(1)*RLK(2)-RKJ(2)*RLK(1))
      UJN=0.0
```

```
      UKN=0.0
      DO 212 I=1,3
      UJN=UJN + UVJ(I)**2
  212 UKN=UKN + UVK(I)**2
      DO 213 I=1,3
      UVJ(I) = UVJ(I)/(SQRT(UJN))
  213 UVK(I) = UVK(I)/(SQRT(UKN))
      CPJK(1)=UVJ(2)*UVK(3)-UVJ(3)*UVK(2)
      CPJK(2)=-UVJ(1)*UVK(3)+UVJ(3)*UVK(1)
      CPJK(3)=UVJ(1)*UVK(2)-UVJ(2)*UVK(1)
      SINJK=0.0
      DO 214 M=1,3
  214 SINJK=SINJK+CPJK(M)*RKJ(M)/DKJR
      TAU=(ASIN(SINJK))/.174532925E-01
      DOTJK = 0.0
      DO 216 I=1,3
  216 DOTJK = DOTJK + UVJ(I)*UVK(I)
      IF(DOTJK)217,218,218
  217 TAU = TAU + 180.0
  218 T=(ABS(TAU))-180.0
      IF(1.0-ABS(T))224,222,222
  222 MT=1
      GO TO 300
  224 IF(30.0-ABS(T)) 230,226,226
  226 MT=2
      GO TO 300
  230 T=ABS(TAU)
      IF(1.0-T) 236,234,234
  234 MT=4
      GO TO 300
  236 IF(30.0-T) 244,240,240
  240 MT=5
      GO TO 300
  244 G=ABS(TAU)-60.0
      IF(ABS(G)-30.0)250,250,254
  250 MT=3
      GO TO 300
  254 MT=6
  300 RETURN
      END
      SUBROUTINE LISTZ
      INTEGER  IFND(200)
      COMMON  /FCON1/ NOK(105),KND(105,10),KODE(105),NOF
      COMMON  /ZEEEL/ COEF(2001),NRW(2001),NCL(2001),NF(2001),NZ
      INTEGER  NUL,NLL,NOUTR(1936),NOUTC(1926),NOUTF(1936)
C
C
      DO 10 I=1,200
      IFND(I)=0
   10 CONTINUE
C
      WRITE(16,25) NZ
   25 FORMAT('TOTAL Z ELEMENTS=',I6)
      DO 20 I=1,NZ
```

```
      IFND(NF(I))=IFND(NF(I))+1
   20 CONTINUE
      WRITE(16,30)
   30 FORMAT(//2X,'FORCE CONSTANTS APPEARING IN Z MATRIX',/5X,
     1       'FORCE CONST.    NUMBER OF OCCUR.')
      DO 40 I=1,200
      IF (IFND(I) .GE. 1) THEN
        WRITE(16,50) I,IFND(I)
   50     FORMAT(5X,I3,12X,I4)
      ENDIF
   40 CONTINUE
C
      WRITE(16,75)
   75 FORMAT(//2X,'F.C. IN VFF BUT NOT USED=')
      DO 60 I=1,NOF
      IF (IFND(NOK(I)) .EQ. 0) THEN
        WRITE(16,70) NOK(I)
   70     FORMAT(5X,I3)
      ENDIF
   60 CONTINUE
C
C DISPLAY PORTIONS OF Z MATRIX
C
      NLL=1
      NUL=43
C
      K=0
      DO 80 I=1,NZ
      IF ((NRW(I).GE.NLL .AND. NRW(I).LE.NUL) .AND.
     1       (NCL(I).GE.NLL .AND. NCL(I).LE.NUL)) THEN
        K=K+1
        NOUTR(K)=NRW(I)
        NOUTC(K)=NCL(I)
        NOUTF(K)=NF(I)
        GO TO 80
      ENDIF
   80 CONTINUE
C
      DO 110 I=1,200
      IFND(I)=0
  110 CONTINUE
C
      DO 120 I=1,K
      IFND(NOUTF(I))=IFND(NOUTF(I))+1
  120 CONTINUE
      WRITE(16,130)
  130 FORMAT(//2X,'FORCE CONSTANTS APPEARING IN Z SUBMATRIX',/5X,
     1       'FORCE CONST.    NO. OCCUR.')
      DO 140 I=1,200
      IF (IFND(I) .GE. 1) THEN
        WRITE(16,150) I,IFND(I)
  150     FORMAT(5X,I3,6X,I4)
      ENDIF
  140 CONTINUE
```

```
C
      WRITE(16,175)
  175 FORMAT(//2X,'F.C. IN VFF BUT NOT USED IN SUBMATRIX=')
      DO 160 I=1,NOF
      IF (IFND(NOK(I)) .EQ. 0) THEN
        WRITE(16,170) NOK(I)
  170     FORMAT(5X,I3)
      ENDIF
  160 CONTINUE
C
      WRITE(16,210) (NOUTR(I),NOUTC(I),NOUTF(I),I=1,K)
  210 FORMAT(3I4)
C
C
      RETURN
      END
      SUBROUTINE BGENER(MXNOB,NOB,NRBB,NCBB,B,MXNOAT,MXNAQ,X)
      INTEGER  NRBB(MXNOB),NCBB(MXNOB),MXNOAT,MXNAQ,NOB
      REAL  B(MXNOB),X(3,120)
      COMMON  /CORD1/ NIC(370,4),NCOD(370),NONIC,NOCTOT
      COMMON  /CORD2/ NICT(101,6,4),NCODT(101,6),NOCOMP(101),NT
C
ALA24350
C
ALA24360
      NOB=0
ALA24370
      JOKER=0
ALA24380
C
ALA24390
C  B ELEMENTS FOR STRETCHES AND BENDS
ALA24400
C
ALA24410
      DO 110 I=1,NOCTOT
ALA24420
      IF(NCOD(I) .EQ. 1) CALL BOST(MXNOB,NOB,NRBB,NCBB,B,I,NIC(I,1),
     1    NIC(I,2),X)
      IF(NCOD(I) .EQ. 2) CALL BEND(MXNOB,NOB,NRBB,NCBB,B,I,NIC(I,1),
     1    NIC(I,2),NIC(I,3),X)
      IF(NCOD(I) .EQ. 3) CALL OPLA(MXNOB,NOB,NRBB,NCBB,B,I,NIC(I,1),
     1    NIC(I,2),NIC(I,3),NIC(I,4),X)
      IF(JOKER .EQ. 0) GO TO 110
        WRITE(16,12) JOKER,I
   12     FORMAT(//2X,'ERROR **** JOKER =',I2,' FOR COORD. NO.',I3)
ALA24490
        CALL EXIT
  110   CONTINUE
ALA24510
C
ALA24520
C  B ELEMENTS FOR TORSIONS
ALA24530
```

```
C
ALA24540
      DO 148 I=1,NT
ALA24550
      K=I+NONIC
        DO 144 J=1,NOCOMP(I)
          CALL TORS(MXNOB,NOB,NRBB,NCBB,B,K,NICT(I,J,1),NICT(I,J,2),
     1         NICT(I,J,3),NICT(I,J,4),X)
ALA24590
          IF(JOKER .EQ. 0) GO TO 144
            WRITE(16,12) JOKER,I
            CALL EXIT
  144       CONTINUE
ALA24630
  148 CONTINUE
ALA24640
C
ALA24650
C
ALA24660
      RETURN
ALA24670
      END
ALA24680
      SUBROUTINE BOST(MXNOB,NOB,NRBB,NCBB,B,NOINT,N1,N2,X)
ALA24690
      INTEGER  NRBB(MXNOB),NCBB(MXNOB)
ALA24700
      REAL  B(MXNOB),X(3,120)
ALA24730
      DIMENSION  RIJ(3)
ALA24740
C
ALA24750
C
ALA24760
C  THIS SUBROUTINE COMPUTES THE B MATRIX ELEMENTS FOR A BOND STRETCH
ALA24770
C  AS DEFINED BY WILSON.
ALA24780
C
ALA24790
  106 I=N1
ALA24800
      J=N2
ALA24810
      DIJSQ=0.0
ALA24820
  109 DO 112 M=1,3
ALA24830
      RIJ(M)=X(M,J)-X(M,I)
ALA24840
  112 DIJSQ=DIJSQ+RIJ(M)*RIJ(M)
ALA24850
```

```
  114 DO 120 M=1,3
ALA24860
      IF(ABS(RIJ(M))-0.00005)120,120,115
ALA24870
  115 NOB=NOB+1
ALA24880
      NRBB(NOB)=NOINT
ALA24890
      NCBB(NOB)=3*(I-1)+M
ALA24900
      B(NOB)=-RIJ(M) /SQRT(DIJSQ)
ALA24910
      NOB=NOB+1
ALA24920
      NRBB(NOB)=NOINT
ALA24930
      NCBB(NOB)=3*(J-1)+M
ALA24940
      B(NOB)= RIJ(M) / SQRT(DIJSQ)
ALA24950
  120 CONTINUE
ALA24960
  132 RETURN
ALA24970
      END
ALA24980
      SUBROUTINE BEND(MXNOB,NOB,NRBB,NCBB,B,NOINT,N1,N2,N3,X)
ALA24990
      INTEGER  NRBB(MXNOB),NCBB(MXNOB)
ALA25000
      REAL  B(MXNOB),X(3,120)
ALA25030
      DIMENSION  RJI(3),RJK(3),RIXJX(3),EJI(3),EJK(3)
ALA25040
C
ALA25050
C  THIS SUBROUTINE COMPUTES THE  B MATRIX ELEMENTS OF A VALENCE
ALA25060
C  ANGLE BENDING  COORDINATE AS DEFINED BY WILSON.
ALA25070
C   I AND K ARE THE NUMBERS  OF THE END ATOMS.
ALA25080
C   J= THE NUMBER OF THE CENTRAL ATOM
ALA25090
      I=N1
ALA25100
  107 J=N2
ALA25110
      K=N3
ALA25120
C     IX=N5
ALA25130
C     JX=N6
ALA25140
```

```
C     IF(IX)110,110,112
ALA25150
  110 IX=1
ALA25160
      JX=1
ALA25170
  112 DJISQ=0.0
ALA25180
      DJKSQ=0.0
ALA25190
      DXSQ=0.0
ALA25200
  115 DO 122 M=1,3
ALA25210
      RJI(M)=X(M,I)-X(M,J)
ALA25220
      RJK(M)=X(M,K)-X(M,J)
ALA25230
      RIXJX(M)=X(M,JX)-X(M,IX)
ALA25240
      DJISQ=DJISQ+RJI(M)*RJI(M)
ALA25250
      DJKSQ=DJKSQ+RJK(M)*RJK(M)
ALA25260
  122 DXSQ=DXSQ+RIXJX(M)*RIXJX(M)
ALA25270
  123 DJI=SQRT(DJISQ)
ALA25280
      DJK=SQRT(DJKSQ)
ALA25290
      DX=SQRT(DXSQ)
ALA25300
      IF(DX)128,127,128
ALA25310
  127 DX=1.0
ALA25320
  128 DOTJ=0.0
ALA25330
  129 DO 132 M=1,3
ALA25340
      EJI(M)=RJI(M)/DJI
ALA25350
      EJK(M)=RJK(M)/DJK
ALA25360
  132 DOTJ=DOTJ+EJI(M)*EJK(M)
ALA25370
      IF(1.0-ABS(DOTJ))152,152,134
ALA25380
  134 SINJ=SQRT(1.0-DOTJ*DOTJ)
ALA25390
  136 DO 144 M=1,3
ALA25400
      SMI=(DX*(DOTJ*EJI(M)-EJK(M)))/ (DJI*SINJ)
ALA25410
```

```
      IF(ABS(SMI)-0.00005)138,138,137
ALA25420
  137 NOB=NOB+1
ALA25430
      NRBB(NOB)=NOINT
ALA25440
      NCBB(NOB)=3*(I-1)+M
ALA25450
      B(NOB)=SMI
ALA25460
  138 SMK= (DX*(DOTJ*EJK(M)-EJI(M)))/ (DJK*SINJ)
ALA25470
      IF(ABS(SMK)-0.00005)140,140,139
ALA25480
  139 NOB=NOB+1
ALA25490
      NRBB(NOB)=NOINT
ALA25500
      NCBB(NOB)=3*(K-1)+M
ALA25510
      B(NOB)=SMK
ALA25520
  140 SUM=SMI+SMK
ALA25530
      IF(ABS(SUM)-0.00005)144,144,142
ALA25540
  142 NOB=NOB+1
ALA25550
      NRBB(NOB)=NOINT
ALA25560
      NCBB(NOB)=3*(J-1)+M
ALA25570
      B(NOB)=-SUM
ALA25580
  144 CONTINUE
ALA25590
      GO TO 154
ALA25600
  152 JOKER=2
ALA25610
  154 RETURN
ALA25620
      END
ALA25630
      SUBROUTINE OPLA(MXNOB,NOB,NRBB,NCBB,B,NOINT,N1,N2,N3,N4,X)
ALA25640
      INTEGER  NRBB(MXNOB),NCBB(MXNOB)
ALA25650
      REAL  B(MXNOB),X(3,120)
ALA25680
C     THIS SUBROUTINE COMPUTES THE B MATRIX ELEMANTS FOR AN OUT OF
C     PLANE WAGGING COORDINATE AS DEFINED  BY WILSON.
C      I= THE END ATOM
C      J= THE APEX ATOM
```

```
C       K AND L = THE ANCHOR ATOMS.
C
        COMMON  /ATOM/  NOAT
C
        DIMENSION RJI(3),RJK(3),RJL(3),RIXJX(3),EJI(3),EJK(3),EJL(3),
       1          C1(3),C2(3),C3(3)
C
  102 IF(NOAT-N4)170,103,103
  103 IF(NOAT-N3)170,104,104
  104 IF(NOAT-N2)170,105,105
  105 IF(NOAT-N1)170,106,106
  106 I=N1
      J=N2
      K=N3
      L=N4
  110 IX=1
      JX=1
  112 DJISQ=0.0
      DJKSQ=0.0
      DJLSQ=0.0
  115 DXSQ=0.0
  116 DO 124 M=1,3
      RJI(M)=X(M,I)-X(M,J)
      DJISQ=DJISQ+RJI(M)*RJI(M)
      RJK(M)=X(M,K)-X(M,J)
      DJKSQ=DJKSQ+RJK(M)*RJK(M)
      RJL(M)=X(M,L)-X(M,J)
      DJLSQ=DJLSQ+RJL(M)*RJL(M)
      RIXJX(M)=X(M,JX)-X(M,IX)
  124 DXSQ=DXSQ+RIXJX(M)*RIXJX(M)
  126 DJI=SQRT(DJISQ)
      DJK=SQRT(DJKSQ)
      DJL=SQRT(DJLSQ)
      DX=SQRT(DXSQ)
  130 IF(DX)132,131,132
  131 DX=1.0
  132 DO 136 M=1,3
      EJI(M)=RJI(M)/DJI
      EJK(M)=RJK(M)/DJK
  136 EJL(M)=RJL(M)/DJL
  137 C1(1)=EJK(2)*EJL(3)-EJK(3)*EJL(2)
      C1(2)=EJK(3)*EJL(1)-EJK(1)*EJL(3)
      C1(3)=EJK(1)*EJL(2)-EJK(2)*EJL(1)
      C2(1)=EJL(2)*EJI(3)-EJL(3)*EJI(2)
      C2(2)=EJL(3)*EJI(1)-EJL(1)*EJI(3)
      C2(3)=EJL(1)*EJI(2)-EJL(2)*EJI(1)
      C3(1)=EJI(2)*EJK(3)-EJI(3)*EJK(2)
      C3(2)=EJI(3)*EJK(1)-EJI(1)*EJK(3)
  139 C3(3)=EJI(1)*EJK(2)-EJI(2)*EJK(1)
  140 DET=EJI(1)*C1(1)+EJI(2)*C1(2)+EJI(3)*C1(3)
      DOTI=0.0
  142 DO 143 M=1,3
  143 DOTI=DOTI+EJK(M)*EJL(M)
  144 IF(1.0-ABS(DOTI))172,172,146
```

```
146 SINI=SQRT(1.0-DOTI*DOTI)
147 SINT=DET/SINI
148 IF(1.0-ABS(SINT))174,174,149
149 COST=SQRT(1.0-SINT*SINT)
150 TANT=SINT/COST
155 DO 168 M=1,3
157 SMI    =((C1(M)/(COST*SINI))-(TANT*EJI(M)))/DJI
    IF(ABS(SMI)-0.00005)160,160,158
158 NOB=NOB+1
    NRBB(NOB)=NOINT
    NCBB(NOB)=3*(I-1)+M
    B(NOB)=DX*SMI
160 SMK=((C2(M)/(COST*SINI))-((TANT*(EJK(M)-DOTI*EJL(M)))/(SINI*SINI))
   1)/DJK
    IF(ABS(SMK)-0.00005)163,163,161
161 NOB=NOB+1
    NRBB(NOB)=NOINT
    NCBB(NOB)=3*(K-1)+M
    B(NOB)=DX*SMK
163 SML=((C3(M)/(COST*SINI))-((TANT*(EJL(M)-DOTI*EJK(M)))/(SINI*SINI))
   1)/DJL
    IF(ABS(SML)-0.00005)166,166,164
164 NOB=NOB+1
    NRBB(NOB)=NOINT
    NCBB(NOB)=3*(L-1)+M
    B(NOB)=DX*SML
166 SUM=SMI+SMK+SML
    IF(ABS(SUM)-0.00005)168,168,167
167 NOB=NOB+1
    NRBB(NOB)=NOINT
    NCBB(NOB)=3*(J-1)+M
    B(NOB)=-DX*SUM
168 CONTINUE
    GO TO 178
170 JOKER=1
    GO TO 178
172 JOKER=2
    GO TO 178
174 JOKER=3
178 RETURN
    END
    SUBROUTINE TORS(MXNOB,NOB,NRBB,NCBB,B,NOINT,N1,N2,N3,N4,X)
ALA25640
    INTEGER  NRBB(MXNOB),NCBB(MXNOB)
ALA25650
    REAL  B(MXNOB),X(3,120)
ALA25680
    DIMENSION  RIJ(3),RJK(3),RKL(3),RIXJX(3),EIJ(3),
ALA25690
     1  EJK(3),EKL(3),CR1(3),CR2(3)
ALA25700
C
ALA25710
```

```
C     THIS SUBROUTINE COMPUTES  THE B MATRIX ELEMENTS FOR THE TORSION
ALA25720
C     AS DEFINED  BY WILSION.
ALA25730
C      I AND L = THE END ATOMS .  I NEARER OBSERVER.
ALA25740
C      J AND K = THE CENTRAL ATOMS. J NEARER OBSERVER.
ALA25750
C
ALA25760
      I=N1
ALA25770
      J=N2
ALA25780
      K=N3
ALA25790
      L=N4
ALA25800
  110 IX=1
ALA25840
      JX=1
ALA25850
  112 DIJSQ=0.0
ALA25860
      DJKSQ=0.0
ALA25870
      DKLSQ=0.0
ALA25880
  115 DXSQ=0.0
ALA25890
  116 DO 124 M=1,3
ALA25900
      RIJ(M)=X(M,J)-X(M,I)
ALA25910
      DIJSQ=DIJSQ+RIJ(M)*RIJ(M)
ALA25920
      RJK(M)=X(M,K)-X(M,J)
ALA25930
      DJKSQ=DJKSQ+RJK(M)*RJK(M)
ALA25940
      RKL(M)=X(M,L)-X(M,K)
ALA25950
      DKLSQ=DKLSQ+RKL(M)*RKL(M)
ALA25960
      RIXJX(M)=X(M,JX)-X(M,IX)
ALA25970
  124 DXSQ=DXSQ+RIXJX(M)*RIXJX(M)
ALA25980
  126 DIJ=SQRT(DIJSQ)
ALA25990
      DJK=SQRT(DJKSQ)
ALA26000
      DKL=SQRT(DKLSQ)
ALA26010
```

```
      DX=SQRT(DXSQ)
ALA26020
  130 IF(DX)132,131,132
ALA26030
  131 DX=1.0
ALA26040
  132 DO 136 M=1,3
ALA26050
      EIJ(M)=RIJ(M)/DIJ
ALA26060
      EJK(M)=RJK(M)/DJK
ALA26070
  136 EKL(M)=RKL(M)/DKL
ALA26080
  138 CR1(1)=EIJ(2)*EJK(3)-EIJ(3)*EJK(2)
ALA26090
      CR1(2)=EIJ(3)*EJK(1)-EIJ(1)*EJK(3)
ALA26100
      CR1(3)=EIJ(1)*EJK(2)-EIJ(2)*EJK(1)
ALA26110
      CR2(1)=EJK(2)*EKL(3)-EJK(3)*EKL(2)
ALA26120
      CR2(2)=EJK(3)*EKL(1)-EJK(1)*EKL(3)
ALA26130
  142 CR2(3)=EJK(1)*EKL(2)-EJK(2)*EKL(1)
ALA26140
  143 DOTPJ=0.0
ALA26150
      DOTPK=0.0
ALA26160
  145 DO 147 M=1,3
ALA26170
      DOTPJ=DOTPJ-EIJ(M)*EJK(M)
ALA26180
  147 DOTPK=DOTPK-EJK(M)*EKL(M)
ALA26190
  148 IF(1.0-ABS(DOTPJ))182,182,149
ALA26200
  149 IF(1.0-ABS(DOTPK))182,182,150
ALA26210
  150 SINPJ=SQRT(1.0-DOTPJ*DOTPJ)
ALA26220
      SINPK=SQRT(1.0-DOTPK*DOTPK)
ALA26230
  152 DO 164 M=1,3
ALA26240
      SMI=-CR1(M)/(DIJ*SINPJ*SINPJ)
ALA26250
      IF(ABS(SMI)-0.00005)156,156,154
ALA26260
  154 NOB=NOB+1
ALA26270
      NRBB(NOB)=NOINT
ALA26280
```

```
      NCBB(NOB)=3*(I-1)+M
ALA26290
      B(NOB)=DX*SMI
ALA26300
  156 F1=(CR1(M)*(DJK-DIJ*DOTPJ))/(DJK*DIJ*SINPJ*SINPJ)
ALA26310
      F2=(DOTPK*CR2(M))/(DJK*SINPK*SINPK)
ALA26320
      SMJ=F1-F2
ALA26330
      IF(ABS(SMJ)-0.00005)158,158,157
ALA26340
  157 NOB=NOB+1
ALA26350
      NRBB(NOB)=NOINT
ALA26360
      NCBB(NOB)=3*(J-1)+M
ALA26370
      B(NOB)=DX*SMJ
ALA26380
  158 SML= CR2(M)/(DKL*SINPK*SINPK)
ALA26390
      IF(ABS(SML)-0.00005)160,160,159
ALA26400
  159 NOB=NOB+1
ALA26410
      NRBB(NOB)=NOINT
ALA26420
      NCBB(NOB)=3*(L-1)+M
ALA26430
      B(NOB)=DX*SML
ALA26440
  160 SUM=SMI+SMJ+SML
ALA26450
      IF(ABS(SUM)-0.00005)164,164,162
ALA26460
  162 NOB=NOB+1
ALA26470
      NRBB(NOB)=NOINT
ALA26480
      NCBB(NOB)=3*(K-1)+M
ALA26490
      B(NOB)=-DX*SUM
ALA26500
  164 CONTINUE
ALA26510
      GO TO 186
ALA26520
  182 JOKER=2
ALA26530
  186 RETURN
ALA26540
      END
ALA26550
```

```
      SUBROUTINE FORMB(MXNOB,NRBB,NCBB,B,NOB,SM1,MXNAQ,NOCTOT)
ALA26580
      INTEGER MXNOB,NRBB(MXNOB),NCBB(MXNOB),NOB,MXNAQ,NOCTOT
ALA26590
      REAL B(MXNOB),SM1(MXNAQ,MXNAQ)
ALA26600
      COMMON  /ATOM/  NOAT
C
C
      NA=3*NOAT
C
C  FORM B-MATRIX AND STORE IN MATRIX SM1
ALA27990
C
ALA28000
      DO 114 I=1,NOCTOT
ALA28010
      DO 114 J=1,NA
ALA28020
      SM1(I,J)=0.0
  114   CONTINUE
      DO 120 L=1,NOB
      I=NRBB(L)
      J=NCBB(L)
      SM1(I,J)=SM1(I,J)+B(L)
  120   CONTINUE
C
      IFX=0
      IF(IFX .EQ. 0) GO TO 100
      WRITE(16,10) NOB
   10 FORMAT(//2X,'NOB= ',I4)
      WRITE(16,25) (NRBB(L),NCBB(L),B(L),L=1,NOB)
   25 FORMAT(///2X,'B ELEMENTS'/(4(3X,2I3,F8.4)))
      WRITE(16,30)
   30 FORMAT(///2X,'BB MATRIX'/)
      DO 142 I=1,NOCTOT
      WRITE(16,400) I
  400   FORMAT(10X,'INT. COORD. ',I3)
      DO 143 J=1,NA/3
        K=3*J
        WRITE(16,401) J,(SM1(I,KK),KK=K-2,K)
  401     FORMAT(15X,I3,3F7.4)
  143   CONTINUE
  142 CONTINUE
  100 CONTINUE
C
ALA26680
C
ALA26690
      RETURN
ALA26700
      END
ALA26710
      SUBROUTINE ZGSYM(SM1,MXNAQ,NOCTOT,NRU,NCU,DU,MXNAQ2,GMAT,SM4,
```

```
     1                    UMAT,SM3,DA)
      INTEGER  MXNAQ,NOCTOT
      INTEGER  NRU(MXNAQ2),NCU(MXNAQ2),MXNAQ2
      INTEGER  NOU,NS,NB(20),NSB,NX
      REAL  SM1(MXNAQ,MXNAQ),DU(MXNAQ2),GMAT(MXNAQ,MXNAQ),DA(MXNAQ)
      REAL  SM4(MXNAQ,MXNAQ),UMAT(MXNAQ,MXNAQ),SM3(MXNAQ,MXNAQ)
      COMMON  /ATOM/  NOAT
      COMMON  /STRUC/ X(3,120),W(120),KIND(120)
C
      NA=3*NOAT
C
      DO 510 I=1,NOCTOT
      DO 510 J=1,NOAT
        KK=(J-1)*3+1
        DO 510 K=KK,KK+2
          SM4(I,K)=SM1(I,K)*SQRT(1.0/W(J))
  510 CONTINUE
C
      IFX=0
      IF(IFX .EQ. 0) GO TO 500
      DO 542 I=1,NOCTOT
      WRITE(16,502) I
  502   FORMAT(10X,'INT. COORD. ',I3)
      DO 543 J=1,NA/3
        K=3*J
        WRITE(16,501) J,(SM4(I,KK),KK=K-2,K)
  501     FORMAT(15X,I3,3F7.4)
  543   CONTINUE
  542 CONTINUE
  500 CONTINUE
C
      CALL DGEMUL(SM4,MXNAQ,'N',SM4,MXNAQ,'T',GMAT,MXNAQ,NOCTOT,NA,
     1              NOCTOT)
      IFX=0
      IF(IFX .EQ. 0) GO TO 122
      WRITE(16,590)
  590 FORMAT(//2X,'G MATRIX')
      DO 600 I=1,NOCTOT
      WRITE(16,527) I,(GMAT(I,J),J=1,NOCTOT)
  527   FORMAT(10X,'ROW',I3/(6F12.6))
  600 CONTINUE
  122 CONTINUE
      DO 130 I=1,MXNAQ
      DO 130 J=1,MXNAQ
      SM4(I,J)=0.0
      SM3(I,J)=0.0
  130 CONTINUE
C
C READ IN U MATRIX, THEN SYMMETRIZE THE G MATRIX; GSYM=U*G*U'
C
      READ(3,650) NOU,NS,NSB
  650 FORMAT(3I3)
      READ(3,655) (NB(I),I=1,NSB)
  655 FORMAT(24I3)
```

```
      NX=1
      DSQ=0.0
      DO 660 I=1,NOU
      READ(3,670) NRU(I),NCU(I),DU(I)
  670   FORMAT(2I3,F12.6)
      IF(NRU(I) .EQ. NX) THEN
        DSQ=DSQ+DU(I)**2
      ELSEIF(NRU(I) .GT. NX) THEN
        DA(NX)=1.0/SQRT(DSQ)
        NX=NX+1
        DSQ=DU(I)**2
      ENDIF
  660 CONTINUE
      DA(NX)=1.0/SQRT(DSQ)
C
      DO 800 I=1,NOU
      J=NRU(I)
      DU(I)=DA(J)*DU(I)
  800 CONTINUE
C
      DO 680 L=1,NOU
      I=NRU(L)
      J=NCU(L)
      UMAT(I,J)=UMAT(I,J)+DU(L)
  680 CONTINUE
C
      IFX=1
      IF(IFX .EQ. 0) GO TO 700
      WRITE(16,685)
  685 FORMAT(//2X,'U MATRIX')
      DO 690 I=1,NS
      WRITE(16,702) I
  702   FORMAT(2X,'ROW ',I3)
      WRITE(16,705) (UMAT(I,J),J=1,NOCTOT)
  705   FORMAT(6F12.6)
  690 CONTINUE
  700 CONTINUE
C
      CALL DGEMUL(GMAT,MXNAQ,'N',UMAT,MXNAQ,'T',SM3,MXNAQ,NOCTOT,
     1            NOCTOT,NOCTOT)
      CALL DGEMUL(UMAT,MXNAQ,'N',SM3,MXNAQ,'N',SM4,MXNAQ,NOCTOT,
     1            NOCTOT,NOCTOT)
C
      IFX=1
      IF(IFX .EQ. 0) GO TO 720
      WRITE(16,722)
  722 FORMAT(//2X,'SYMMETRIZED G MATRIX')
      DO 710 I=1,NS
      WRITE(16,702) I
      WRITE(16,715) (SM4(I,J),J=1,NOCTOT)
  715   FORMAT(6F12.6)
  710 CONTINUE
  720 CONTINUE
C
```

```
      CALL ZSYM(NRU,NCU,NOU,NS,NSB,NB,DU,MXNAQ2,NOCTOT,SM4,MXNAQ)
C
C
      RETURN
      END
      SUBROUTINE ZSYM(NRU,NCU,NOU,NS,NSB,NB,DU,MXNAQ2,NOCTOT,SM4,MXNAQ)
      INTEGER  NRU(MXNAQ2),NCU(MXNAQ2),NOU,MXNAQ2,MXNAQ
      INTEGER  NS,NB(20),NSB,NOCTOT,NZ1,I2(4),J2(4),II2(4),JJ2(4)
      REAL  DU(MXNAQ2),SM4(MXNAQ,MXNAQ)
      DIMENSION       DZ(2000),NR1(2000),NC1(2000),DU1(2000),
     1                NRZ(500),NCZ(500),NBL(101),NRS(101),
     2                NCS(101),NFC(101),FS(101),NB3(2000),DA(500),
     3                U(500),FU(500),UF(500),NRO(4),NCO(4),NPI(4),
     4                DAT(4),NR(2000),NC(2000),NFO(2000),Z(500)
      COMMON  /FCON1/ NOK(105),KND(105,10),KODE(105),NOF
      COMMON  /FCON2/ VAL(105),ANGLE(105),ZFACT(105)
      COMMON  /ZEEEL/ COEF(2001),NRW(2001),NCL(2001),NF(2001),NZ
C
C WRITE FORCE CONSTANTS TO FILE
C
      WRITE(4,988) (VAL(I),I=1,NOF)
  988 FORMAT(6F12.6)
C
      NREC=0
      IFSK=0
      NE=0
      IFREP=0
      NST=0
      L=0
      NWY=0
      REWIND 1
      DO 10 I=1,NZ
      NR(I)=NRW(I)
      NC(I)=NCL(I)
      NFO(I)=ABS(NF(I))
      DZ(I)=1.0
   10 CONTINUE
      NOZ=NZ
      NOU=NOU+1
      NRU(NOU)=-3
      NCU(NOU)=0
      DU(NOU)=0.0
      NU=NOU-1
      DO 184 K=1,NU
      NR1(K)= NRU(K)
      NC1(K)=NCU(K)
  184 DU1(K)=DU(K)
C
      IFX=0
      IF(IFX .EQ. 0) GO TO 101
      DO 102 I=1,NZ
        WRITE(16,103) I,NR(I),NC(I),NFO(I),DZ(I)
  103     FORMAT(4I3,F12.6)
  102   CONTINUE
```

```
      DO 104 I=1,NOU
        WRITE(16,105) I,NRU(I),NCU(I),DU(I)
  105     FORMAT(3I3,F12.6)
  104   CONTINUE
      DO 106 I=1,NSB
        WRITE(16,107) I,NB(I)
  107     FORMAT(2I3)
  106   CONTINUE
  101 CONTINUE
C
      NO=1
  186 NZ1=0
1070
      DO 190 K=1,NOZ
1080
      IF(NO-NFO(K))190,188,190
1090
  188 NZ1=NZ1+1
1100
      NRZ(NZ1)=NR(K)
1110
      NCZ(NZ1)=NC(K)
1120
      Z(NZ1)=DZ(K)
1130
  190 CONTINUE
1140
      IF(NZ1)600,192,220
1150
  192 NO=NO+1
1160
      IF(NO-NOF)186,186,295
1170
  220 NL=1
1180
      NX=2
1190
      NUT=1
1200
      NUB=1
1210
      NJ=1
1220
  230 NP=NB(NL)
1230
      NT=NB(NX)
1240
  236 DO 238 I=1,NOCTOT
1250
      FU(I)=0.0
1260
  238 U(I)=0.0
1270
```

```
      DO 250 K=NUB,NOU
1280
      IF(NRU(K)-NJ)240,248,240
1290
  240 DO 246 L=1,NZ1
1300
      I=NRZ(L)
1310
      J=NCZ(L)
1320
      FU(I)=FU(I)+Z(L)*U(J)
1330
      IF(I-J)244,246,244
1340
  244 FU(J)=FU(J)+Z(L)*U(I)
1350
  246 CONTINUE
1360
      GO TO 252
1370
  248 JU=NCU(K)
1380
  250 U(JU)=DU(K)
1390
  252 NUB=K
1400
      DO 254 I=NJ,NS
1410
  254 UF(I)=0.0
1420
      ASSIGN 262 TO JOKE
1430
      L=0
      DO 265 L=NUT,NU
1440
      GO TO JOKE,(262,264)
1450
  262 IF(NR1(L)-NJ)605,264,263
1460
  263 ASSIGN 264 TO JOKE
1470
      NWY=L
1480
  264 I=NR1(L)
1490
      J=NC1(L)
1500
  265 UF(I)=UF(I)+DU1(L)*FU(J)
1510
      NUT=NWY
1520
      DO 280 J=NJ,NS
1530
```

```
      IF(0.00005-ABS(UF(J)))270,280,280
1540
  270 IF(NT-J)271,271,272
1550
  271 WRITE(16,72)NJ,J
1560
   72 FORMAT('ERROR,ERROR,ERROR- Z NOT FACTORING.ROW',I4,'COLUMN',I4)
1570
  272 NE=NE+1
1580
      IF(101-NE)273,273,274
1590
  273 WRITE (1)(NBL(I),NRS(I),NCS(I),NFC(I),FS(I),I=1,100)
1600
      NREC=NREC+1
1610
      NE=1
1620
  274 NRS(NE)=NJ-NP+1
1630
      NCS(NE)=J-NP+1
1640
      NBL(NE)=NL
1650
      NFC(NE)=NO
1660
      FS(NE)=UF(J)
1670
  280 CONTINUE
1680
      NJ=NJ+1
1690
      IF(NT-NJ)284,284,236
1700
  284 NL=NL+1
1710
      NX=NX+1
1720
      IF(NSB-NX)290,230,230
1730
  290 NO=NO+1
1740
      IF(NOF-NO)295,186,186
1750
  295 IF(NREC)296,296,298
1760
  296 NOZ=0
1770
      GO TO 321
1780
  298 WRITE (1)(NBL(I),NRS(I),NCS(I),NFC(I),FS(I),I=1,NE)
1790
  300 REWIND 1
1800
```

```
  302 DO 312 L=1,NREC
1810
      READ  (1)(NBL(I),NRS(I),NCS(I),NFC(I),FS(I),I=1,100)
1820
      DO 312 K=1,100
1830
      NZ=100*(L-1)+K
1840
      NB3(NZ)=NBL(K)
1850
      NR(NZ)=NRS(K)
1860
      NC(NZ)=NCS(K)
1870
      NFO(NZ)=NFC(K)
1880
  312 DZ(NZ)=FS(K)
1890
      NOZ=NZ1
1900
  315 IF(NE)330,330,320
1910
  320 READ  (1)(NBL(I),NRS(I),NCS(I),NFC(I),FS(I),I=1,NE)
1920
  321 DO 324 K=1,NE
1930
      NZ1=NOZ+K
1940
      NB3(NZ1)=NBL(K)
1950
      NR(NZ1)=NRS(K)
1960
      NC(NZ1)=NCS(K)
1970
      NFO(NZ1)=NFC(K)
1980
  324 DZ(NZ1)=FS(K)
1990
  330 NSO=1
2000
  331 NT=0
2010
      NX=0
2020
      NKK=NB(NSO+1)-NB(NSO)
      WRITE(4,77) NKK,NKK
   77 FORMAT(' -6',2I3,6X,'-1 0'/)
  332 DO 340 I=1,NZ1
      IF(NSO-NB3(I))340,336,340
  336 NX=NX+1
      IF(101-NX)337,337,338
  337 WRITE (4,86)   (NRS(L),NCS(L),NFC(L),FS(L),L=1,100)
   86 FORMAT    (3I3,F9.6,3I3,F9.6,3I3,F9.6,3I3,F9.6)
```

```
      NT=NT+100
2110
      NX=1
2120
  338 NRS(NX)=NR(I)
2130
      NCS(NX)=NC(I)
2140
      NFC(NX)=NFO(I)
2150
      FS(NX)=DZ(I)
2160
  340 CONTINUE
2170
      IF(NX)344,344,342
2180
  342 WRITE (4,86)    (NRS(L),NCS(L),NFC(L),FS(L),L=1,NX)
      NT=NT+NX
  344 WRITE(16,76)NT
   76 FORMAT(2X,' NOZ=',I4)
C
C OUTPUT SYMMETRIZED BLOCK OF G MATRIX
C
      N1=NB(NSO)
      N2=NB(NSO+1)-1
      II=0
      NK=0
      DO 120 I1=N1,N2
      JJ=II
      II=II+1
      DO 120 J1=I1,N2
      JJ=JJ+1
      IF(ABS(SM4(I1,J1)) .GT. 0.00005) THEN
        NK=NK+1
        I2(NK)=I1
        J2(NK)=J1
        II2(NK)=II
        JJ2(NK)=JJ
        IF(NK .EQ. 4) THEN
          WRITE(4,125) (II2(K),JJ2(K),SM4(I2(K),J2(K)),K=1,4)
  125       FORMAT(4(2I3,F12.6))
          NK=0
        ENDIF
      ENDIF
  120 CONTINUE
      WRITE(4,125) (II2(K),JJ2(K),SM4(I2(K),J2(K)),K=1,NK)
C
      NSO=NSO+1
      IF(NSB-NSO)400,400,331
  600 WRITE(16,56)L,NRO(L),NCO(L),NPI(L),DAT(L)
   56 FORMAT(' Z MATRIX ERROR FIELD', I3,'READS',3I4,F12.6)
      GO TO 400
  605 WRITE(16,58)L,NRO(L),NCO(L),DAT(L)
   58 FORMAT(' U MATRIX ERROR FIELD',I3,'READS',2I4,F12.6)
```

```
      GO TO 400
C
C
  400 RETURN
      END
      SUBROUTINE TFORM(TRC,MXNC,NUMC,IC,JC,KC,TC,X)
      INTEGER  MXNC,NUMC,IC(MXNC),JC(MXNC),KC(MXNC),TC(MXNC)
      REAL  TRC(MXNC,3,3),B1(3),B2(3)
ALA27610
      REAL  XXS(3),YXS(3),ZXS(3),X(3,120)
ALA27620
C
ALA27630
      DO 10 I=1,NUMC
ALA27650
      IF (TC(I) .EQ. 1) THEN
        DO 200 J=1,3
          YXS(J)=X(J,IC(I))-X(J,JC(I))
          XXS(J)=0.0
          ZXS(J)=0.0
  200     CONTINUE
        CALL MKUNIT(YXS,3)
      ELSEIF ((TC(I).EQ.2).OR.(TC(I).EQ.3)) THEN
        DO 20 J=1,3
          B1(J)=X(J,JC(I))-X(J,IC(I))
          B2(J)=X(J,KC(I))-X(J,JC(I))
          XXS(J)=X(J,KC(I))-X(J,IC(I))
   20     CONTINUE
        CALL MKUNIT(XXS,3)
        CALL XPROD(B1,B2,ZXS,3)
        CALL MKUNIT(ZXS,3)
        CALL XPROD(XXS,ZXS,YXS,3)
        IF (TC(I).EQ.3) THEN
          ZXS(1)=-ZXS(1)
          ZXS(2)=-ZXS(2)
          ZXS(3)=-ZXS(3)
        ENDIF
      ELSEIF ((TC(I).GE.4).AND.(TC(I).LE.6)) THEN
        DO 90 J=1,3
          YXS(J)=X(J,JC(I))-X(J,KC(I))
          B2(J)=X(J,IC(I))-X(J,JC(I))
   90     CONTINUE
        CALL MKUNIT(YXS,3)
        CALL XPROD(YXS,B2,ZXS,3)
        CALL MKUNIT(ZXS,3)
        IF (TC(I).EQ.6) THEN
          ZXS(1)=-ZXS(1)
          ZXS(2)=-ZXS(2)
          ZXS(3)=-ZXS(3)
        ENDIF
        IF (TC(I).EQ.4) THEN
          CALL XPROD(YXS,ZXS,XXS,3)
        ELSE
          CALL XPROD(ZXS,YXS,XXS,3)
```

```
        ENDIF
      ELSE
        DO 100 J=1,3
          XXS(J)=0.0
          YXS(J)=0.0
          ZXS(J)=0.0
  100     CONTINUE
        XXS(1)=1.0
        YXS(2)=1.0
        ZXS(3)=1.0
      ENDIF
C
      DO 30 J=1,3
          TRC(I,1,J)=XXS(J)
          TRC(I,2,J)=YXS(J)
          TRC(I,3,J)=ZXS(J)
   30   CONTINUE
ALA28110
   10 CONTINUE
ALA28120
C
ALA28130
      IFX=0
ALA28140
      IF (IFX .NE. 0) THEN
ALA28150
      WRITE(16,70)
   70   FORMAT(//,'T MATRIX')
ALA28170
      DO 40 I=1,NUMC
        WRITE(16,80) I
   80     FORMAT(/5X,'LOCAL AXIS NO.',I4)
ALA28200
        DO 50 J=1,3
          WRITE(16,60) (TRC(I,J,K), K=1,3)
   60       FORMAT(10X,3(F12.6))
ALA28230
   50     CONTINUE
ALA28240
   40   CONTINUE
ALA28250
      ENDIF
ALA28260
C
ALA28270
      RETURN
ALA28280
      END
ALA28290
      SUBROUTINE MKUNIT(VEC,LTH)
ALA28300
      REAL  VEC(LTH),TOTMAG
ALA28310
```

```
      INTEGER  LTH
ALA28320
C
ALA28330
      TOTMAG=0.0
ALA28340
      DO 10 I=1,3
ALA28350
      TOTMAG=VEC(I)**2+TOTMAG
   10 CONTINUE
ALA28370
      TOTMAG=SQRT(TOTMAG)
ALA28380
      DO 20 I=1,3
ALA28390
      VEC(I)=VEC(I)/TOTMAG
   20 CONTINUE
ALA28410
C
ALA28420
      RETURN
ALA28430
      END
ALA28440
      SUBROUTINE XPROD(VEC1,VEC2,VECOUT,LTH)
ALA28450
      REAL  VEC1(LTH),VEC2(LTH),VECOUT(LTH)
ALA28460
      INTEGER  LTH
ALA28470
C
ALA28480
      VECOUT(1)=VEC1(2)*VEC2(3)-VEC1(3)*VEC2(2)
ALA28490
      VECOUT(2)=VEC1(3)*VEC2(1)-VEC1(1)*VEC2(3)
ALA28500
      VECOUT(3)=VEC1(1)*VEC2(2)-VEC1(2)*VEC2(1)
ALA28510
C
ALA28520
      RETURN
ALA28530
      END
ALA28540
      SUBROUTINE FREQNC(MXNAQ,FP,FR,SM1,SM2,SM3,ED,MXNAQ2,ROWDAT,
ALA27780
     1  MXNAQE,WTINV,MXNOAT,CAX,NGPTOT)
ALA27790
      INTEGER  MXNAQ,MXNAQ2,MXNOAT,CAX(MXNAQ),NGPTOT
ALA27820
      REAL  FP(MXNAQ),FR(MXNAQ)
ALA27850
      REAL  SM1(MXNAQ,MXNAQ),SM2(MXNAQ,MXNAQ),SM3(MXNAQ,MXNAQ)
ALA27860
```

```
      REAL  ED(MXNAQE),ROWDAT(MXNAQ2),WTINV(MXNAQ)
ALA27870
      COMMON  /ATOM/  NOAT
      COMMON  /CORD1/ NIC(370,4),NCOD(370),NONIC,NOCTOT
      COMMON  /FCON1/ NOK(105),KND(105,10),KODE(105),NOF
      COMMON  /FCON2/ VAL(105),ANGLE(105),ZFACT(105)
      COMMON  /STRUC/ X(3,120),W(120),KIND(120)
      COMMON  /ZEEEL/ COEF(2001),NRW(2001),NCL(2001),NF(2001),NZ
C
ALA27950
C
ALA27960
      NA=3*NOAT
ALA27970
C
ALA28100
C  FORM F-MATRIX AND STORE IN MATRIX SM3
ALA28140
C
ALA28150
      DO 125 I=1,NOCTOT
ALA28160
      DO 125 J=1,NOCTOT
ALA28170
      SM3(I,J)=0.0
  125   CONTINUE
C
    VALIN=0.0
    DO 130 L=1,NZ
    I=NRW(L)
    J=NCL(L)
    K=NF(L)
    IFNEG=0
    IF(K .LT. 0) THEN
      K=-K
      IFNEG=1
    ENDIF
    IFFND=0
    DO 127 L2=1,NOF
      IF (K .EQ. NOK(L2)) THEN
        VALIN=VAL(L2)
        IFFND=1
        GO TO 129
      ENDIF
127   CONTINUE
129   CONTINUE
    IF (IFFND .EQ. 0) THEN
      WRITE(16,500)
500     FORMAT(//2X,'ERROR!! FC FOR F MATRIX NOT FOUND IN FC LIST')
      CALL EXIT
    ENDIF
    IF(IFNEG .EQ. 1) VALIN=-VALIN
    SM3(I,J)=SM3(I,J)+VALIN
```

```
  130 CONTINUE
ALA28250
C
ALA28260
      DO 134 I=1,NOCTOT
ALA28270
      DO 134 J=I,NOCTOT
ALA28280
      SM3(J,I)=SM3(I,J)
  134   CONTINUE
ALA28300
C
ALA28310
C     WRITE(16,16) (SM3(1,J), J=1,NOCTOT)
C  16 FORMAT(//2X,'FIRST ROW OF F'//(10X,5F10.4))
C
      IFX=1
      IF(IFX .EQ. 1) GO TO 150
      LIMNQ=NOCTOT
      LIMNA=NA
      LIMNOZ=NZ
      WRITE(16,21) NOCTOT,NA,NZ
   21 FORMAT(///2X,'NOCTOT,NA,NZ=',2I4,2I5)
      WRITE(16,24) (NRW(L),NCL(L),NF(L),L=1,LIMNOZ)
   24 FORMAT(///2X,' Z ELEMENTS'/(5(3X,3I3)))
      WRITE(16,26)
   26 FORMAT(///2X,'FF MATRIX'/)
      DO 140 I=1,LIMNQ
  140 WRITE(16,27) I,(SM3(I,J),J=1,LIMNQ)
   27 FORMAT(10X,'ROW',I3/(10F7.4))
ALA28550
C
ALA28750
C  MULT. BY PAIRS TO FORM   FX=(B'*F)*B  WHICH ENDS UP IN SM3
ALA28760
C     AT THIS POINT:  SM1=B AND SM3=F
ALA28770
C
ALA28780
  150   CALL DGEMUL(SM1,MXNAQ,'T',SM3,MXNAQ,'N',SM2,MXNAQ,NA,NOCTOT,
ALA28800
     1               NOCTOT)
      CALL DGEMUL(SM2,MXNAQ,'N',SM1,MXNAQ,'N',SM3,MXNAQ,NA,NOCTOT,
     1               NA)
C
ALA28830
C  FORM HX = (W**-0.5)'*FX*(W**-0.5)
ALA28840
C
ALA28850
      DO 222 I=1,NOAT
ALA28860
      DO 220 M=1,3
        K=3*(I-1)+M
```

```
        WTINV(K)=SQRT(1.0/W(I))
  220     CONTINUE
ALA28900
  222       CONTINUE
ALA28910
C
ALA28920
      N=0
        DO 258 I=1,NA
          DO 257 J=I,NA
            N=N+1
            ROWDAT(N)=SM3(I,J)*WTINV(I)*WTINV(J)
  257         CONTINUE
ALA28980
  258       CONTINUE
ALA28990
C
ALA29000
      IFHX=1
ALA29010
      IF(IFHX .EQ. 0) THEN
ALA29020
        WRITE(16,32) (ROWDAT(I),I=1,NA)
   32     FORMAT(//2X,'FIRST ROW OF HX'/(10F7.4))
      ENDIF
C
ALA29350
C  DIAGONALIZE HX:  CX'*HX*CX = SM3'*ROWDAT*SM3
ALA29360
C
ALA29370
      IFX=1
ALA29380
      IF(IFX .EQ. 0) THEN
ALA29390
        WRITE(16,81)
   81     FORMAT(///2X,'FIRST ROW OF FX MATRIX'/)
        I=1
        WRITE(16,82) I,(SM3(I,J),J=1,NA)
   82     FORMAT(10X,'ROW',I3/(10F7.4))
      ENDIF
C
        NNA2=NA*2
        CALL DSPEV(1,ROWDAT,FP,SM3,MXNAQ,NA,ED,NNA2)
C -------------------XXXXX
c       WRITE(*,*)'-------->>> CHECK FP:'
c       WRITE(*,*)(FP(J),J=1,NA)
C
C -------------------XXXXX
c       WRITE(*,*)'-------->>> CHECK SM3 after DSPEV:'
c       DO 346 I=1,NA
c       WRITE(*,*)I
c c     WRITE(*,*)(SM3(J,I),J=1,NA)
c  346  CONTINUE
```

```
C
C
C  CALC. FREQENCIES IN CM-1 AND
C  FORM EIGENVEC.    L = BB*(WT**-0.5)'*CX = SM2
C
C -------------------XXXXX
c       WRITE(*;*)'-------->>> CHECK WTINV:'
c       WRITE(*,*)(WTINV(J),J=1,NA)
C
      DO 340 I=1,NA
      S=1.0
      IF(FP(I) .LT. 0.0) S=-S
      FR(I)=S*SQRT(S*FP(I)/5.88852E-7)
        DO 338 J=1,NA
          SM3(I,J)=SM3(I,J)*WTINV(I)
  338     CONTINUE
  340   CONTINUE
C -------------------XXXXX
c       WRITE(*,*)'-------->>> CHECK SM1:'
c       DO 342 I=1,NA
c       WRITE(*,*)I
c       WRITE(*,*)(SM1(J,I),J=1,NOCTOT)
c  342  CONTINUE
C
C -------------------XXXXX
c       WRITE(*,*)'-------->>> CHECK SM3:'
c       DO 348 I=1,NA
c       WRITE(*,*)I
c       WRITE(*,*)(SM3(J,I),J=1,NA)
c  348  CONTINUE
C
C
      CALL DGEMUL(SM1,MXNAQ,'N',SM3,MXNAQ,'N',SM2,MXNAQ,NOCTOT,NA,NA)
C -------------------XXXXX
c       WRITE(*,*)'-------->>> CHECK SM2:'
c       DO 350 I=1,NA
c       WRITE(*,*)I
c       WRITE(*,*)(SM2(J,I),J=1,NOCTOT)
c  350  CONTINUE
C
      RETURN
      END
      SUBROUTINE OUTL(MXNAQ,FP,FR,SM2,XC,IFTAU,IFR)
      INTEGER  MXNAQ,IFTAU,IFR
      REAL  FP(MXNAQ),FR(MXNAQ),SM2(MXNAQ,MXNAQ),XC(3,120)
ALA30000
      COMMON  /PROBN/ REC(36)
COM00010
      COMMON  /ATOM/  NOAT
      COMMON  /CORD1/ NIC(370,4),NCOD(370),NONIC,NOCTOT
      COMMON  /STRUC/ X(3,120),W(120),KIND(120)
C
C
      NAQ=3*NOAT
```

```
      WRITE(9,108) (REC(I),I=1,18)
  108 FORMAT(2X,18A4)
      WRITE(9,110) NAQ-6,NOCTOT
  110 FORMAT(2I6)
      WRITE(9,17) (FR(K),0.0,K=7,NAQ)
ALA30080
   17 FORMAT(5(F8.2,F6.1))
ALA30090
C
ALA30110
      WRITE(9,23) ((SM2(I,K),I=1,NOCTOT),K=7,NAQ)
ALA30170
   23 FORMAT(7E10.4)
ALA30180
C
      IF ((IFTAU .EQ. 0).OR.(IFR .EQ. 0)) THEN
      WRITE(9,14) ((X(M,I),M=1,3),I=1,NOAT)
   14   FORMAT(6F12.6)
      ELSE
      WRITE(9,14) ((XC(M,I),M=1,3),I=1,NOAT)
      ENDIF
C
ALA30200
C
ALA30210
      RETURN
ALA30220
      END
ALA30230
C***  SUBROUTINE LISTFR(MXNAQ,FP,FR,SM2)
ALA29980
      SUBROUTINE LISTFR(MXNAQ,FP,FR,SM2,IFL,IFS)
C***  INTEGER  MXNAQ
      INTEGER  MXNAQ, IFL,IFS
      REAL  FP(MXNAQ),FR(MXNAQ),SM2(MXNAQ,MXNAQ)
      COMMON  /ATOM/  NOAT
      COMMON  /CORD1/ NIC(370,4),NCOD(370),NONIC,NOCTOT
C
C
      NAQ=3*NOAT
      IF(IFS.EQ.1) THEN
        RETURN
      ENDIF
      WRITE(16,10)
   10 FORMAT(//2X,'FREQUENCIES FOR MOLECULE'//)
      DO 125 K=NAQ,1,-1
      WRITE(16,17) NAQ+1-K,FR(K)
   17   FORMAT(10X,I3,2X,F8.2)
  125   CONTINUE
C***  IFNC=1
      IFNC=IFL
C***
      IF(IFNC.EQ.2) THEN
       RETURN
```

```
      ENDIF
C***
      IF(IFNC .EQ. 0) RETURN
ALA30130
      WRITE(16,21)
   21 FORMAT(//2X,'EIGENVALUES AND EIGENVECTORS'/)
ALA30150
      DO 129 K=NAQ,1,-1
ALA30160
          WRITE(16,23) NAQ+1-K,FR(K),(SM2(I,K),I=1,NOCTOT)
   23       FORMAT(/4X,'MODE NO.',I3,3X,'FREQ. =',F8.2/(8(F8.4)))
ALA30180
  129   CONTINUE
ALA30190
C
ALA30200
C
ALA30210
      RETURN
ALA30220
      END
ALA30230
      SUBROUTINE INTIN2(NGC,COF,MXNAQ,DIPMAG,SM1,SM2,SM3,NNEWNO,RI,
ALA30850
     1  IFREOR,NICTOT,NGPC,MXPOLP,KIC,NGPSET,MXNTOR,KON,NGPTOT,
ALA30860
     2  TRC,CAX,DIPCOM,MXNC,FR)
ALA30870
      INTEGER  NNEWNO(MXNAQ),NGC(MXNAQ),NGPSET,CAX(MXNAQ)
ALA30880
      INTEGER  MXNAQT,MXNAQ,NGPC(MXPOLP),MXPOLP,MXNC
ALA30890
      INTEGER  KIC(MXNAQ),MXNTOR,KON(MXNTOR),NGPTOT
ALA30900
      INTEGER  NFR
ALA30910
      REAL  COF(MXNAQ),RI(MXNAQ),DIPMAG(MXPOLP,2),TRC(MXNC,3,3)
ALA30920
      REAL  DIPCOM(MXNAQ,3),RINT(3),FR(MXNAQ),WAGANS
ALA30930
      REAL  SM1(MXNAQ,MXNAQ),SM2(MXNAQ,MXNAQ),SM3(MXNAQ,MXNAQ)
ALA30940
      COMMON  /ATOM/  NOAT
      COMMON  /PROBN/ REC(36)
COM00010
      COMMON  /CORD1/ NIC(370,4),NCOD(370),NONIC,NOCTOT
C
ALA31040
C  FORM U-MATRIX
ALA31050
C
ALA31060
      DO 110 I=1,MXNAQ
ALA31070
```

```
      DO 110 J=1,MXNAQ
ALA31080
      SM1(I,J)=0.0
  110   SM3(I,J)=0.0
C
ALA31100
      DO 128 I=1,NICTOT
ALA31110
        II=NGC(I)
        JJ=KIC(I)
        SM1(II,JJ)=COF(I)
  128   CONTINUE
ALA31150
      NAQ=3*NOAT
C
C  FORM PRODUCT U*L ( U=SM1, L=SM2, U*L=SM3)
ALA31170
C
ALA31180
      CALL DGEMUL(SM1,MXNAQ,'N',SM2,MXNAQ,'N',SM3,MXNAQ,NGPTOT,
ALA31190
     1            NAQ,NAQ)
C
C     NFR=135
ALA42410
C     DO 200 K=NAQ,1,-1
ALA42430
C       IF ((FR(K) .GE. 917.0).AND.(FR(K) .LE. 926.0)) THEN
ALA42440
C         WRITE(16,215) FR(K),(KON(I),I=1,NTOR)
C 215     FORMAT(F12.6,3X,5(I1))
ALA42460
C       ENDIF
ALA42470
C       IF (NAQ+1-K .EQ. NFR) THEN
ALA42480
C         WRITE(16,235) NAQ+1-K,FR(K),(SM3(I,K),I=1,NGPTOT)
C 235     FORMAT(/4X,'MODE NO.',I3,3X,'FREQ. =',F8.2/(8(F8.4)))
ALA42500
C       ENDIF
ALA42510
C 200 CONTINUE
ALA42520
C
ALA31200
C  PUT PWR. PAR. INTO U*L MATRIX(=SM3)
ALA31210
C
ALA31220
      DO 300 K=1,NAQ
ALA31230
      DO 310 MM=1,3
        RINT(MM)=0.0
        NCG=0
```

```
          DO 320 IS=1,NGPSET
            DO 330 KK=1,NGPC(IS)
              NCG=NCG+1
              DO 340 J=1,3
              RINT(MM)=DIPMAG(IS,1)*SM3(NCG,K)*DIPCOM(NCG,J)*
     1                       TRC(CAX(NCG),J,MM)+RINT(MM)
ALA31410
  340           CONTINUE
ALA31430
  330         CONTINUE
ALA31440
  320       CONTINUE
ALA31450
  310    CONTINUE
ALA31460
       RI(K)=RINT(1)**2+RINT(2)**2+RINT(3)**2
  300 CONTINUE
ALA31480
C
ALA31490
C
ALA31500
       RETURN
ALA31510
       END
ALA31520
       SUBROUTINE ADD2(MXNEL,DS,SA,MXNAQ,FP,FR,SM2,RI,WTS)
C
c       Adding up the spectra from each molecule
c           Modification:
c           When IFL=9, it will use the weight factor WTS
c                       Xiaozhen Yang July 10, 1996
c
       INTEGER  MXNEL
ALA32460
       INTEGER  MXNAQ
ALA32470
       REAL  FP(MXNAQ),FR(MXNAQ),SM2(MXNAQ,MXNAQ)
ALA32480
       REAL  DS(MXNEL),SA(MXNEL)
ALA32490
       REAL  RI(MXNAQ)
ALA32500
       COMMON  /CORD1/ NIC(370,4),NCOD(370),NONIC,NOCTOT
       COMMON  /MAINC/ IFR,IFL,NMOL,NCM,NMTOT
       COMMON  /B12/ FH,FL,FDEL,NEL
ALA32520
C
ALA32530
C
       if(IFL.ne.9) WTS=1.0
       DO 130 K=1,NOCTOT
ALA32550
       IF(FR(K) .LT. 0.001) GO TO 130
```

```
      IF(FR(K) .GT. FH .OR. FR(K) .LT. FL) GO TO 130
      N=(FR(K)-FL)/FDEL+1.0
      DS(N)=DS(N)+1.0*WTS
      SA(N)=SA(N)+RI(K)*WTS
  130   CONTINUE
ALA32610
C
ALA32620
C
ALA32630
      RETURN
ALA32650
      END
ALA32660
      SUBROUTINE PLOT3(MXNEL,DS,SA,TEMP)
ALA33790
      INTEGER  MXNEL
ALA33800
      REAL  DS(MXNEL),SA(MXNEL),TEMP
ALA33810
      COMMON  /CORD1/ NIC(370,4),NCOD(370),NONIC,NOCTOT
      COMMON  /B12/ FH,FL,FDEL,NEL
ALA33830
      COMMON  /B14/ DSCALE,SSCALE
ALA33840
C
ALA33850
C
ALA33860
      CALL SCALE(MXNEL,DS,SA,NEL,DSCALE,SSCALE)
ALA33870
      CALL DSFILE(MXNEL,DS,SA,FH,FL,FDEL,NEL,TEMP)
ALA33880
C
ALA33890
C
ALA33900
      RETURN
ALA33910
      END
ALA33920
      SUBROUTINE SCALE(MXNEL,DS,SA,NEL,DSCALE,SSCALE)
ALA33930
      INTEGER  MXNEL
ALA33940
      REAL  DS(MXNEL),SA(MXNEL)
ALA33950
C
ALA33960
C
ALA33970
      DMAX=DS(1)
ALA33980
```

```
      SMAX=SA(1)
ALA33990
C
ALA34000
      DO 133 I=2,NEL
ALA34010
      IF(DS(I) .GT. DMAX) DMAX=DS(I)
ALA34020
      IF(SA(I) .GT. SMAX) SMAX=SA(I)
ALA34030
  133   CONTINUE
ALA34040
C
ALA34050
      DSCALE=10.0/DMAX
ALA34060
      SSCALE=10.0/SMAX
ALA34070
C
ALA34080
      DO 145 I=1,NEL
ALA34090
      DS(I)=DS(I)*DSCALE
      SA(I)=SA(I)*SSCALE
  145   CONTINUE
ALA34120
C
ALA34130
      RETURN
ALA34140
      END
ALA34150
      SUBROUTINE DSFILE(MXNEL,DS,SA,FH,FL,FDEL,NEL,TEMP)
ALA34160
      INTEGER  MXNEL
ALA34170
      REAL  DS(MXNEL),SA(MXNEL),TEMP
ALA34180
      COMMON  /PROBN/ REC(36)
C
ALA34210
C
      open(7,file='dsfile.nca',status='unknown')
      WRITE(7,13) NEL,FH,FL,FDEL,TEMP
ALA34230
   13 FORMAT(I6,4F12.6)
ALA34240
      WRITE(7,14) (REC(I),I=1,18)
ALA34250
   14 FORMAT(18A4)
ALA34260
      WRITE(7,15) (DS(I),I=1,NEL)
ALA34270
```

```
   15 FORMAT(6F12.6)
ALA34280
      WRITE(7,15) (SA(I),I=1,NEL)
      close(7)
C
C
      RETURN
      END
      SUBROUTINE STAT(MXNEL,DS,SA)
      INTEGER  MXNEL
      REAL  DS(MXNEL),SA(MXNEL)
      COMMON  /MAINC/ IFR, IFL,NMOL,NCM,NMTOT
      COMMON  /CORD2/ NICT(101,6,4),NCODT(101,6),NOCOMP(101),NT
      COMMON  /STAT1/ KOUNT(7),KOUNTB(50,3)
ALA12730
      COMMON  /S1/ XSTAT(7),XSTATB(50,3)
ALA32100
C
ALA32110
C
ALA32120
      IF(NMTOT .EQ. 0) RETURN
ALA32130
      DO 112 I=1,3
ALA32140
      XSTAT(I)=KOUNT(I)/(REAL(NMTOT)*REAL(NT))
      DO 110 K=1,NT
      XSTATB(K,I)=KOUNTB(K,I)/REAL(NMTOT)
  110     CONTINUE
ALA32180
  112   CONTINUE
ALA32190
C
ALA32200
      XT=0.0
ALA32210
      DO 120 I=4,7
ALA32220
      XT=XT+KOUNT(I)
  120   CONTINUE
ALA32240
      IF(XT .EQ. 0.0) RETURN
ALA32250
      DO 122 I=4,7
ALA32260
      XSTAT(I)=KOUNT(I)/XT
ALA32270
  122   CONTINUE
ALA32280
C
      WRITE(16,13)
   13 FORMAT(///2X,'**** CALC. RESULTS ****')
ALA32400
```

```
C
ALA32410
      CALL CONSTA
ALA32420
ccc       IF (NMTOT .NE. 0) CALL RESULT1(MXNEL,DS,SA,IFL)
C
ALA32290
C
ALA32300
      RETURN
ALA32310
      END
ALA32320
      SUBROUTINE CONSTA
ALA32480
      COMMON  /MAINC/ IFR, IFL,NMOL,NCM,NMTOT
      COMMON  /CORD2/ NICT(101,6,4),NCODT(101,6),NOCOMP(101),NT
      COMMON  /S1/ XSTAT(7),XSTATB(50,3)
ALA32100
      COMMON  /CON4/ VTOTSQ(50)
ALA10900
      COMMON  /ETORS/ KTNUM(50),NSTATE(50),KTTYP(50),KTANG(50,3),
     1                TENER(50,3),KTYN,KARTAU(50)
C
ALA32550
C
ALA32560
      WRITE(16,34) NMOL,NMTOT
   34 FORMAT(///2X,'CONFORM. STAT.'//6X,
ALA32580
     1  'NO. OF CONF. CONSIDERED =',I5/6X,'NO. OF CONF. USED =',I5)
ALA32590
      XG=XSTAT(2)+XSTAT(3)
ALA32610
      WRITE(16,36) XSTAT(1),XG
   36 FORMAT(//6X,'T BONDS =',F7.4
ALA32630
     1         /6X,'G BONDS =',F7.4)
ALA32640
      WRITE(16,38) (XSTAT(I),I=4,7)
   38 FORMAT(//6X,'TT PAIRS =',F7.4
ALA32660
     1        /6X,'GT PAIRS =',F7.4
ALA32670
     2        /6X,'GG PAIRS =',F7.4
ALA32680
     3        /6X,'GG* PAIRS =',F7.4)
ALA32690
C
ALA32700
      WRITE(16,44)
   44 FORMAT(//2X,'CONFORM. STAT. FOR EACH BOND POSITION.'
ALA32720
```

```
     1  //5X,'NO.',5X,'T',8X,'G',8X,'G*',5X,'STD. DEV.'/)
ALA32730
      DO 120 K=1,NT
ALA32740
      STDTAU=SQRT(VTOTSQ(KARTAU(K))/NMOL)
      WRITE(16,46) K,(XSTATB(K,I),I=1,3),STDTAU
   46   FORMAT(5X,I2,3(3X,F6.4),5X,F8.4)
ALA32760
  120   CONTINUE
ALA32770
C
ALA32780
C
ALA32830
      RETURN
ALA32840
      END
ALA32850
      SUBROUTINE LISTRI(MXNAQ,FP,FR,SM2,RI)
ALA31950
      INTEGER  MXNAQ
ALA31960
      REAL  FP(MXNAQ),FR(MXNAQ),SM2(MXNAQ,MXNAQ)
ALA31970
      REAL  RI(MXNAQ)
ALA31980
      COMMON  /MAINC/ IFR, IFL,NMOL,NCM,NMTOT
      COMMON  /ATOM/  NOAT
C
ALA32000
C
ALA32010
      NAQ=3*NOAT
ALA32020
      WRITE(16,10) NMTOT
   10 FORMAT(///2X,'CALC. FP(K), FR(K), AND PWR(K) FOR MOL. NO.',I3)
      WRITE(16,12)
   12 FORMAT(10X,'NO.',4X,'FR.PAR.',2X,'FREQ.',5X,'POWER'/)
      DO 111 I=NAQ,1,-1
  111   WRITE(16,14) NAQ+1-I,FP(I),FR(I),RI(I)
   14   FORMAT(10X,I3,3X,F7.4,2X,F7.2,2X,F9.6)
      DO 100 I=7,NAQ
      WRITE(16,110) FR(I),RI(I)*100.0
  110   FORMAT(F8.2,F12.6,'  1   1.0')
  100 CONTINUE
C
C
      RETURN
      END
      SUBROUTINE LISTX(X,XC)
      REAL  X(3,120),XC(3,120)
      COMMON  /ATOM/  NOAT
C
C
```

```
      WRITE(16,12)
   12 FORMAT(///2X,'CARTESIAN COORD.'/
     1  20X,'X',11X,'Y',11X,'Z'/)
C
      IFX=0
      IF (IFX .EQ. 0) THEN
      DO 111 I=1,NOAT
  111     WRITE(16,14) I,(X(M,I),M=1,3)
   14     FORMAT(10X,I3,2X,3F12.6)
      ELSE
      DO 112 I=1,NOAT
  112     WRITE(16,14) I,(XC(M,I),M=1,3)
      ENDIF
C
C
      RETURN
      END
      SUBROUTINE RESULT1(MXNEL,DS,SA,Key,temp,NAME)
c
c  Output the calculated spetra, modified by Xiaozhen Yang (1996)
c
      INTEGER  MXNEL
      REAL  DS(MXNEL),SA(MXNEL),WV(2000),SPR(2000),SPD(2000),
     &  AD(1000),AR(1000),B(1000)
      character*32 NAME
      COMMON  /B12/ FH,FL,FDEL,NEL
      COMMON  /B14/ DSCALE,SSCALE
C
C
      WRITE(16,30)
   30 FORMAT(///2X,'CALC. DENS. OF STATES AND POWER')
C
      WRITE(16,31)
   31 FORMAT(/7X,'SCALE FACTORS: DIV. LIST VAL. BY FACTOR TO GET',
     1  1X,'TRUE VAL.')
      WRITE(16,32) DSCALE,SSCALE
   32 FORMAT(/10X,'DSCALE =',2X,E12.4/10X,'PSCALE =',2X,E16.8)
C
      NN=0
      WRITE(16,35)
   35 FORMAT(////11X,'NO.',5X,'FREQ',7X,'D. OF S.',6X,'POWER'//)
      DO 220 I=1,NEL
      IF(DS(I) .EQ. 0.0) GO TO 220
      NN=NN+1
      FQ=FL+(I-1)*FDEL+0.5*FDEL
        B(NN)=FQ
      AD(NN)=DS(I)
      AR(NN)=SA(I)
      WRITE(16,40) NN,I,FQ,DS(I),SA(I)
   40   FORMAT(5X,I3,2X,I4,F10.2,5X,F8.4,5X,F8.4)
  220   CONTINUE
C        ----------------------
C         Calculate the spectra
C               ----------------------
```

```
          open(12,file=NAME,status='unknown')
C               C - the band width; D - the ratio of L/G.
        C=8
        D=0.9
C
C       NN - number of peaks;  NF - number of points along frequency
axis.
C
  255    NF=(FH-FL)/FDEL+1
C
        DO 300 I=1,NF
        WV(i)=FL+FDEL*(I-1)
        SPD(I)=0.0
        SPR(I)=0.0
        DO 300 J=1,NN
         P1=SHAPE1(AD(J),B(J),C,D,WV(i))
         P2=SHAPE1(AR(J),B(J),C,D,WV(i))
        SPD(I)=SPD(I)+P1
        SPR(I)=SPR(I)+P2
  300  CONTINUE
  310  format(f15.1,f15.4,e18.6)
            do 330 i=1,NF
          if(WV(i).lt.1.0E-6) goto 330
          p=WV(i)*3.0E+10
            p1=p*6.626E-11/temp/1.380622
          p1=exp(-p1)
            p=(1-p1)*p
          SPR(i)=SPR(i)/p*1.0E+15
  330           continue
        WRITE(12,310)(WV(I),SPD(I),SPR(I),I=1,NF)
        CLOSE(12)
C
C                   Prepare data for specific intensity optimization
C
            if(Key.ne.3) goto 900
C
            open(12,file='freq.opt',status='old')
            read(12,*)n
            read(12,*)(B(i),i=1,n)
            close(12)
c
            open(12,file='intens.opt',status='unknown')
            j=1
            do 400 i=1,NF
            if(B(j).ne.WV(i)) goto 400
            SPD(j)=SPR(i)
            j=j+1
  400   continue
c
c     Normalization of the intensities
c
            pmax=SPD(1)
            do 500 i=1,n
            if(pmax.lt.SPD(i)) pmax=SPD(i)
```

```
  500   continue
            do 600 i=1,n
            SPD(i)=SPD(i)/pmax
  600   continue
C
            write(12,*)n
            write(12,*)(SPD(i),i=1,n)
            close(12)
C
  900  continue
       RETURN
       END
       FUNCTION SHAPE1(A,B,C,D,X)
C
C         This function generates a curve of psuedo Lorientzian and
Gausian band shape
C
       P=X-B
       P2=P*P
       P4=P2*P2
       C2=C*C
       C4=C2*C2
       SHAPE1=A/(1+D*P2/C2+(1-D)*P4/C4)
       RETURN
       END

       SUBROUTINE DGEMUL(A,MAX1,STR1,B,MAX2,STR2,C,MAX3,M1,M2,M3)
C
C       This subroutine for multification of A & B matrices
C           There is an option for the normal or the transition
C           of the matrices:
C                       'N' - normal matrix for;
C                       'T' - transition matrix.
C                   difined to str1 and str2.
C                       (M1 x M2) - the orders of A matrix;
C                       (M2 x M3) - the orders of B matrix.
C           then we have
C       A(M1,M2)*B(M2,M3)=>C(M1,M3)
C                       MAX? - determines the dimension of matrices.
C
C                            by Xiaozhen YANG, May 8, 1995
C
       DIMENSION A(MAX1,MAX1),B(MAX2,MAX2),C(MAX3,MAX3)
       CHARACTER*1 STR1,STR2
       IF(STR1.EQ.'N'.AND.STR2.EQ.'N') THEN
             N1=M1
             N2=M3
             N3=M2
       DO 4777 I=1,N1
       DO 4777 J=1,N2
       C(I,J)=0.0
       DO 4777 K=1,N3
c       IF(ABS(A(I,K)).LT.1.0D-6) GO TO 4775
c       IF(ABS(B(K,J)).LT.1.0D-6) GO TO 4775
```

```
      C(I,J)=C(I,J)+A(I,K)*B(K,J)
 4775   continue
 4777 CONTINUE
      GO TO 10000
      ENDIF
      IF(STR1.EQ.'N'.AND.STR2.EQ.'T') THEN
            N1=M1
            N2=M3
            N3=M2
      DO 5777 I=1,N1
      DO 5777 J=1,N2
      C(I,J)=0.0
      DO 5777 K=1,N3
c      IF(ABS(A(I,K)).LT.1.0D-6) GO TO 5775
c      IF(ABS(B(J,K)).LT.1.0D-6) GO TO 5775
      C(I,J)=C(I,J)+A(I,K)*B(J,K)
 5775   continue
 5777 CONTINUE
      GO TO 10000
      ENDIF
      IF(STR1.EQ.'T'.AND.STR2.EQ.'N') THEN
            N1=M1
            N2=M3
            N3=M2
      DO 6777 I=1,N1
      DO 6777 J=1,N2
      C(I,J)=0.0
      DO 6777 K=1,N3
c      IF(ABS(A(K,I)).LT.1.0D-6) GO TO 6775
c      IF(ABS(B(K,J)).LT.1.0D-6) GO TO 6775
      C(I,J)=C(I,J)+A(K,I)*B(K,J)
 6775   continue
 6777 CONTINUE
      GO TO 10000
      ENDIF
      IF(STR1.EQ.'T'.AND.STR2.EQ.'T') THEN
            N1=M1
            N2=M3
            N3=M2
      DO 7777 I=1,N1
      DO 7777 J=1,N2
      C(I,J)=0.0
      DO 7777 K=1,N3
c      IF(ABS(A(K,I)).LT.1.0D-6) GO TO 7775
c      IF(ABS(B(J,K)).LT.1.0D-6) GO TO 7775
      C(I,J)=C(I,J)+A(K,I)*B(J,K)
 7775   continue
 7777 CONTINUE
      GO TO 10000
      ENDIF
      WRITE(*,*)'*****************************ERROR IN DGEMUL'
10000   CONTINUE
      RETURN
      END
```

```
      SUBROUTINE DSPEV(IFU, ROW, FP, U, NH, N, ED, N2)
c-----------------------------------------------------------------------
---
c       This is a JACOBI subroutine modified from Michigen version
MV.FOR
c       in order to meet Snyder's new version TOPOVIB1
c                          --- by Xiaozhen YANG, May 8, 1995
C
C       Some useless staff: ED and N2
c-----------------------------------------------------------------------
---
      parameter (MXNAQ=400)
c       DOUBLE PRECISION H(MXNAQ,MXNAQ)
      DIMENSION U(NH,NH), FP(NH), ED(NH*2),ROW(NH*NH),H(MXNAQ,MXNAQ)
c       DOUBLE PRECISION SUM,FIN,OFFMAX,HII,HJI,HJJ,HIJ,TANG,HIK,UKI
C       The adjusting parameter is FIN for a minimum
      FIN=1.0D-06
C
C       Transfer ROW(NH**2) to H(NH,NH)
C
      DO 1000 I=1,N
      DO 1000 J=1,N
 1000   H(I,J)=0.0
      K=0
      DO 1010 I=1,N
      DO 1010 J=I,N
      K=K+1
      H(I,J)=ROW(K)
c        WRITE(*,*)'-----> I, J :',I,J,H(I,J)
 1010   CONTINUE
      DO 1020 I=1,N
      DO 1020 J=I,N
 1020   H(J,I)=H(I,J)
C-CCCCC----------------------------------------
      GO TO (1,4), IFU
 1    DO 3 I=1,N
      DO 2 J=1,N
 2    U(I,J) = 0.0
 3    U(I,I) = 1.0
 4    IF(N .EQ. 1)  GO TO 100
      NS1 = N - 1
      SUM = 0.0
      DO 6 I= 1, NS1
      IA1 = I + 1
      DO 5 J=IA1, N
 5    SUM = SUM + H(I,J)*H(I,J)
 6    CONTINUE
      IF(SUM .LT. FIN*FIN)    GO TO 100
      OFFMAX = SQRT(SUM+SUM)
 7    OFFMAX = OFFMAX/FLOAT(N)
      IF(OFFMAX .LT. FIN)   OFFMAX = FIN
 8    MEMO = 1
      DO 17 I=1, NS1
```

```
      IA1 = I + 1
      DO 17 J= IA1, N
      IF(ABS(H(I,J)) . LT. OFFMAX)    GO TO 17
      MEMO = 2
      HII = H(I,I)
      HJJ = H(J,J)
      HIJ = H(I,J)
      TANG =                          SIGN(2.0, (HII-HJJ))*HIJ
     1    / (  ABS(HII-HJJ) + SQRT((HII-HJJ)**2 + HIJ**2*4.0)    )
      COSIN = 1.0/SQRT(1.0 + TANG**2)
      SINE = TANG*COSIN
      IS1 = I - 1
      IF(IS1 .EQ. 0 )      GO TO 10
      DO 9 K = 1, IS1
      HKI = H(K,I)
      H(K,I) = HKI*COSIN + H(K,J)*SINE
      H(K,J) = -HKI*SINE + H(K,J)*COSIN
 9    CONTINUE
 10   H(I,I) = HII*COSIN**2 + HJJ*SINE**2 + HIJ*SINE*COSIN*2.0
      H(J,J) = HII*SINE**2 + HJJ*COSIN**2 - HIJ*SINE*COSIN*2.0
      JS1 = J - 1
      IF(IA1 .GT. JS1)    GO  TO 12
      DO 11 K=IA1 , JS1
      HIK = H(I,K)
      H(I,K) = HIK*COSIN + H(K,J)*SINE
      H(K,J) = -HIK*SINE + H(K,J)*COSIN
 11   CONTINUE
 12   H(I,J) = 0.0
      IF(J .EQ. N)    GO TO 14
      JA1 = J + 1
      DO 13 K = JA1, N
      HIK = H(I,K)
      H(I,K) = HIK*COSIN + H(J,K)*SINE
      H(J,K) = -HIK*SINE + H(J,K)*COSIN
 13   CONTINUE
 14   GO TO (15,17),  IFU
 15   DO 16 K=1,N
      UKI = U(K,I)
      U(K,I) = UKI*COSIN + U(K,J)*SINE
      U(K,J) = -UKI*SINE + U(K,J)*COSIN
 16   CONTINUE
 17   CONTINUE
      GO TO (18,8), MEMO
 18   IF(OFFMAX .GT. FIN*1.01)    GO TO 7
 100  CONTINUE
      DO 200 I=1,N
      FP(I)=H(I,I)
 200    CONTINUE
c       WRITE(*,*)'-----> CHECK THE ORDER:'
c       WRITE(*,*)(FP(I),I=1,N)
c       check U
c       WRITE(*,*)'--------------> EIGENVECTORS:'
c       DO 210 I=1,N
c       WRITE(*,*)I
```

```
c       WRITE(*,*)(U(J,I),J=1,N)
c  210  CONTINUE
cc
c       Put the output in ascending order
c
      DO 250 I=1,N-1
      DO 245 J=I+1,N
      IF(FP(I).LE.FP(J)) GO TO 245
      P=FP(I)
      FP(I)=FP(J)
      FP(J)=P
      DO 240 K=1,N
      ED(K)=U(K,I)
      U(K,I)=U(K,J)
      U(K,J)=ED(K)
  240   CONTINUE
  245   CONTINUE
  250   CONTINUE
c       WRITE(*,*)'-----> CHECK THE ORDER after:'
c       WRITE(*,*)(FP(I),I=1,N)
c       check U
c       WRITE(*,*)'--------------> EIGENVECTORS after:'
c       DO 260 I=1,N
c       WRITE(*,*)I
c       WRITE(*,*)(U(J,I),J=1,N)
c  260  CONTINUE
      RETURN
      END

      SUBROUTINE DGEEV(IFU, H, NH, FP, U, NU, EC, N1, ED, N2)
c
c       This is a JACOBI subroutine modified from Michigen version
MV.FOR
c       in order to meet Snyder's new version TOPOVIB1
c                        --- by Xiaozhen YANG, May 8, 1995
c
c       Some useless staff: EC, N1, ED, N2
c
      DIMENSION H(NH,NH), EC(NH*2), ED(NH*2)
      COMPLEX U(NU,NU), FP(NH)
C       The adjusting parameter is FIN for a minimum
      N=NH
      FIN=1.0e-6
      GO TO (1,4), IFU
 1    DO 3 I=1,N
      DO 2 J=1,N
 2    U(I,J) = 0.0
 3    U(I,I) = 1.0
 4    IF(N .EQ. 1)  GO TO 100
      NS1 = N - 1
      SUM = 0.0
      DO 6 I= 1, NS1
      IA1 = I + 1
      DO 5 J=IA1, N
```

```
5     SUM = SUM + H(I,J)*H(I,J)
6     CONTINUE
      IF(SUM .LT. FIN*FIN)     GO TO 100
      OFFMAX = SQRT(SUM+SUM)
7     OFFMAX = OFFMAX/FLOAT(N)
      IF(OFFMAX .LT. FIN)    OFFMAX = FIN
8     MEMO = 1
      DO 17 I=1, NS1
      IA1 = I + 1
      DO 17 J= IA1, N
      IF(ABS(H(I,J)) . LT. OFFMAX)    GO TO 17
      MEMO = 2
      HII = H(I,I)
      HJJ = H(J,J)
      HIJ = H(I,J)
      TANG =                        SIGN(2.0, (HII-HJJ))*HIJ
     1    / (  ABS(HII-HJJ) + SQRT((HII-HJJ)**2 + HIJ**2*4.0)    )
      COSIN = 1.0/SQRT(1.0 + TANG**2)
      SINE = TANG*COSIN
      IS1 = I - 1
      IF(IS1 .EQ. 0 )      GO TO 10
      DO 9 K = 1, IS1
      HKI = H(K,I)
      H(K,I) = HKI*COSIN + H(K,J)*SINE
      H(K,J) = -HKI*SINE + H(K,J)*COSIN
9     CONTINUE
10    H(I,I) = HII*COSIN**2 + HJJ*SINE**2 + HIJ*SINE*COSIN*2.0
      H(J,J) = HII*SINE**2 + HJJ*COSIN**2 - HIJ*SINE*COSIN*2.0
      JS1 = J - 1
      IF(IA1 .GT. JS1)   GO  TO 12
      DO 11 K=IA1 , JS1
      HIK = H(I,K)
      H(I,K) = HIK*COSIN + H(K,J)*SINE
      H(K,J) = -HIK*SINE + H(K,J)*COSIN
11    CONTINUE
12    H(I,J) = 0.0
      IF(J .EQ. N)    GO TO 14
      JA1 = J + 1
      DO 13 K = JA1, N
      HIK = H(I,K)
      H(I,K) = HIK*COSIN + H(J,K)*SINE
      H(J,K) = -HIK*SINE + H(J,K)*COSIN
13    CONTINUE
14    GO TO (15,17),  IFU
15    DO 16 K=1,N
      UKI = U(K,I)
      U(K,I) = UKI*COSIN + U(K,J)*SINE
      U(K,J) = -UKI*SINE + U(K,J)*COSIN
16    CONTINUE
17    CONTINUE
      GO TO (18,8), MEMO
18    IF(OFFMAX .GT. FIN*1.01)    GO TO 7
100   CONTINUE
      DO 200 I=1,N
```

```
      FP(I)=H(I,I)
 200    CONTINUE
      RETURN
      END

      SUBROUTINE DGEICD(R, NH, N, IFU, Rp, EC, D, N2)
c
c       This is an inverse subroutine modified from yang's version
NVAS04.FOR
c       in order to meet Snyder's new version TOPOVIB1
c                        --- by Xiaozhen YANG, May 8, 1995
c
C ***    Some useless staff: Rp, EC, D and N2.
C
      DIMENSION R(NH,NH), U(3,3), EC(2)
C       The adjusting parameter is FIN for a minimum
      FIN=1.0e-20
ccccc      SUBROUTINE RCPR(R,N)
ccccc      DIMENSION R(45,45)
      DO 111 K=1,N
      DO 100 I=1,N
      DO 100 J=1,N
      IF(ABS(R(K,K)).LT.FIN) GO TO 107
   99 IF(I.EQ.K) GO TO 100
      IF(J.EQ.K) GO TO 100
      R(I,J)=R(I,J)-R(I,K)*R(K,J)/R(K,K)
  100 CONTINUE
      DO 105 J=1,N
      IF(J.EQ.K) GO TO 105
      R(K,J)=R(K,J)/R(K,K)
      R(J,K)=-R(J,K)/R(K,K)
  105 CONTINUE
      R(K,K)=1.0/R(K,K)
      GO TO 111
  107 WRITE(3,120)R(K,K)
      DO 108 II=1,N
      R(II,K)=0.0
  108 R(K,II)=0.0
  111 CONTINUE
  120 FORMAT(1X,'???????? THIS NUMBER IS SO SMALL :',E16.8)
      RETURN
      END

      SUBROUTINE DNRAND(SEED,N,RD,AUX,N2)
C
C       This is for meeting to Snyder's program TOPOVIB1
C       SEED is seed;
C       N - the number of random numbers generated
C       RD(N) - the random number
C       AUX - an working unit with a length of N/2.
C       N2 = 1
C
      INTEGER SEED
      REAL RD(N),AUX(N2,2)
```

```
C
      I=1
  300   IF(I.GT.N2) GO TO 400
      J1=2*I-1
      J2=2*I
      RD(J1)=RAND(SEED)
      RD(J2)=RAND(SEED)
C
      AUX(I,1)=2*RD(J1)-1.0
      AUX(I,2)=2*RD(J2)-1.0
C
      P=AUX(I,1)**2+AUX(I,2)**2
      IF(P.GE.1.0) GO TO 300
      X= SQRT((-2.0*LOG(P))/P)
      RD(J1)= AUX(I,1)*X
      RD(J2)= AUX(I,2)*X
      I=I+1
      GO TO 300
  400 CONTINUE
      RETURN
      END

      SUBROUTINE DURAND(SEED,N,RD)
C
C       This is for meeting to Snyder's program TOPOVIB1
C       SEED is seed;
C       N is the number of random numbers to be generated
C              here N=1.
C       RD - the random number
C
      integer SEED
C
      DO 100 I=1,N
      RD=RAND(SEED)
  100   CONTINUE
      RETURN
      END

      FUNCTION RAND(IX)
C
C       RANDOM NUMBER GENERATOR
C
C       USUS THE RECURSION   IX=IX*A(MOD P)
C       INITIALIZE WITH SEED:   0 < SEED < 2**31-1
C       USE EITHER RAND:  0 < RAND < 1
C              OR   IX:  0 < IX < 2**31-1
C       CHECKING VALUES:  IF IX(0)=1, THEN IX(1000)=522329230
C       IX IN CALLING LIST MUST BE INTEGER*4 IN CALLING PROGRAM
C
      INTEGER A,P,IX,B15,B16,XHI,XALO,LEFTLO,FHI,K
C              7**5, 2**15, 2**16, 2**31-1
      DATA A/16807/, B15/32768/, B16/65536/, P/2147483647/
      XHI=IX/B16
      XALO=(IX-XHI*B16)*A
```

```
      LEFTLO=XALO/B16
      FHI=XHI*A+LEFTLO
      K=FHI/B15
      IX=(((XALO-LEFTLO*B16)-P)+(FHI-K*B15)*B16)+K
      IF(IX.LT.0) IX=IX+P
      RAND=FLOAT(IX)*4.656612875E-10
      RETURN
      END

      SUBROUTINE EXIT
C
      RETURN
      END
```

BIBLIOGRAPHY

Adamson, A. W. (1990). Physical Chemistry of Surfaces. New York, John Wiley & Sons, Inc.

Alamo, R. G.;Galante, M. J.;Lucas, J. C. and Mandelkern, L. (1995). Polymer Preprints **36**(1): 285.

Allegra, G.;Ganis, P. and Corradini, P. (1963). Makromol. Chem. **61**: 225.

Allerhand, A. and Schleyer, P. v. R. (1963). J. Amer. Chem. Soc. **85**: 371.

Asakura, T.;Aoki, A.;Takeshi, D.;Demura, M. and Asanuma, T. (1996). Polym. J. **28**: 24.

Baret, J. F. (1981). Phase Transitions in Two-Dimensional Amphiphilic Systems. Progress in Surface and Membrane Science. New York, Academic Press. 291.

Bauer, R. and Magat, M. (1938). J. Phys. Radium **9**: 319.

Biskup, U. and Cantow, H.-J. (1972). Macromolecules **5**: 546.

Bohan, S. P.;Strauss, H. L. and Snyder, R. G. (1990). Journal of Physical Chemistry **94**: 2801.

Boor, J. J. and Youngman, E. A. (1966). J. Polym. Sci: Part A-1 **4**: 1861.

Cates, D. A.;Strauss, H. L. and Snyder, R. G. (1994). J. Phys. Chem. **98**: 4482.

Chalmers, J. M. (1977). Polymer **18**(July): 681.

Chalmers, J. M.;Edwards, H. G. M.;Lees, J. S.;Long, D. A.;Mackenzie, M. W. and Willis, H. A. (1991). Journal of Raman Spectroscopy **22**: 613.

Chatani, Y.;Maruyama, H.;Asanuma, T. and Shiomura, T. (1991). J. Polym. Sci. Polym. Phys. Ed. **29**: 1649.

Chatani, Y.;Maruyama, H.;Noguchi, K.;Asanuma, T. and Shiomura, T. (1990). J. Polym. Sci. Polym. Phys. Lett. **28**: 393.

Chen, H.;Hsu, S. L.;Tirrell, D. A. and Stidham, H. D. (1997). Langmuir **30**(4): 840.

Corradini, P.;Natta, G.;Ganis, P. and Temussi, P. A. (1967). Journal of Polymer Science, Part C **16**: 2477.

Cyvin, S. J. and Brunvoll, J. (1969). Journal of Molecular Spectroscopy **29**(2): 159.

Damaschun, V. G. (1962). Kolloid-Zeitschrift, Zeitschrift fur Polymere **180**(1): 65.

Ewen, J. A.;Jones, R. L.;Razavi, A. and Ferrara, J. D. (1988). J. Am. Chem. Soc. **110**: 6255.

Flory, P. J. (1969). Statistical Mechanics of Chain Molecules. New York, Interscience Publishers.

Flory, P. J.;Mark, J. E. and Abe, A. (1966). Journal of the American Chemical Society **88**(4): 639.

Fox, H. W.;Taylor, P. W. and Zisman, W. A. (1947). Industrial and Engineering Chemistry : 1401.

Garrett, W. D. and Zisman, W. A. (1970). J. Phys. Chem. **70**: 1796.

Gornick, F. and Mandelkern, L. (1962). Journal of Applied Physics **33**(3): 907.

Granick, S.;Clarson, S. J.;Formoy, T. R. and Semlyen, J. A. (1985). Polymer **26**: 925.

Hahn, T. D.;Stidham, H. D. and Hsu, S. L. (1997). Macromolecules **30**: 87.

Hallmark, V. M.;Bohan, S. P.;Strauss, H. L. and Snyder, R. G. (1991). Macromolecules **24**: 4025.

Hutchinson, J. W. (1995). Prog. Polym. Sci. **20**: 703.

Isasi, J. R.;Mandelkern, L. and Alamo, R. G. (1996). Polymer Preprints **37**(2): 239.

Jean, Y. C. and Deng, Q. (1992). Journal of Polymer Science: Part B: Polymer Physics Edition **30**: 1359.

Kluin, J.-E.;Yu, Z.;Vleeshouwers, S.;McGervey, J. D.;Jamieson, A. M.;Simha, R. and Sommer, K. (1993). Macromolecules **26**(1853):

Kobayashi, Y.;Zheng, W.;Meyer, E. F. and McGervey, J. D. (1989). Macromolecules **22**: 2302.

Konopka, R. and Stojczyk, B. (1971). Acta Physica Polonica **A40**: 537.

Lamarre, L. and Sung, C. S. P. (1983). Macromolecules **16**: 1729.

Lee, L. T.;Langevin, D.;Mann, E. K. and Farnoux, B. (1994). Physica B **198**: 83.

Lee, L. T.;Mann, E. K.;Langevin, D. and Farnoux, B. (1991). Langmuir **7**: 3076.

Lenk, T. J.;Lee, D. H. T. and Koberstein, J. T. (1994). Langmuir **10**: 1857.

Lotz, B.;Lovinger, A. J. and Cais, R. E. (1988). Macromolecules **21**: 2375.

Lovinger, A. J.;B., L.;Davis, D. D. and Paden, F. J. (1993). Macromolecules **26**: 2494.

Lovinger, A. J.;Lotz, B.;Davis, D. D. and Schumacher, M. (1994). Macromolecules **27**: 6603.

Mann, E. K.;Henon, S.;Langevin, D. and Meunier, J. (1992). J. Phys. II, France **2**: 1683.

Mann, E. K. and Langevin, D. (1991). Langmuir **7**: 1112.

Mann, E. K.;Langevin, D.;Henon, S.;Meunier, J. and Lee, L. T. (1994). Ber. Bunsenges. Phys. Chem. **98**: 519.

Masetti, G.;Cabassi, F. and Zerbi, G. (1980). Polymer **21**: 143.

Mattice, W. L. and Suter, U. W. (1994). Conformational Theory of Large Molecules. The Rotational Isomeric State Model in Macromolecular Systems. New York, John Wiley and Sons, Inc.

McConnell, H. M. (1991). Annual Review of Physical Chemistry **42**: 171.

Mohwald, H. (1990). Annual Review of Physical Chemistry **41**: 441.

MSI This program was developed by Molecular Simulations Incorporated.

Nakaoki, T.;Ohira, Y.;Hayashi, H. and Horii, F. (1998). Macromolecules **31**: 2705.

Natta, G. and Corradini, P. (1960). Nuovo Chim. Suppl. **15**: 40.

Natta, G.;Peraldo, M. and Allegra, G. (1964). Die Makromolekulare Chemie **75**: 215.

Noll, W.;Steinbach, H. and Sucker, C. (1971). Journal of Polymer Science: Part C **34**: 123.

Peraldo, M. and Cambini, M. (1965). Spectrochimica Acta **21**: 1509.

Porto, S. P. S. (1966). Journal of the Optical Society of America **56**(11): 1585.

Ren, Y.;Meuse, C. W. and Hsu, S. L. (1994). J. Phys. Chem. **98**: 8424.

Ren, Y.;Shoichet, M. S.;McCarthy, T. J.;Stidham, H. D. and Hsu, S. L. (1995). Macromolecules **28**: 358.

Riou, S. A.;Hsu, S. L. and Stidham, H. D. (1997). J. Polym. Sci. - Phys. Ed. **35**: 2843.

Royal, J. S.;Victor, J. G. and Torkelson, J. M. (1992). Macromolecules **25**: 729.

Royal, R. S. and Torkelson, J. M. (1992). Macromolecules **25**: 1705.

Royal, R. S. and Torkelson, J. M. (1993). Macromolecules **26**: 5331.

Schachtschneider, J. H. and Snyder, R. G. (1965). Spectrochimica Acta **21**: 1527.

Smith, A. L. (1960). Spectrochimica Acta **16**: 87.

Snyder, R. G. (1967). J. Chem. Phys. **47**: 1316.

Snyder, R. G. (1992). J. Chem. Soc. Faraday Trans **88**(13): 1823.

Snyder, R. G. and Kim, Y. (1991). J. Phys. Chem **95**: 602.

Snyder, R. G. and Schachtschneider, J. H. (1964). Spectrochim. Acta **20**: 853.

Sozzani, P.;Simonutti, R. and Comoti, A. (1994). Magnetic Resonance in Chemistry **32**: s45.

Sozzani, P.;Simonutti, R. and Galimberti, M. (1993). Macromolecules **26**: 5782.

Stocker, W.;Schumacher, M.;Graff, S.;Lang, J.;Wittmann, J. C.;Lovinger, A. J. and Lotz, B. (1994). Macromolecules **27**: 6948.

Struik, L. C. E. (1978). Physical Aging in Amorphous Polymers and Other Materials. New York, Elsevier Scientific Publishing Company.

Suter, U. W. and Flory, P. J. (1975). Macromolecules **8**(6): 765.

Tang, J. and Albrecht, A. C. (1970). Chapter 2, Developments in the Theories of Vibrational Raman Intensities. Raman Spectroscopy: Theory and Practice. New York, Plenum Press. 33.

Tao, H. J.;MacKnight, W. J.;Gagnon, K. D. and Lenz, R. W. (1995). Macromolecules **28**: 2016.

Tonneli, A. E. and Schilling, F. C. (1981). Acc. Chem. Res. **14**: 233.

Tsay, F. D.;Hong, S. D.;Maocanin, J. and Gupta, A. (1982). Journal of Polymer Science: Polymer Physics Edition **20**: 763.

Turner-Jones, A.;Aizlewood, J. M. and Beckett, D. R. (1964). Makromol. Chem. **75**: 134.

Uehara, H.;Yamazaki, Y. and Kanamoto, T. (1996). Polymer **37**(1): 57.

Wang, Y.;Hahn, T. D.;Hsu, S. L.;Stidham, H. D. and Seidle, A. (1998). : Manuscript in Preparation.

Wang, Y. Y.;Nakanishi, H. and Jean, Y. C. (1990). Journal of Polymer Science: Part B: Polymer Physics **28**: 1431.

Weis, R. M. (1991). Chemistry and Physics of Lipids **57**: 227.

Wilmshurst, J. K. (1957). Journal of Chemical Physics **26**: 426.

Wilson Jr., E. B.;Decius, J. C. and Cross, P. C. (1955). Molecular vibrations. New York, McGraw-Hill Book Company.

Woodward, L. A. (1972). Introduction to the theory of molecular vibrations and vibrational spectroscopy. Oxford, Oxford University Press.

Wright, N. and Hunter, M. J. (1947). The Journal of the American Chemical Society **69**: 803.

Yang, X.;He, L.;An , B. and Ma, D. (1993). Polymer **34**(21): 4542.

Yang, X.;Su, Z.;Wu, D.;Hsu, S. L. and Stidham, H. D. (1997). Macromolecules **30**: 3796.

Yoon, S.;Ichikawa, K.;J., M. W. and Hsu, S. L. (1995). Macromolecules **28**: 4278.

Yoon, S.;Ichikawa, K.;MacKnight, W. J. and Hsu, S. L. (1995). Macromolecules **28**: 5063.

Zambelli, A.;Locatelli, P.;Bajo, G. and Bovey, F. A. (1975). Macromolecules **8**: 687.

Zambelli, A.;Natta, G. and Pasquon, I. (1963). Journal of Polymer Science: C **4**: 411.

Zbinden, R. (1964). Infrared Spectroscopy of High Polymers. New York, Academic Press, Inc.

Zerbi, G.;Gussoni, M. and Ciampelli, F. (1967). Spectrochimica Acta **23A**: 301.

Zerbi, G. and Piseri, L. (1968). The Journal of Chemical Physics **49**(9): 3840.